Modeling Oil Spill Trajectories in Baffin Bay and Lancaster Sound

FINAL REPORT

June 13, 2016

Submitted to:
Paul Crowley, Vice-President, Arctic
WWF-Canada

Contributing Authors:
Danielle Ameen Reich, Shoal's Edge Consulting
Dagmar Schmidt Etkin, Environmental Research Consulting
Greg Rowe, Growe Geospatial
Stefanie Zamorski, Shoal's Edge Consulting

This report contains information intended for use by WWF-Canada and is not intended for third-party use without prior written consent from WWF-Canada. Modeling is predictive in nature and, while this report is based on information from sources that Shoal's Edge Consulting considers reliable, the accuracy and completeness of said information cannot be guaranteed. Therefore, Shoal's Edge Consulting and its directors, agents, assigns, and employees accept no liability for the result of any action taken or not taken on the basis of the information given in this report, nor for any negligent misstatements, errors, and omissions. The statements in this report are the opinions of the authors and may not reflect the views of WWF-Canada.

CONTACT

Danielle Ameen Reich

dreich@shoalsedge.com

(772) 206-0989

www.shoalsedge.com

TABLE OF CONTENTS

1.0 INTRODUCTION 1
2.0 MODEL DESCRIPTIONS 4
2.1 OILMAP DEEP 4
2.2 SIMAP 4
3.0 MODELING APPROACH 7
3.1 Blowout Near-Field Modeling 7
3.1.1 Description of a Blowout 7
3.1.2 Blowout Near-field Modeling Approach 8
3.2 Far-field Modeling 9
3.2.1 Stochastic Modeling Approach 9
3.2.2 Deterministic Modeling Approach 12
3.3 Modeling Oil Interactions in Ice 12
3.3.1 Oil Transport in Sea Ice 13
3.3.2 Oil Interaction with Landfast Ice 14
3.3.3 Effects of Ice on Oil Fates and Behavior Processes 14
4.0 DATA INPUTS 16
4.1 Currents and Ice 16
4.1.1 Regional Overview 16
4.1.2 Currents and Sea Ice Dataset 19
4.1.3 Landfast Ice Dataset 21
4.1.4 Eclipse Sound Tidal Currents Model 22
4.2 Winds 23
4.2.1 Regional Overview 23
4.2.2 Wind Dataset 24
4.3 Temperature, Density, and Salinity 24
4.4 Shoreline Geometry and Type 24
4.5 Bathymetry 25
4.6 Oil Properties 25
4.7 Consequence Thresholds 26
5.0 SCENARIOS 1A AND 1B – MELVILLE BAY BLOWOUTS 28
5.1 Scenario Development 28
5.2 Environmental Analysis 30
5.3 Near-field Modeling 37
5.4 Stochastic Modeling 39
5.4.1 Stochastic Scenario Parameters 39
5.4.2 Stochastic Results 40
5.5 Deterministic Modeling 45
5.5.1 Deterministic Scenario Parameters 46
5.5.1.1 Response Parameters 47
5.5.2 Deterministic Results 51
5.6 Conclusions 70
6.0 SCENARIOS 2A AND 2B – BAFFIN BAY BLOWOUTS 72
6.1 Scenario Development 72
6.2 Environmental Analysis 74
6.3 Near-field Modeling 81
6.4 Stochastic Modeling 83
6.4.1 Stochastic Scenario Parameters 83
6.4.2 Stochastic Results 84

6.5 Deterministic Modeling 90
6.5.1 Deterministic Scenario Parameters 90
6.5.1.1 Response Parameters 90
6.5.2 Deterministic Results 94
6.6 Conclusions 107
7.0 SCENARIO 3 – GREENLAND COAST CRUISE SHIP SPILL 109
7.1 Scenario Development 109
7.2 Environmental Analysis 111
7.3 Stochastic Modeling 117
7.3.1 Stochastic Scenario Parameters 117
7.3.2 Stochastic Results 117
7.4 Deterministic Modeling 121
7.4.1 Deterministic Scenario Parameters 122
7.4.2 Deterministic Results 122
7.5 Conclusions 129
8.0 SCENARIO 4 – LANCASTER SOUND PRODUCT TANKER SPILL 130
8.1 Scenario Development 130
8.2 Environmental Analysis 131
8.3 Stochastic Modeling 137
8.3.1 Stochastic Scenario Parameters 137
8.3.2 Stochastic Results 138
8.4 Conclusions 142
9.0 SCENARIOS 5A AND 5B – ECLIPSE SOUND BULK CARRIER SPILLS 143
9.1 Scenario Development 143
9.2 Environmental Analysis 145
9.3 Stochastic Modeling 153
9.3.1 Stochastic Scenario Parameters 153
9.3.2 Stochastic Results 154
9.4 Deterministic Modeling 159
9.4.1 Deterministic Scenario Parameters 160
9.4.2 Deterministic Results 160
9.5 Conclusions 173
10.0 REFERENCES 174

LIST OF FIGURES

Figure 1. Spill site locations for base cases 1, 2, 3, 4, and 5 2
Figure 2. General schematic showing profile and associated characteristics of a deep well blowout. 7
Figure 3. Examples of four individual spill trajectories predicted by SIMAP for a generic spill scenario. All 100+ individual trajectories are overlain (shown as the stacked runs on the right), and the frequency of contact with given locations is used to calculate the probability of impacts during a spill. 11
Figure 4. Probability of surface oil exceeding a given threshold for the example scenario. This figure overlays 100+ individual model runs to calculate the percentage of runs that caused oiling above the threshold in a given area. This figure does not depict the areal extent of a single trajectory/spill. 11
Figure 5. General schematic showing dynamics and characteristics of sea ice and oil interaction at the sea surface. (Source: Original figure by Alan A. Allen). 13
Figure 6. Schematic of general circulation in the Baffin Bay region (Source: Hamilton and Wu, 2013). 17
Figure 7. Approximate extent of the North Water Polynya is shown in dark blue. Data provided by WWF-Canada. 18
Figure 8. The entire domain of the outer model of TOPAZ4 Arctic and Atlantic Oceans. Coloration shows a snapshot of sea surface height. (Source: Samuelsen and Bertino, 2013). 20
Figure 9. Example current speed output from the operational version of TOPAZ4 showing the dataset's coverage in the area of interest. 20
Figure 10. Snapshot of the monthly average landfast ice cover data used in modeling. Data displayed is for the month of March. 22
Figure 11. HYDROMAP grid for the vicinity of Eclipse Sound, showing the varying resolutions of the nested grid. 23
Figure 12. GEBCO bathymetry in the study area. 25
Figure 13. Location of the selected spill site in Melville Bay (scenarios 1A and 1B). 28
Figure 14. Location of the Melville Bay Nature Reserve (red outline). Source: IUCN and UNEP-WCMC, 2016. 29
Figure 15. TOPAZ4 monthly averaged surface current roses near the Melville Bay spill site, averaged over the period of 2011-2015. Direction convention is standard (i.e., direction currents are moving to). 31
Figure 16. TOPAZ4 current statistics: monthly average (grey solid) and 95th percentile (orange dash) current speed at the surface near the Melville Bay spill site for 2011-2015. 32
Figure 17. TOPAZ4 monthly averaged ice roses near the Melville Bay spill site, averaged over the period of 2011-2015. Ice roses are presented for the surface. Direction convention is standard (i.e., direction ice is moving to). 33
Figure 18. Average monthly cover of sea ice and landfast ice near the Melville Bay spill site. 34
Figure 19. ECMWF monthly averaged wind roses near the Melville Bay spill site, averaged over the period of 2011-2015. Wind speeds are in knots, using meteorological convention (i.e., direction wind is coming from). 35
Figure 20. ECMWF wind statistics: monthly average (grey solid) and 95th percentile (orange dash) wind speed near the Melville Bay spill site for 2011-2015. 36
Figure 21. Vertical profile of average temperature (red), salinity (purple), and density (green) near the Melville Bay spill site for July to October. Data from the World Ocean Atlas 2013. 37
Figure 22. Predicted blowout plume centerline velocity and plume radius versus elevation above release point for the Melville Bay blowout events (scenarios 1A and 1B). 38

Figure 23. Predicted droplet size distribution and droplet rise times to the surface for the Melville Bay blowout events (scenarios 1A and 1B). 39
Figure 24. Scenario 1A (1-day blowout of 3,340 m^3 crude oil) stochastic results – Probability of water surface oiling above the socioeconomic threshold of 0.01 g/m^2 (top panel) and probability of water surface oiling above the ecological threshold of 10 g/m^2 (bottom panel). 42
Figure 25. Scenario 1A (1-day blowout of 3,340 m^3 crude oil) stochastic results – Probability of shoreline oiling above the ecological threshold of 100 g/m^2. 43
Figure 26. Scenario 1B (34-day blowout of 113,560 m^3 crude oil) stochastic results – Probability of water surface oiling above the socioeconomic threshold of 0.01 g/m^2 (top panel) and probability of water surface oiling above the ecological threshold of 10 g/m^2 (bottom panel). 44
Figure 27. Scenario 1B (34-day blowout of 113,560 m^3 crude oil) stochastic results – Probability of shoreline oiling above the ecological threshold of 100 g/m^2. 45
Figure 28. Nearshore and offshore response zones for scenarios 1A and 1B. 48
Figure 29. Scenario 1A: Worst-case (95th percentile) trajectory for shoreline length oiled above 100 g/m^2, with spill response (surface dispersant, mechanical containment/recovery, and *in situ* burning) – Maximum concentration (g/m^2) of floating oil that passed by a given area during the simulation and the subsurface area swept by dissolved aromatics (top panel); and total concentration (g/m^2) of oil on the shoreline at the end of the simulation (bottom panel). 53
Figure 30. Scenario 1A: Worst-case (95th percentile) trajectory for shoreline length oiled above 100 g/m^2, with spill response (surface dispersant, mechanical containment/recovery, and *in situ* burning) – Mass balance graph. 54
Figure 31. Scenario 1A: Worst-case (95th percentile) trajectory for water surface area oiled above 10 g/m^2 within the North Water Polynya, with spill response (surface dispersant, mechanical containment/recovery, and *in situ* burning) – Maximum concentration (g/m^2) of floating oil that passed by a given area during the simulation and the subsurface area swept by dissolved aromatics (top panel); and total concentration (g/m^2) of oil on the shoreline at the end of the simulation (bottom panel). 56
Figure 32. Scenario 1A: Worst-case (95th percentile) trajectory for water surface area oiled above 10 g/m^2 within the North Water Polynya, with spill response (surface dispersant, mechanical containment/recovery, and *in situ* burning) – Mass balance graph. 57
Figure 33. Scenario 1B: Worst-case (95th percentile) trajectory for shoreline length oiled above 100 g/m^2, with no spill response – Maximum concentration (g/m^2) of floating oil that passed by a given area during the simulation and the subsurface area swept by dissolved aromatics (top panel); and total concentration (g/m^2) of oil on the shoreline at the end of the simulation (bottom panel). 59
Figure 34. Scenario 1B: Worst-case (95th percentile) trajectory for shoreline length oiled above 100 g/m^2, with no spill response – Mass balance graph. 60
Figure 35. Scenario 1B: Worst-case (95th percentile) trajectory for water surface area oiled above 10 g/m^2 within the North Water Polynya, with no spill response – Maximum concentration (g/m^2) of floating oil that passed by a given area during the simulation and the subsurface area swept by dissolved aromatics (top panel); and total concentration (g/m^2) of oil on the shoreline at the end of the simulation (bottom panel). 62
Figure 36. Scenario 1B: Worst-case (95th percentile) trajectory for water surface area oiled above 10 g/m^2 within the North Water Polynya, with no spill response – Mass balance graph. 63
Figure 37. Scenario 1B: Worst-case (95th percentile) trajectory for water surface area oiled above 10 g/m^2 within the North Water Polynya, with spill response (surface dispersant, mechanical containment/recovery, and *in situ* burning) – Maximum concentration (g/m^2)

of floating oil that passed by a given area during the simulation and the subsurface area swept by dissolved aromatics (top panel); and total concentration (g/m^2) of oil on the shoreline at the end of the simulation (bottom panel). 65
Figure 38. Scenario 1B: Worst-case (95th percentile) trajectory for water surface area oiled above 10 g/m^2 within the North Water Polynya, with spill response (surface dispersant, mechanical containment/recovery, and *in situ* burning) – Mass balance graph....66
Figure 39. Scenario 1B: Worst-case (95th percentile) trajectory for volume of oil in the water column, with no spill response – Maximum concentration (g/m^2) of floating oil that passed by a given area during the simulation and the subsurface area swept by dissolved aromatics (top panel); and total concentration (g/m^2) of oil on the shoreline at the end of the simulation (bottom panel). 68
Figure 40. Scenario 1B: Worst-case (95th percentile) trajectory for volume of oil in the water column, with no spill response – Mass balance graph. 69
Figure 41. Location of the selected spill site in Baffin Bay (scenarios 2A and 2B)....72
Figure 42. TOPAZ4 monthly averaged surface current roses near the Baffin Bay spill site, averaged over the period of 20011-2015. Direction convention is standard (i.e., direction currents are moving to). 75
Figure 43. TOPAZ4 current statistics: monthly average (grey solid) and 95th percentile (orange dash) current speed at the surface near the Baffin Bay spill site for 2011-2015. 76
Figure 44. TOPAZ4 monthly averaged ice roses near the Baffin Bay spill site averaged over the period of 2011-2015. Ice roses are presented for the surface. Direction convention is standard (i.e., direction ice is moving to). 77
Figure 45. Average monthly cover of sea ice and landfast ice near the Baffin Bay spill site....78
Figure 46. ECMWF monthly averaged wind roses near the Baffin Bay spill site, averaged over the period of 2011-2015. Wind speeds are in knots, using meteorological convention (i.e., direction wind is coming from). 79
Figure 47. ECMWF wind statistics: monthly average (grey solid) and 95th percentile (orange dash) wind speed near the Baffin Bay spill site for 2011-2015. 80
Figure 48. Vertical profile of average temperature (red), salinity (purple), and density (green) near the Baffin Bay spill site for June to October. Data from the World Ocean Atlas 2013. ...81
Figure 49. Predicted blowout plume centerline velocity and plume radius versus elevation above release point for the Baffin Bay blowout events (scenarios 2A and 2B). 82
Figure 50. Predicted droplet size distribution and droplet rise times to the surface for the Baffin Bay blowout events (scenarios 2A and 2B). 83
Figure 51. Scenario 2A (1-day blowout of 3,340 m^3 crude oil) stochastic results – Probability of water surface oiling above the socioeconomic threshold of 0.01 g/m^2 (top panel) and probability of water surface oiling above the ecological threshold of 10 g/m^2 (bottom panel). 86
Figure 52. Scenario 2A (1-day blowout of 3,340 m^3 crude oil) stochastic results – Probability of shoreline oiling above the ecological threshold of 100 g/m^2....87
Figure 53. Scenario 2B (34-day blowout of 113,560 m^3 crude oil) stochastic results – Probability of water surface oiling above the socioeconomic threshold of 0.01 g/m^2 (top panel) and probability of water surface oiling above the ecological threshold of 10 g/m^2 (bottom panel). 88
Figure 54. Scenario 2B (34-day blowout of 113,560 m^3 crude oil) stochastic results – Probability of shoreline oiling above the ecological threshold of 100 g/m^2....89
Figure 55. Oil-brine interfacial tension as a function of Dispersant to Oil Ratio (DOR) (1 mN/m = 1 dyne/cm). The plot is using logarithmic scales in both axis....92
Figure 56. Predicted droplet size distribution for scenario 2B, with and without subsurface dispersant treatment (DOR 1:100). Note: the x-axis is logarithmic....93

Figure 57. Predicted rise time to the surface based on free rise velocity for the droplet size distributions associated with the untreated and treated (DOR 1:100) simulations for scenario 2B. Note: the x-axis is logarithmic. 94
Figure 58. Scenario 2B: Worst-case (95th percentile) trajectory for shoreline length oiled above 100 g/m^2, with no spill response – Maximum concentration (g/m^2) of floating oil that passed by a given area during the simulation and the subsurface area swept by dissolved aromatics (top panel); and total concentration (g/m^2) of oil on the shoreline at the end of the simulation (bottom panel). 96
Figure 59. Scenario 2B: Worst-case (95th percentile) trajectory for shoreline length oiled above 100 g/m^2, with no spill response – Mass balance graph. 97
Figure 60. Scenario 2B: Worst-case (95th percentile) trajectory for shoreline length oiled above 100 g/m^2, with spill response (subsurface dispersant injection) – Maximum concentration (g/m^2) of floating oil that passed by a given area during the simulation and the subsurface area swept by dissolved aromatics (top panel); and total concentration (g/m^2) of oil on the shoreline at the end of the simulation (bottom panel). 99
Figure 61. Scenario 2B: Worst-case (95th percentile) trajectory for shoreline length oiled above 100 g/m^2, with spill response (subsurface dispersant injection) – Mass balance graph. 100
Figure 62. Scenario 2B: Worst-case (95th percentile) trajectory for water surface area oiled above 10 g/m^2, with no spill response – Maximum concentration (g/m^2) of floating oil that passed by a given area during the simulation and the subsurface area swept by dissolved aromatics (top panel); and total concentration (g/m^2) of oil on the shoreline at the end of the simulation (bottom panel). 102
Figure 63. Scenario 2B: Worst-case (95th percentile) trajectory for water surface area oiled above 10 g/m^2, with no spill response – Mass balance graph. 103
Figure 64. Scenario 2B: Worst-case (95th percentile) trajectory for volume of oil in the water column, with no spill response – Maximum concentration (g/m^2) of floating oil that passed by a given area during the simulation and the subsurface area swept by dissolved aromatics (top panel); and total concentration (g/m^2) of oil on the shoreline at the end of the simulation (bottom panel). 105
Figure 65. Scenario 2B: Worst-case (95th percentile) trajectory for volume of oil in the water column, with no spill response – Mass balance graph. 106
Figure 66. Location of the selected spill site off the Greenland coast near Disko Island (scenario 3). 109
Figure 67. TOPAZ4 monthly averaged surface current roses near the Greenland coast spill site averaged over the period of 2011-2015. Direction convention is standard (i.e., direction currents are moving to). 112
Figure 68. TOPAZ4 current statistics: monthly average (grey solid) and 95th percentile (orange dash) current speed at the surface near the Greenland coast spill site for 2011-2015. 113
Figure 69. ECMWF monthly averaged wind roses near the Greenland coast spill site, averaged over the period of 2011-2015. Wind speeds are in knots, using meteorological convention (i.e., direction wind is coming from). 114
Figure 70. ECMWF wind statistics: monthly average (grey solid) and 95th percentile (orange dash) wind speed near the Greenland coast spill site for 2011-2015. 115
Figure 71. Average monthly cover of sea ice and landfast ice near the Greenland coast spill site during the period of interest. 116
Figure 72. Vertical profile of average temperature (red), salinity (purple), and density (green) near the Greenland coast spill site for July to September. Data from the World Ocean Atlas 2013. 117
Figure 73. Scenario 3 (surface spill of 280 m^3 IFO 180) stochastic results – Probability of water surface oiling above the socioeconomic threshold of 0.01 g/m^2 (top panel) and

probability of water surface oiling above the ecological threshold of 10 g/m^2 (bottom panel). 120
Figure 74. Scenario 3 (surface spill of 280 m^3 IFO 180) stochastic results – Probability of shoreline oiling above the ecological threshold of 100 g/m^2. 121
Figure 75. Scenario 3: Worst-case (95th percentile) trajectory for shoreline length oiled above 100 g/m^2, with no spill response – Maximum concentration (g/m^2) of floating oil that passed by a given area during the simulation and the subsurface area swept by dissolved aromatics (top panel); and total concentration (g/m^2) of oil on the shoreline at the end of the simulation (bottom panel). 124
Figure 76. Scenario 3: Worst-case (95th percentile) trajectory for shoreline length oiled above 100 g/m^2, with no spill response – Mass balance graph. 125
Figure 77. Scenario 3: Worst-case (95th percentile) trajectory for water surface area oiled above 10 g/m^2, with no spill response – Maximum concentration (g/m^2) of floating oil that passed by a given area during the simulation and the subsurface area swept by dissolved aromatics (top panel); and total concentration (g/m^2) of oil on the shoreline at the end of the simulation (bottom panel). 127
Figure 78. Scenario 3: Worst-case (95th percentile) trajectory for water surface area oiled above 10 g/m^2, with no spill response – Mass balance graph. 128
Figure 79. Location of the selected spill site in Lancaster Sound (scenario 4). 130
Figure 80. TOPAZ4 monthly averaged surface current roses near the Lancaster Sound spill site averaged over the period of 2011-2015. Direction convention is standard (i.e., direction currents are moving to). 132
Figure 81. TOPAZ4 current statistics: monthly average (grey solid) and 95th percentile (orange dash) current speed at the surface near the Lancaster Sound spill site for 2011-2015. 133
Figure 82. ECMWF monthly averaged wind roses near the Lancaster Sound spill site, averaged over the period of 2011-2015. Wind speeds are in knots, using meteorological convention (i.e., direction wind is coming from). 134
Figure 83. ECMWF wind statistics: monthly average (grey solid) and 95th percentile (orange dash) wind speed near the Lancaster Sound spill site for 2011-2015. 135
Figure 84. Average monthly cover of sea ice and landfast ice near the Lancaster Sound spill site during the period of interest. 136
Figure 85. Vertical profile of average temperature (red), salinity (purple), and density (green) near the Lancaster Sound spill site for June to September. Data from the World Ocean Atlas 2013. 137
Figure 86. Scenario 4 (surface spill of 2,400 m^3 Arctic diesel) stochastic results – Probability of water surface oiling above the socioeconomic threshold of 0.01 g/m^2 (top panel) and probability of water surface oiling above the ecological threshold of 10 g/m^2 (bottom panel). 140
Figure 87. Scenario 4 (surface spill of 2,400 m^3 Arctic diesel) stochastic results – Probability of shoreline oiling above the ecological threshold of 100 g/m^2. 141
Figure 88. Location of the selection spill site in Eclipse Sound (scenarios 5A and 5B). 143
Figure 89. Shipping routes to Milne Port, Baffinland Mines (Baffinland Iron Mines Corporation, 2015). The purple line shows the shipping route in the open water season; the green line shows the route during the ice-covered season. 144
Figure 90. TOPAZ4 monthly averaged surface current roses near the Eclipse Sound spill site, averaged over the period of 2011-2015. Direction convention is standard (i.e., direction currents are moving to). 146
Figure 91. TOPAZ4 current statistics: monthly average (grey solid) and 95th percentile (orange dash) current speed at the surface near the Eclipse Sound spill site for 2011-2015. 147

Figure 92. TOPAZ4 monthly averaged ice roses near the Eclipse Sound spill site, averaged over the period of 2011-2015. Ice roses are presented for the surface. Direction convention is standard (i.e., direction ice is moving to). TOPAZ4 ice velocity data are not available for the spill site during January and February. 148
Figure 93. Average monthly cover of sea ice and landfast ice near the spill site for the Eclipse Sound spill site. 149
Figure 94. Time-averaged HYDROMAP surface current rose near the Eclipse Sound spill site. Direction convention is standard (i.e., direction currents are moving to). 150
Figure 95. HYDROMAP tidal current stick plot for the Eclipse Sound spill site. 150
Figure 96. ECMWF monthly averaged wind roses near the Eclipse Sound spill site averaged over the period of 2011-2015. Wind speeds are in knots, using meteorological convention (i.e., direction wind is coming from). 151
Figure 97. ECMWF wind statistics: monthly average (grey solid) and 95th percentile (orange dash) wind speed near the Eclipse Sound spill site for 2011-2015. 152
Figure 98. Vertical profile of average temperature (red), salinity (purple), and density (green) near the Eclipse Sound spill site for ice-covered (June-July, November-March) and open water (August-October) periods. Data from the World Ocean Atlas 2013. 153
Figure 99. Scenario 5A (surface spill of 1,000 m^3 IFO 380 in open water conditions) stochastic results – Probability of water surface oiling above the socioeconomic threshold of 0.01 g/m^2 (top panel) and probability of water surface oiling above the ecological threshold of 10 g/m^2 (bottom panel). 156
Figure 100. Scenario 5A (surface spill of 1,000 m^3 IFO 380 in open water conditions) stochastic results – Probability of shoreline oiling above the ecological threshold of 100 g/m^2. 157
Figure 101. Scenario 5B (surface spill of 1,000 m^3 IFO 380 in ice conditions) stochastic results – Probability of water surface oiling above the socioeconomic threshold of 0.01 g/m^2 (top panel) and probability of water surface oiling above the ecological threshold of 10 g/m^2 (bottom panel). 158
Figure 102. Scenario 5B (surface spill of 1,000 m^3 IFO 380 in ice conditions) stochastic results – Probability of shoreline oiling above the ecological threshold of 100 g/m^2. 159
Figure 103. Scenario 5: Representative (50th percentile) trajectory for water surface area oiled above 10 g/m^2 for spills originating in the month of July, with no spill response – Maximum concentration (g/m^2) of floating oil that passed by a given area during the simulation and the subsurface area swept by dissolved aromatics (top panel); and total concentration (g/m^2) of oil on the shoreline at the end of the simulation (bottom panel). 162
Figure 104. Scenario 5: Representative (50th percentile) trajectory for water surface area oiled above 10 g/m^2 for spills originating in the month of July, with no spill response – Mass balance graph. 163
Figure 105. Scenario 5: Representative (50th percentile) trajectory for water surface area oiled above 10 g/m^2 for spills originating in the month of August, with no spill response – Maximum concentration (g/m^2) of floating oil that passed by a given area during the simulation and the subsurface area swept by dissolved aromatics (top panel); and total concentration (g/m^2) of oil on the shoreline at the end of the simulation (bottom panel). 165
Figure 106. Scenario 5: Representative (50th percentile) trajectory for water surface area oiled above 10 g/m^2 for spills originating in the month of August, with no spill response – Mass balance graph. 166
Figure 107. Scenario 5: Representative (50th percentile) trajectory for water surface area oiled above 10 g/m^2 for spills originating in the month of October, with no spill response – Maximum concentration (g/m^2) of floating oil that passed by a given area during the

simulation and the subsurface area swept by dissolved aromatics (top panel); and total concentration (g/m^2) of oil on the shoreline at the end of the simulation (bottom panel). 168
Figure 108. Scenario 5: Representative (50th percentile) trajectory for water surface area oiled above 10 g/m^2 for spills originating in the month of October, with no spill response – Mass balance graph. 169
Figure 109. Scenario 5: Worst-case (95th percentile) trajectory for water surface area oiled above 10 g/m^2, with no spill response – Maximum concentration (g/m^2) of floating oil that passed by a given area during the simulation and the subsurface area swept by dissolved aromatics (top panel); and total concentration (g/m^2) of oil on the shoreline at the end of the simulation (bottom panel). 171
Figure 110. Scenario 5: Worst-case (95th percentile) trajectory for water surface area oiled above 10 g/m^2, with no spill response – Mass balance graph. 172

LIST OF TABLES

Table 1. Spill matrix summarizing the eight spill scenarios selected for modeling. 1
Table 2. Percent ice coverage thresholds for oil fates and behavior processes applied in the SIMAP model. 15
Table 3. Shore width and oil holding capacities for various generic shoreline types (French et al., 1996). 25
Table 4. Key properties of the oils used in model simulations. 26
Table 5. Consequence thresholds used in modeling. 27
Table 6. Stochastic scenario input parameters for scenarios 1A and 1B. 39
Table 7. Scenarios 1A and 1B stochastic results – shoreline oiling statistics. 40
Table 8. Scenarios 1A and 1B stochastic results – surface oiling and water column oiling statistics. 41
Table 9. Selected deterministic cases for scenarios 1A and 1B. 46
Table 10. Environmental and physical thresholds for effective response used in model simulations. 49
Table 11. Timing and daily oil removal/treatment capacities assumed for the response operations in scenarios 1A and 1B. 50
Table 12. Summary of deterministic results for the Melville Bay 1-day and 34-day blowout scenarios. 51
Table 13. Stochastic scenario input parameters for scenarios 2A and 2B. 83
Table 14. Scenarios 2A and 2B stochastic results – shoreline oiling statistics. 84
Table 15. Scenarios 2A and 2B Stochastic results – surface oiling and water column oiling statistics. 85
Table 16. Selected deterministic cases for scenario 2B. 90
Table 17. Subsurface dispersant injection modeling assumptions for scenario 2B. 91
Table 18. Summary of deterministic results for the Baffin Bay 34-day blowout scenarios. 95
Table 19. Stochastic scenario input parameters for scenario 3. 117
Table 20. Scenario 3 stochastic results – shoreline oiling statistics. 118
Table 21. Scenario 3 stochastic results – surface oiling and water column oiling statistics. 118
Table 22. Selected deterministic cases for scenario 3. 122
Table 23. Summary of deterministic results for the Greenland coast cruise ship scenarios. 123
Table 24. Stochastic scenario input parameters for scenario 4. 137
Table 25. Scenario 4 stochastic results – shoreline oiling statistics. 138
Table 26. Scenario 4 stochastic results – surface oiling and water column oiling statistics. 138

Table 27. Stochastic scenario input parameters for scenarios 5A and 5B. 153
Table 28. Scenarios 5A and 5B stochastic results – shoreline oiling statistics. 154
Table 29. Scenarios 5A and 5B stochastic results – surface oiling and water column oiling statistics. 155
Table 30. Selected deterministic cases for scenario 5. 160
Table 31. Summary of deterministic results for the Eclipse Sound bulk carrier scenarios. 161

LIST OF APPENDICES

Appendix A Spill Scenario Development, Spill Probability Analysis, and Spill Response Development

1.0 INTRODUCTION

World Wildlife Fund Canada (WWF-Canada) contracted Shoal's Edge Consulting (SEC), Environmental Research Consulting (ERC), and Growe Geospatial to perform an oil spill trajectory study of hypothetical oil spills in the Lancaster Sound and Baffin Bay region. This study investigated possible spill events associated with vessel traffic and offshore petroleum exploration and development. The results of this analysis are intended to inform local risk perception, prepare for oil spill response planning, and inform integrated ocean management and planning.

The results of this study will be used by WWF-Canada to assist in communicating the potential impacts of oil spills in the "Last Ice Area" (i.e., northern Greenland, the Canadian High Arctic Archipelago, and associated waters), identifying areas that are particularly vulnerable to oil spill impacts, influencing planning and preparation for oil spill responses, and informing integrated ocean management and planning in Nunavut, Canada and Greenland.

WWF-Canada requested that five different types of spill events be evaluated for this project. These included:

1. An offshore oil platform blowout, occurring within the existing license areas off Melville Bay in northwestern Greenland;
2. An offshore oil platform blowout, occurring within the existing license areas in Baffin Bay located to the east of the entrance to Lancaster Sound;
3. A passenger cruise ship spill due to a grounding off the coast of Greenland near Disko Island;
4. An oil product tanker spill in Lancaster Sound; and
5. A bulk carrier spill in Eclipse Sound.

The development of spill scenarios for modeling is not a straightforward task because of the sheer number of possible combinations of spill volume, spill type, location, duration, season, and oil type. Given WWF-Canada's stated objectives, SEC and ERC developed a spill matrix consisting of a focused set of 8 spill scenarios (Table 1) that reflect both highly damaging potential spills (which have a very low likelihood of occurrence), as well as smaller, more probable spills. The selected spill site locations for each base case are shown in Figure 1.

Table 1. Spill matrix summarizing the eight spill scenarios selected for modeling.

Base Case #	Location	Spill Type	# of Oil Types	# of Spill Volumes/ Durations	# of Seasons	Total # of Scenarios
1	Melville Bay license areas	Subsurface blowout	1	2	1	2
2	Baffin Bay license areas (near entrance of Lancaster Sound)	Subsurface blowout	1	2	1	2
3	Greenland coast near Ilulissat	Surface spill (cruise ship grounding)	1	1	1	1
4	Lancaster Sound	Surface spill (product tanker)	1	1	2	2
5	Eclipse Sound	Surface spill (bulk carrier)	1	1	1	1
					TOTAL	**8**

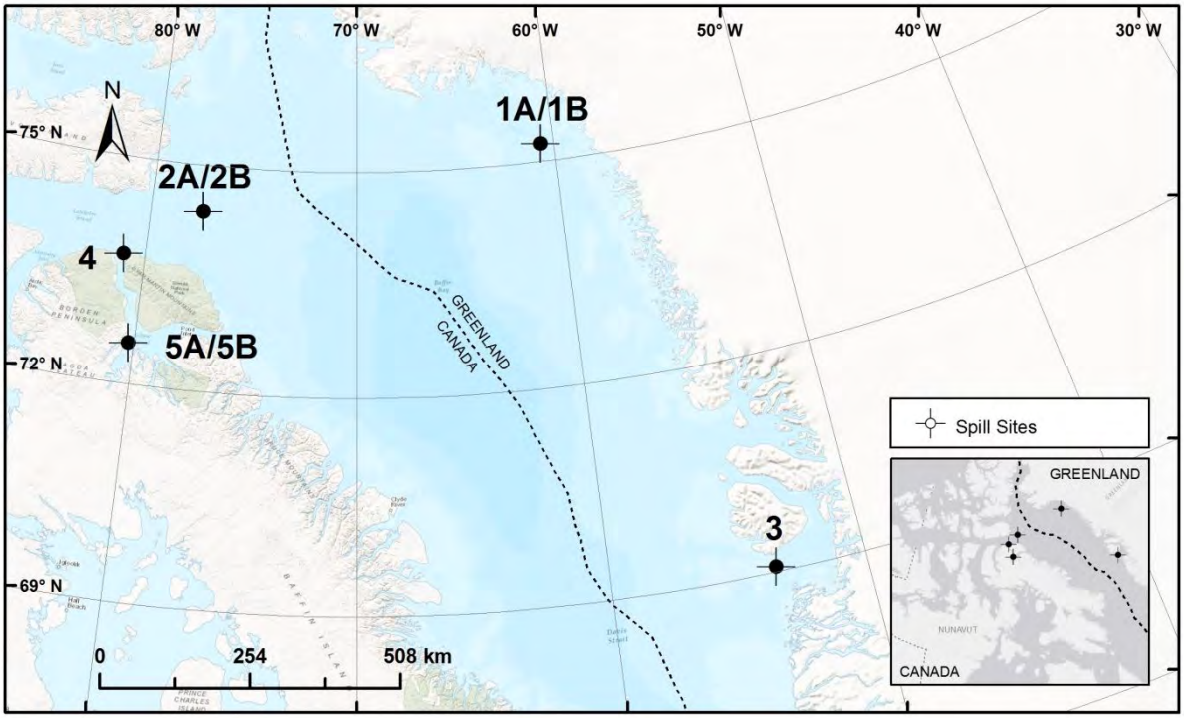

Figure 1. Spill site locations for base cases 1, 2, 3, 4, and 5.

To develop the specific spill scenario parameters necessary for modeling, ERC conducted background research on existing shipping, cruising, exploration, and operational activities in the region of interest. Interested stakeholders also provided information to support the development of spill scenario parameters, including individuals from WWF-Canada, WWF-Denmark, Government of Greenland, Greenland Institute of Natural Resources, Association of Arctic Expedition Cruise Operators, Danish Metrological Institute, communities of Upernavik and Qaanaq, Qikiqtani Inuit Association, and Baffinland Iron Mines Corporation. The result was a suite of credible spill scenarios that adequately represent the range of oil types, spill volumes, locations, and seasonal timing that may reasonably be expected in the area of interest.

The oil spill scenarios were simulated and analyzed using RPS ASA's SIMAP oil spill modeling system with the goal of assessing the potential impact of different release scenarios on the nearby surface water, water column, and shoreline. Evaluation of each of the spill scenarios included stochastic and deterministic model simulations. Near-field modeling in RPS ASA's OILMAP Deep modeling system was also conducted for the subsurface blowout scenarios (scenarios 1 and 2). The near-field simulations provide an estimate of the initial plume geometry and plume termination height as well as the oil droplet size distributions associated with the blowouts. The near-field simulation results are subsequently used to define the initial release of subsurface oil in the stochastic and deterministic simulations.

The stochastic modeling approach uses multiple model runs to characterize the probable consequences of a spill scenario under typical yet varying environmental conditions. For each scenario, the model was run more than 100 times, each with a randomly selected hypothetical start

date and time, thereby sampling the variability of meteorological and oceanographic conditions in the study area. The stochastic model results were evaluated statistically and provide insight into the probable behavior of potential oil spills in response to varying environmental conditions in the study area.

The deterministic trajectory and fate simulations provided an estimate of the trajectory (movement) and fate (weathering) for a particular individual (e.g., worst-case) spill event. The individual trajectory simulations provided estimates of the oil's fate and transport for a specific set of environmental conditions, whereas the stochastic output provided the overall probability of oiling extent given a wide range of possible environmental conditions. Oil spill response measures (e.g., subsurface dispersant injection, surface dispersant application, mechanical containment/recovery, and *in situ* burning) were evaluated in the deterministic simulations for selected spill scenarios.

This report presents an overview of the modeling software (Section 2.0), a summary of the general modeling approach (Section 3.0), and a description of the environmental, physical, and geographic input data utilized for modeling (Section 4.0). Following these background sections, the remainder of the report is organized into self-contained sections for each base case (Sections 5.0 through 9.0). These sections describe the spill scenario development, environmental analysis, near-field modeling inputs and results (for scenarios 1 and 2 only), stochastic modeling inputs and results, and deterministic modeling inputs and results for each base case. Additional supporting information is provided in Appendix A, which contains a report compiled by ERC addressing spill scenario development, spill probabilities, and spill response measures.

2.0 MODEL DESCRIPTIONS

Oil spill modeling was carried out in RPS ASA's SIMAP modeling system. RPS ASA's OILMAP Deep model was also used to analyze the subsurface blowout scenarios in Melville Bay and Baffin Bay (scenarios 1 and 2).

2.1 OILMAP DEEP

RPS ASA's OILMAP Deep model was developed as an enhanced version of the OILMAP modeling system and is based on published work on plume formation and behavior as well as droplet formation. The OILMAP Deep model contains two major sub-models, the droplet size distribution model and the plume model.

The droplet size distribution model employs a character diameter calculation (d95 hereby referred to as maximum diameter) and the Rosin Rammler distribution (Yapa et al., 2001) based on the oil properties (primarily the interfacial tension between oil and seawater) and the energy of the release through calculation of the dimensionless Weber number associated with the release. The Weber number is based on the volumetric release rate, the pipe diameter and receiving water density in the numerator, and the oil interfacial tension (IFT) in the denominator. The maximum droplet diameter for a release is related to the Weber number, i.e. a larger Weber number results in larger droplet size. Therefore lowering the IFT or increasing exit velocity results in a distribution of relatively smaller droplets.

The plume model solves equations for the conservation of water mass, momentum, buoyancy, and gas mass using integral plume theory, following work outlined in McDougall (1978), Spaulding (1982), and Fanneløp and Sjøen (1980). A simplified integral jet theory is employed for the vertical and horizontal motions of the gas-oil plume. The necessary model parameters defining the rates of entrainment and spreading of the jet are obtained from laboratory studies. The plume model calculates the evolution of the blowout plume as it rises and entrains water until it eventually either surfaces or comes in to equilibrium with the receiving water. The receiving water is characterized by a site-specific, depth-variable temperature and density profile. These water column properties influence the plume properties since the state of gas is a function of the temperature and pressure. Similarly, temperature and pressure are used to adjust plume bulk density, based on the volume of entrained seawater, to determine the depth at which the plume bulk density approaches the receiving water density. At the point the plume bulk density is equal to that of the receiving water, plume ascension ceases and the plume becomes trapped at what is referred to as the termination (trap) height. The plume dynamics account for oil and gas buoyancy, gas compression and expansion as a function of depth, hydrate formation, dynamic gas bubble size distribution formulation, gas dissolution, and seawater entrainment and plume spreading processes.

2.2 SIMAP

RPS ASA's SIMAP oil spill modeling system is a computer modeling software application that estimates the physical fates and biological effects of releases of oil. In SIMAP, both the physical fates and biological effects models are three-dimensional. There is also a three-dimensional stochastic model for risk assessment and contingency planning applications. The models are coupled to a geographic information system (GIS) containing environmental and

biological data, and also to databases of physical-chemical properties and biological abundance, providing the necessary inputs for the models.

SIMAP was derived from the physical fates and biological effects sub-models in the Natural Resource Damage Assessment Models for Coastal and Marine and Great Lakes Environments (NRDAM/CME and NRDAM/GLE), which were developed for the U.S. Department of the Interior as the basis of the Comprehensive Environmental Response, Compensation and Liability Act of 1980 (CERCLA) Natural Resource Damage Assessment (NRDA) regulations for Type A assessments (French et al., 1996; Reed et al., 1996). The physical fates model has been validated with more than 20 case histories, including the Exxon Valdez and other large spills (French McCay, 2003, 2004; French McCay and Rowe, 2004), as well as test spills designed to verify the model's transport algorithms (French et al., 1997). The technical documentation for SIMAP is in French McCay (2003; 2004; 2009).

Applications for SIMAP include impact assessment, hindcast/forecast of spill response, Natural Resource Damage Assessment, contingency planning, ecological risk assessment, cost-benefit analysis, and drills and education. The model may be run for a hindcast/forecast of a specific release, or be used in stochastic mode to evaluate the probable distribution of contamination. SIMAP contains several major components:

- The physical fates model estimates surface distribution and subsurface concentrations of the spilled oil and its components over time.
- The biological effects model estimates impacts resulting from a spill scenario on fish, invertebrates, wildlife, and for each of a series of habitats (environments) affected by the spill.
- The probability of impact from an oil discharge is quantified using the three-dimensional stochastic model.
- Currents that transport contaminant(s) and organisms are entered using the graphical user interface or generated using a (separate) hydrodynamic model. Alternatively, existing current data sets may be imported.
- Environmental, chemical, and biological databases supply required information to the model for computation of fates and effects.
- The user supplies information about the spill (time, place, oil type, and amount spilled) and environmental conditions (such as temperature and wind data).

As with RPS ASA's other modeling systems, SIMAP is easily applied to a wide variety of conditions. It is set up and runs within RPS ASA's standard GIS or ESRI's ArcView GIS, and can be applied to any aquatic environment (fresh or salt) in the world. It uses a variety of hydrodynamic data file formats (1-, 2- and 3-dimensional; time varying or constant) and allows 2-D vertically-averaged current files to be created within the program system when modeled currents are not available. Outputs include easily interpreted visual displays of dissolved and particulate (oil droplet) concentrations and trajectories over time. The biological exposure model evaluates areas and volumes exposed above concentrations of concern and predicts the potential impacts on exposed fish and wildlife.

SIMAP specifically simulates the following oil fate processes:

- Oil spreading (gravitational and shearing);
- Transport and vertical and horizontal dispersion;

- Emulsification
- Entrainment (natural and facilitated by dispersant);
- Dissolution;
- Evaporation and volatilization (to atmosphere);
- Transport and dispersion of entrained oil and dissolved aromatics in the water column;
- Adsorption of entrained oil and dissolved aromatics to suspended sediments;
- Sedimentation and re-suspension;
- Natural degradation;
- Tarball formation;
- Interactions with mobile sea ice and immobile landfast ice;
- Shoreline entrainment; and
- Oil spill response (e.g., mechanical containment/recovery, dispersant application, *in situ* burning).

3.0 MODELING APPROACH

SEC's general approach was to use the OILMAP Deep and SIMAP modeling systems to estimate potential oil spill impacts on the environment (i.e., the water column, shoreline, and water surface) for a variety of subsurface and surface spill scenarios. The subsurface blowout scenarios (scenarios 1 and 2) were evaluated on two spatial scales, the near-field and the far-field. The near-field modeling in OILMAP Deep describes the oil/gas plume generated by the blowout that is driven mainly by vertical processes (momentum and relative buoyancy). The far-field analysis then predicts the long term transport and weathering of the released oil mixture, a process driven primarily by environmental conditions (e.g., winds, currents). Far-field modeling in SIMAP consisted of both stochastic (probabilistic) and deterministic approaches.

3.1 Blowout Near-Field Modeling

To reproduce near-field dynamic and complex processes associated with the subsurface blowout scenarios, a near-field analysis using OILMAP Deep was performed prior to simulating the far-field movement of the oil with SIMAP. The objective of this first step in modeling was to characterize the plume mixture (oil, gas and water) discharged in the vicinity of the wellhead (Figure 2). In most blowout cases, this near-field region occurs within a few hundred meters of the wellhead.

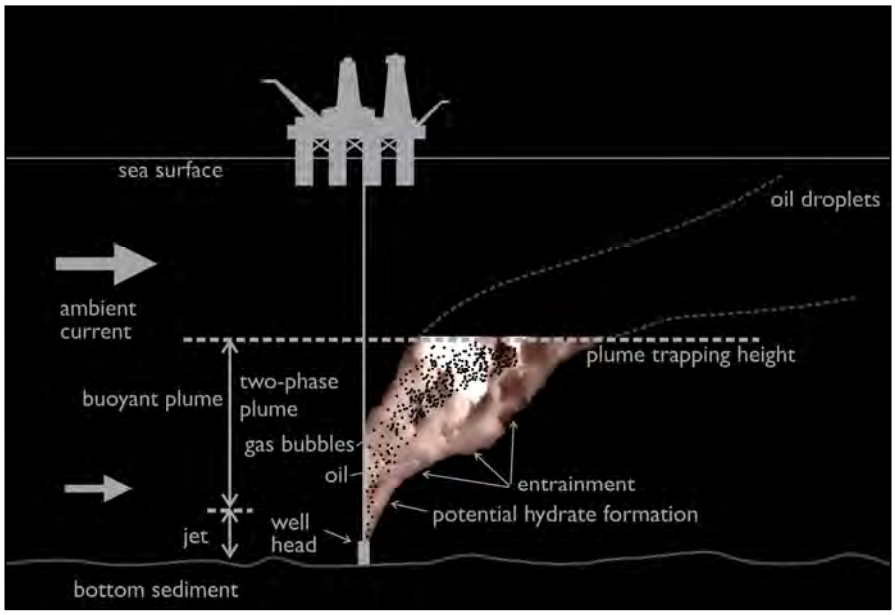

Figure 2. General schematic showing profile and associated characteristics of a deep well blowout.

3.1.1 Description of a Blowout

In a subsurface well blowout, discharged materials consisting of a mixture of gaseous and liquid hydrocarbon go through three phases: momentum jet, buoyant density plume, and free rise and advection/diffusion.

1) Momentum jet

The immediate pressure difference between inside the well and the ambient water drives the discharge. Due to the high-density of the deep ocean water, this jet momentum dissipates quickly and is confined to the vicinity of the seabed (on the order of meters).

2) Buoyant density plume

As the discharge moves upward, the density difference between the expanding gas bubbles in the plume and the receiving water results in a buoyant force which drives the plume. As the plume rises, it continues to entrain sea water, reducing the plume's velocity and buoyancy and increasing its radius.

The oil in the release is rapidly mixed due to turbulence in the plume, resulting in a break up into small droplets. These droplets (typically a few micrometers to millimeters in diameter) are transported upward by the rising plume; their individual rise velocities contributing little to their upward motion.

3) Free rise and advection-diffusion

As the plume reaches the sea surface or its termination height (when all momentum is lost), it can be deflected in a radial pattern within a horizontal/surface flow zone without appreciable loss of momentum. This radial jet carries the oil particles rapidly away from the center of the plume, while the velocity and oil concentrations in this surface flow zone decrease.

Subsequently, oil particles ascend to the surface solely by their own buoyancy. Rise velocities of oil droplets are much slower than the velocity of a buoyant gas-liquid plume, resulting in particle transport that may take considerably longer to reach the surface and result in transport farther (horizontally) from the release site due to ambient currents.

3.1.2 Blowout Near-field Modeling Approach

The key inputs to the near-field model include flow rate, gas-to-oil ratio (GOR), aperture or pipe diameter, and a vertical profile of water temperature and density.The near-field modeling results provide a description of the plume characteristics, including the plume location (namely plume trap height), plume geometry, and the oil droplet size distribution. The results of the near-field model are then used to provide the initial conditions for the stochastic and deterministic far-field modeling in SIMAP, including:

- Termination height (trap height) of the plume;
- Diameter of the plume; and
- Oil droplet size distribution.

The characterization of the plume height and radius may be helpful information for oil spill responders, as it aids in determining the area with the highest concentration of oil in a dispersed/dissolved form. In the near-field plume, during the jet momentum and buoyant density plume phases, concentrations of oil are the highest. After the oil leaves these phases, oil droplets begin to rise under their own buoyancy and are transported away from the discharge by advection

and diffusion, both vertically and horizontally. Therefore, any sort of subsurface collection of the oil or application of dispersants would likely be most effective within the defined dimensions of the plume.

The oil droplet size distribution has a profound effect on how oil is transported after the initial plume, as the size dictates how long the oil droplet will remain suspended in the water column. Large droplets will reach the surface faster, potentially generating a floating oil slick that will drift with surface winds and currents. Small droplets will remain in the water column longer and be subjected to subsurface advection-diffusion transport. As the oil is transported by subsurface currents away from the well site, natural dispersion of the oil droplets quickly reduces hydrocarbon component concentrations in the water column, with decreasing concentration at increasing distance away from the well site. However, lower rise velocities of the oil droplets correspond to longer residence times of oil suspended in the water column and thus a larger volume of affected water.

From a response perspective, a turbulent blowout that results in the formation of very small oil droplets essentially acts as a natural dispersion mechanism, as these smaller size particles effectively keep the oil from surfacing. On the other hand, with large particle sizes, there will be quick surfacing of oil which will limit the subsurface volume exposed to oil, but result in a larger surface oil slick.

3.2 Far-field Modeling

RPS ASA's 3-D oil spill modeling system, SIMAP, was used for all far-field simulations performed in this study.

3.2.1 Stochastic Modeling Approach

For each of the eight spill scenarios, SIMAP's stochastic model was used to determine the range of distances and directions oil spills are likely to travel from the spill sites, and the associated probabilities. The stochastic modeling approach uses multiple model runs (typically 100 or more) of the same spill event to characterize the probable consequences of a spill scenario under typical yet varying environmental conditions. Each individual trajectory is randomly assigned a different start date/time. Individual trajectories are computed in SIMAP for each of these start dates/times, thereby sampling the variability of meteorological and oceanographic conditions in the study area (and the resulting variability in the transport of spilled oil). By statistically evaluating all of these individual trajectories together, the outputs of the stochastic model provide a variety of information, including:

- The probability of exceeding consequence thresholds of concern (surface, shore, water column);
- The footprint of water surface and shoreline areas that may be oiled (and associated probability); and
- Minimum travel times.

For this study, the stochastic analysis for most of the eight spill scenarios consisted of 200 individual model runs. The only exception was the two 34-day blowout scenarios (scenarios 1B and 2B), which utilized 120 individual model runs due to file size and computational limitations.

The following figures illustrate the stochastic modeling process for an example spill scenario. The left panel of Figure 3 shows four individual trajectories predicted by SIMAP for the example scenario. Because these trajectories started on different dates/times, they were exposed to varying environmental conditions, and thus traveled in different directions. To compute the stochastic results, all 100+ individual trajectories (like the four shown) are overlain and the number of times that a given location is reached by different trajectories is used to calculate the probability of oiling for that location. This is shown as the stacked runs in the right panel of Figure 3. One of the main outputs of this process is the stochastic "footprint," as shown in the generic example in Figure 4. It is important to note that a single trajectory/spill would encounter only a relatively small portion of this footprint, and that this figure does not depict the areal extent of a single trajectory/spill.

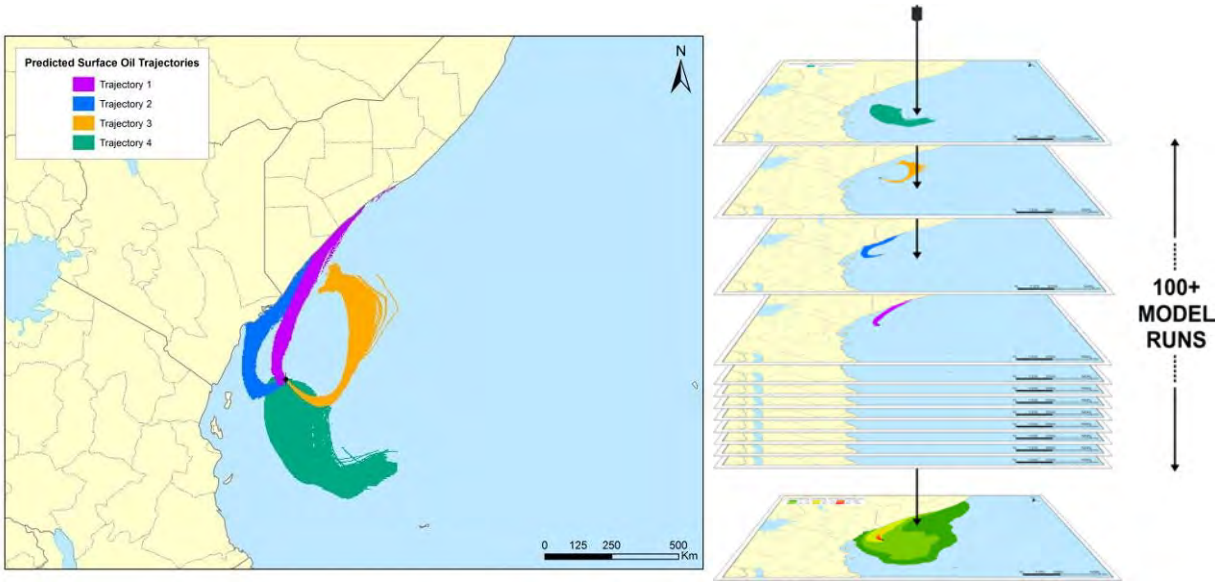

Figure 3. Examples of four individual spill trajectories predicted by SIMAP for a generic spill scenario. All 100+ individual trajectories are overlain (shown as the stacked runs on the right), and the frequency of contact with given locations is used to calculate the probability of impacts during a spill.

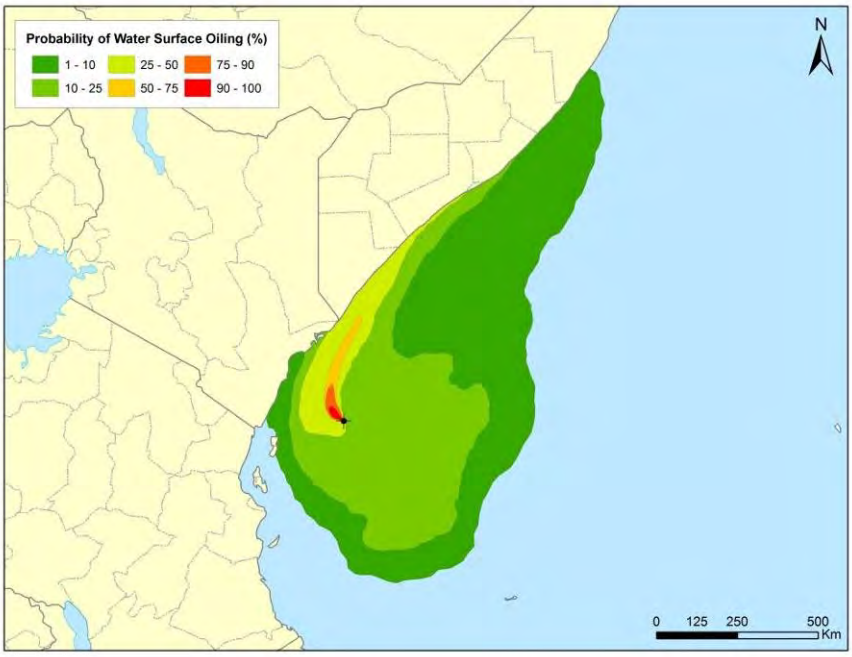

Figure 4. Probability of surface oil exceeding a given threshold for the example scenario. This figure overlays 100+ individual model runs to calculate the percentage of runs that caused oiling above the threshold in a given area. This figure does not depict the areal extent of a single trajectory/spill.

3.2.2 Deterministic Modeling Approach

While the stochastic analysis provides insight into the probable behavior of oil spills given historic wind and current data for the region, it does not provide detailed oil weathering information or mass balance for individual spill events. Therefore, for the second phase of the study, individual 3-D or "deterministic" trajectories were rerun in SIMAP to produce fates and weathering information for particular runs selected from the stochastic scenario based on pre-defined criteria. Different parameters or criteria can be used to select individual trajectories for deterministic analysis. For example, deterministic trajectories can be "representative" or "worst-case" for a variety of consequence metrics (e.g., shoreline length oiled, time to shore, volume of oil ashore, water column contamination, water surface area swept). The selection criteria for each spill scenario varied depending on WWF-Canada's goals and objectives, and are described in the sections corresponding to each individual spill site (Sections 5.0 through 9.0).

The results of the deterministic simulations provide additional graphical and numerical data describing the trajectory, as well as a time history of oil weathering over the duration of the spill (mass balance).

3.3 Modeling Oil Interactions in Ice

Oil interactions with mobile sea ice or immobile landfast ice involve several processes that affect transport and fate of the oil. If oil is released at or above the water surface, it may spill into water and/or onto the surface of the ice. Oil deposited on ice may absorb into surface snow, run off and become trapped between cracks or in open water fields between floes, and/or become encapsulated in the ice. Oil released into and under water may become trapped under the ice in ridges and keels, or build up along and become trapped in sea or landfast ice edges (Figure 5) (Drozdowski et al., 2011). Many of these interactions and processes are at a finer scale than can be captured in oil spill models using inputs from large scale meteorological, hydrodynamic, and coupled ocean-ice models. However, the influence of ice on net transport and fate processes is simulated in SIMAP by considering the potential reduction in the surface area of the oil and the water in contact with the atmosphere, which changes the wave environment, spreading, movements, volatilization, and mixing. Oil-ice interactions modeled in the stochastic and deterministic simulations are described in the following sections.

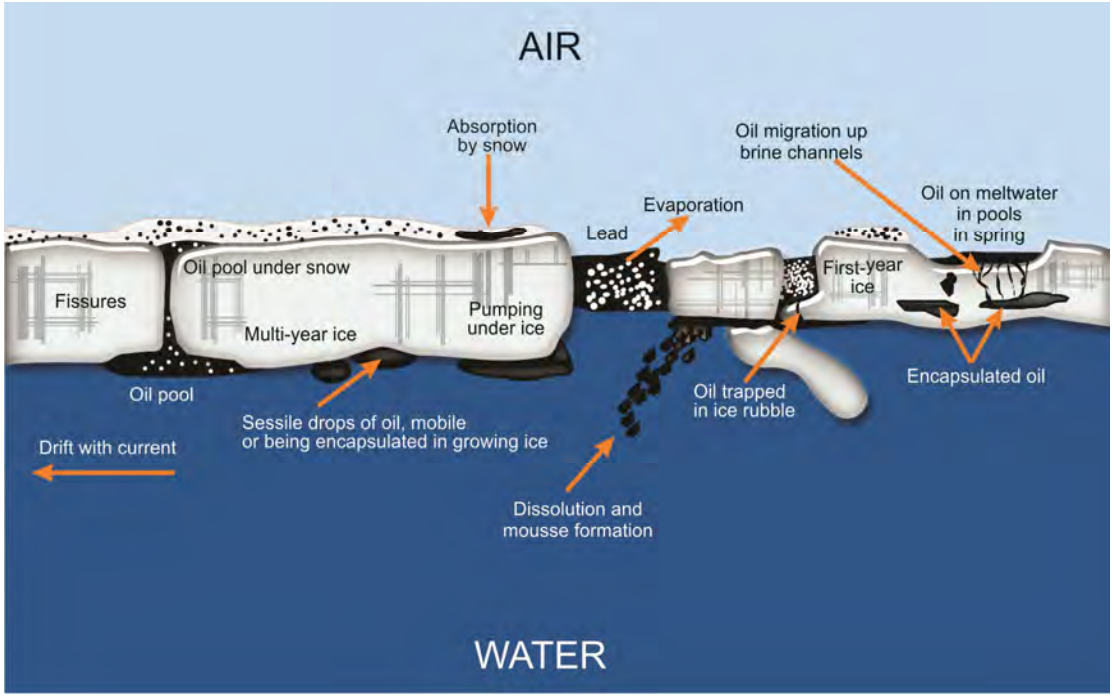

Figure 5. General schematic showing dynamics and characteristics of sea ice and oil interaction at the sea surface. (Source: Original figure by Alan A. Allen).

3.3.1 Oil Transport in Sea Ice

When oil interacts with mobile sea ice, some fraction of that oil will become contained (either on top, in, or underneath the ice) and will then travel with the ice floe (Drozdowski et al., 2011). Sea ice fields can drift rapidly and over great distances in the Arctic (Peterson et al., 2008). The fraction of oil moving with the ice versus in open water depends on the conditions and specifics of the release. In some cases, all of the oil becomes completely trapped in the ice and remains there until it melts. This scenario is readily modeled (i.e., 100% of oil drifts with ice). However, since sea ice can be patchy, only partial amounts may become either encapsulated or trapped (e.g., between ice fragments or under ice sheet in small cavities), depending on ice coverage, subsurface roughness, winds and currents, and ice formation/melting dynamics (Drozdowski et al., 2011).

To simplify the problem, the ice coverage or concentration information provided by the ice data or model can be used as an indicator of whether oil is transported by the surface currents or the ice currents. Ice coverage information available in coupled hydrodynamics and ice models typically comes from remotely sensed satellite data. A rule of thumb followed in past modeling studies is that oil will generally drift with ice when ice coverage is greater than 30% (Drozdowski et al., 2011; Venkatesh et al., 1990).

When a coupled ocean-ice model is available and provides currents and ice velocities, the SIMAP model uses the ice coverage data to determine whether floating (or ice-trapped) oil moves with the surface water currents or the ice. If the ice coverage is less than 30%, the oil is assumed not to be trapped and thus moves with surface water currents. If ice coverage exceeds this

threshold, the ice is assumed to have ample spatial coverage to trap the oil in it or between floes, and oil is transported along with the ice using the ice velocities from the coupled ocean-ice model.

To simulate oil transport in this study, the TOPAZ4 coupled ocean-ice model (described in Section 4.1.2) was used in SIMAP to provide sea ice coverage, ocean currents, and the ice currents or ice velocities.

3.3.2 Oil Interaction with Landfast Ice

Immobile or fixed landfast ice, which seasonally extends out from the coast, may act as a natural barrier where oil collects. The ice edge is complex with ridges, keels, cracks and crevices where oil can become trapped. During landfast ice melt, oil that has been stored along the edge may either release back into open water or may retreat back with the ice towards the coast (Drozdowski et al., 2011).

In the SIMAP model, when oil encounters landfast ice at the surface of the ocean it is assumed to trap along the ice edge and remain immobile until the ice retreats. When landfast ice is no longer present at the trapped oil's location, the oil is released back into the water as floating oil. In areas deep enough for landfast ice to have subsurface open channels (i.e., where the ice sheet may not extend completely to the seabed), entrained oil is allowed to circulate underneath the surface ice using subsurface current data for transport. Monthly representations of the landfast edge along the entire coast (capturing average growth and retreat patterns) were prepared as data inputs to the model (Section 4.1.3).

3.3.3 Effects of Ice on Oil Fates and Behavior Processes

The presence of ice can shelter oil from the wind and waves (Drozdowski et al., 2011). Thus, weathering processes such as evaporation and emulsification, and behaviors such as spreading and entrainment, are slowed (Spaulding, 1988). Field data show evaporation, dispersion, and emulsification significantly slowed in ice leads, contrary to some laboratory experiments. Wave-damping, the limitations on spreading dictated by the presence of sea ice, and temperature appear to be the primary factors governing observed spreading and weathering rates (Sørstrøm et al., 2010).

As with transport, the ice coverage or concentration variable provided in the ice model is used as an index to control oil weathering and behavior processes (Table 2). Oil behaves as it would in open water when ice coverage is less than 30%. Ice coverage exceeding 80% is assumed to be fast (pack) ice and effectively continuous ice cover. Evaporation and volatilization of oil under/in ice, as well as spreading, emulsification, and entrainment into the surface water are halted in pack ice. Oil spilled on top of pack ice is allowed to evaporate, but does not spread from the initial condition of the release. Dissolution of soluble aromatics and oil degradation proceeds for subsurface oil and oil under ice using the normal open-water algorithms (French McCay, 2004).

In ice coverage between 30% and 80%, a linear reduction in wind speed from the open-water value (<30% ice coverage) to zero in pack ice (>80% ice coverage) is applied to simulate shielding from wind effects. This reduces the evaporation, volatilization, emulsification, and entrainment rates due to reduced wind and wave energy. Terminal thickness of oil is increased in proportion to ice coverage in this range (i.e., oil is thickest at >80% ice coverage).

Table 2. Percent ice coverage thresholds for oil fates and behavior processes applied in the SIMAP model.

Ice Cover (Percent)	Advection	Evaporation & Emulsification	Entrainment	Spreading
0 – 30 (Drift Ice)	Surface oil moves as in open water	As in open water	As in open water	As in open water
30 – 80 (Ice Patches and Leads)	Surface oil moves with the ice	Linear reduction with ice cover to zero at 80% ice cover	Linear reduction with ice cover to zero at 80% ice cover	Terminal thickness increased in proportion to ice coverage
80 – 100 (Pack Ice)	Surface oil moves with the ice	No evaporation or emulsification	No entrainment	No spreading

Assumptions applied to fates and behavior processes of oil in ice are not well quantified by field experiments or other studies. Also, the coupled ocean-ice models available to date do not resolve the details of leads, fractures, and ice roughness. This presents a major modeling limitation. The applied ice coverage thresholds (i.e., the discrete bands of 0 to 30, 30 to 80, and 80 to 100 percent cover) may not accurately reflect the fate of oil in real ice cover, particularly at fine scales.

4.0 DATA INPUTS

The environmental and physical data inputs used in the modeling are described in the following sections.

4.1 Currents and Ice

4.1.1 Regional Overview

Baffin Bay is a marginal sea of the North Atlantic Ocean located between Baffin Island and the southwest coast of Greenland that connects the Arctic Ocean and the Northwest Atlantic. Baffin Bay is around 1,400 km by 550 km in size, with the deepest depths in the central region over 2,300 m (Tang et al., 2004). The continental shelf is relatively narrow and is deeply cut by canyons running across the shelf. In the south, Baffin Bay is connected to the Labrador Sea, and thus to the Atlantic, by the Davis Strait. This is the deepest channel, with depths of 650 m and a width of 320 km at 66.25°N (Tang et al., 2004). Baffin Bay's connection to the Arctic is more restrictive with three relatively small passages through the Canadian Arctic Archipelago islands, including Lancaster Sound, Jones Sound, and Nares Strait, with sill depths around 125, 190 and 220 m, respectively. The Nares Strait is only 25 km wide (Münchow et al., 2013).

The two main features of Baffin Bay circulation are the cold and buoyant near-surface Baffin Island Current (BIC) and the warm and salty sub-surface West Greenland Current (WGC) (Figure 6). The BIC advects Arctic ice, water, and coinciding water characteristics southward towards Davis Strait, while the WGC advects Atlantic water northward towards Cape York in northern Baffin Bay (Münchow et al., 2013). The broad, surface intensified BIC is formed by the cold Arctic water that flows southward through the Nares Strait, Jones Sound, and Lancaster Sound. The BIC flows southward along the east coast of Baffin Island and into the western half of Davis Strait, which eventually feeds the Labrador Current (Hamilton and Wu, 2013). The WGC originates where the cold, Arctic East Greenland Current (EGC) is joined by the warm, saline Irminger Current (Hamilton and Wu, 2013). The WGC flows northward along the west Greenland coast, and transports both the cold, fresh Arctic water northward as a continuation of the EGC and the relatively warmer and salty waters from the Irminger Sea. The fresh Arctic water that enters the eastern side of Davis Strait continues northward along the west Greenland slope as far north as 78°N before turning west to join the BIC. Most of the Irminger Sea water circulates counterclockwise around the northern Labrador Sea, though a portion continues northward along the slope into Baffin Bay as a continuation of the WGC (Hamilton and Wu, 2013). This cyclonic rotation transports heat and salt into northern Baffin Bay, and colder and fresher water southward. The variations of currents with depth, season, and region are complex, but there are some evident trends. Currents throughout the water column area stronger during summer and fall than during winter and spring. One of the regions with the largest seasonal variation occurs at the mouth of Lancaster Sound and the Baffin Island slope (Tang et al., 2004).

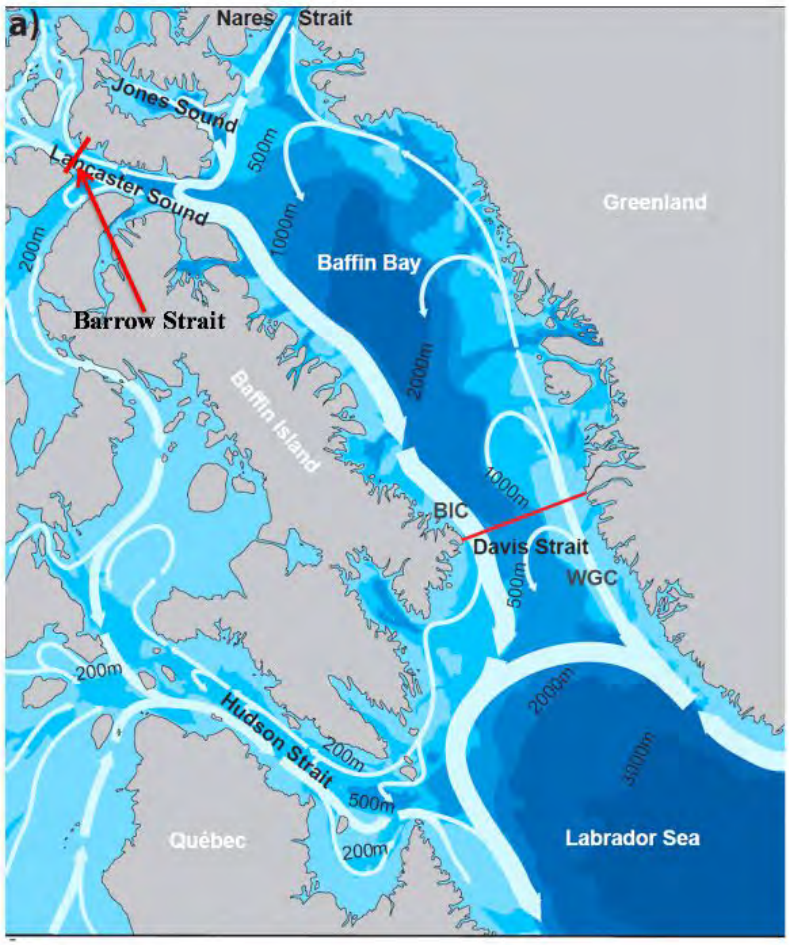

Figure 6. Schematic of general circulation in the Baffin Bay region (Source: Hamilton and Wu, 2013).

Baffin Bay is partially covered by sea-ice throughout the year, except for the months of August and September (Tang et al., 2004). Ice begins to form in open water in September and increases steadily in coverage until March, where the entire bay except eastern Davis Strait is covered by ice. The western half of Baffin Bay always has more ice cover than the eastern half due to the inflow of the relatively warm WGC on the eastern side. The ice coverage begins to decrease in April, and by July, less than half of the area is covered by ice (Tang et al., 2004).

Observational ice velocity data is scarce in Baffin Bay. A typical ice velocity in winter and early spring is 10 cm/s in the southern part of Baffin Bay. In Davis Strait, ice velocity is higher, around 20 to 30 cm/s, and decreasing to 10 to 15 cm/s along the Baffin Island coast toward Hudson Strait (Tang et al., 2004). Ice thickness varies spatially as well. Ice thickness from satellite images indicate that the ice field in Baffin Bay is a combination of first-year medium (0.7–1.2 m), first-year thin (0.3–0.7 m), young ice (0.1–0.3 m) and new ice (0–0.1 m) (Tang et al., 2004). The dominant thickness is first-year medium ice, and only a small amount of multi-year ice drifts into Baffin Bay from Nares Strait and Lancaster Sound. A distribution map of mean ice thickness produced by J.E. Markham (Valeur et al., 1996) showed that the mean thickness of level ice

decreased from 1.75 m in the northwest, to less than 0.75 m in the southeast. The mean thickness along the coast of Baffin Bay was 1.25–1.5 m.

In regions where sea ice persists, there are important oceanographic features known as polynyas. Polynyas are areas of open water surrounded by ice (Sterling, 1980). In the Canadian Arctic, the largest and best known polynya is the North Water Polynya (Figure 7). Polynyas can be caused by numerous factors, such as currents, tidal fluctuations, wind, upwelling, or a combination of these. Polynyas are important for various reasons. They are a source of heat and moisture to the atmosphere, thus affecting the weather in the surrounding areas. In addition, they are important to Arctic birds and wildlife for feeding, reproduction and migration. Since polynyas persist for a sustained period of time, and due to upwelling bringing nutrients to the surface, phytoplankton thrive in polynyas. The North Water Polynya is thought to be a latent heat polynya driven by a persistent north wind and south-flowing current (Melling et al., 2001). A latent heat polynya is classified as being formed at locations where persistent winds and currents carry newly formed ice away from a shoreline or stable ice edge. The conditions that create latent heat polynya also promote upwelling and mixing. The upwelling brings heat to the surface, thereby decreasing albedo (reflective power), and further increasing the absorption of solar radiation at the surface. The North Water Polynya is closely connected to Lancaster Sound, Baffin Bay, and Melville Bay due to the regional ocean current system. The WGC runs parallel to the coastline, moving warm and salty Atlantic water north to the North Water Polynya. Upwelling of warmer water in this polynya helps keep the area partially ice-free throughout the year, even when the surrounding areas are frozen (Sterling, 1980). The North Water Polynya evolves seasonally from a relatively small area in winter to a larger area of ice-free water in June and in summer ceases to exist as a distinct ice-free boundary within the Baffin Bay. The North Water Polynya region is fed by the cold inflow of the Arctic Ocean that flows southward through the Smith Sound and by a warmer inflow of water from the southeast that is derived from the WGC (Sadler, 1976; Mueller et al., 2010).

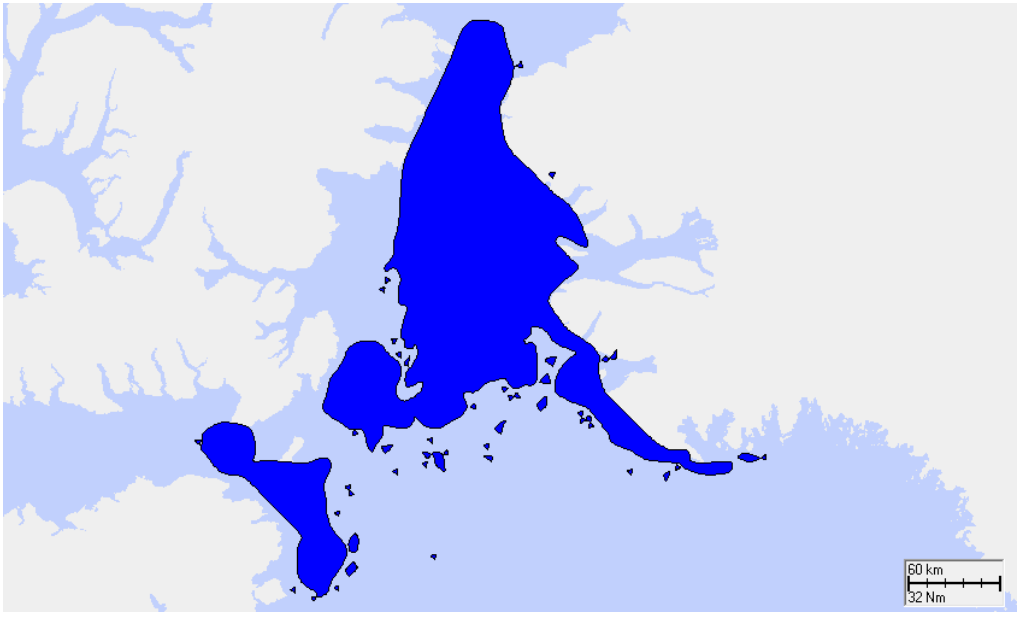

Figure 7. Approximate extent of the North Water Polynya is shown in dark blue. Data provided by WWF-Canada.

4.1.2 Currents and Sea Ice Dataset

In order to reproduce the natural variability of ocean currents and sea ice in the study area, the SIMAP model requires spatially- and temporally-varying input data. The favored approach is to use actual historically-observed currents and ice data and perform the model simulations over a time period coincident with the observations. Since site-specific long-term historical observations are often not available, the alternative is to use long-term records of data from the outputs of an ocean circulation model.

For this study, the TOPAZ4 long-term coupled ocean-sea ice circulation dataset for the Arctic Ocean was used to provide the necessary current and sea ice data. The TOPAZ4 dataset is a coupled ocean-sea ice data assimilation system for the North Atlantic and the Arctic. The dataset was developed by Nansen Environmental and Remote Sensing Center (NERSC) and is publically available through the Norwegian Meteorological Institute. TOPAZ4 incorporates the hybrid coordinate ocean model (HYCOM, version 2.2) (Bleck, 2002) coupled with a sea-ice model (Hunke and Dukowicz, 1997), and a 100-member ensemble Kalman filter (EnKF) (Evensen, 1994) assimilating both *in situ* observations and satellite data. Wind stress for the TOPAZ4 model is from the ERA-40 (ECMWF RE-ANALYSIS) wind model (described in Section 4.2.2). TOPAZ4 is the only operational, large-scale, eddy-resolving ocean data assimilation system that uses a deterministic formulation of the EnKF in the Arctic region. The EnKF assimilates remotely-sensed sea level anomalies, sea surface temperature, sea ice concentration, Lagrangian sea ice velocities, as well as temperature and salinity profiles from Argo floats. From the results of a 6-year pilot reanalysis, TOPAZ4 has been shown to produce a realistic estimate of the mesoscale ocean circulation in the North Atlantic, as well as the sea ice variability within the Arctic (Sakov et al., 2012).

In the implementation of HYCOM for the TOPAZ4 system, the vertical coordinate is isopycnal in the stratified open ocean and z-coordinate in the unstratified surface mixed layer (Sakov et al., 2012). HYCOM was found to be the most suitable model for the large-scale Arctic water masses that span the stratified open ocean, regions of steep topography, and extensive sea ice. HYCOM is also flexible in that it provides sigma coordinates in coastal regions. However, sigma coordinates were not adopted because resolving coastal areas was not a primary objective of the TOPAZ4 project.

The model domain covers the North Atlantic and Arctic Ocean basins (Figure 8), including the area of interest for this study (Figure 9). The model grid is horizontal and created by a conformal mapping with the poles shifted to the side of the globe. This allows for a quasi-homogeneous grid size (Bentsen et al., 1999, Sakov et al., 2012). The model grid has 880 x 800 horizontal grid points and with horizontal spacing of approximately 12-16 km in the open ocean (about 12.5 km at the north pole, equivalent to 1/8 degree). There are 28 hybrid layers (or z layers) in the vertical from the surface to a depth of 5,500 m. Z-layer thickness can range from a minimum of 3 m to a maximum of 450 m (to resolve the deep mixed layer of the sub-polar gyre). The model bathymetry is based on the General Bathymetric Chart of the Oceans database (GEBCO) at 1-min resolution (GEBCO, 2009).

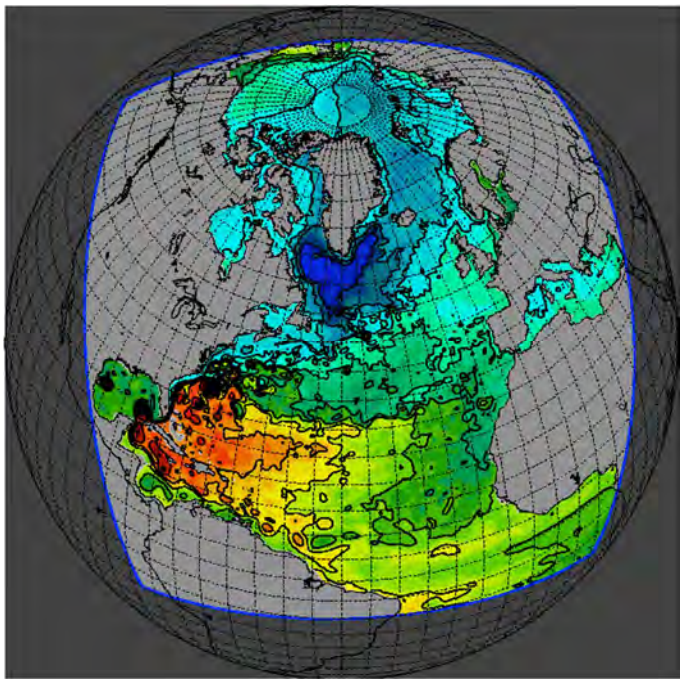

Figure 8. The entire domain of the outer model of TOPAZ4 Arctic and Atlantic Oceans. Coloration shows a snapshot of sea surface height. (Source: Samuelsen and Bertino, 2013).

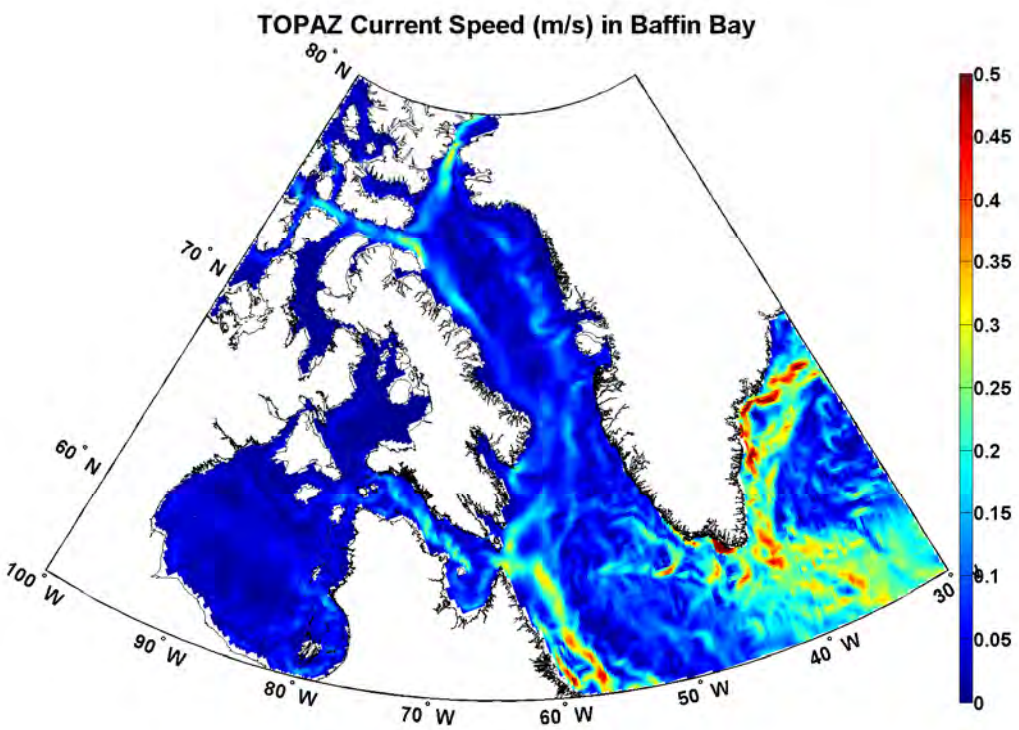

Figure 9. Example current speed output from the operational version of TOPAZ4 showing the dataset's coverage in the area of interest.

TOPAZ4 is coupled with a sea-ice model based on elastic-viscous-plastic (EVP) rheology (Hunke and Dukowicz, 1997). EVP is the standard fluid dynamics model used to predict the behavior of free moving sea ice. The EVP treats pack ice as a visco-plastic material that flows plastically under typical stress conditions, but behaves as a linear viscous fluid where strain rates are small and the ice becomes nearly rigid (Hunke and Dukowicz, 1997). Predicted currents and wind stress, together with the EVP accounting for behavior, are used to derive modeled sea ice velocities. These ice currents are then assimilated with remotely-sensed sea ice concentration (CRESAT) and Lagrangian sea ice velocities using the EnKF. For more information, refer to Sakov et al. (2012) for detailed documentation of the complete TOPAZ4 Data Assimilation System.

The TOPAZ4 reanalysis long-term dataset provides monthly mean data from 1991 to 2010, whereas daily mean data from 2011 to present is available through the operational TOPAZ4 system. Overall, temporal and spatial data quality was found to be highest for 2011-present. Data from both the reanalysis and operational versions of TOPAZ4 are available at http://myocean.met.no/.

Daily mean 3-dimensional current speed and direction, surface sea ice drift speed and direction, ice thickness, and ice coverage fraction were acquired from the TOPAZ4 operational system and processed for October 2011 to October 2015. Only a subset of the Arctic grid was retrieved for the region of interest. The geographical coordinates of the subset are approximately 46°N to 87°N, and 134°W to 40°W.

Raw TOPAZ4 data was provided using a polar stereographic projection with velocity vectors orthogonal to the curvilinear grid. An inversion projection was applied to transform the coordinates of the grid into latitude and longitude. The raw velocity data was transformed using an inverse polar stereographic vector projection for an eastward northward reference frame for the SIMAP model.

4.1.3 Landfast Ice Dataset

Landfast ice coverage was available for the study area from the National Snow and Ice Data Center (NSIDC) (Konig Beatty, 2007; 2012). Monthly data from the years 1991 through 1998 were composited into mean monthly landfast ice coverage. This dataset includes ice concentration percentages for each raster cell. Cells with a concentration of greater than 15% were considered to have landfast ice. This concentration level is based on a comparative analysis of the lower resolution NSIDC dataset with a higher resolution landfast ice dataset for the north slope of Alaska (Mahoney et al., 2012). This analysis determined that 15% is a reasonable value for defining landfast ice cover in the lower resolution NSIDC dataset (Schroeder Gearon et al., 2014).

The resulting dataset of monthly mean landfast ice coverage has a resolution of 0.2 degrees by 0.2 degrees. A snapshot of the monthly mean landfast ice coverage data is shown in Figure 10. The resolution and age (i.e., 1991-1998) of the dataset is not ideal; however, at the time of this study it was the best dataset available in a format that could be processed for use in the oil spill modeling software.

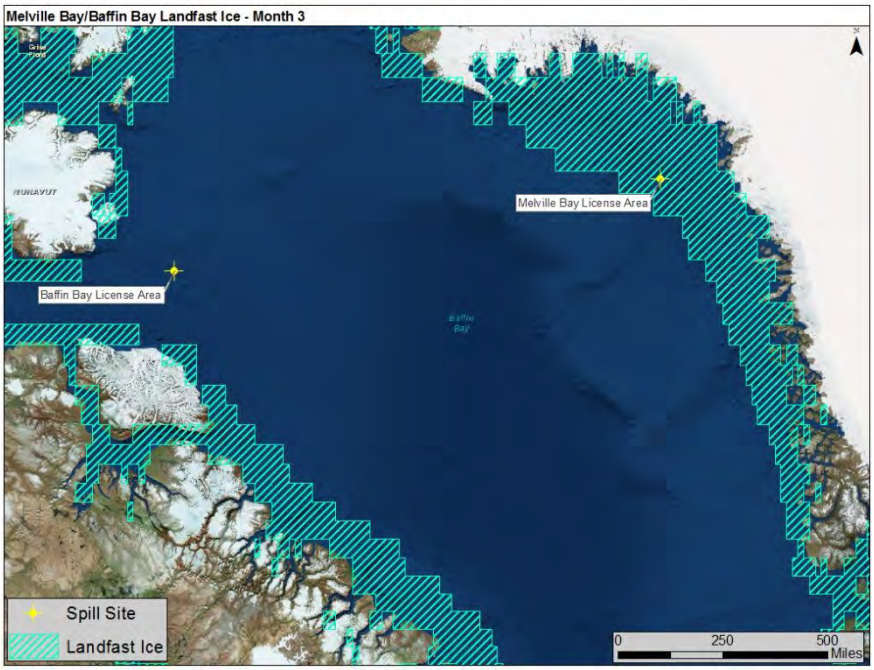

Figure 10. Snapshot of the monthly average landfast ice cover data used in modeling. Data displayed is for the month of March.

4.1.4 Eclipse Sound Tidal Currents Model

The TOPAZ4 data do not include complete coverage of the geographic complexity of Eclipse Sound and its associated inlets. In order to reproduce tidal currents and provide additional currents data coverage, RPS ASA's HYDROMAP model was used to perform hydrodynamic simulations in the Eclipse Sound region. HYDROMAP is a globally re-locatable three-dimensional hydrodynamic model (Isaji et al., 2001a; 2001b) capable of simulating complex circulation patterns due to tidal forcing, wind stress, and fresh water flows. This model has been applied in numerous transport studies in the U.S. and worldwide.

HYDROMAP employs a novel step-wise-continuous-variable rectangular gridding strategy with up to six levels of resolution. The term "step-wise continuous" implies that the boundaries between successively smaller and larger grids are managed in a consistent integer step. The numerical solution methodology follows that of Owen (1980). HYDROMAP incorporates a spatially-variable global tidal database characterization of tidal constituents for use in specifying water surface elevation (tidal) boundary conditions. Alternatively, boundary specific water level records can be used to generate water surface elevation boundary conditions. HYDROMAP creates harmonic models that are not time-stamped.

The study area was represented by HYDROMAP's 2-step nested grid system with the coarser, outer grid having a resolution of approximately 2 km, and the finest grid system having a resolution of 0.45 km (Figure 11). The geographical coordinates of the HYDROMAP grid are approximately 69.7°N to 71.6°N, and 87.6°W to 75.3°W. At the boundary, 8 tidal harmonic components (M2, K2, N2, S2, P1, O1, Q1, K1) from the TPXO global tide database (Egbert and

Erofeeva, 2002) were applied. The simulation time step was 5 minutes. In the model simulation, tidal currents from HYDROMAP were merged with TOPAZ4 currents data where overlap occurred.

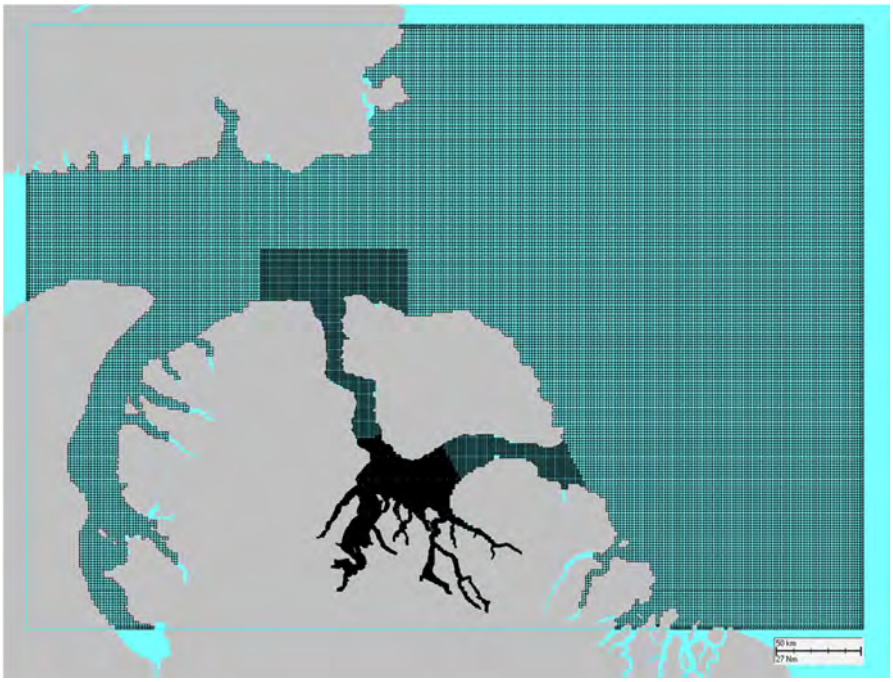

Figure 11. HYDROMAP grid for the vicinity of Eclipse Sound, showing the varying resolutions of the nested grid.

While the supplementary currents file generated from HYDROMAP provides the necessary current forcings to run the model, it does not provide coupled sea ice data. To incorporate sea ice into areas lacking TOPAZ4 data coverage, GIS polygons were created in data gap areas to represent average sea ice coverage. The coverage values for these polygons were based on the monthly average sea ice coverage from nearby TOPAZ4 data.

4.2 Winds

4.2.1 Regional Overview

Baffin Bay meteorological conditions are primarily influenced by the North American and Greenland land masses, local sea-ice and ocean conditions, and the Arctic atmospheric system. Baffin Bay is north of the westerlies and the zone of cyclonic activities. The climate is characterized by high east-west gradients during winter, while summer temperatures are nearly uniform across the region (Tang et al., 2004). January is the coldest month, with temperatures as low as -35°C, while the warmest temperatures occur in July. Air temperatures vary greatly during winter (January, February, March), with average temperatures of -28.6°C. This variability of temperature contributes to the sea-ice variability. In addition, wind stresses over Baffin Bay differ seasonally. From January to April there are weak stresses in central and northern Baffin Bay, and strong stresses at Davis Strait and in the Northern Labrador Sea (Tang et al., 2004). In winter, the strong wind stresses are a major factor in moving sea-ice from Baffin Bay to the Labrador Sea. Between April and May, there is a rapid decline in wind stress that lasts through August. September to October is the transition period between summer and winter conditions.

4.2.2 Wind Dataset

As for ocean currents data, the favored approach for wind data is to use actual historically-observed winds. Since site-specific long-term historical observations of winds are often not available for large geographic study areas, the alternative is to use long-term records from the outputs of an atmospheric model.

For this study, wind data was obtained from the ERA-40 (ECMWF RE-ANALYSIS) wind model. This model was developed and is operated by the European Center for Medium-range Weather Forecast (ECMWF). This model has global domain coverage with 0.75° resolution. A long-term (January 2011 to August 2015) gridded wind data record was extracted from the ECMWF database (http://www.ecmwf.int/products/data/archive/descriptions/e4/) and processed into a file format compatible with the SIMAP modeling system. This dataset contains 3-hourly (8 times a day) wind speed and direction readings at all grid nodes included in the region of interest.

ERA-40 is the wind forcing dataset that is used in the TOPAZ4 ocean circulation model (see Section 4.1.2). Therefore the ECMWF RE-ANALYSIS wind dataset was the most appropriate choice for use in the oil spill modeling.

4.3 Temperature, Density, and Salinity

A definition of the physical properties of the water column in the area of interest is an important input for oil spill modeling, especially for subsurface releases. Water temperature dictates many physical attributes and weathering processes including the viscosity and evaporation rate of the spilled oil. Temperature and salinity also dictate the density of the surrounding water body, which influences the speed at which entrained oil can re-surface. Similarly, these physical attributes play an important role in the near-field mechanics of a subsurface blowout.

For this study, monthly vertical profiles of temperature, salinity, and density, were obtained from the publicly available World Ocean Atlas 2013 (Boyer et al., 2013). The dataset is compiled and maintained by the U.S. National Oceanographic Data Center. The dataset consists of decades of observations from various global data management projects. The World Ocean Atlas originated from the Climatological Atlas of the World Ocean (Levitus, 1982) and has been updated with new records several times. Records were obtained using a variety of oceanographic instruments from millions of collection stations. After a comprehensive quality control process, the remaining data were averaged yearly, seasonally, and monthly and interpolated to fit a grid with ¼ degree horizontal resolution and up to 33 depth bins.

4.4 Shoreline Geometry and Type

RPS ASA's oil spill models include an oil-shoreline interaction algorithm that is used to estimate the amount of oil that will be retained onshore when oil reaches the coast based on the definition of shoreline type. Shoreline type is an important parameter in understanding the potential oiling in an area. For example, flat sandy beaches typically retain much more oil than steep rocky coast. Oil that cannot be retained on the shore is susceptible to further transport, thereby potentially affecting additional areas.

It was not within the scope of the project to develop detailed characterizations of shoreline type for the study area. Therefore, for the purpose of this study, the entire coast within the model

domain was assigned a default shoreline type of cobble/gravel beach. Table 3 lists the oil holding capacities for some generic beach types.

Table 3. Shore width and oil holding capacities for various generic shoreline types (French et al., 1996).

Type of Shore	Width (m)	Oil Holding Capacity (mm)		
		Oil Viscosity < 30 cSt	Oil Viscosity 30 – 2,000 cSt	Oil Viscosity > 2,000 cSt
Rocky Shore	3	1	2	2
Cobble/Gravel Beach	6	2	9	15
Sand Beach	20	4	17	25
Artificial Shore	0.1	0.01	0.1	0.1

Coastline geometry definition (i.e. distinction of the land and water boundaries) was obtained from the Open Street Map dataset (http://www.openstreetmap.org) for use in this study. The Open Street Map dataset is based on the U.S. National Geospatial-Intelligence Agency's Prototype Global Shoreline Data, which is a satellite-derived approximation of the high water line. The resolution of the dataset is approximately 50 m.

4.5 Bathymetry

Bathymetry data for the study area were obtained from the General Bathymetric Chart of the Oceans (GEBCO) Digital Atlas (GEBCO, 2014). The GEBCO Digital Atlas consists of a global one-arc-minute grid. The grid is largely generated by combining quality-controlled ship depth soundings with interpolation between points guided by satellite-derived gravity data. A subset of the gridded GEBCO data was extracted to generate the depth grids used as an input to the SIMAP model (Figure 12).

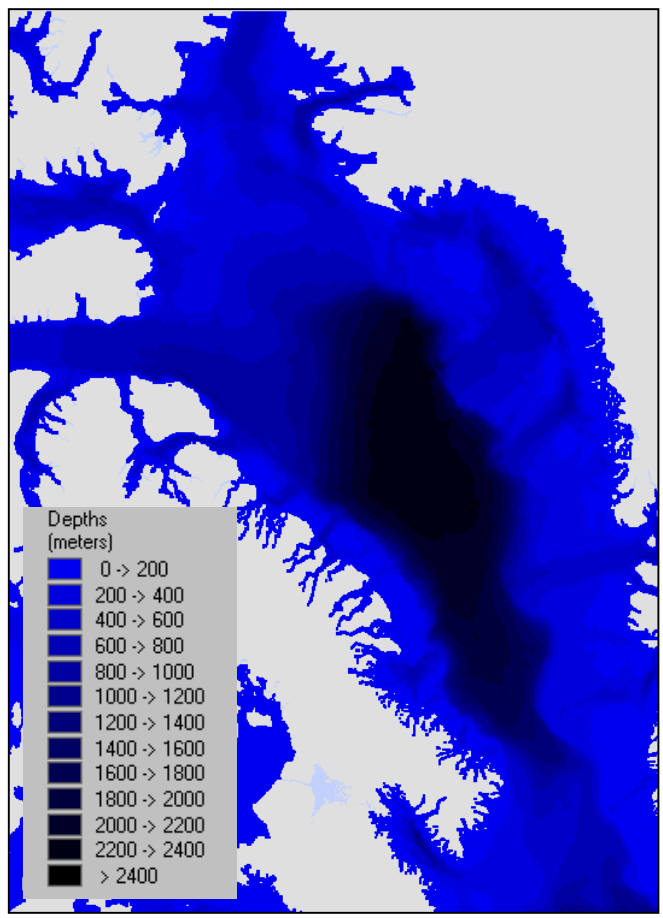

Figure 12. GEBCO bathymetry in the study area.

4.6 Oil Properties

Accurate characterization of oil properties is critical for accurate trajectory and fate modeling, as these properties strongly influence the behavior and movement of oil in the marine environment. Table 4 summarizes the key characteristics of the hydrocarbon products that were used for this study, which included a medium crude oil, two intermediate fuel oils (IFO 180 and IFO 380), and Arctic diesel. Since the exact properties of the oils that could be spilled in the region are unknown,

SEC assumed representative proxy oils to define the properties necessary to run the oil spill model. These properties were based on characterizations from the Environmental Canada Oil Property Database (described in Jokuty et al., 1999) and proprietary databases provided by RPS ASA. In the event that further information becomes available about the properties of specific products being used or extracted in the region, the characterization of the oils used in this modeling study should be reviewed to ensure that the representative oils are suitable.

Table 4. Key properties of the oils used in model simulations.

Oil Type	Density (g/cm^3 at 15.6°C)	API Gravity	Viscosity (cP at 15°C)	Surface Tension (dyne/cm)	Pour Point (°C)	Emulsion Maximum Water Content (%)
Medium Crude	0.871305	30.9	11.5	27.3	-32.0	72.9
IFO 180	0.967191	14.8	2,324.0	31.4	-10.0	69.0
IFO 380	0.995077	10.7	29,850.0	32.6	-6.0	45.0
Arctic Diesel	0.830887	38.8	2.8	27.5	-50.0	0.0

Viscosity and surface tension affect the degree of spreading of the surface oil, which in turn influences the rates of evaporation, dissolution, dispersion, and photo-oxidation. The maximum water content is a measure, obtained in a laboratory, of the emulsion-formation tendency of the oil. Oils that form water-in-oil emulsions tend to be more persistent in the marine environment, as they are less likely to be dissolved and/or evaporated; this increases their potential for reaching the shoreline. Light products such as diesel have no tendency in forming an emulsion, thus they are less persistent on the water surface relative to heavier oils (such as crude).

4.7 Consequence Thresholds

The modeling approach involves estimating the areas of water surface, lengths of shoreline, and volumes of water exposed above consequence thresholds for each spill scenario. For water surface impacts, a thickness of 0.01 g/m^2 (approximately 0.01 µm), which would appear as a barely visible sheen or scattered tarballs, was used as the threshold for impacts on socioeconomic resources because fishing may be prohibited in areas with any visible oil to prevent contamination of fishing gear and catch. A thickness of 10 g/m^2 was used as the threshold for ecological impacts to the water surface, as this level of oiling has been observed to be enough to mortally impact birds and other wildlife associated with the water surface (French et al., 1996; French McCay, 2009). This thickness is also roughly equivalent to the minimum threshold for recovery operations.

For shoreline impacts, a thickness of 100 g/m^2 was used as the threshold for ecological impacts to shoreline habitats based on synthesis of the literature showing that shoreline (invertebrate) life has been affected by this degree of oiling (French et al., 1996; French McCay, 2009).

For water column impacts on both ecological and socioeconomic resources, the volume of water with dissolved aromatic concentrations exceeding 1 ppb was used as a screening threshold for sensitive organisms (based on French McCay, 2009).

These consequence thresholds are summarized in Table 5 below.

Table 5. Consequence thresholds used in modeling.

Consequence Threshold	Value	Oil Appearance [1]	Rationale
Shoreline impact – ecological	100 g/m^2	Black oil	Based on a literature synthesis, this level of oiling may affect shoreline life (French et al., 1996; French McCay, 2009)
Water surface impact – socioeconomic	0.01 g/m^2	Colorless and silver sheen	Fishing may be prohibited in areas with visible oil to prevent contamination of gear and catch.
Water surface impact – ecological	10 g/m^2	Dark brown sheen	This level of oiling has been observed to be enough to mortally impact birds and other wildlife associated with the water surface (French et al., 1996; French McCay, 2009).
Water column impact	1 ppb	-	A contamination level of 1 ppb is used as a screening threshold for sensitive water column organisms (French McCay, 2009).

[1] Oil appearance listed in the table is for a continuous area of oil of the same thickness. In reality, the degree of oiling in the model is based on the amount of oil averaged over a large area (dependent on the resolution of the model). For example, 0.01 g/m^2 of oil on the water surface could appear as a barely visible sheen, oil patches of various amounts of oil, and/or scattered tarballs.

5.0 SCENARIOS 1A AND 1B – MELVILLE BAY BLOWOUTS

5.1 Scenario Development

The spill site selected for the hypothetical well blowouts in Melville Bay (Figure 13) is located within Pitu Block (also called Block 6) in Cairn Energy's exploration license areas. The specific location is 75.231740°N, 60.645321°W. The site was selected to be within Cairn Energy's license area for credibility as a potential blowout location, but also because of its relative proximity to shore and to several sensitive resources of concern to stakeholders, particularly the North Water Polynya area and the Melville Bay Nature Reserve (Figure 14), which is an important habitat area for polar bear, narwhal, and beluga. The North Water Polynya is also designated as a Priority 1 marine area for ecological value and sensitivity (Christensen et al., 2012).

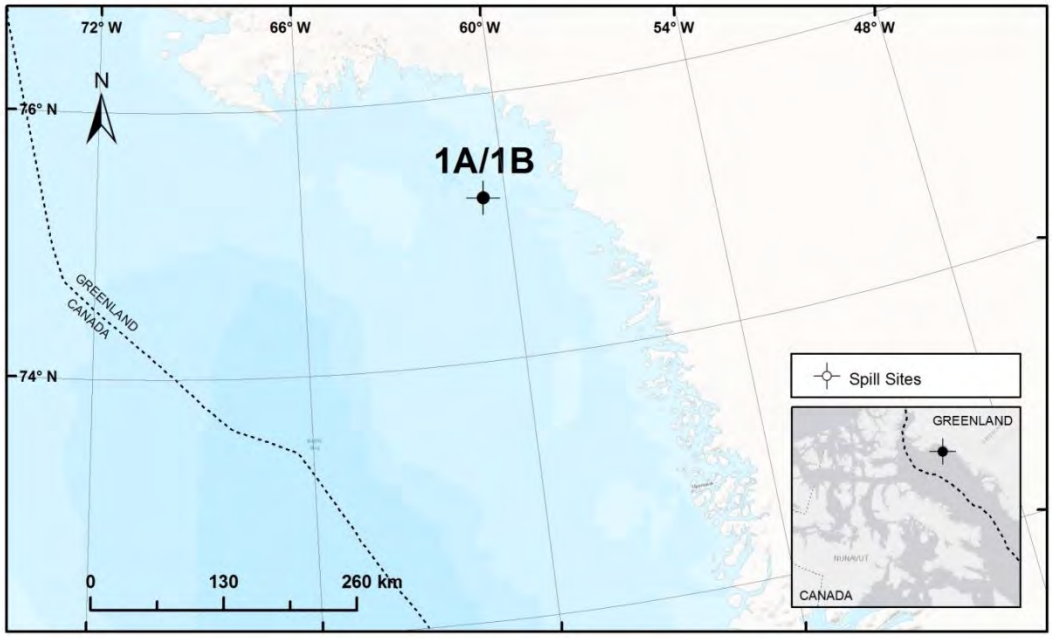

Figure 13. Location of the selected spill site in Melville Bay (scenarios 1A and 1B).

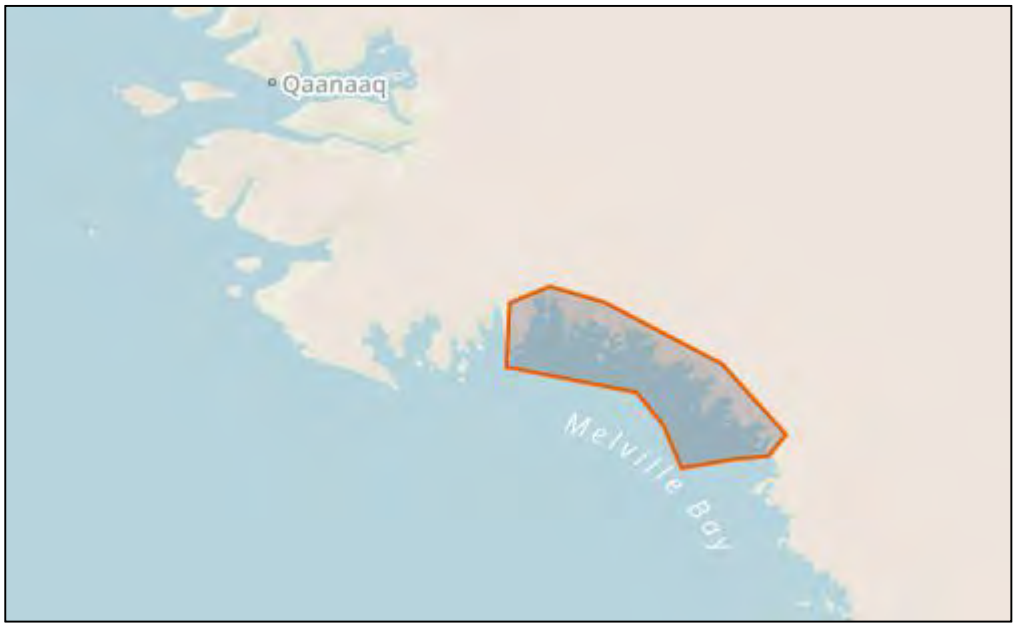

Figure 14. Location of the Melville Bay Nature Reserve (red outline). Source: IUCN and UNEP-WCMC, 2016.

For the Melville Bay spill site, two subsurface well blowout scenarios were developed, reflecting two different blowout durations (and associated total volume spilled):

- Scenario 1A: a flow rate of 3,340 m^3 per day for 1 day (assumes that natural bridging will stop the flow of oil) for a total of 3,340 m^3 (21,008 bbl) spilled; and
- Scenario 1B: a flow rate of 3,340 m^3 per day for 34 days (assumes a relief well is needed to stop the flow of oil) for a total of 113,560 m^3 (714,271 bbl) spilled.

The season evaluated for scenarios 1A and 1B corresponds to “open water” conditions, and was based on analysis of average monthly ice coverage data from TOPAZ4 at the spill site (2011-2015). Average ice cover of less than 30% was defined as “open water.” This time period corresponded to July through October.

The oil type selected for scenarios 1A and 1B was similar to Statfjord (medium) crude, which is a crude oil that represents the characteristics of crudes found in other exploration wells in the region (Mosbech et al., 2007; Perry and Bright, 2010). The precise characteristics of crude oil from a particular well can only be known after direct sampling from that well, which is not possible in this case, as the Pitu Block has not yet been explored or developed.

The rate of flow from a particular well is dependent on the characteristics of the well itself, particularly the reservoir pressure, but also the type of well (development, exploratory, etc.). The actual flow rate of a well can often not be predicted in advance and will be determined only when the actual well is drilled. Flow rates can vary during the course of oil extraction, including variations in the amount of crude oil versus water or brine in the flow. The flow rates that are described for wells are generally the average flow rate. The flow rate assumed for the modeling of scenarios 1A and 1B was 3,340 m^3 per day, which corresponds to 21,008 barrels (bbl) per day. This flow rate was assumed based on other studies conducted in the region (Mosbech et al., 2007; Perry and

Bright, 2010), and was deemed to be a reasonable approximation of the magnitude of flow rate that might be expected for a well in this license area.

Given an average flow rate for a particular well, the total volume will depend on the duration of flow – the length of time that the well continues to release crude oil to the environment. The duration of flow is determined by the length of time that it takes for the well to either bridge naturally (fill in with enough sediment to naturally stop flowing without any human intervention), to be capped and contained, or to be intercepted by a relief well(s) to stop the flow. For the Melville Bay blowout scenarios, two durations of flow were assumed. The first assumed that there would be natural bridging that occurs within one day; the second assumed that a relief well operation successfully stopped the flow at the end of the 34th day of flow, as per the Cairn Oil Spill Contingency Plan (Cairn Energy, 2011).[1] For these scenarios, capping and containment was not considered. Generally, relief well operations take longer than capping and containment operations, and would represent the worst-case with respect to flow duration and ultimate spill volume.

Studies indicate that about 84% of well blowouts bridge naturally, that is, the flow is stopped as sediment naturally fills in the wellbore without any intervention in 0.5 to 5 days (Dyb et al., 2012, Holand, 2013). Generally, the duration of flow is relatively short, which would limit the total volume of spillage. In the other 16% of cases, human intervention in the form of relief wells and/or containment and capping is required to stop the flow of oil. Worldwide, about 10% of blowouts have been stopped with relief wells and 6% by capping and containment operations. Fifty percent of relief well operations took less than five days, 75% less than 10 days, and 90% less than 25 days. The 34-day relief well operation assumed in scenario 1B represents the estimated 95th percentile case with respect to flow duration.

See Appendix A for additional discussion regarding the development of spill scenario parameters; benchmarking blowout flow rates, durations, and total volumes; and blowout likelihood.

5.2 Environmental Analysis

Figure 15 presents monthly TOPAZ4 surface current roses at the Melville Bay spill site. Throughout the year, surface currents are predominantly directed northwestward; however, some seasonality exists. In December-May, surface currents are north-northwestward before transitioning to a more variable and stronger flow in summer (June–August). Direction becomes primarily northwestward in fall and remains northwestward for the rest of the year. Surface current speeds are weaker during winter and spring (January–May), and strongest during fall (October–November).

Figure 16 presents monthly statistics (average and 95th percentile) describing TOPAZ4 current speeds at the surface. The lowest average monthly speed occurs in March (around 2.5 cm/s), while the highest occurs in November at over 7 cm/s. Surface speeds are lowest in the early part of the year and increase gradually until reaching a maximum in November, then sharply declining in December.

[1] The Cairn Oil Spill Contingency Plan (Cairn Energy, 2011) was developed for activities in a different license area of West Greenland, located well to the south of Pitu Block. However, it is the best available information, as no contingency plans are currently available for the Pitu Block area.

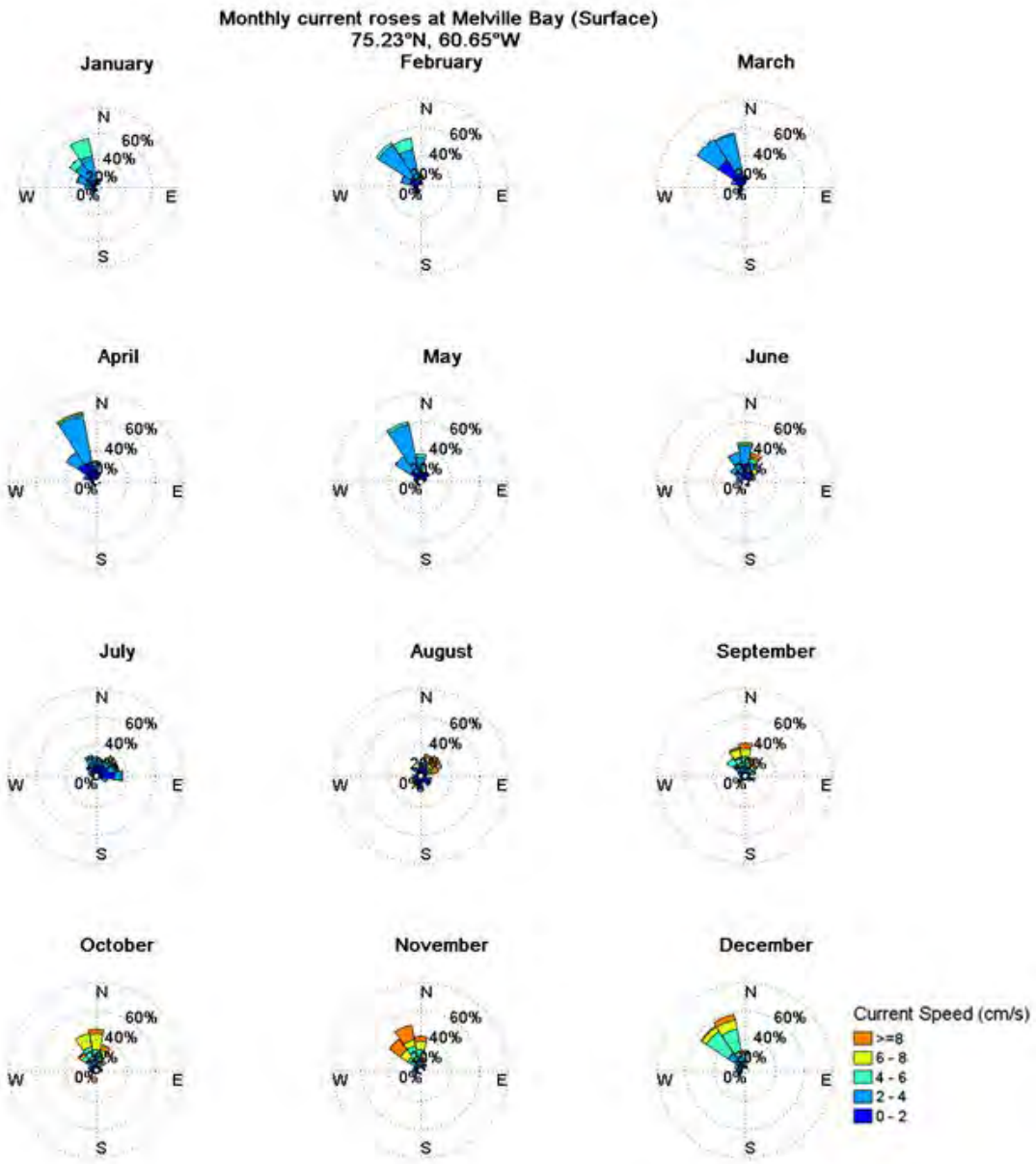

Figure 15. TOPAZ4 monthly averaged surface current roses near the Melville Bay spill site, averaged over the period of 2011-2015. Direction convention is standard (i.e., direction currents are moving to).

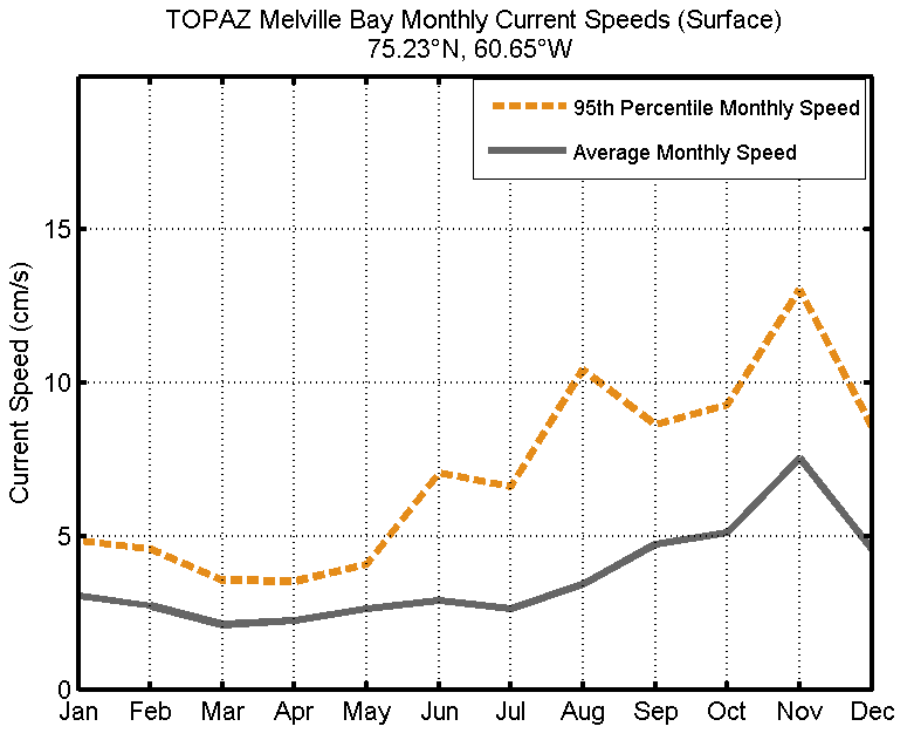

Figure 16. TOPAZ4 current statistics: monthly average (grey solid) and 95th percentile (orange dash) current speed at the surface near the Melville Bay spill site for 2011-2015.

The following figure (Figure 17) presents monthly TOPAZ4 ice roses at the Melville Bay spill site. Ice is present during the majority of the year, except for August and September. Ice speeds are variable throughout the year. During winter and spring (December–May), direction is divided between north-northwestward and southeastward movement. In June, ice is primarily directed northwestward, while in July ice begins to diminish and decrease in speed. After an ice-free period during August and September, ice begins to form again. Direction is variable during October and November before returning to a predominantly northwestward and southeastward direction.

Monthly average sea ice and landfast ice cover near the spill site are shown in Figure 18. Sea ice coverage is based on data from TOPAZ4 (2011-2015) and landfast ice coverage is based on data from the National Snow and Ice Data Center (1991 through 1998).

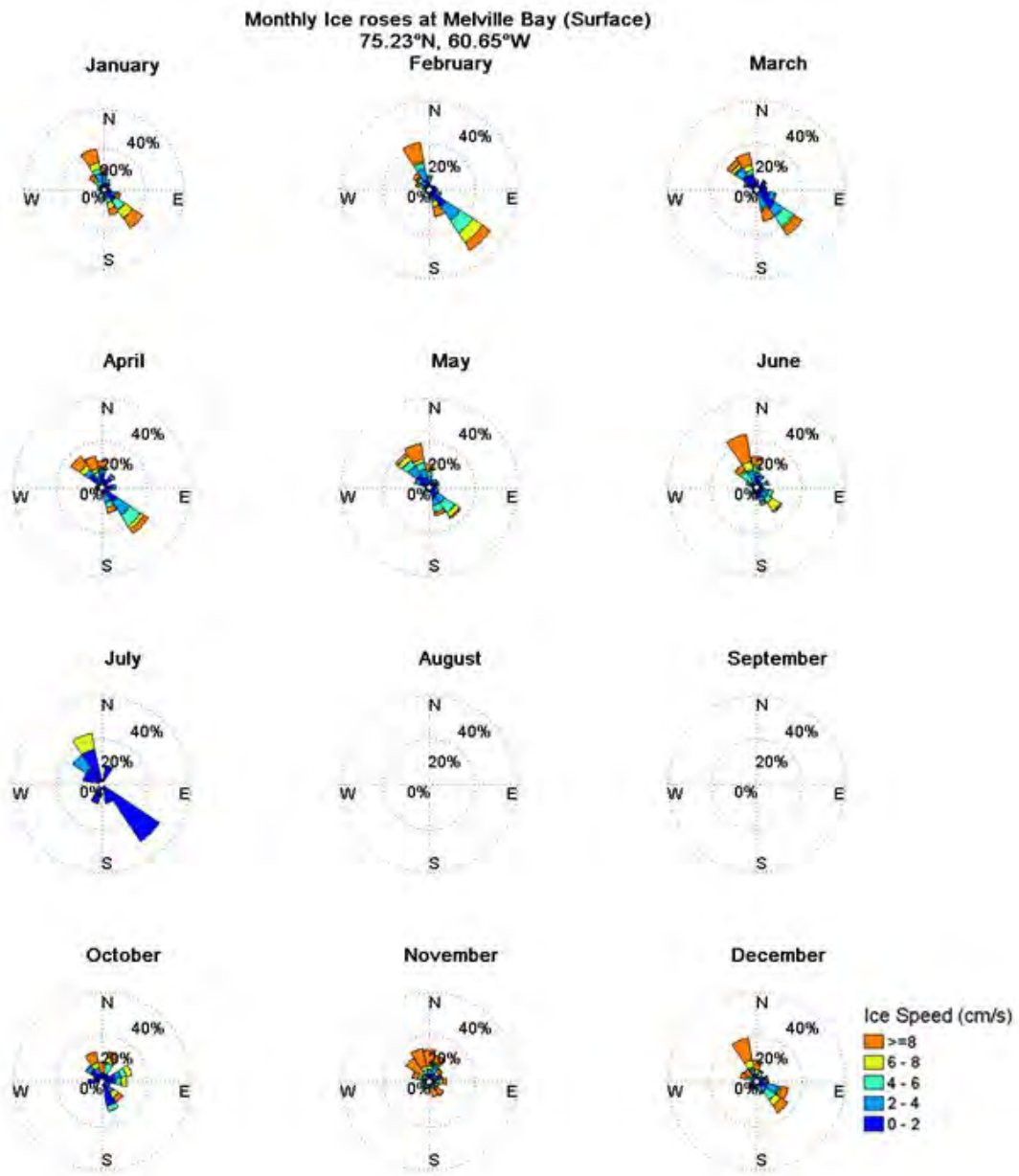

Figure 17. TOPAZ4 monthly averaged ice roses near the Melville Bay spill site, averaged over the period of 2011-2015. Ice roses are presented for the surface. Direction convention is standard (i.e., direction ice is moving to).

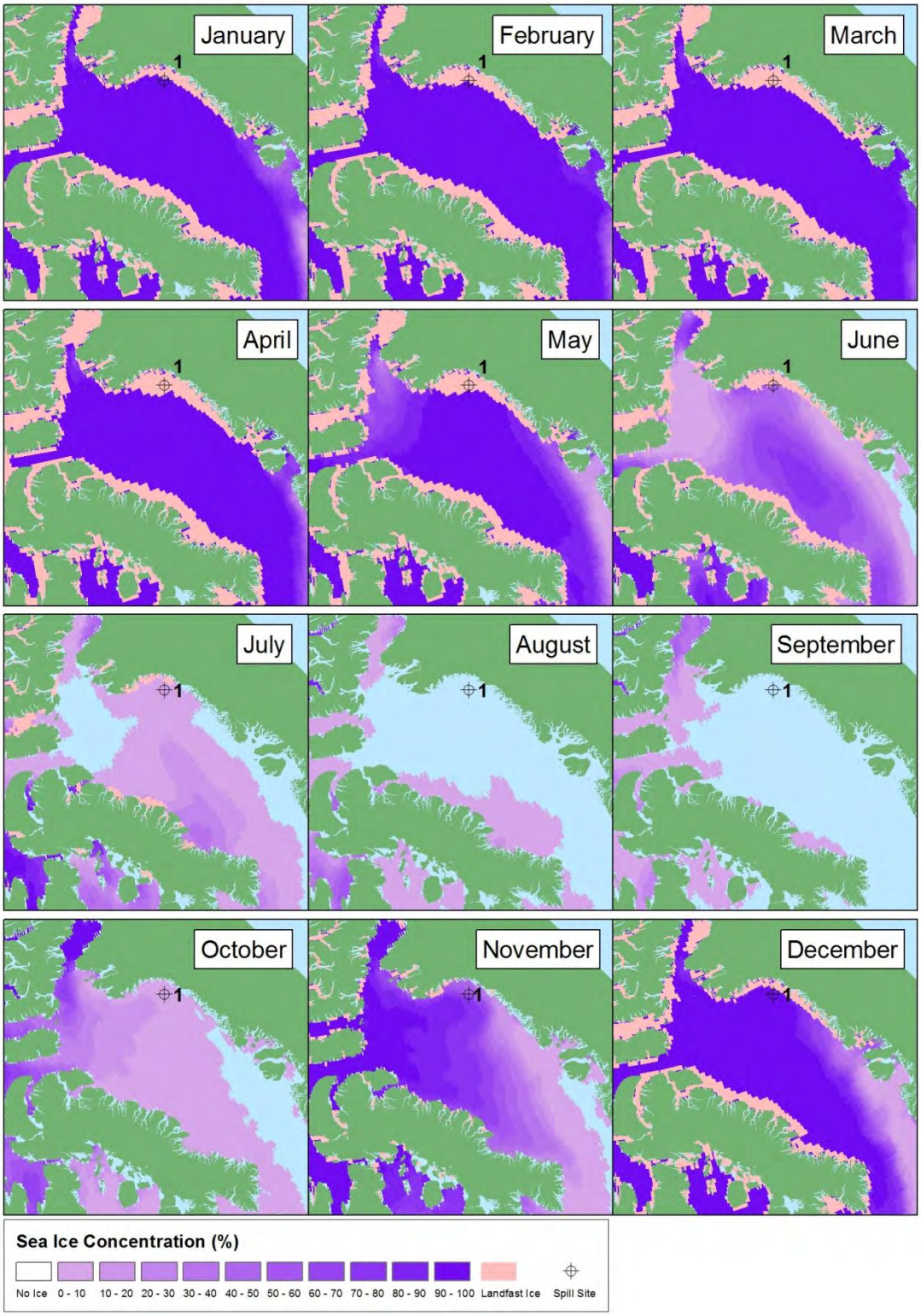

Figure 18. Average monthly cover of sea ice and landfast ice near the Melville Bay spill site.

Figure 19 displays monthly ECMWF wind roses for the Melville Bay spill site. The wind direction is divided between primarily southeasterly and northwesterly. Winds are stronger during summer and fall (June–November), with the strongest winds coming from the southeast at over 20 knots. Wind direction is more southeasterly during June through September and becomes more variable during winter.

Monthly wind speeds from ECMWF at the Melville Bay spill site indicate that average speeds are fairly consistent throughout the year, varying between approximately 6 to 8 knots (Figure 20). The lowest monthly average speed occurs in April and the maximum occurs in November.

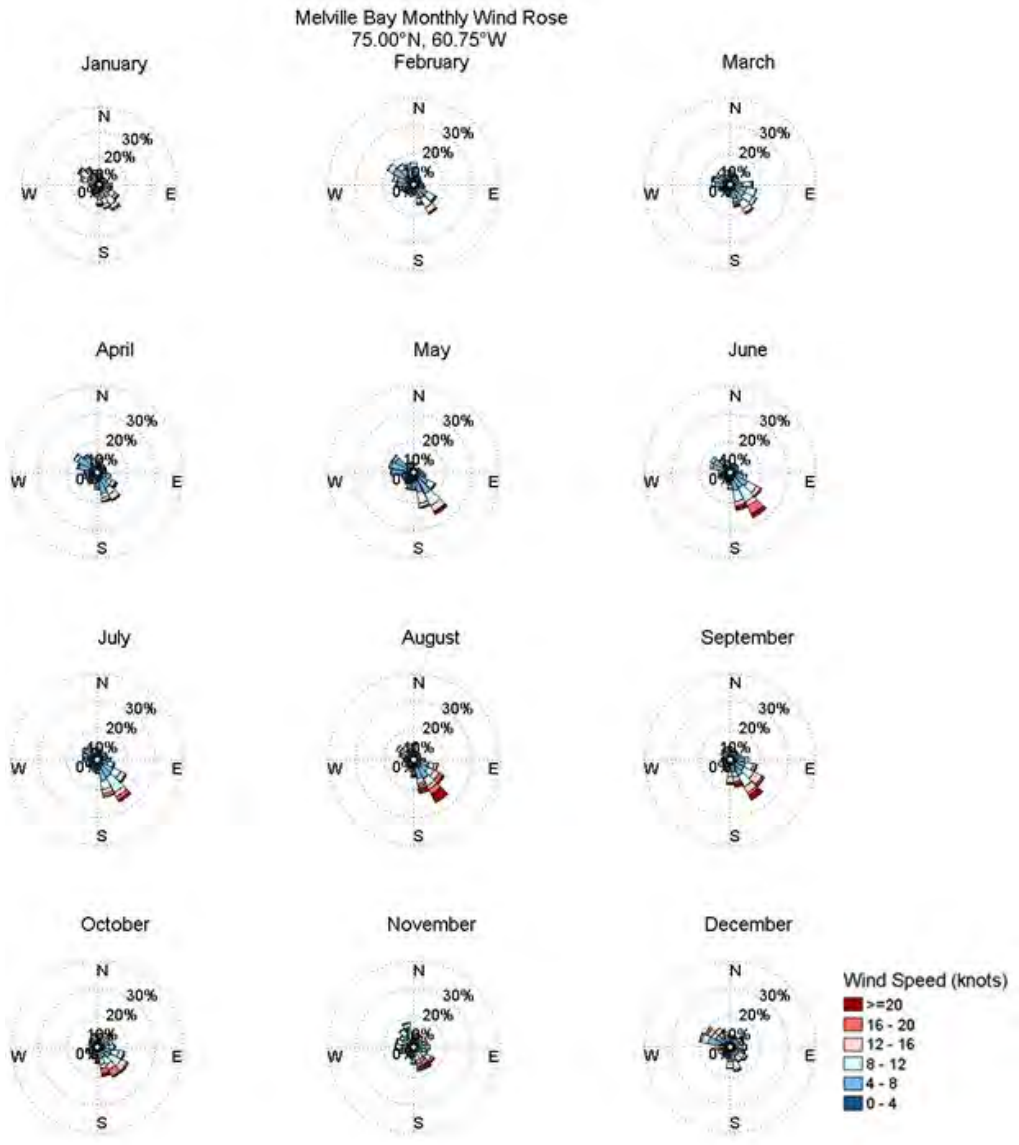

Figure 19. ECMWF monthly averaged wind roses near the Melville Bay spill site, averaged over the period of 2011-2015. Wind speeds are in knots, using meteorological convention (i.e., direction wind is coming from).

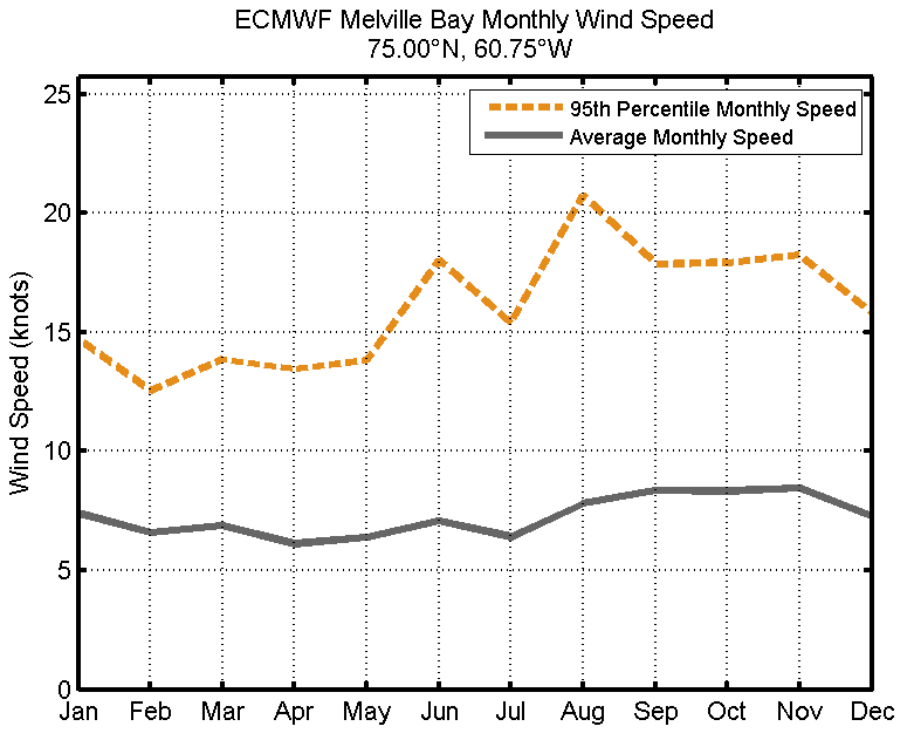

Figure 20. ECMWF wind statistics: monthly average (grey solid) and 95th percentile (orange dash) wind speed near the Melville Bay spill site for 2011-2015.

The vertical profile of temperature, salinity, and density at the Melville Bay spill site for July through October is shown in Figure 21. Salinity is approximately 31 psu at the surface and increases to 34.5 psu near the sea floor. Temperature at the surface is approximately 1.9 ºC and decreases quickly to -0.7 ºC at 60 m before increasing gradually to 1.8 ºC at 425 m. The temperature then decreases to 0.4 ºC near the sea floor. Density at the surface is 24.8 kg/m^3 and increases to 27.7 kg/m^3 near the sea floor.

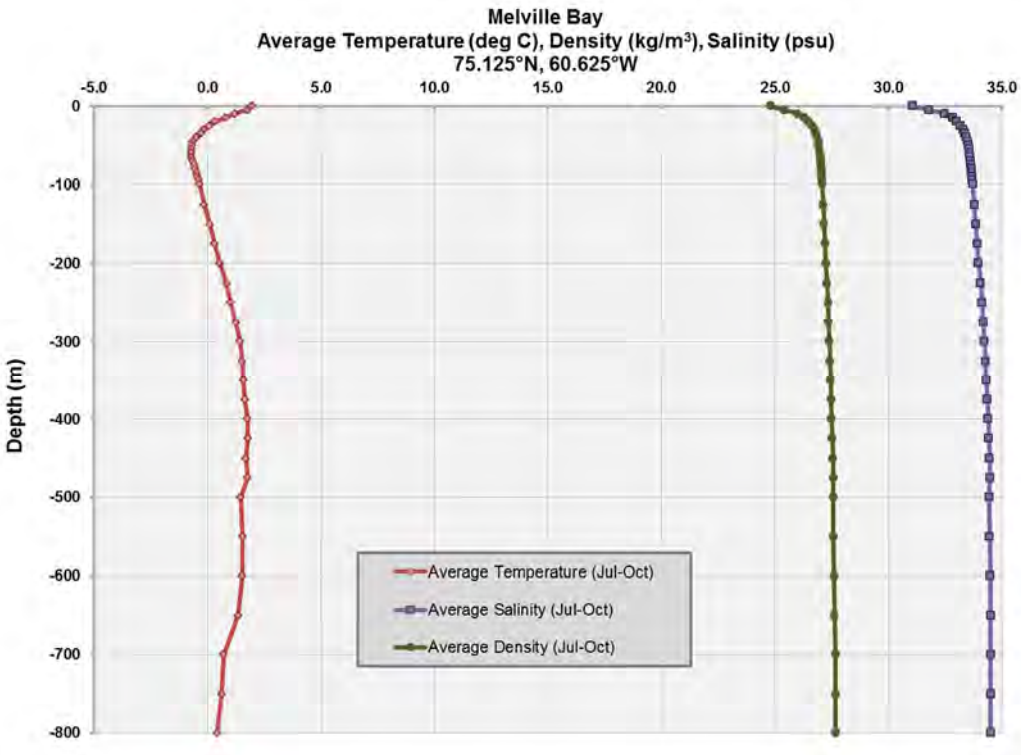

Figure 21. Vertical profile of average temperature (red), salinity (purple), and density (green) near the Melville Bay spill site for July to October. Data from the World Ocean Atlas 2013.

5.3 Near-field Modeling

The key inputs to the near-field model include flow rate, gas-to-oil ratio, aperture or pipe diameter, and a vertical profile of water temperature and density. For both scenarios 1A and 1B, the gas-to-oil ratio was assumed to be 1,000 scf/stb (standard cubic feet per stock tank barrel), and the pipe diameter was assumed to be 38.1 cm. In the absence of site-specific information for the area of interest, these values are considered to be reasonable proxy values based on past modeling experience.

The near-field modeling results provide a description of the plume characteristics, including the plume location (namely plume trap height), plume geometry, and the release droplet size distribution. The results of the near-field model are then used to provide the initial conditions for the stochastic and deterministic far-field modeling in SIMAP, including:

- Termination height (trap height) of the plume;
- Diameter of the plume; and
- Oil droplet size distribution.

Figure 22 and Figure 23 present the OILMAP Deep modeling results for scenarios 1A and 1B. Despite the difference in duration between the two scenarios (1 day vs. 34 days), plume formation and behavior as well as droplet formation are identical.

Figure 22 shows the plume radius plotted as a function of the height above the sea floor (wellhead), and plume velocity along the centerline of the blowout as a function of the height above the seafloor. Plume centerline velocity defines the vertical movement of the mixture of gas, oil, and water along the center of the plume. The model indicates that the velocity of the plume decreases quickly at heights further from the discharge point as it entrains heavier ambient seawater. As the plume continues to rise and entrain more ambient seawater, the centerline velocity gradually decreases, and approaches zero at about 238 m above the wellhead (a depth of 570 m below the water surface). From this termination height, gas and oil droplets will ascend to the water surface under free rise velocities determined by Stokes law. The plume is expected to reach a maximum radius of approximately 43 m.

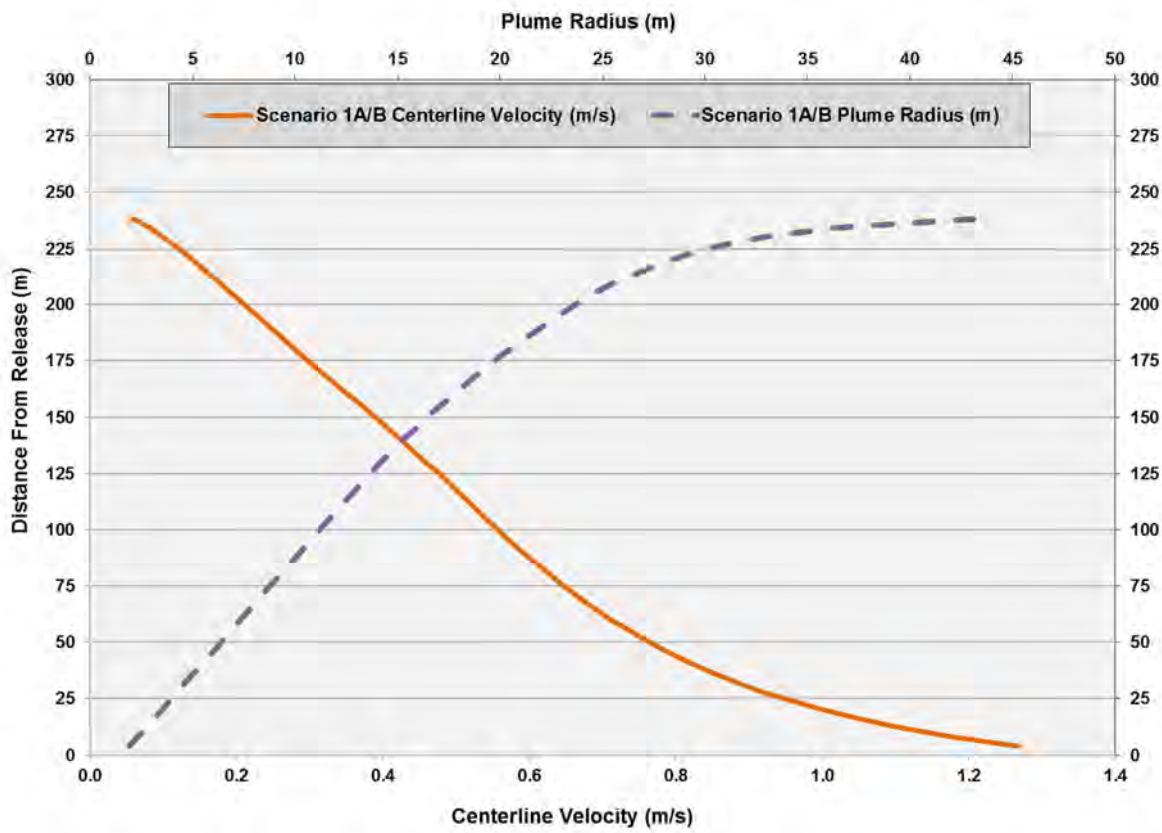

Figure 22. Predicted blowout plume centerline velocity and plume radius versus elevation above release point for the Melville Bay blowout events (scenarios 1A and 1B).

The near-field modeling results also provide a characterization of the oil droplet size distribution generated by the blowout. This distribution has a profound effect on how oil is transported after the initial plume, as the droplet size dictates how long the oil droplet will remain suspended in the water column. Figure 23 shows the model-estimated droplet size distribution and droplet rise times to the surface for scenarios 1A and 1B. The oil droplet sizes for these scenarios are relatively large, and would tend to reach the surface quickly. The minimum droplet size was 500 µm; a droplet this size would be expected to surface in about 14.7 hours. The maximum droplet size was 10,000 µm, which would surface in about 1.3 hours.

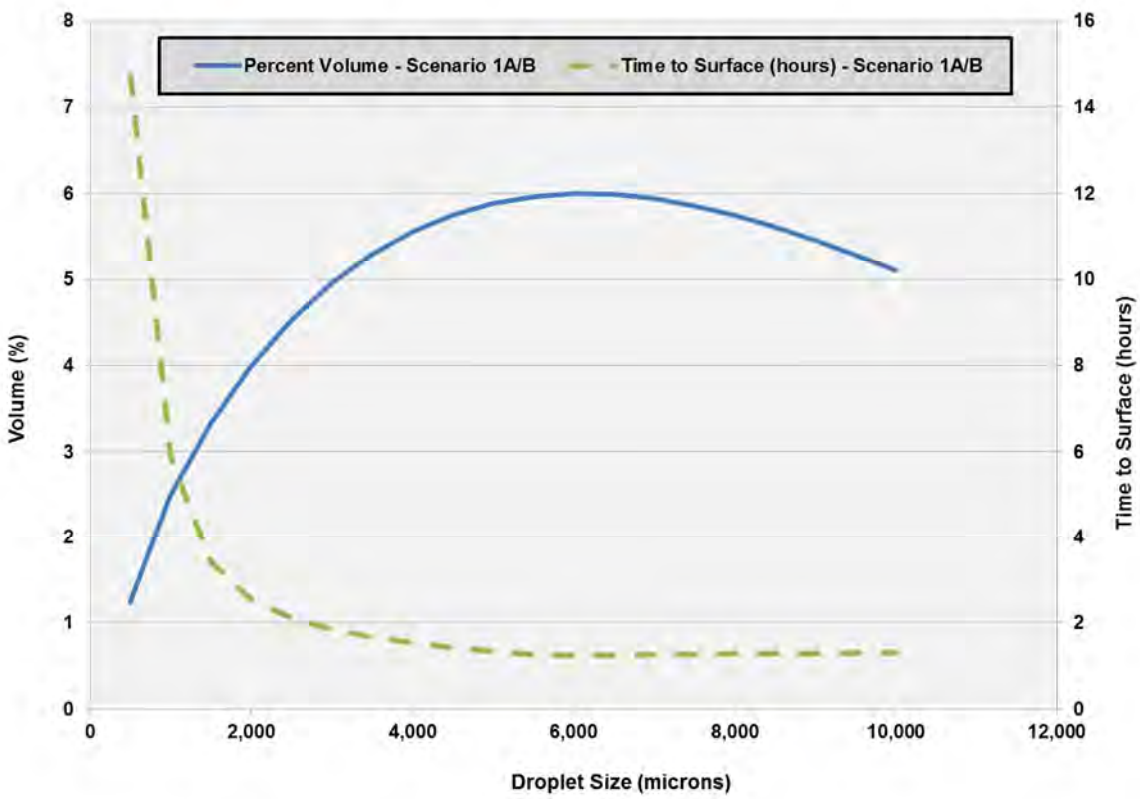

Figure 23. Predicted droplet size distribution and droplet rise times to the surface for the Melville Bay blowout events (scenarios 1A and 1B).

5.4 Stochastic Modeling

Using the near-field model results as initial conditions for the far-field modeling, the SIMAP stochastic model was used to predict the statistical footprint of oiling associated with the blowout scenarios.

5.4.1 Stochastic Scenario Parameters

The stochastic scenario input parameters developed for 1A and 1B (see Section 5.1) are summarized in Table 6 below. Each scenario was simulated (tracked) for 45 days beyond the end of the blowout release. No spill response measures were included in the stochastic simulations for these scenarios.

Table 6. Stochastic scenario input parameters for scenarios 1A and 1B.

ID #	Spill Type	Location	Release Depth (m)	Oil Type	Spill Rate	Spill Duration (days)	Total Volume (m^3)	Season	Simulation Duration (days)
1A	Subsurface blowout	75.231740°N, 60.645321°W	808	Medium crude	3,340 m^3/day	1	3,340	July to October	46
1B	Subsurface blowout	75.231740°N, 60.645321°W	808	Medium crude	3,340 m^3/day	34	113,560	July to October	79

5.4.2 Stochastic Results

The results of the stochastic model simulations for scenarios 1A and 1B are shown in Table 7 and Table 8.

Table 7 presents shoreline oiling statistics for both scenarios, including the percentage of simulations reaching shore, time to shore, peak volume of oil ashore, and the shoreline length oiled above the ecological threshold of 100 g/m^2. The percentage of simulations reaching shore indicates the likelihood that a particular spill event will reach nearby coastal areas with a level of shoreline oiling greater than 100 g/m^2. The percentage of simulations reaching shore is based on the total number of trajectories out of the ensemble of 100+ individual runs that reached the coast in the stochastic analysis. Note that a spill event with high probability of shoreline oiling does not imply that a particular section of the coast will be oiled, only that there is a high probability of oil reaching the coastline *at some location*.

Both scenarios had a high probability of causing shoreline oiling above 100 g/m^2, with 85% of trajectories reaching shore for scenario 1A, and 100% of trajectories reaching shore for scenario 1B. As expected, the volume of oil ashore and the shoreline length oiled was substantially higher for the longer duration, larger volume blowout (scenario 1B). On average, the peak volume of oil ashore for scenario 1A is about 37% of the total volume spilled, and about 10% of the total volume spilled for scenario 1B. The minimum time to reach shore was similar between the two scenarios, at about 2-3 days.

Table 7. Scenarios 1A and 1B stochastic results – shoreline oiling statistics.

ID	Spill Event	Total Volume Spilled (m^3)	Simulations Reaching Shore (%)[1]	Time to Reach Shore (days)		Peak Volume of Oil Ashore (m^3)		Shoreline Length Oiled Above 100 g/m^2 (km)	
				Min.	Avg.	Max.	Avg.	Max.	Avg.
1A	Melville Bay – 1-Day Blowout	3,340	85	2.3	10.5	1,975	1,228	373	135
1B	Melville Bay – 34-Day Blowout	113,560	100	2.8	12.5	24,753	11,521	1,303	631

[1] Percentage of simulations reaching shore is calculated based on the number of individual trajectories that resulted in shoreline oiling above a threshold of 100 g/m^2 of oil.

Table 8 presents surface oiling and water column oiling statistics. The 1-day blowout (scenario 1A) resulted in a water surface footprint of, on average, about 74 km^2 oiled above the ecological threshold of 10 g/m^2. The water surface oiling footprint for the 34-day blowout (scenario 1B) was approximately 1,145 km^2 oiled on average. Because of the relatively large size of the oil droplets from the blowouts (Section 5.3), the droplets tend to surface quickly and the residence time in the water column is relatively short. As such, entrainment of oil in the water column was relatively low for both scenarios. On average, the peak volume of oil entrained in the water column was about 17% of the total volume for scenario 1A, and about 3% of the total volume for scenario 1B.

Table 8. Scenarios 1A and 1B stochastic results – surface oiling and water column oiling statistics.

ID	Spill Event	Total Volume Spilled (m^3)	Water Surface Area Oiled Above 0.01 g/m^2 (km^2)		Water Surface Area Oiled Above 10 g/m^2 (km^2)		Volume of Oil in Water Column (m^3)	
			Max.	Avg.	Max.	Avg.	Max.	Avg.
1A	Melville Bay – 1-Day Blowout	3,340	11,023	1,619	86	74	2,046	582
1B	Melville Bay – 34-Day Blowout	113,560	118,260	34,780	1,545	1,145	6,041	3,229

The following figures (Figure 24 through Figure 27) illustrate the spatial extent of water surface oiling and shoreline oiling probabilities for scenarios 1A and 1B. For each scenario, three figures are presented:

1. **Probability of Water Surface Oiling Above 0.01 g/m^2**: The map defines the area in which water surface oiling above the socioeconomic threshold of 0.01 g/m^2 may be expected and the associated probability of oiling (based on analysis of the 200 or 120[2] individual trajectories run for each spill scenario). The map does not imply that the entire contoured area would be covered with oil in the event of a spill. The map also does not provide any information about the quantity of oil in a given area.

2. **Probability of Water Surface Oiling Above 10 g/m^2**: The map defines the area in which water surface oiling above the ecological threshold of 10 g/m^2 may be expected and the associated probability of oiling (based on analysis of the 200 or 120 individual trajectories run for each spill scenario). The map does not imply that the entire contoured area would be covered with oil in the event of a spill. The map also does not provide any information about the quantity of oil in a given area.

3. **Probability of Shoreline Oiling Exceeding 100 g/m^2**: This map shows the probability of shoreline oiling above the ecological threshold of 100 g/m^2 (based on analysis of the 200 or 120 individual trajectories run for each spill scenario). The map does not imply that the entire shoreline extent would be oiled in the event of a spill. The map also does not provide any information about the quantity of oil in a given area.

A brief summary of each stochastic simulation follows the figures for each case.

[2] For the 34-day blowout scenario, 120 individual model runs were simulated instead of 200 due to file size and computational limitations.

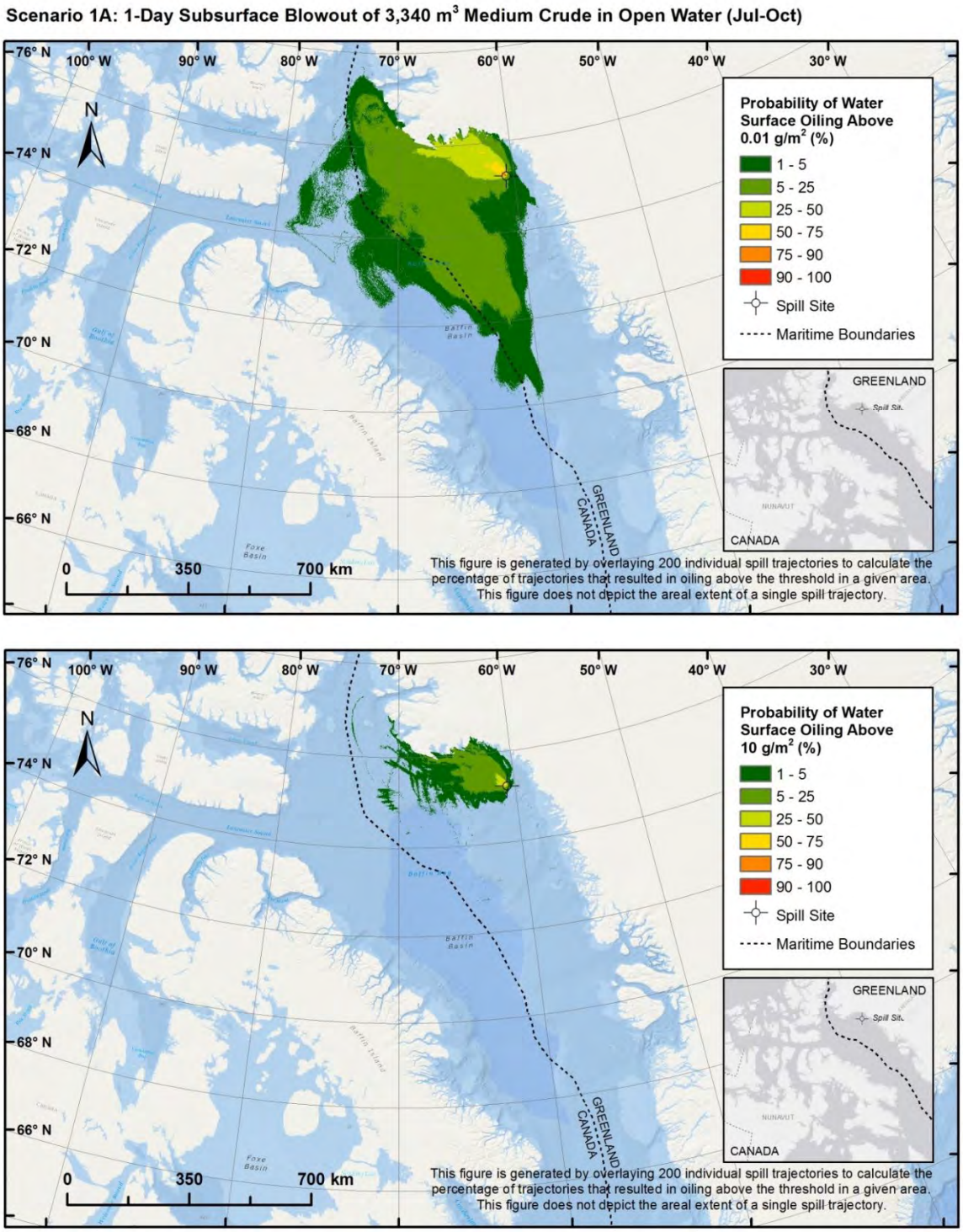

Figure 24. Scenario 1A (1-day blowout of 3,340 m^3 crude oil) stochastic results – Probability of water surface oiling above the socioeconomic threshold of 0.01 g/m^2 (top panel) and probability of water surface oiling above the ecological threshold of 10 g/m^2 (bottom panel).

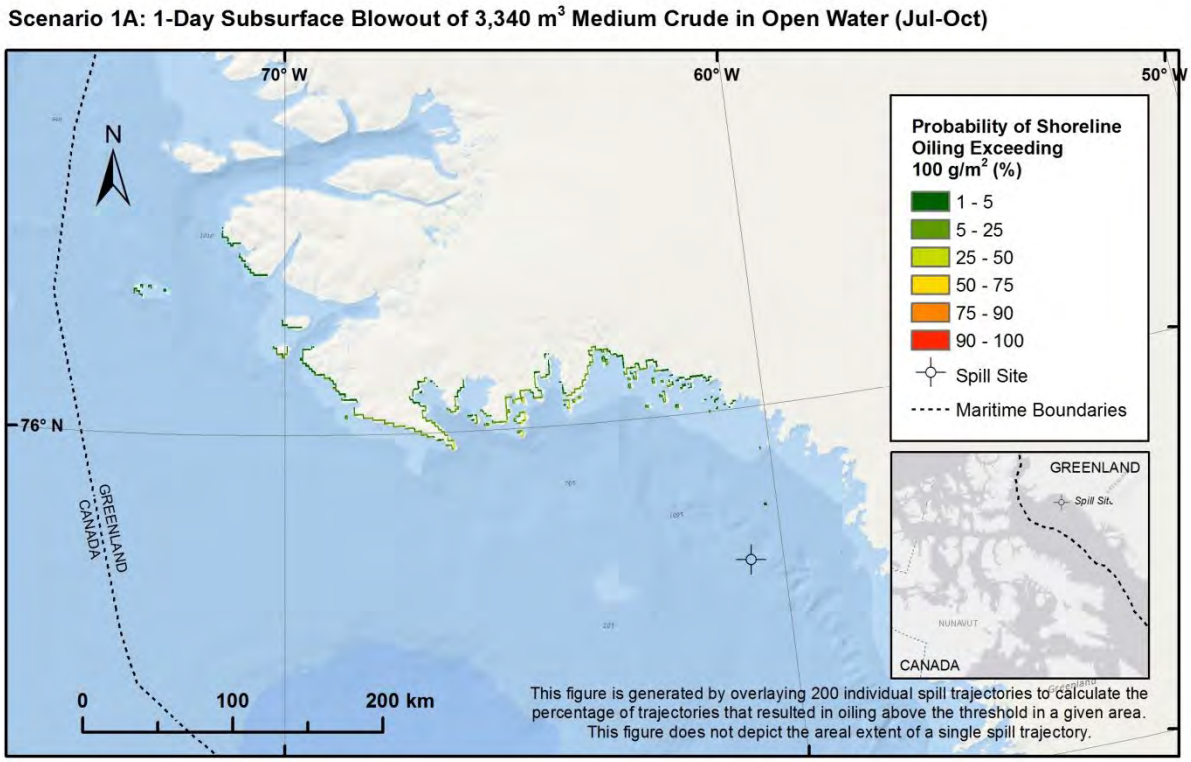

Figure 25. Scenario 1A (1-day blowout of 3,340 m^3 crude oil) stochastic results – Probability of shoreline oiling above the ecological threshold of 100 g/m^2.

As shown in Figure 24, the highest probabilities in the stochastic surface water oiling footprint for scenario 1A are predominately oriented to the northwest of the spill site, towards Greenlandic shoreline. For the socioeconomic threshold of 0.01 g/m^2, there are low (<25%) probabilities of surface oil being transported into the North Water Polynya area to the northwest and to the south into Baffin Bay. There is also a low probability of water surface oiling above the threshold in Canadian territorial waters. For the ecological threshold of 10 g/m^2, the stochastic surface oiling footprint is restricted to Greenlandic waters, with lower overall probabilities.

There is an approximately 85% chance that shoreline oiling above 100 g/m^2 will occur at some location in the study area (Table 25). However, the highest probability of any individual segment of the coastline being oiled above the threshold is 39% (Figure 25). The highest probability of oiling is for shorelines to the northwest of the spill site near the settlement of Savissivik, Greenland.

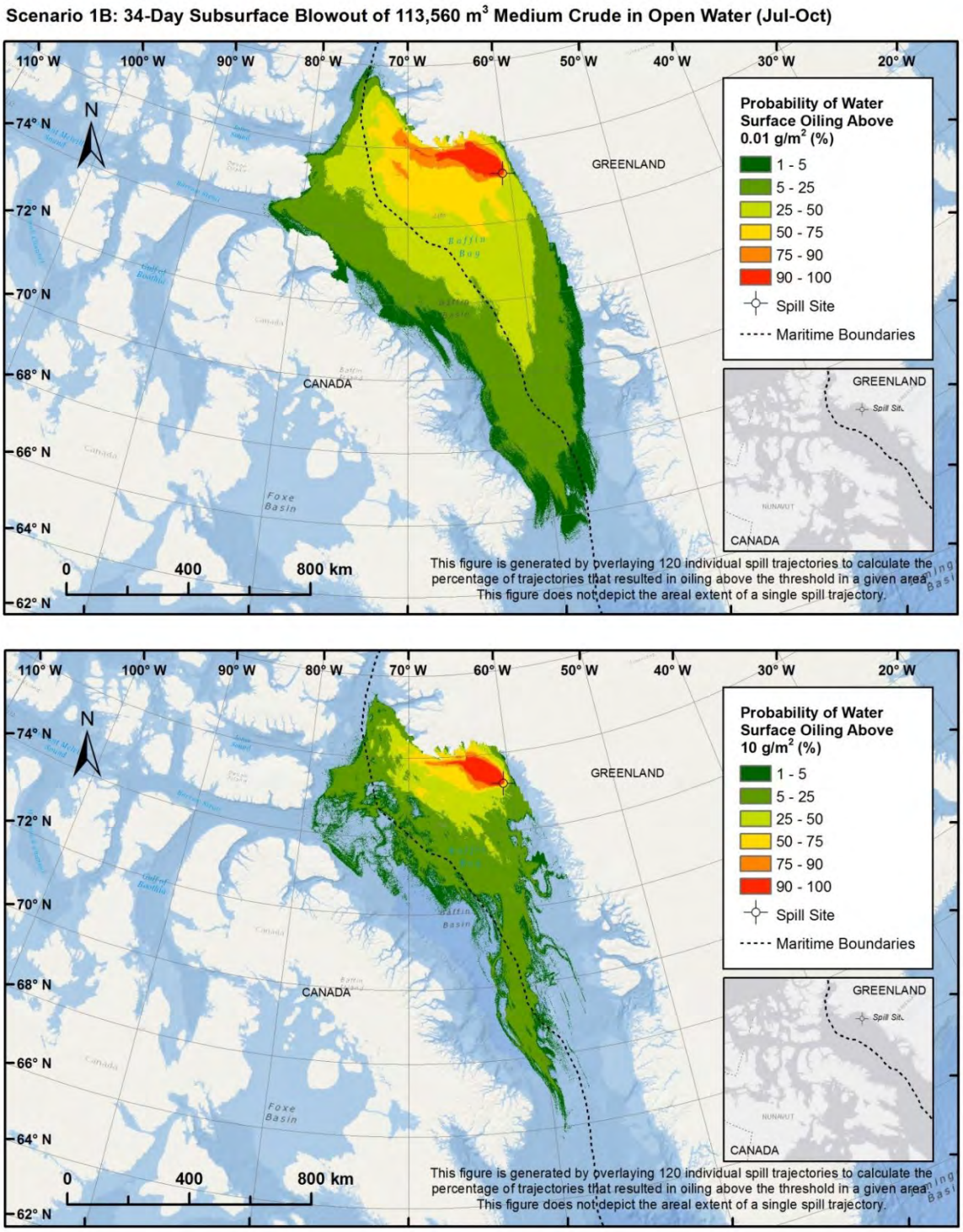

Figure 26. Scenario 1B (34-day blowout of 113,560 m^3 crude oil) stochastic results – Probability of water surface oiling above the socioeconomic threshold of 0.01 g/m^2 (top panel) and probability of water surface oiling above the ecological threshold of 10 g/m^2 (bottom panel).

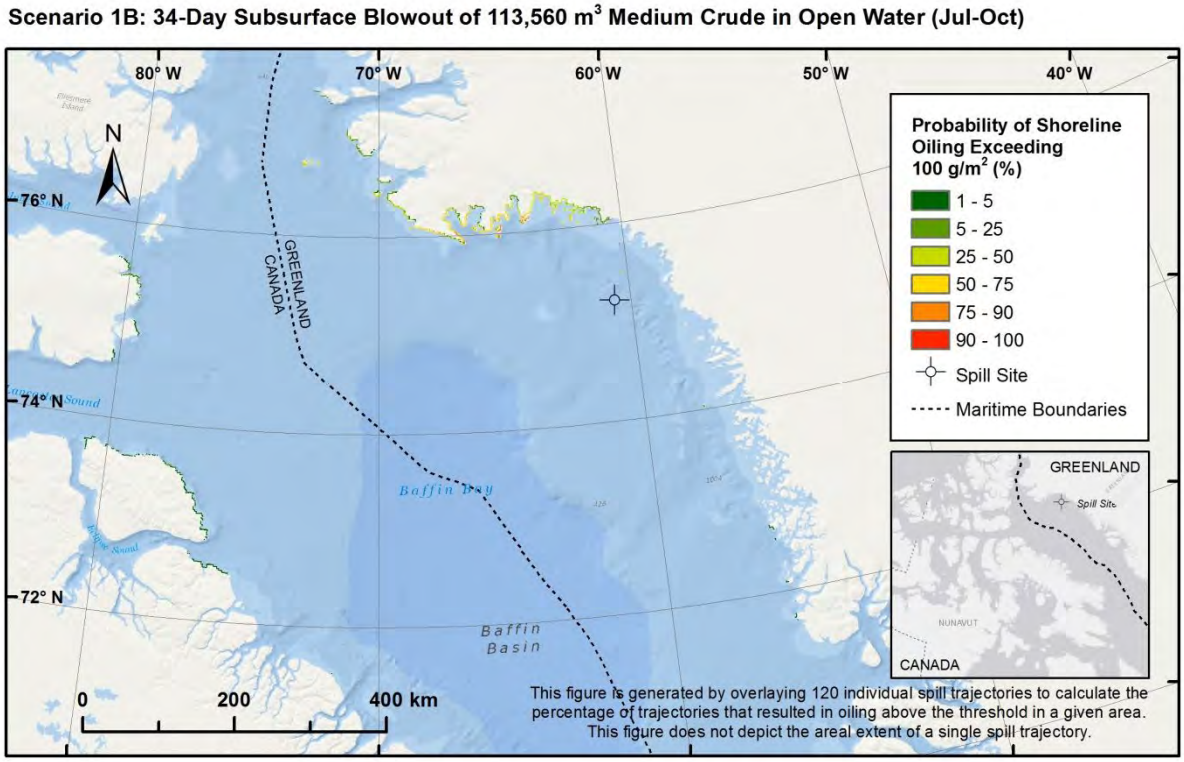

Figure 27. Scenario 1B (34-day blowout of 113,560 m^3 crude oil) stochastic results – Probability of shoreline oiling above the ecological threshold of 100 g/m^2.

Like scenario 1A, the highest probabilities in the stochastic surface water oiling footprint for scenario 1B are predominately oriented to the northwest of the spill site, towards Greenlandic shoreline and the North Water Polynya area (Figure 26). For the socioeconomic threshold, there are high (>50%) probabilities of surface oil being transported into the North Water Polynya area to the northwest and to the south into Baffin Bay. There is a moderate probability of oiling above the threshold in Canadian territorial waters, especially offshore of Bylot and Devon Islands. For the ecological threshold, the stochastic surface oiling footprint includes both Greenlandic and Canadian waters, with lower overall probabilities. The probability of water surface oiling above the ecological threshold within the North Water Polynya area is moderate to high.

The probability that shoreline oiling above 100 g/m^2 will occur at some location in the study area is 100% (Table 7). The highest probability of any individual segment of the coastline being oiled above the threshold is 90% (Figure 27). The highest probability of oiling is for shorelines to the northwest of the spill site near the settlement of Savissivik, Greenland. There is a very low (<5%) probability of shoreline oiling above the threshold in Canada along the coastlines of Devon Island, Bylot Island, and Baffin Island.

5.5 Deterministic Modeling

The deterministic trajectory and fate simulations provide an estimate of the 3-D trajectory (movement) and fate (weathering) for a particular individual spill event.

5.5.1 Deterministic Scenario Parameters

Trajectories were selected from the stochastic scenario based on pre-defined criteria. Different parameters or criteria can be used to select individual trajectories for deterministic analysis. For example, deterministic trajectories can be "representative" or "worst-case" for a variety of consequence metrics (e.g., shoreline length oiled, time to shore, volume of oil ashore, water column contamination, water surface area swept). The selected deterministic cases for scenarios 1A and 1B are summarized in Table 9. At the request of WWF-Canada, the deterministic scenarios were simulated (tracked) for longer than the corresponding stochastic scenario in order to provide more information about the ultimate fate of the spilled oil. The chosen simulation durations were based on test simulations and were selected to reflect either:

- The point at which zero or minimal oil remains on the water surface;
- The point beyond which oil begins to leave the extent of the environmental input data (e.g., currents, winds); or
- The point beyond which the duration begins to reduce the credibility of model results (due to increasing uncertainly with longer post-spill durations).

Three of the deterministic cases included response simulations based on the strategies and capabilities described in Cairn Energy's Oil Spill Response Plan (Cairn Energy, 2011), which was developed for a different West Greenland license area located well to the south of Pitu Block. No contingency plans are currently available for the Pitu Block area. Spill response parameters are described in Section 5.5.1.1 below.

Table 9. Selected deterministic cases for scenarios 1A and 1B.

ID	Spill Event	Type of Deterministic Case[1]	Spill Response Type	Spill Start Date	Simulation Duration (Days)
1A	Melville Bay – 1-Day Blowout	Worst-case Shoreline Length Oiled	Surface dispersant application, mechanical containment/recovery, *in situ* burning	17 August 2012	100
1A	Melville Bay – 1-Day Blowout	Worst-case Water Surface Area Oiled within the North Water Polynya	Surface dispersant application, mechanical containment/recovery, *in situ* burning	1 July 2012	100
1B	Melville Bay – 34-Day Blowout	Worst-case Shoreline Length Oiled	None	9 July 2012	120
1B	Melville Bay – 34-Day Blowout	Worst-case Water Surface Area Oiled within the North Water Polynya	None	27 August 2012	120
1B	Melville Bay – 34-Day Blowout	Worst-case Water Surface Area Oiled within the North Water Polynya	Surface dispersant application, mechanical containment/recovery, *in situ* burning	27 August 2012	120
1B	Melville Bay – 34-Day Blowout	Worst-case Volume of Oil in the Water Column	None	31 July 2014	120

[1] The "worst case" for a given consequence metric was defined as the trajectory with the 95th percentile value for oiling above the ecological threshold (i.e., 100 g/m^2 for the shoreline, and 10 g/m^2 for the water surface).

5.5.1.1 Response Parameters

The spill response simulations for scenarios 1A and 1B involved a multi-faceted approach including mechanical containment/recovery operations, *in situ* burning, and the application of surface dispersants. Modeling of spill response operations in SIMAP involves setting various parameters for oil removal rates for each type of response activity, based on user inputs. The user defines reasonable assumptions regarding operations and logistics, maximized removal rates, thresholds for effectiveness, response timing, and areas of response operations.

SIMAP then simulates the behavior of the oil based on its chemical and physical properties in the particular environment into which the oil is released. Oil removal is assumed to occur in the areas designated by the user as long as certain criteria are met and designated thresholds are not exceeded. SIMAP essentially determines whether oil removal is possible given the specific environmental conditions (wave height, winds, etc.) and the behavior of the oil (spreading on the water surface, viscosity, etc.).

For both scenarios 1A and 1B, the different response types were applied to two response zones, the offshore area near the well site and in deeper waters (the offshore response zone) and the nearshore areas along the coast (the nearshore response zone). The extents of these two response operation zones can be seen in Figure 28. The operational zones were based on criteria of the approximate spread of the thickest oil, water depth, and distance from shore. Generally, response vessels and aircraft would be expected to work relatively near to the well site to remove the freshest oil. This oil would tend to be thicker on the water surface, less spread out, and less viscous to allow for greater removal efficiency. Responders may choose to follow larger oil patches up to a certain point offshore (about 180 km). Further offshore operations would cause safety concerns, as well as operational/logistical issues with regard to fueling. In the simulations, mechanical containment/recovery and surface dispersant application took place in both the nearshore and offshore zones. *In situ* burning was only applied in the offshore zone (i.e., a minimum distance of 10 kilometers from shore) (Steiner, 2011).

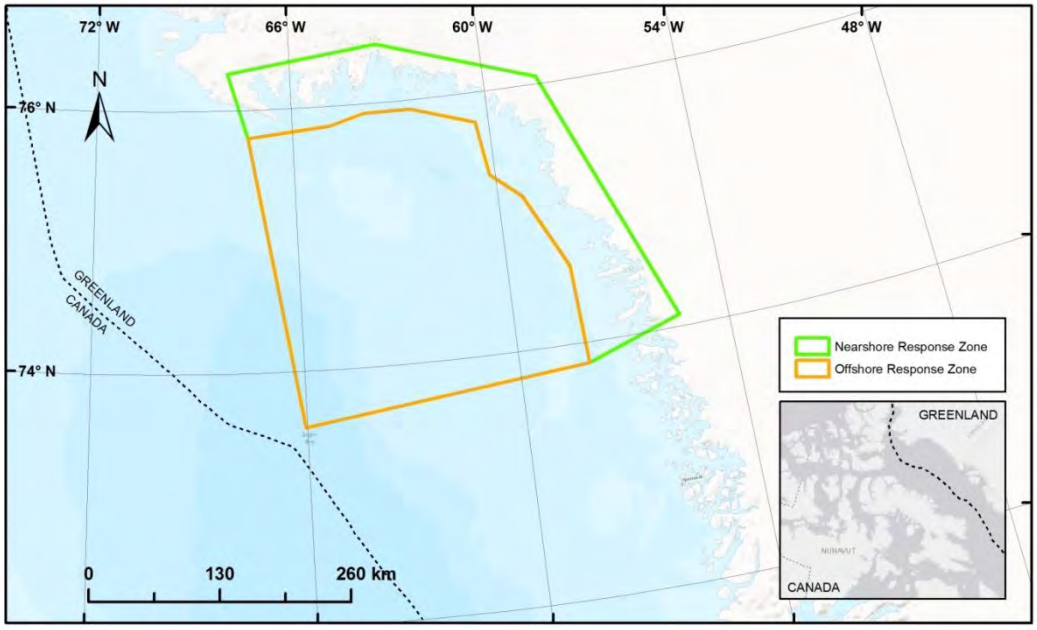

Figure 28. Nearshore and offshore response zones for scenarios 1A and 1B.

In order for response operations to be reasonably effective, certain environmental and physical parameters must be met. If these thresholds are exceeded (or not met, in the case of minimum oil thickness, minimum water depth, and minimum wind speed), response operations are assumed to cease until the conditions next meet the criteria.

For mechanical containment/recovery, the oil needs to be thick enough on the water surface for skimming equipment to be effective. In addition, the winds, currents, and sea state need to be such that containment booms are effective and there is no splashing over or entrainment (oil moving under the boom). Offshore and nearshore mechanical recovery operations are compromised when ice coverage exceeds about 20%, and becomes relatively ineffective above about 40% cover (Evers et al., 2006). Another factor that significantly affects mechanical removal effectiveness in the field is the viscosity of the oil. Mechanical recovery (skimming) systems are usually most effective on relatively fresh oil. Once emulsification occurs, the oil becomes more viscous (by as much as 1,000 times) and increases its water content to about 70% (Fingas, 2001; 2011). These changes in oil properties present challenges for spill response operations. Many oil skimmers work considerably less efficiently (if at all) on emulsified, viscous oil, though some types of systems work better with increasing viscosity. The high water content of emulsified oil means considerably more volume of oil-water emulsion to recover, which increases the requirements for temporary storage capacity and transport for disposal or processing. Based on research into skimmer effectiveness (Dale, 2011a; 2011b), the thresholds for viscosity (i.e., the viscosities above which skimmers are ineffective) were assumed to be 80 cP in the nearshore zone, where the equipment would be mainly weir skimmers, and 15,000 cP in the offshore zone, where the equipment would mainly be oleophilic skimmers (Cairn Energy, 2011).

For surface dispersant application, the response is effective only if the environmental and physical criteria are met and there are sufficient chemical dispersants available (until the supply

runs out). Dispersant operations would only be successful if the oil were of sufficient thickness on the water surface and of a viscosity below 20,000 cP. In order to be effective, there needs to be sufficient mixing energy in the water, which requires a minimum wind speed of 3 knots. The maximum wind speed would be 27 knots, which is not related to mixing energy, but rather to the safety of flying aircraft. In order not to cause damages to nearshore organisms through higher concentrations of chemically-dispersed oil, a minimum water depth of 10 meters was assumed. Offshore and nearshore surface dispersant operations are assumed to be compromised when ice coverage exceeds about 30%.

For *in situ* burning, oil needs to be thick enough on the water surface and relatively free of emulsification, because water content above 60% would hinder ignition and burning. Wind speed needs to be low enough to allow burning to occur and to hinder the smoke plume from moving too far. Sea state and current speed need to be below thresholds that would significantly reduce the effectiveness of containment boom, since oil needs to be contained within fire boom to allow for burning to be effective. Ice coverage needs to be less than 30% or more than 70%. These values are based on the fact that the oil needs to be either held by ice, be on top of ice, or be in relatively open water for the burning operations to be effective.

The environmental and physical thresholds for effective response that were applied in the model simulations are summarized in Table 10.

Table 10. Environmental and physical thresholds for effective response used in model simulations.

Response Type	Response Zone	Min. Wind Speed (knots)	Max. Wind Speed (knots)	Max. Current Speed (knots)	Max. Wave Height (m)	Ice Cover (%)	Min. Water Depth (m)	Min. Oil Thickness (µm)	Max. Oil Viscosity (cP)	Max. Oil Water Content (%)
Mechanical containment/ recovery	Nearshore	-	30	0.7	1.07	<20	-	8	80	-
Mechanical containment/ recovery	Offshore	-	30	0.7	1.07	<20	-	8	15,000	-
In situ burning	Offshore	-	30	0.7	0.3	<30, >70	-	8	-	60
Surface dispersant application	Nearshore and Offshore	3	27	-	-	<30	10	8	20,000	-

Table 11 summarizes the timing and daily oil removal/treatment capacities assumed for the simulated response operations for scenarios 1A and 1B. The initial starting times for all spill response operations were assumed to be 48 hours after the onset of the oil release from the well, based on information in the Cairn Oil Spill Contingency Plan (Cairn Energy, 2011) and Steiner (2011). Response operations were assumed to continue until hindered by ice coverage or the various thresholds for response effectiveness were exceeded (Table 10), including the lack of recoverable oil on the water surface.

Table 11. Timing and daily oil removal/treatment capacities assumed for the response operations in scenarios 1A and 1B.

Response Type	Response Zone	Response Start (hrs after spill start)	Response End	Response Timeframe	Oil Removed/ Treated per Day (m^3)
Mechanical containment/ recovery	Nearshore	48	End of simulation or end of response timeframe (whichever is sooner)	July to November	30
Mechanical containment/ recovery	Offshore	48	End of simulation or end of response timeframe (whichever is sooner)	July to October	90
In situ burning	Offshore	48	End of simulation	Year-round	878
Surface dispersant application	Nearshore and Offshore	48	Day 36 post-spill start, or end of response timeframe (whichever is sooner)	July to October	888

In the case of surface dispersant application operations, the Cairn Oil Spill Contingency Plan (Cairn Energy, 2011) states that responders have access to 400,000 gallons of dispersant for surface applications. This volume of dispersant can treat 8 million gallons of oil (190,476 bbl or 30,284 m^3 total) at a 1:20 dispersant to oil ratio. Based on the operating assumptions described above, this volume of dispersant would be exhausted after 34 days of operations. Based on the monthly average ice cover data from TOPAZ4, it was expected that dispersants would only be applied during July through October.

Mechanical containment/recovery was assumed to continue until the end of the model simulation, or until the end of the possible response timeframe (based on monthly average ice cover), whichever was sooner. In the offshore operations zone, the window for mechanical recovery operations was assumed to be July through October. For the nearshore area, the possible response timeframe was assumed to be July through November. It was assumed that there would be no seasonal restrictions (due to ice cover) on *in situ* burning activities in the simulations.

All spill response operations are assumed to occur for 12 hours a day with a 12-hour rest period. In the per-day removal rates in Table 11, the operational period or “day” is assumed to be 12 hours. While daylight hours would exceed 12 hours for significant portions of the response operations in these northern latitudes, the operational period is still considered to be 12 hours. The reason for this is that there will always be issues related to required down-time for equipment maintenance, mobilization times (on site), disposal of recovered liquids, and rest periods for workers (even with shift changes). This assumption is based on the consensus of response experts and research studies into this issue.

In addition to the daily 12-hour operational periods, another restriction was added with respect to logistical and safety concerns related to weather. Research studies (e.g., DeCola et al., 2006, Nuka Research and Planning Group, 2014) have indicated that spill response operations in Arctic conditions, even during open water and summer seasons, are compromised by weather, cold temperatures, and other factors that affect effectiveness about 52% of the time. When operations are halted, curtailed, or postponed due to weather issues, it generally takes another 20% of that time to re-mobilize and resume normal operations. For all of the surface response

operations, an assumption of 62.5% of non-operation time was assumed on top of the existing 12-hour operational time frames.

For additional discussion regarding the development of the spill response assumptions, see Appendix A.

5.5.2 Deterministic Results

Note: Because the deterministic simulations for this spill site were run longer than the corresponding stochastic simulations (i.e., 100 vs. 46 days for scenario 1A and 120 vs. 79 days for scenario 1B), the deterministic results presented herein are not directly comparable to the stochastic results reported in Section 5.4.2. Similarly, the selection criteria used to identify the deterministic cases from the stochastic analysis should be interpreted with caution. For example, the worst case shoreline length oiled trajectory in the stochastic analysis (79-day simulation) may no longer be the worst case shoreline length oiled trajectory when simulated for 120 days in the deterministic analysis.

Key results from the deterministic simulations for the Melville Bay blowout scenarios are summarized in Table 12, including volume of water exceeding 1 ppb of dissolved aromatics (the most toxic components of oil), water surface area oiled, shoreline length oiled, time to first reach shore, and peak volume of oil ashore.

Table 12. Summary of deterministic results for the Melville Bay 1-day and 34-day blowout scenarios.

ID	Deterministic Case	Volume of Water Exceeding 1 ppb of Dissolved Aromatics (m^3)	Water Surface Area Oiled Above 0.01 g/m^2 (km^2)	Water Surface Area Oiled Above 10 g/m^2 (km^2)	Shoreline Length Oiled Above 100 g/m^2 (km)	Time to Shore (Days)	Peak Volume of Oil Ashore (m^3)
1-day Blowout							
1A	Worst-case Shoreline Length Oiled, with Response	2.6×10^9	544.6	40.7	91.8	22.8	452.3
1A	Worst-case Water Surface Area Oiled within the North Water Polynya, with Response	3.3×10^9	104.1	60.5	84.6	23.6	835.3
34-day Blowout							
1B	Worst-case Shoreline Length Oiled	2.9×10^{10}	7,660.6	1,183.8	1,310.5	16.6	22,435.3
1B	Worst-case Water Surface Area Oiled within the North Water Polynya	2.4×10^{10}	17,671.2	895.4	945.8	12.6	19,178.2
1B	Worst-case Water Surface Area Oiled within the North Water Polynya, with Response	3.9×10^{10}	14,514.2	681.5	878.9	12.7	17,061.9
1B	Worst-case Volume of Oil in the Water Column [1]	1.7×10^{10}	19,639.7	1,054.4	793.6	8.3	14,347.4

[1]Note: This case was selected from the stochastic analysis based on the 95th percentile case for total hydrocarbons in the water column, which is used as a proxy for evaluating water column contamination. The detailed deterministic modeling provides more specific water column contamination metrics, namely the volume of water

contaminated above 1 ppb of dissolved aromatics (a screening threshold for impacts on sensitive water column organisms). The worst case volume of total hydrocarbons in the water column does not necessarily result in the worst case volume of water contaminated above 1 ppb of dissolved aromatics, as many factors are involved (including simulation length).

The following figures (Figure 29 through Figure 40) present the results of the deterministic simulations for each scenario. Three figures are shown for each deterministic case:

1. **Maximum Floating Oil Concentration**: This map shows the maximum concentration (g/m^2) of floating oil that passed through a given area at some point during the simulation. This map also displays the approximate subsurface area swept by dissolved aromatic concentrations greater than 1 ppb. This concentration is used as a screening threshold for potential impacts on sensitive water column organisms (based on French McCay, 2009).

2. **Shoreline Oil Concentration**: This map shows the concentration (g/m^2) of oil on the shoreline at the end of the simulation.

3. **Mass Balance**: This graph shows a time history of the fate and weathering of the spilled oil during the simulation. Components of the oil tracked over time include amount of oil on the sea surface, on the shoreline, in the water column (subsurface), in subsea sediments, evaporated into the atmosphere, removed (for simulations including mechanical removal and/or burning), and decayed (e.g., by photo-oxidation, biodegradation).

A brief description of each deterministic scenario follows the figures for each case.

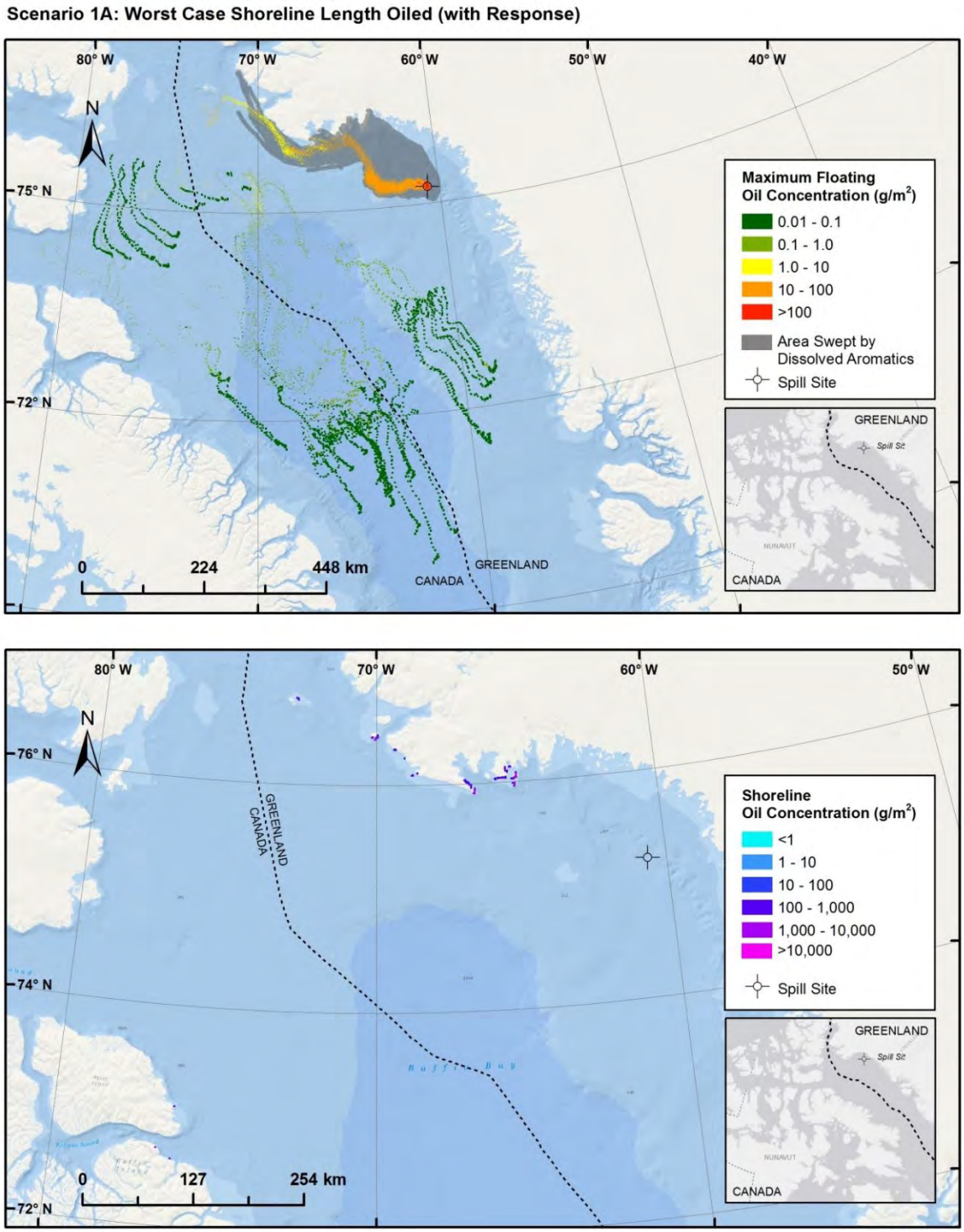

Figure 29. Scenario 1A: Worst-case (95th percentile) trajectory for shoreline length oiled above 100 g/m^2, with spill response (surface dispersant, mechanical containment/recovery, and *in situ* burning) – Maximum concentration (g/m^2) of floating oil that passed by a given area during the simulation and the subsurface area swept by dissolved aromatics (top panel); and total concentration (g/m^2) of oil on the shoreline at the end of the simulation (bottom panel).

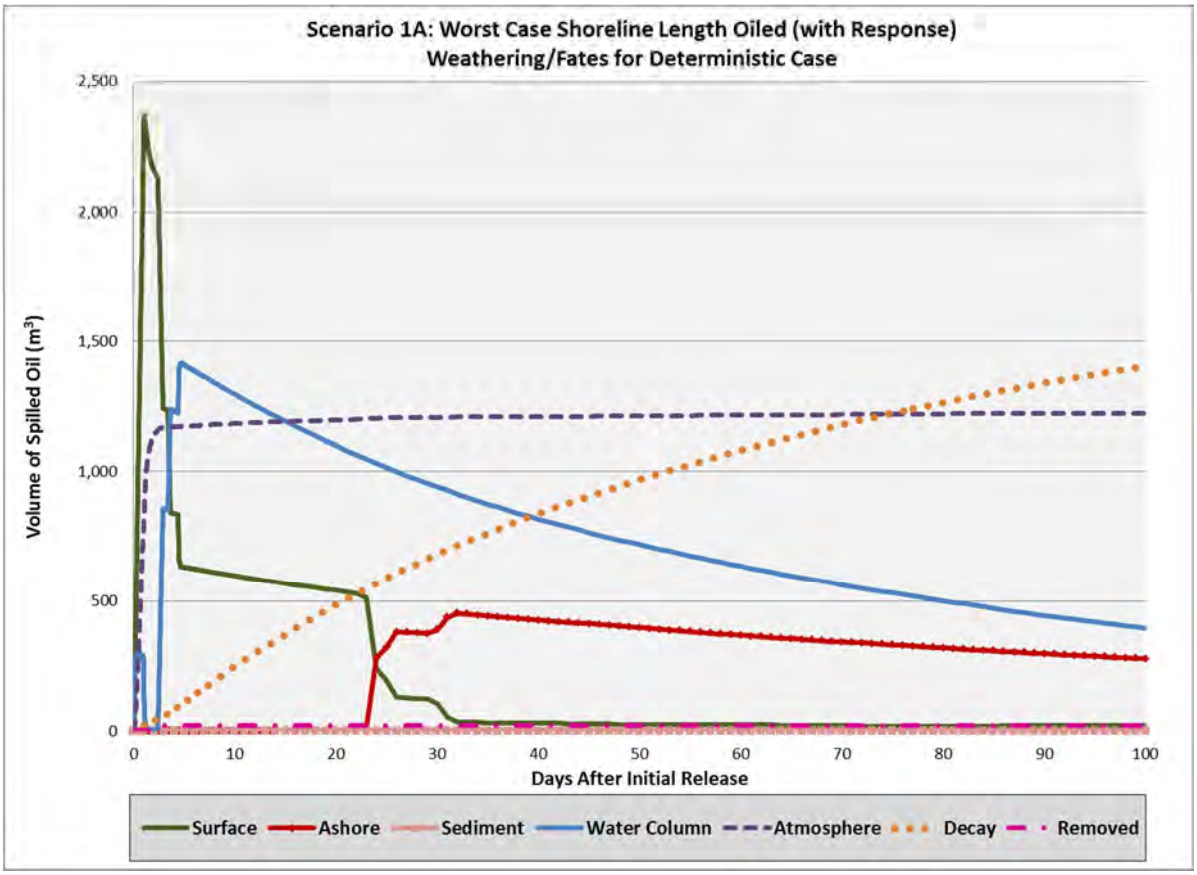

Figure 30. Scenario 1A: Worst-case (95th percentile) trajectory for shoreline length oiled above 100 g/m^2, with spill response (surface dispersant, mechanical containment/recovery, and *in situ* burning) – Mass balance graph.

For scenario 1A, the worst-case trajectory for shoreline length oiled was modeled with spill response, including surface dispersant application, mechanical containment/recovery, and *in situ* burning (Figure 29 and Figure 30).

The spill trajectory initially heads to the west of the spill site, turning north at about 20 days after the start of the spill, and oiling shoreline near the settlement of Savissivik, Greenland at 22.8 days into the simulation. Lower concentrations of floating oil then continue to travel west along the coast of Greenland and north into the North Water Polynya area, oiling shorelines near Kap York, Kap Atholl, and Carey Islands. Discontinuous areas of low concentration surface oil are found in Baffin Bay late in the simulation (visible on Figure 29 as patchy lines). By 32 days post-spill, <1% of the volume spilled remains on the water surface.

The mass balance graph (Figure 30) shows that the response effort (beginning 2 days post-spill start) reduces the amount of oil on the water surface. This was mainly due to the surface application of dispersants, which reduced the amount of surface floating oil, but increased the amount of oil in the water column. Mechanical containment/recovery and *in situ* burning activities were ineffective after about 1 day of operation, and ultimately removed <1% of the total volume spilled. This is attributable to the spreading of oil on the water surface to thicknesses not amenable to recovery and the chemical dispersant operations that reduced surface oil. Increasing oil viscosity may also have played a role. As viscosity increases, the removal capability of the mechanical

recovery equipment and burning effectiveness are limited. Both of these methods work best on very fresh oil.

Evaporation plays a major role in removal, with about 37% of the spilled volume evaporated, most of which occurred during the first 2 days. Natural decay processes also play a large role, with about 42% of the spilled volume removed by natural decay processes such as biodegradation and photo-oxidation by the end of the 100-day simulation. The peak volume on the shoreline was 452.3 m^3, at 32 days after the spill start. At the end of the simulation, 277.5 m^3 of oil remains on shore, with a total of 91.8 km of shoreline oiled above the ecological threshold of 100 g/m^2.

In general, the subsurface area swept by dissolved aromatics (the most toxic components of oil) followed the same trajectory as the surface oil, extending somewhat beyond the surface oil footprint and sweeping the area between the spill site and the shoreline to the north. The peak volume of water exceeding 1 ppb of dissolved aromatics (a screening threshold for impacts on sensitive water column organisms) was 2.6×10^9 m^3. At the end of the simulation, about 395.6 m^3 of oil remains entrained in the water column and over time will tend to move with the prevailing subsurface currents.

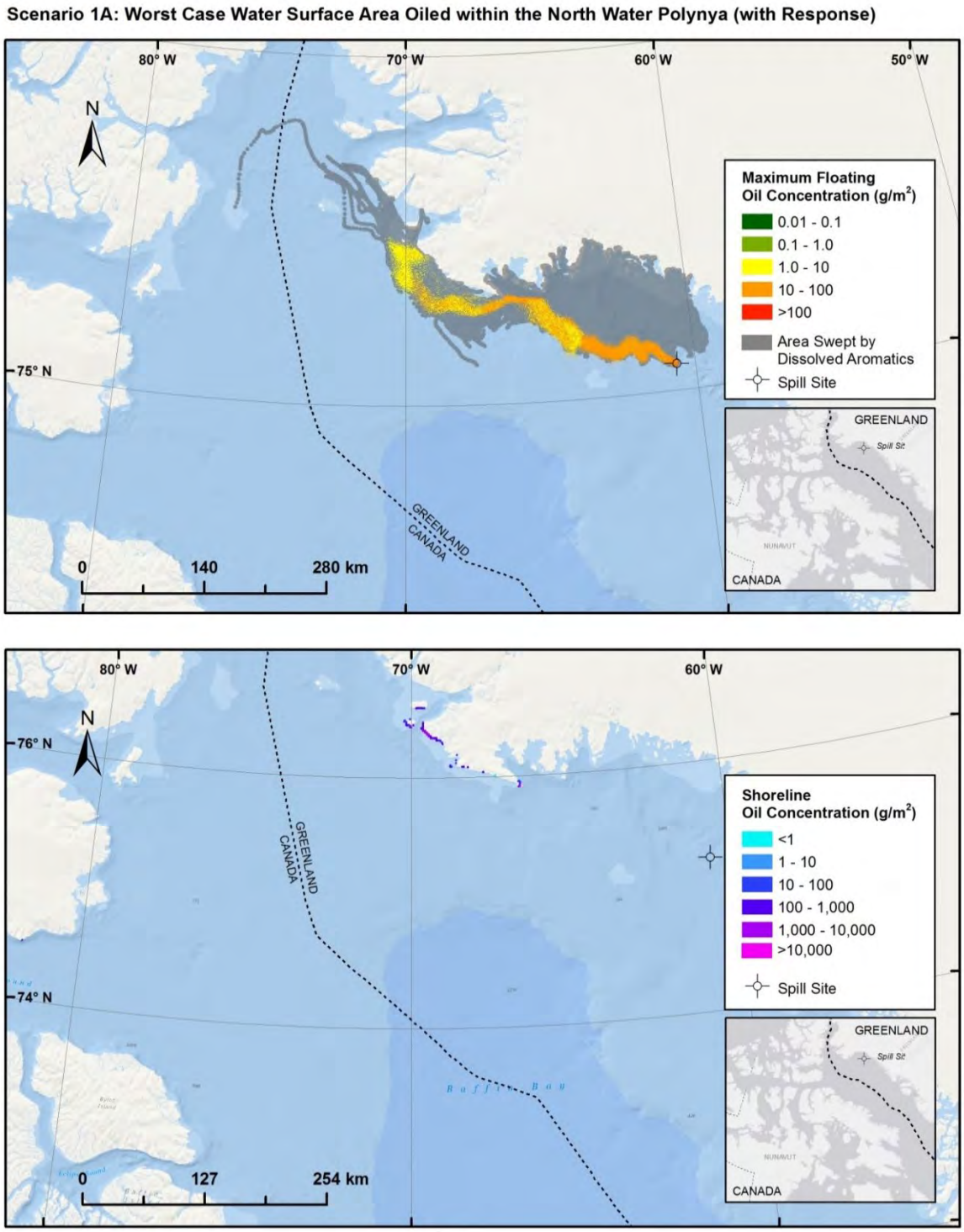

Figure 31. Scenario 1A: Worst-case (95th percentile) trajectory for water surface area oiled above 10 g/m^2 within the North Water Polynya, with spill response (surface dispersant, mechanical containment/recovery, and *in situ* burning) – Maximum concentration (g/m^2) of floating oil that passed by a given area during the simulation and the subsurface area swept by dissolved aromatics (top panel); and total concentration (g/m^2) of oil on the shoreline at the end of the simulation (bottom panel).

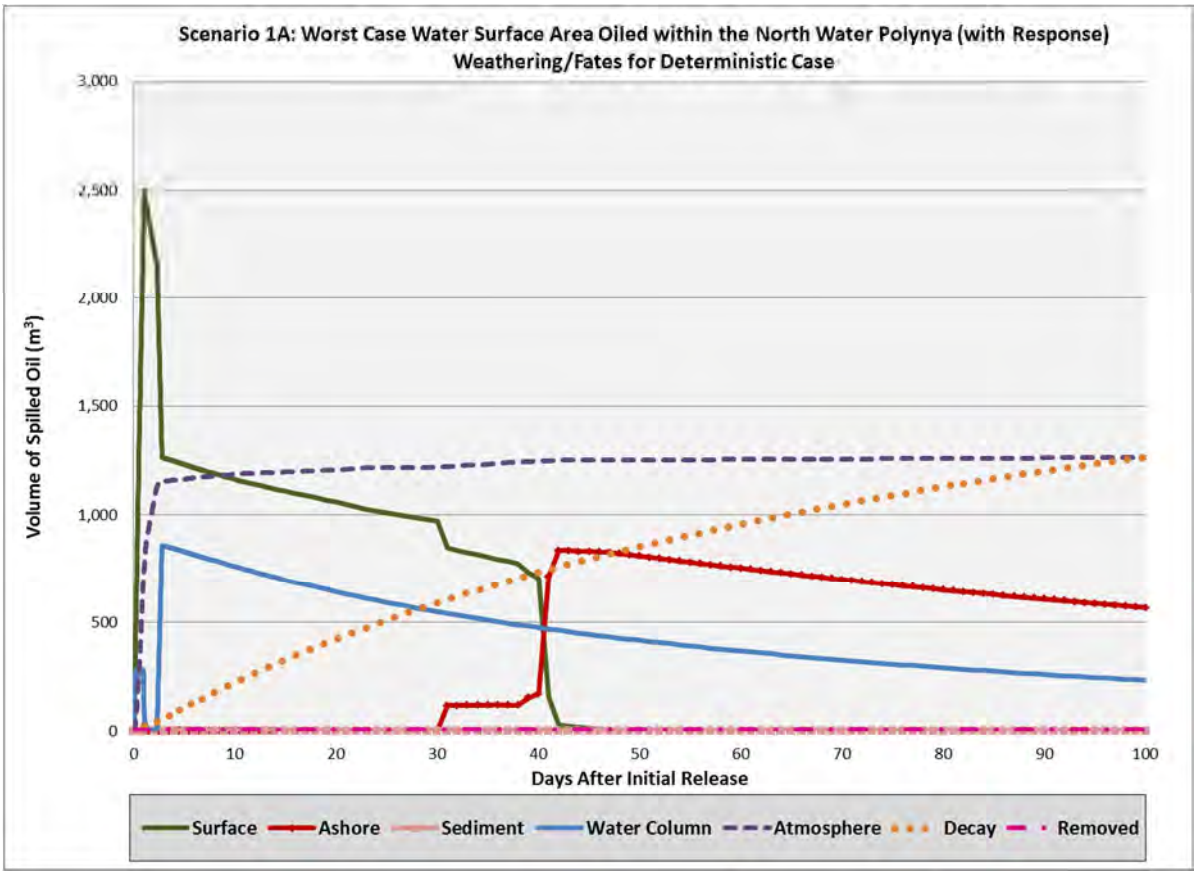

Figure 32. Scenario 1A: Worst-case (95th percentile) trajectory for water surface area oiled above 10 g/m^2 within the North Water Polynya, with spill response (surface dispersant, mechanical containment/recovery, and *in situ* burning) – Mass balance graph.

For scenario 1A, the worst-case trajectory for water surface oiling within the North Water Polynya was modeled with spill response, including surface dispersant application, mechanical containment/recovery, and *in situ* burning (Figure 31 and Figure 32).

The spill trajectory initially heads to the northwest of the spill site, becoming trapped against the edge of landfast ice between the settlement of Savissivik and Kap York and first reaching shore to the west of Kap York at 23.6 days into the simulation. Upon retreat of the landfast ice, the trapped floating oil is released and continues to travel west along the coast of Greenland and north into the North Water Polynya area, oiling shorelines near Kap York and Kap Atholl. A small amount of oil reaches the shoreline of south Devon Island at 87 days into the simulation. By 42 days post-spill, <1% of the volume spilled remains on the water surface.

The mass balance graph (Figure 32) shows that response effort (beginning 2 days post-spill start) reduces the amount of oil on the water surface. This was mainly due to the surface application of dispersants, which reduced the amount of surface floating oil, but increased the amount of oil in the water column. Mechanical containment/recovery and *in situ* burning activities were ineffective after about half a day of operation, and ultimately removed <0.2% of the total volume spilled. This is attributable to the spreading of oil on the water surface to thicknesses not amenable to recovery and the chemical dispersant operations that reduced surface oil. Increasing

oil viscosity may also have played a role. As viscosity increases, the removal capability of the mechanical recovery equipment and burning effectiveness are limited. Both of these methods work best on very fresh oil.

Evaporation plays a major role in removal, with about 38% of the spilled volume evaporated, most of which occurred during the first 2 days. Natural decay processes also play a large role, with about 38% of the spilled volume removed by natural decay processes such as biodegradation and photo-oxidation by the end of the 100-day simulation. The peak volume on the shoreline was 835.3 m^3, at 42 days after the spill start. At the end of the simulation, 568.6 m^3 of oil remains on shore, with a total of 84.6 km of shoreline oiled above the ecological threshold of 100 g/m^2.

In general, the subsurface area swept by dissolved aromatics (the most toxic components of oil) followed the same trajectory as the surface oil, extending beyond the surface oil footprint and sweeping the area between the spill site and the shoreline to the north. The peak volume of water exceeding 1 ppb of dissolved aromatics (a screening threshold for impacts on sensitive water column organisms) was 3.3×10^9 m^3. At the end of the simulation, about 232.9 m^3 of oil remains entrained in the water column and over time will tend to move with the prevailing subsurface currents.

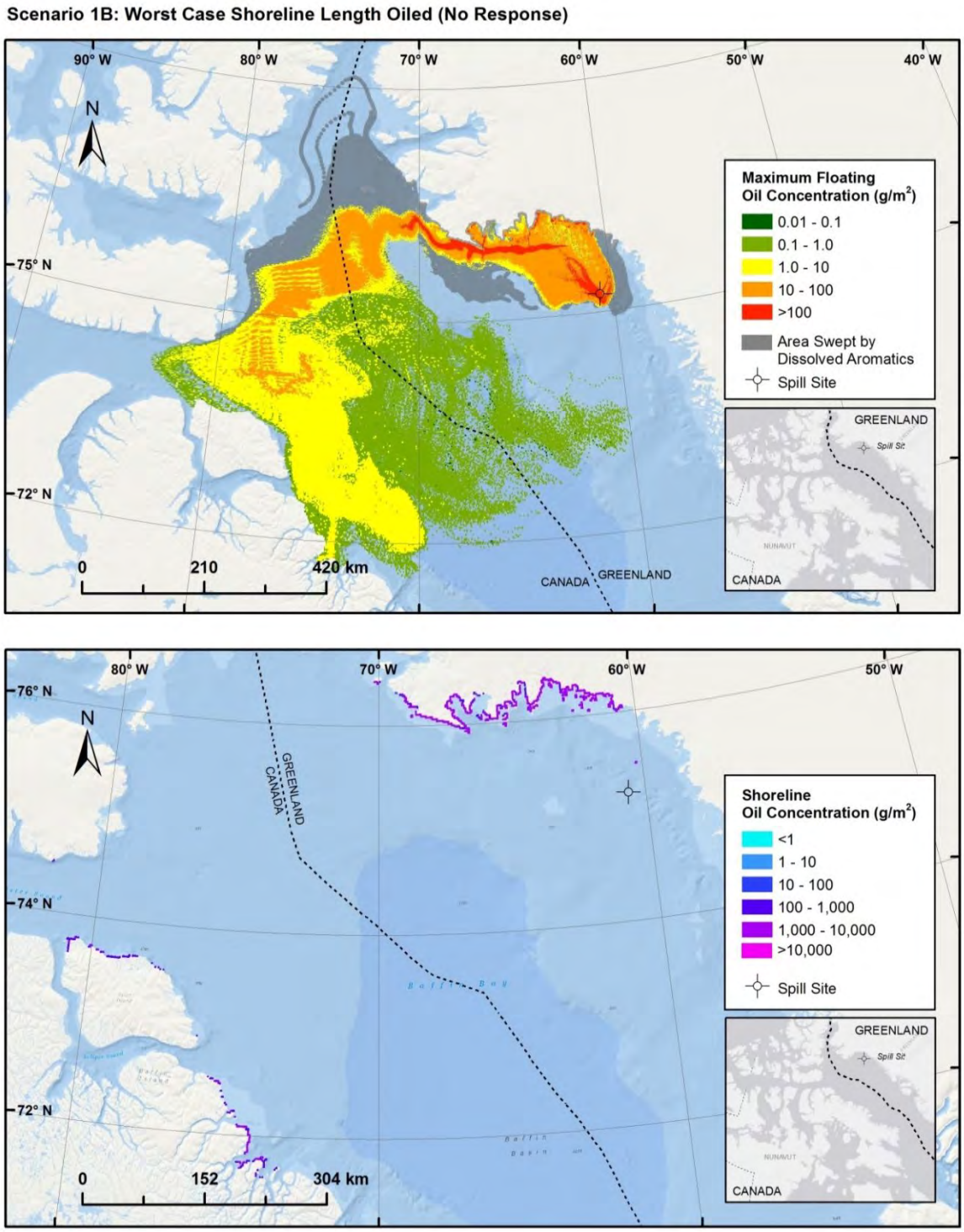

Figure 33. Scenario 1B: Worst-case (95th percentile) trajectory for shoreline length oiled above 100 g/m^2, with no spill response – Maximum concentration (g/m^2) of floating oil that passed by a given area during the simulation and the subsurface area swept by dissolved aromatics (top panel); and total concentration (g/m^2) of oil on the shoreline at the end of the simulation (bottom panel).

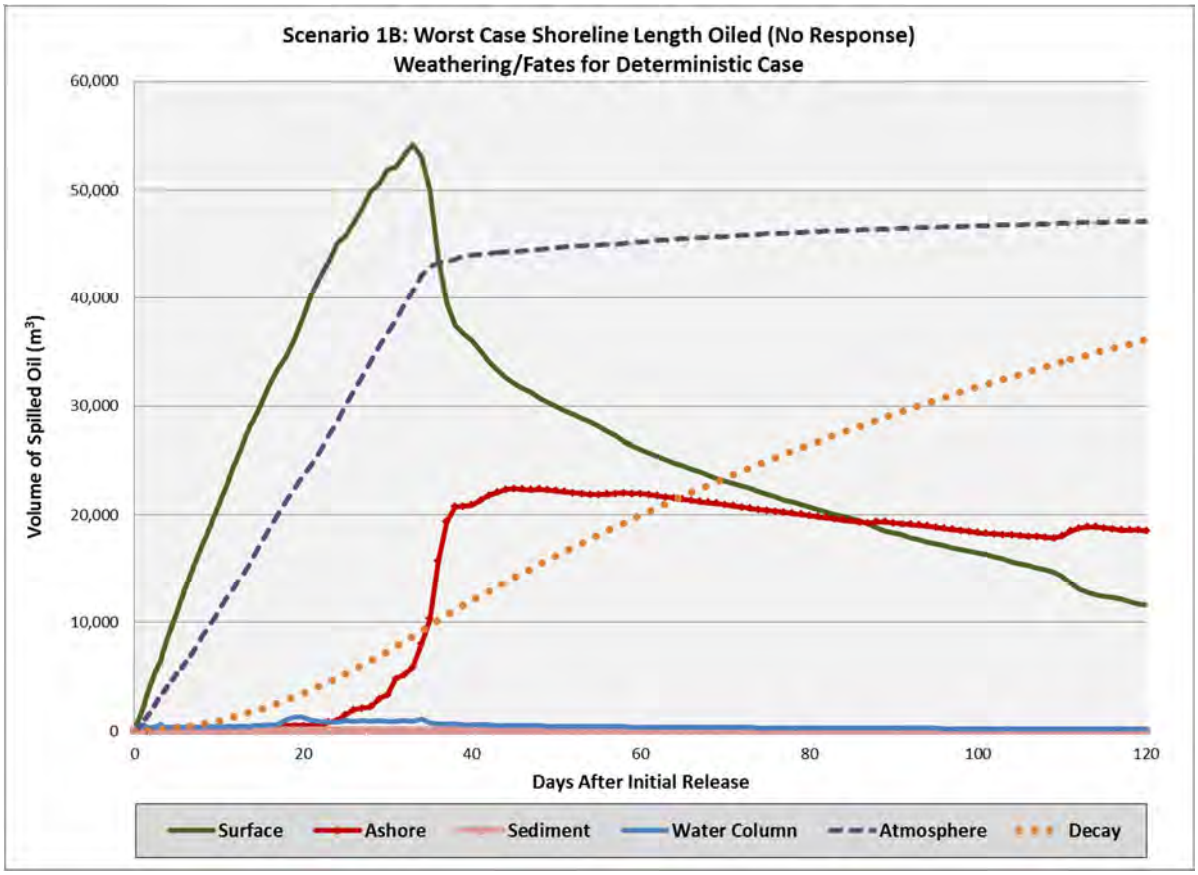

Figure 34. Scenario 1B: Worst-case (95th percentile) trajectory for shoreline length oiled above 100 g/m^2, with no spill response – Mass balance graph.

For scenario 1B, the worst-case trajectory for shoreline length oiled was modeled without spill response (Figure 33 and Figure 34).

The spill trajectory initially heads to the northwest of the spill site, then turns north-northwest, becoming trapped against the edge of landfast ice near the settlement of Savissivik and first reaching shore to the east of Savissivik at 16.6 days into the simulation. Upon retreat of the landfast ice, the trapped floating oil is released and continues to travel west along the coast of Greenland and north into the North Water Polynya area, oiling the Greenlandic coastline along Savissivik, Kap York, and Kap Atholl. At about 34 days into the simulation, floating oil to the west of the spill site also pushes northward into the Greenlandic coast, oiling shoreline areas within the Melville Bay Nature Reserve, nearly as far east as Kap Walker. Floating oil not retained on shore continues to travel westward and southwestward, reaching the shoreline of Devon Island at about 83 days after the spill start, and Bylot Island at about 87 days after the spill start, and Baffin Island at about 108 days after the spill start. At the end of the 120-day simulation, 11,592.4 m^3 of oil (about 10% of the volume spilled) remains on the water surface in Baffin Bay, mostly bound in sea ice. Over time, this oil would continue to move with the ice currents, potentially oiling other areas.

Evaporation plays a major role in removal, with about 41% of the spilled volume evaporated, most of which occurred during the first 34 days. Natural decay processes also play a large role, with about 32% of the spilled volume removed by natural decay processes such as

biodegradation and photo-oxidation by the end of the simulation. The peak volume of oil on the shoreline was 22,435.3 m^3, at 45 days after the spill start. At the end of the simulation, 18,540.0 m^3 of oil remains on shore with 1,310.5 km of shoreline oiled above the ecological threshold of 100 g/m^2.

In general, the subsurface area swept by dissolved aromatics (the most toxic components of oil) followed the same trajectory as the surface oil, extending farther north into the North Water Polynya area. The peak volume of water exceeding 1 ppb of dissolved aromatics (a screening threshold for impacts on sensitive water column organisms) was 2.9×10^{10} m^3. At the end of the simulation, about 159.7 m^3 of oil remains entrained in the water column and over time will tend to move with the prevailing subsurface currents.

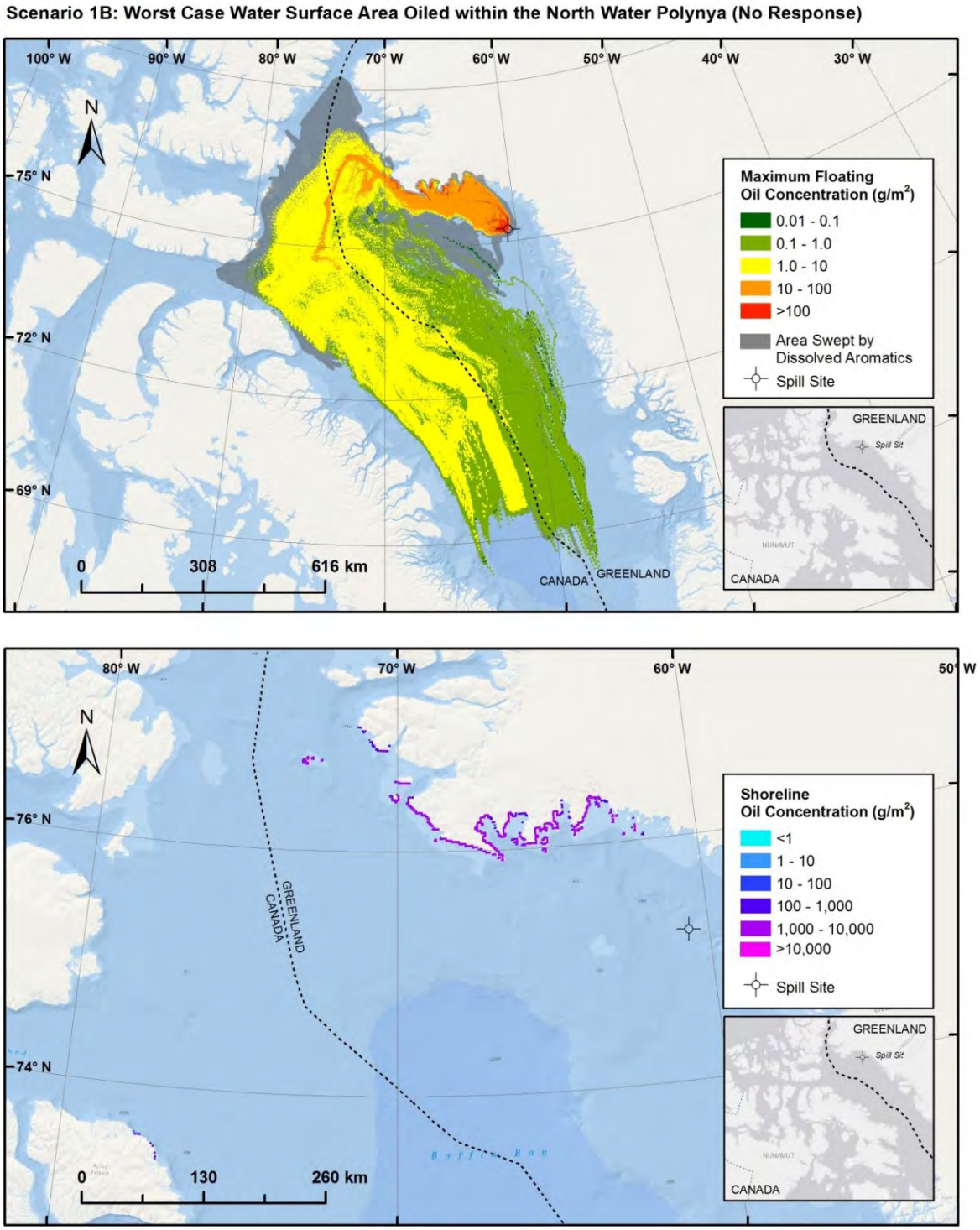

Figure 35. Scenario 1B: Worst-case (95th percentile) trajectory for water surface area oiled above 10 g/m^2 within the North Water Polynya, with no spill response – Maximum concentration (g/m^2) of floating oil that passed by a given area during the simulation and the subsurface area swept by dissolved aromatics (top panel); and total concentration (g/m^2) of oil on the shoreline at the end of the simulation (bottom panel).

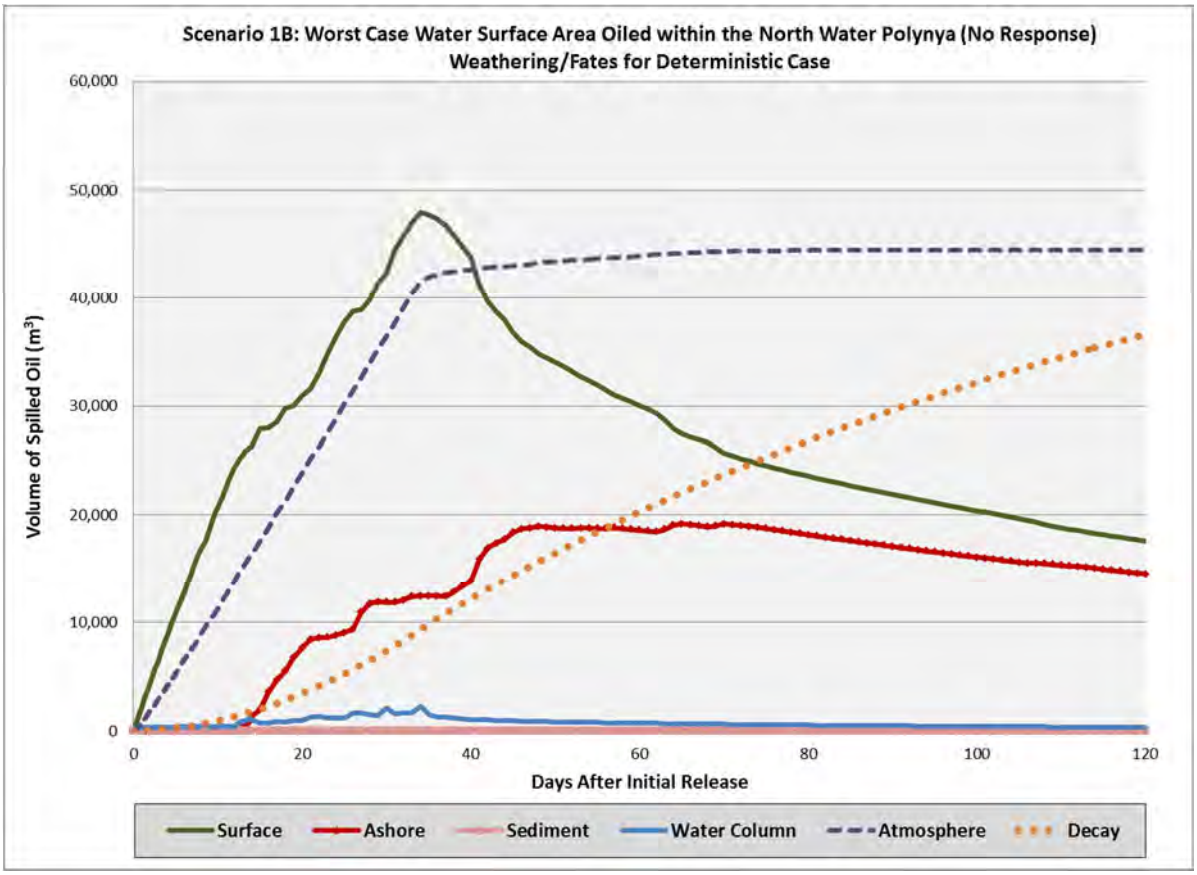

Figure 36. Scenario 1B: Worst-case (95th percentile) trajectory for water surface area oiled above 10 g/m^2 within the North Water Polynya, with no spill response – Mass balance graph

For scenario 1B, the worst-case trajectory for water surface area oiled within the North Water Polynya was modeled without spill response (Figure 35 and Figure 36) and with spill response including surface dispersant application, mechanical containment/recovery, and *in situ* burning (Figure 37 and Figure 38).

For the no-response scenario, the spill trajectory initially heads to the west of the spill site, turning north approximately 8 days after the spill start, and oiling the Greenlandic coast to the north of the spill site within the Melville Bay Nature Reserve at 12.6 days into the simulation. The floating oil trajectory continues to travel northwest along the coast of Greenland and north into the North Water Polynya area, oiling additional shoreline areas including along the settlement of Savissivik, Kap York, Kap Atholl, Kap Parry, and Carey Islands. Floating oil not retained on shore continues to travel westward and southwestward, passing offshore of Devon Island and reaching the shoreline of Bylot Island at about 61 days after the spill start. The remaining floating oil generally travels southeastward in Baffin Bay for the rest of the simulation. By about 65 days into the simulation, the majority of the remaining surface oil is bound in sea ice and moving with the ice currents. At the end of the 120-day simulation, 17,583.2 m^3 of oil (about 15% of the volume spilled) remains on the water surface in Baffin Bay, mostly bound in sea ice. Over time, this oil would continue to move with the ice currents, potentially oiling other areas.

Evaporation plays a major role in removal, with about 39% of the spilled volume evaporated, most of which occurred during the first 34 days. Natural decay processes also play a large role, with about 32% of the spilled volume removed by natural decay processes such as biodegradation and photo-oxidation by the end of the simulation. The peak volume of oil on the shoreline was 19,178.2 m^3, at 70 days after the spill start. At the end of the simulation, 14,543.9 m^3 of oil remains on shore, with a total of 945.8 km of shoreline oiled above the ecological threshold of 100 g/m^2.

In general, the subsurface area swept by dissolved aromatics (the most toxic components of oil) followed the same trajectory as the surface oil, extending farther north into the North Water Polynya area. The peak volume of water exceeding 1 ppb of dissolved aromatics (a screening threshold for impacts on sensitive water column organisms) was 2.4×10^{10} m^3. At the end of the simulation, about 325.8 m^3 of oil remains entrained in the water column and over time will tend to move with the prevailing subsurface currents.

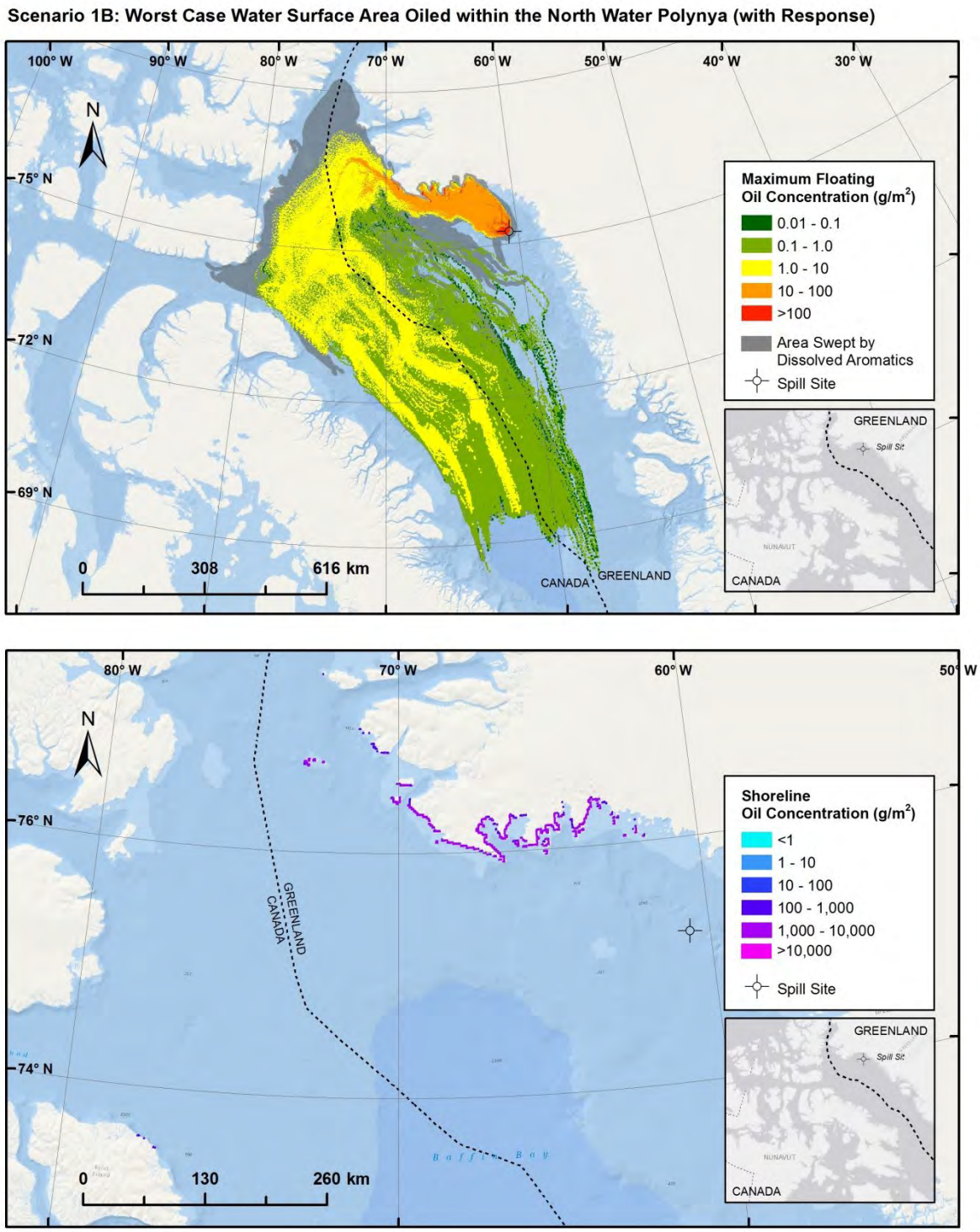

Figure 37. Scenario 1B: Worst-case (95th percentile) trajectory for water surface area oiled above 10 g/m^2 within the North Water Polynya, with spill response (surface dispersant, mechanical containment/recovery, and *in situ* burning) – Maximum concentration (g/m^2) of floating oil that passed by a given area during the simulation and the subsurface area swept by dissolved aromatics (top panel); and total concentration (g/m^2) of oil on the shoreline at the end of the simulation (bottom panel).

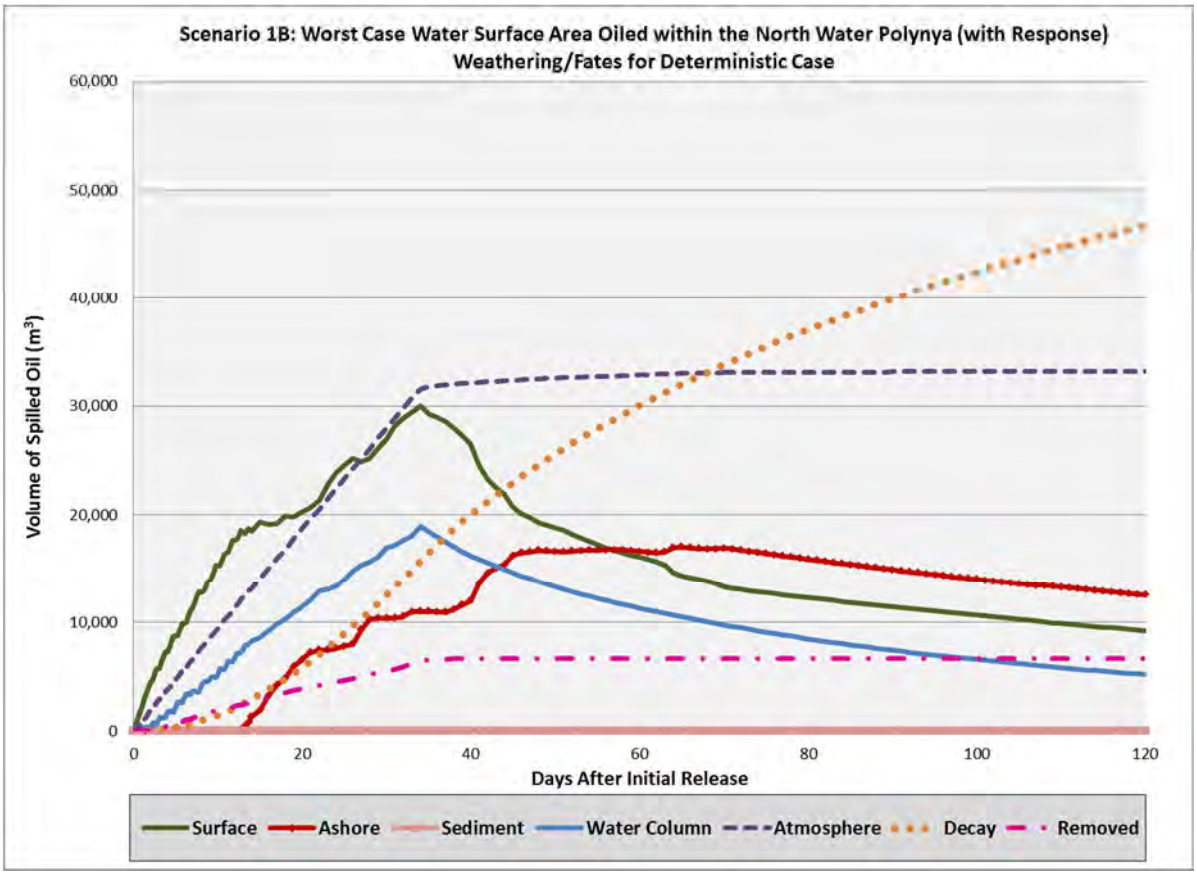

Figure 38. Scenario 1B: Worst-case (95th percentile) trajectory for water surface area oiled above 10 g/m^2 within the North Water Polynya, with spill response (surface dispersant, mechanical containment/recovery, and *in situ* burning) – Mass balance graph

For the scenario 1B worst-case trajectory for water surface area oiled within the North Water Polynya with spill response (Figure 37 and Figure 38), the floating oil follows the same general trajectory described for the no-response scenario in the previous paragraphs. The trajectory initially heads to the west of the spill site, turning north approximately 8 days after the spill start, and oiling the Greenlandic coast to the north of the spill site within the Melville Bay Nature Reserve at 12.7 days into the simulation. The floating oil trajectory continues to travel northwest along the coast of Greenland and north into the North Water Polynya area, oiling additional shoreline areas including along the settlement of Savissivik, Kap York, Kap Atholl, Kap Parry, and Carey Islands. Floating oil not retained on shore continues to travel westward and southwestward, passing offshore of Devon Island and reaching the shoreline of Bylot Island at about 61 days after the spill start. The remaining floating oil generally travels southeastward in Baffin Bay for the rest of the simulation. By about 65 days into the simulation, the majority of the remaining surface oil is bound in sea ice and moving with the ice currents. Over time, this oil would continue to move with the ice currents, potentially oiling other areas.

Though the trajectory is similar between the response and no-response scenarios, the volume of oil on the water surface and on the shoreline is reduced when response (beginning 2 days post-spill start) is applied. At the end of the 120-day simulation, 9,259.3 m^3 of oil (about 8% of the volume spilled) remains on the water surface in Baffin Bay. This is reduced from 17,583.2 m^3

(about 15% of the volume spilled) in the no-response case. The peak volume of oil on the shoreline was 17,061.9 m^3, at 65 days after the spill start, compared to 19,178.2 m^3 in the no-response case. At the end of the simulation, 12,552.1 m^3 of oil remains on shore, with a total of 878.9 km of shoreline oiled above the ecological threshold of 100 g/m^2 (reduced from 945.8 km in the no-response case).

Mechanical containment/recovery and *in situ* burning activities were ineffective after about 37 days of operation, and ultimately removed about 6% of the total volume spilled. This is attributable to the spreading of oil on the water surface to thicknesses not amenable to recovery and the chemical dispersant operations that reduced surface oil. Increasing oil viscosity may also have played a role. As viscosity increases, the removal capability of the mechanical recovery equipment and burning effectiveness are limited. Over the course of the 34-days of release from the well, the response worked best on the fresh oil that had just been released and had more limited effectiveness on the weathered oil released during the previous days.

The removal of oil from the water surface and shoreline was mainly due to the surface application of dispersants, which increased the volume of oil entrained in the water column at the end of the simulation from 325.8 m^3 in the no-response case to 5,196.1 m^3 in the response case. The application of dispersants also increased the subsurface area swept by dissolved aromatics (the most toxic components of oil), extending beyond the surface footprint is nearly all directions. The peak volume of water exceeding 1 ppb of dissolved aromatics (a screening threshold for impacts on sensitive water column organisms) was 3.9×10^{10} m^3 (increased from 2.4×10^{10} in the no-response case).

Like the no-response case, evaporation plays a role in removal, with about 29% of the spilled volume evaporated, most of which occurred during the first 34 days. Natural decay processes also play a large role, with about 41% of the spilled volume removed by natural decay processes such as biodegradation and photo-oxidation by the end of the simulation.

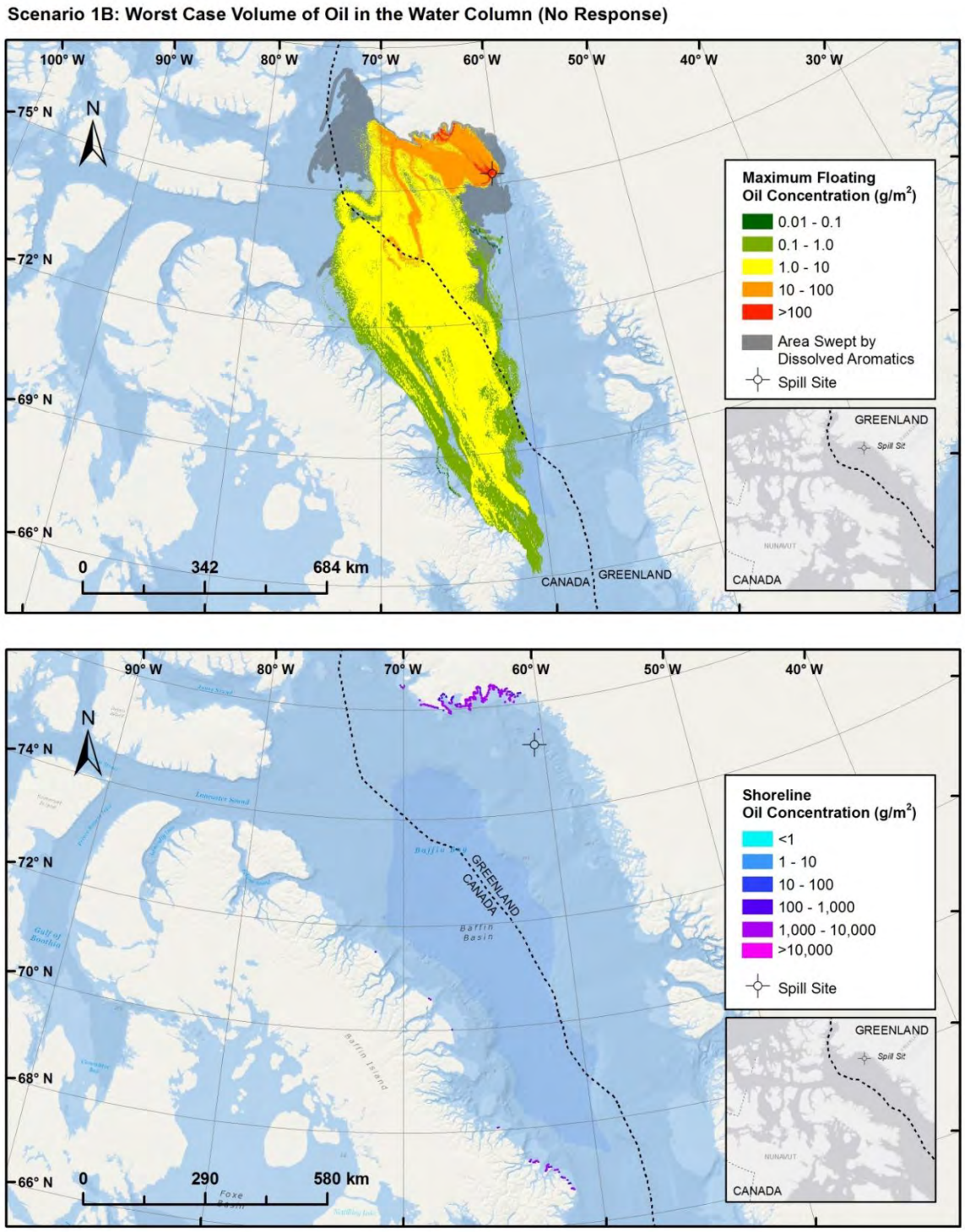

Figure 39. Scenario 1B: Worst-case (95th percentile) trajectory for volume of oil in the water column, with no spill response – Maximum concentration (g/m^2) of floating oil that passed by a given area during the simulation and the subsurface area swept by dissolved aromatics (top panel); and total concentration (g/m^2) of oil on the shoreline at the end of the simulation (bottom panel).

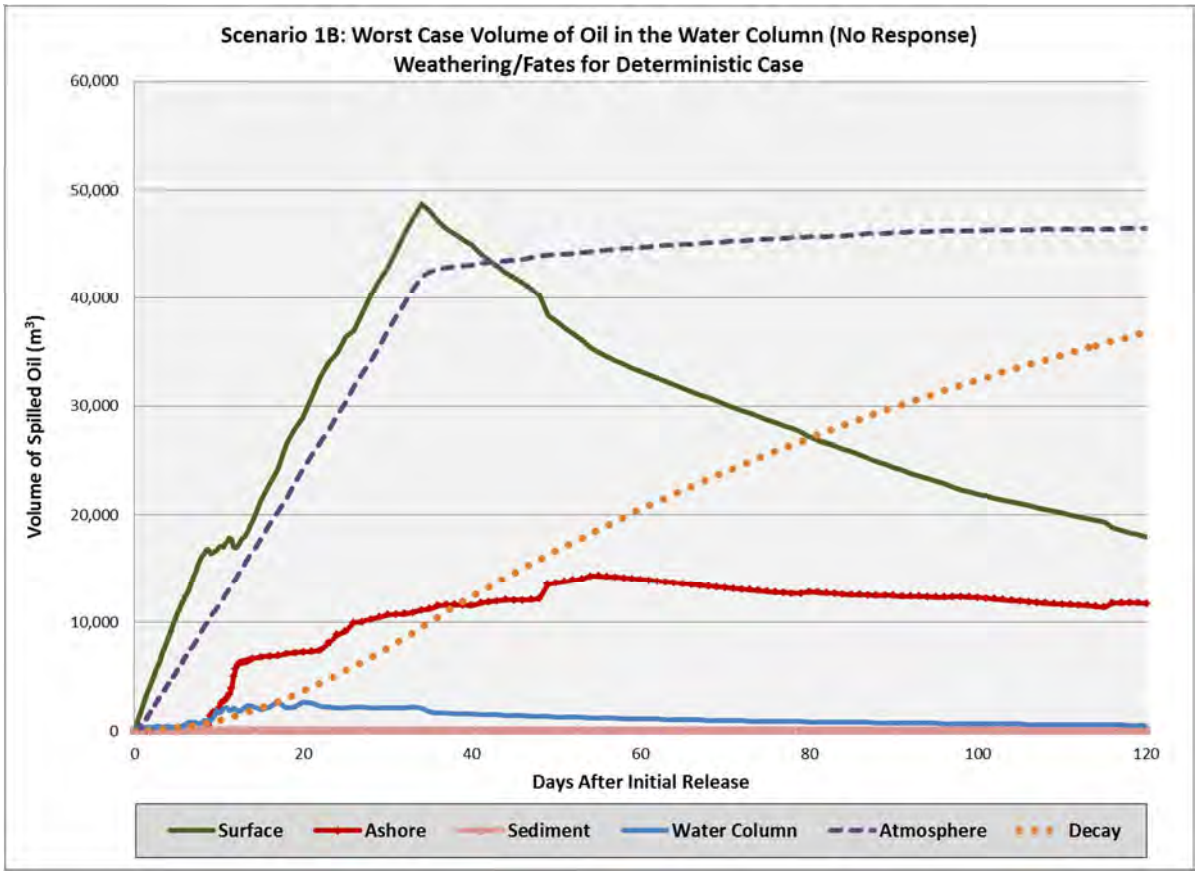

Figure 40. Scenario 1B: Worst-case (95th percentile) trajectory for volume of oil in the water column, with no spill response – Mass balance graph.

For scenario 1B, the worst-case trajectory for volume of oil in the water column was modeled without spill response (Figure 39 and Figure 40).

The spill trajectory initially heads to the northwest of the spill site, first oiling shoreline to the east of the settlement of Savissivik at 8.3 days into the simulation. Floating oil continues to travel north, northwest, and west along the coast of Greenland and into the North Water Polynya area, oiling the Greenlandic coastline within the Melville Bay Nature Reserve and including the settlement of Savissivik and Kap York. Floating oil not retained on shore begins to turn south at about 52 days after the spill start, and travels generally southward through Baffin Bay for the remainder of the simulation. By about day 90 of the simulation, that majority of the remaining floating oil is bound in sea ice and moving with the ice currents. Oil reaches the shoreline of Baffin Island at various locations at about 95, 111, and 115 days after the spill start, including areas as far south as Cape Dyer. At the end of the 120-day simulation, 17,998.9 m^3 of oil (about 16% of the volume spilled) remains on the water surface in Baffin Bay, mostly bound in sea ice. Over time, this oil would continue to move with the ice currents, potentially oiling other areas.

Evaporation plays a major role in removal, with about 41% of the spilled volume evaporated, most of which occurred during the first 34 days. Natural decay processes also play a large role, with about 32% of the spilled volume removed by natural decay processes such as biodegradation and photo-oxidation by the end of the simulation. The peak volume of oil on the

shoreline was 14,347.4 m^3, at 55 days after the spill start. At the end of the simulation, 11,775.8 m^3 of oil remains on shore, with a total of 793.6 km of shoreline oiled above the ecological threshold of 100 g/m^2.

In general, the subsurface area swept by dissolved aromatics (the most toxic components of oil) followed the same trajectory as the surface oil, extending farther north into the North Water Polynya area and slightly south and east of the spill site. The peak volume of water exceeding 1 ppb of dissolved aromatics (a screening threshold for impacts on sensitive water column organisms) was 1.7 x 10^{10} m^3. At the end of the simulation, about 515.9 m^3 of oil remains entrained in the water column and over time will tend to move with the prevailing subsurface currents.

5.6 Conclusions

The hypothetical scenario 1B blowout (34 days of flow for a total spill volume of 113,560 m^3), if it were to occur, would be the fourth largest well blowout ever in the world, based on current records. Only 0.5% of blowouts have ever been of this size or larger. The smaller scenario 1A (1 day of flow for a total spill volume of 3,340 m^3) – would be the 15th largest well blowout incident worldwide. Only 2% of blowouts have ever been this size or larger. Both of these scenarios represent relatively extreme volumes for blowouts, with a very low likelihood of occurrence.[3]

Based on the stochastic analyses, both of the scenarios are highly likely to cause shoreline oiling above the ecological threshold of 100 g/m^2 along the Greenlandic coastline to the northwest of the spill site. The larger blowout could potentially also oil shorelines in Canada along the coastlines of Devon, Bylot, and Baffin Islands. For the larger blowout (scenario 1B), there is a moderate to high probability of water surface oiling above the ecological threshold of 10 g/m^2 within the North Water Polynya area. Because of the relatively large size of the oil droplets from the blowouts (as indicated by the near-field modeling), the droplets tend to surface quickly and the residence time in the water column is relatively short. As such, entrainment of oil in the water column was relatively low for both scenarios.

Of the response scenarios modeled in the deterministic analysis (i.e., surface dispersant application, mechanical containment/recovery, and *in situ* burning) the most effective response strategy was surface dispersant application. Mechanical containment/recovery and *in situ* burning were largely ineffective in the deterministic simulations because of rapid weathering and spreading of the oil, as well as environmental conditions. These strategies were only effective when relatively fresh oil was present and ultimately removed <1% of the volume spilled for scenario 1A, and 6% of the volume spilled for scenario 1B. These removal rates are what would be expected under most offshore removal operations.

Even under relatively “ideal” conditions, mechanical containment and recovery operations typically remove about 2% to 25% of the oil. In the Macondo MC252 (Deepwater Horizon) spill in the U.S. Gulf of Mexico, an estimated 3% of the spilled oil was removed mechanically. In this effort, all available response equipment was employed with a very large work force. It is only under the

[3] See Appendix A for additional discussion of benchmarking blowout flow rates, durations, and total volumes, as well as a discussion of blowout likelihood.

very unusual circumstances of a spill in a very sheltered location, usually with a pre-boomed vessel during transfer or lightering operations, that a higher percentage of oil recovery is possible.[4]

Taken together, the response measures simulated in this study for the 34-day blowout scenario (scenario 1B) reduced the peak amount of oil on the water surface by about 37% and the peak amount of oil on the shoreline by about 11%. The shoreline length oiled above the ecological threshold of 100 g/m^2 was also reduced by about 7%. However, though the dispersant reduced the volume of oil ashore, shore length oiled, and the volume of oil on the water surface, it does not remove oil from the environment, but rather displaces it. As such, the peak volume of oil in the water column was increased by 746% and the volume of water exceeding 1 ppb of dissolved aromatics (a screening threshold for impacts on sensitive water column organisms) was increased by 63% when response measures were included in the simulation.

Dispersants reduce the interfacial tension of oil, facilitating increased entrainment of oil into the water column as microscopic droplets. This leads to more oil in the water column, increased dissolution rates of soluble hydrocarbons (mostly aromatics), and enhanced biodegradation rates. Application of dispersants can reduce the effects of shoreline oil and surface floating oil on birds and other wildlife, but the trade-off is increased risks to fish and invertebrates in the water column.

[4] Many reports of “recovered oil” are actually for oil-water mixtures. A small percentage of the recovered oil-water mixture is oil. This means that the *oil* recovery represents a much lower percentage.

6.0 SCENARIOS 2A AND 2B – BAFFIN BAY BLOWOUTS

6.1 Scenario Development

The spill site selected for the hypothetical well blowouts in Baffin Bay (Figure 41) is near the entrance to Lancaster Sound near the Hope Structure, which is an area of hydrocarbon potential. The precise location is 74.401196°N, 77.467675°W. The spill site is within the Shell license area,[5] as well as near an upwelling feature near the mouth of Lancaster Sound, which was mentioned by stakeholders as an area of concern with respect to the influence of the upwelling feature on oil transport.

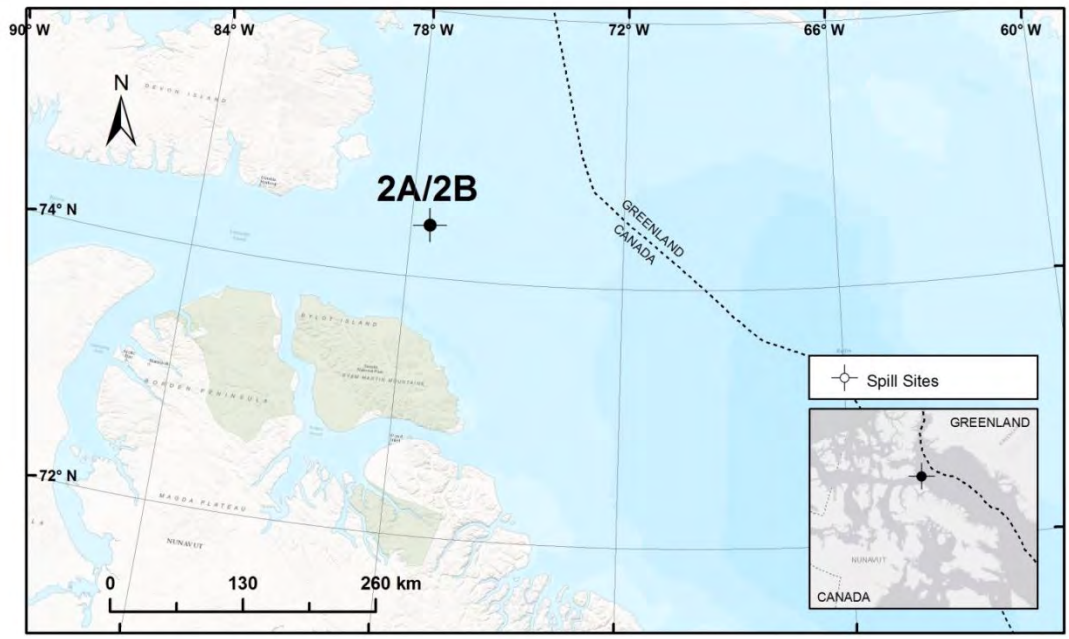

Figure 41. Location of the selected spill site in Baffin Bay (scenarios 2A and 2B).

For the Baffin Bay spill site, two subsurface well blowout scenarios (2A and 2B) were developed, reflecting two different blowout durations (and associated total volume spilled):

- Scenario 2A: a flow rate of 3,340 m^3 per day for 1 day (assumes that natural bridging will stop the flow of oil) for a total of 3,340 m^3 (21,008 bbl) spilled; and
- Scenario 2B: a flow rate of 3,340 m^3 per day for 34 days (assumes a relief well is needed to stop the flow of oil) for a total of 113,560 m^3 (714,271 bbl) spilled.

The season evaluated for scenarios 2A and 2B corresponds to “open water” conditions, and was based on analysis of average monthly ice coverage data from TOPAZ4 at the spill site (2011-

[5] Shell announced June 8, 2016 that it was relinquishing its exploration permits for this license area. The permits were relinquished to the Nature Conservancy of Canada for use in marine conservation efforts in the Arctic (http://www.cbc.ca/news/canada/north/shell-lancaster-sound-permits-1.3620681).

2015). Average ice cover of less than 30% was defined as "open water." This time period corresponded to June through October.

The oil type selected for scenarios 2A and 2B was similar to Statfjord (medium) crude, which is a crude oil that represents the characteristics of crudes found in other exploration wells in the region (Mosbech et al., 2007; Perry and Bright, 2010). The precise characteristics of crude oil from a particular well can only be known after direct sampling from that well, which is not possible in this case, as the license area has not been explored or developed.

The rate of flow from a particular well is dependent on the characteristics of the well itself, particularly the reservoir pressure, but also the type of well (development, exploratory, etc.). The actual flow rate of a well can often not be predicted in advance and will be determined only when the actual well is drilled. Flow rates can vary during the course of oil extraction, including variations in the amount of crude oil versus water or brine in the flow. The flow rates that are described for wells are generally the average flow rate. The flow rate assumed for the modeling of scenarios 2A and 2B was 3,340 m^3 per day, which corresponds to 21,008 barrels (bbl) per day. This flow rate was assumed based on other studies conducted in the region (Mosbech et al., 2007; Perry and Bright, 2010), and was deemed to be a reasonable approximation of the magnitude of flow rate that might be expected for a well in this license area.

Given an average flow rate for a particular well, the total volume will depend on the duration of flow – the length of time that the well continues to release crude oil to the environment. The duration of flow is determined by the length of time that it takes for the well to either bridge naturally (fill in with enough sediment to naturally stop flowing without any human intervention), to be capped and contained, or to be intercepted by a relief well(s) to stop the flow. For the Baffin Bay blowout scenarios, two durations of flow were assumed. The first assumed that there would be natural bridging that occurs within one day; the second assumed that a relief well operation successfully stopped the flow at the end of the 34th day of flow. For these scenarios, capping and containment was not considered. Generally, relief well operations take longer than capping and containment operations, and would represent the worst-case with respect to flow duration and ultimate spill volume.

Studies indicate that about 84% of well blowouts bridge naturally, that is, the flow is stopped as sediment naturally fills in the wellbore without any intervention in 0.5 to 5 days (Dyb et al., 2012, Holand, 2013). Generally, the duration of flow is relatively short, which would limit the total volume of spillage. In the other 16% of cases, human intervention in the form of relief wells and/or containment and capping is required to stop the flow of oil. Worldwide, about 10% of blowouts have been stopped with relief wells and 6% by capping and containment operations. Fifty percent of relief well operations took less than five days, 75% less than 10 days, and 90% less than 25 days. The 34-day relief well operation assumed in scenario 2B represents the estimated 95th percentile case with respect to flow duration.

See Appendix A for additional discussion regarding the development of spill scenario parameters; benchmarking blowout flow rates, durations, and total volumes; and blowout likelihood.

6.2 Environmental Analysis

Monthly TOPAZ4 surface current roses at the Baffin Bay spill site are presented in Figure 42. The surface current flow is predominantly to the east-southeast from January to August. September surface current flow is variable with westward to northward components evident. During October to December, surface currents transition back to primarily eastward flow. The strongest current speed (25 cm/s) occurs in June and is directed to the east.

Monthly TOPAZ4 current speed statistics (average and 95th percentile) at the Baffin Bay spill site show seasonality in intensity of surface current speeds (Figure 43). The highest monthly surface current speeds occur in June, at around 17 cm/s, before rapidly decreasing to lower speeds during September to January. The minimum occurs in December with surface current speeds slightly over 5 cm/s.

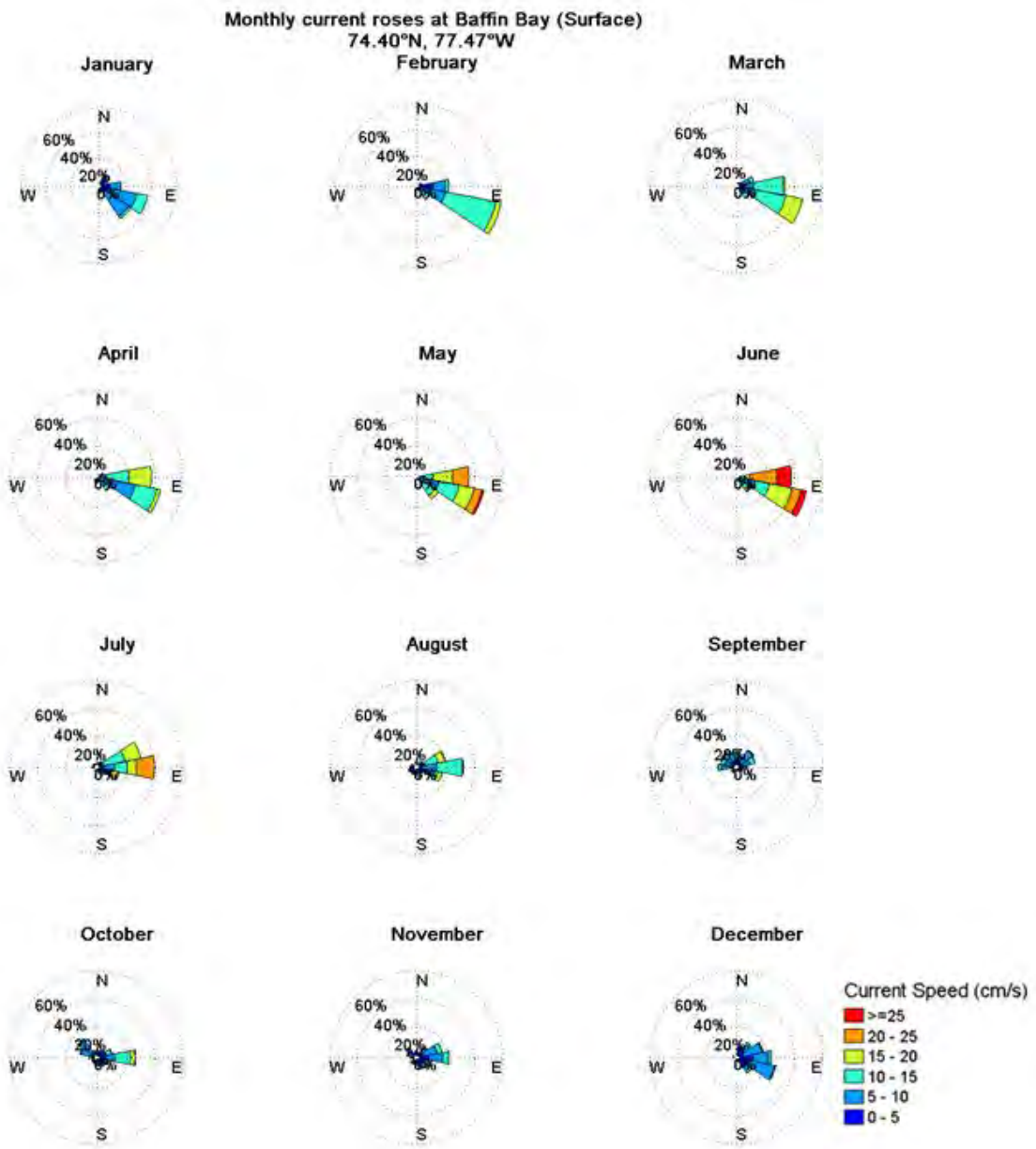

Figure 42. TOPAZ4 monthly averaged surface current roses near the Baffin Bay spill site, averaged over the period of 20011-2015. Direction convention is standard (i.e., direction currents are moving to).

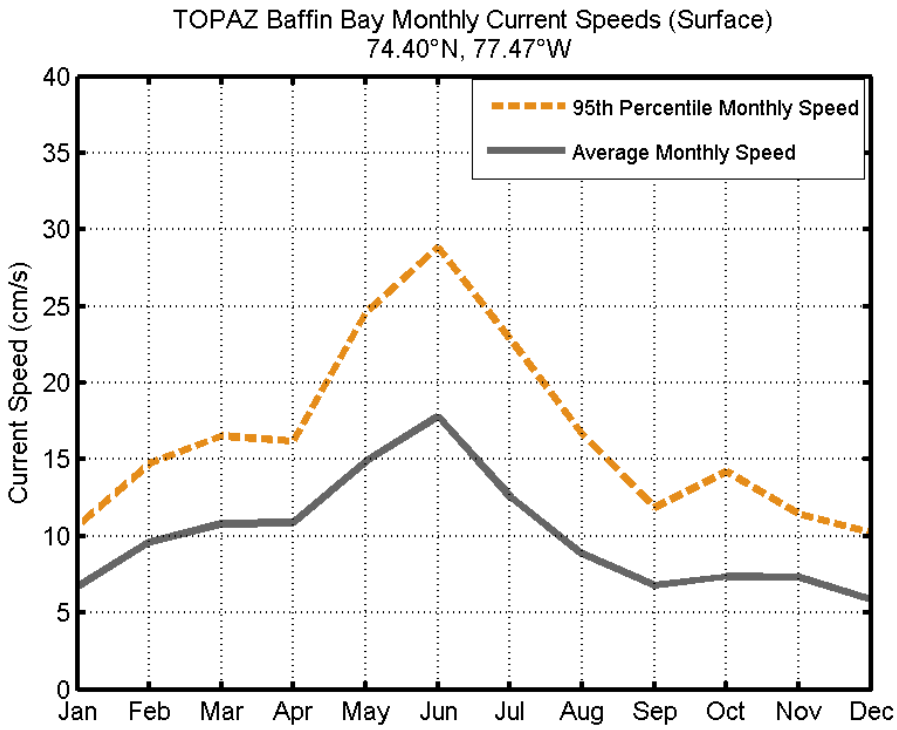

Figure 43. TOPAZ4 current statistics: monthly average (grey solid) and 95th percentile (orange dash) current speed at the surface near the Baffin Bay spill site for 2011-2015.

Monthly TOPAZ4 ice roses at the Baffin Bay spill site indicate that the primary of direction of movement is to the southeast and east (Figure 44). Ice coverage begins to decline in June, with no coverage at this site during July and August. Ice begins to form again in September through the end of the year. Ice speeds can exceed 25 cm/s directed to the east-southeast.

Monthly average sea ice and landfast ice cover near the spill site are shown in Figure 45. Sea ice coverage is based on data from TOPAZ4 (2011-2015) and landfast ice coverage is based on data from the National Snow and Ice Data Center (1991 through 1998).

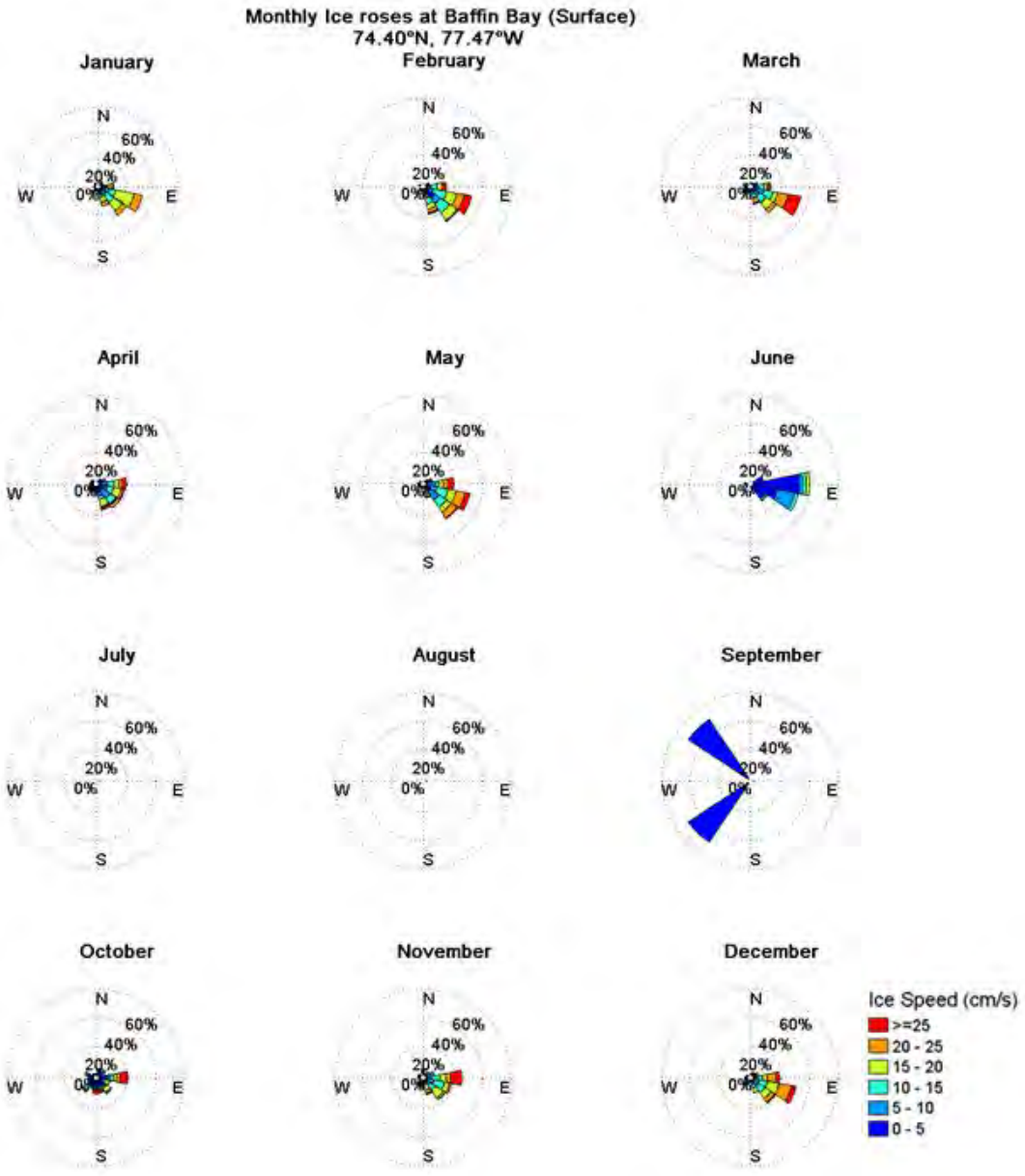

Figure 44. TOPAZ4 monthly averaged ice roses near the Baffin Bay spill site averaged over the period of 2011-2015. Ice roses are presented for the surface. Direction convention is standard (i.e., direction ice is moving to).

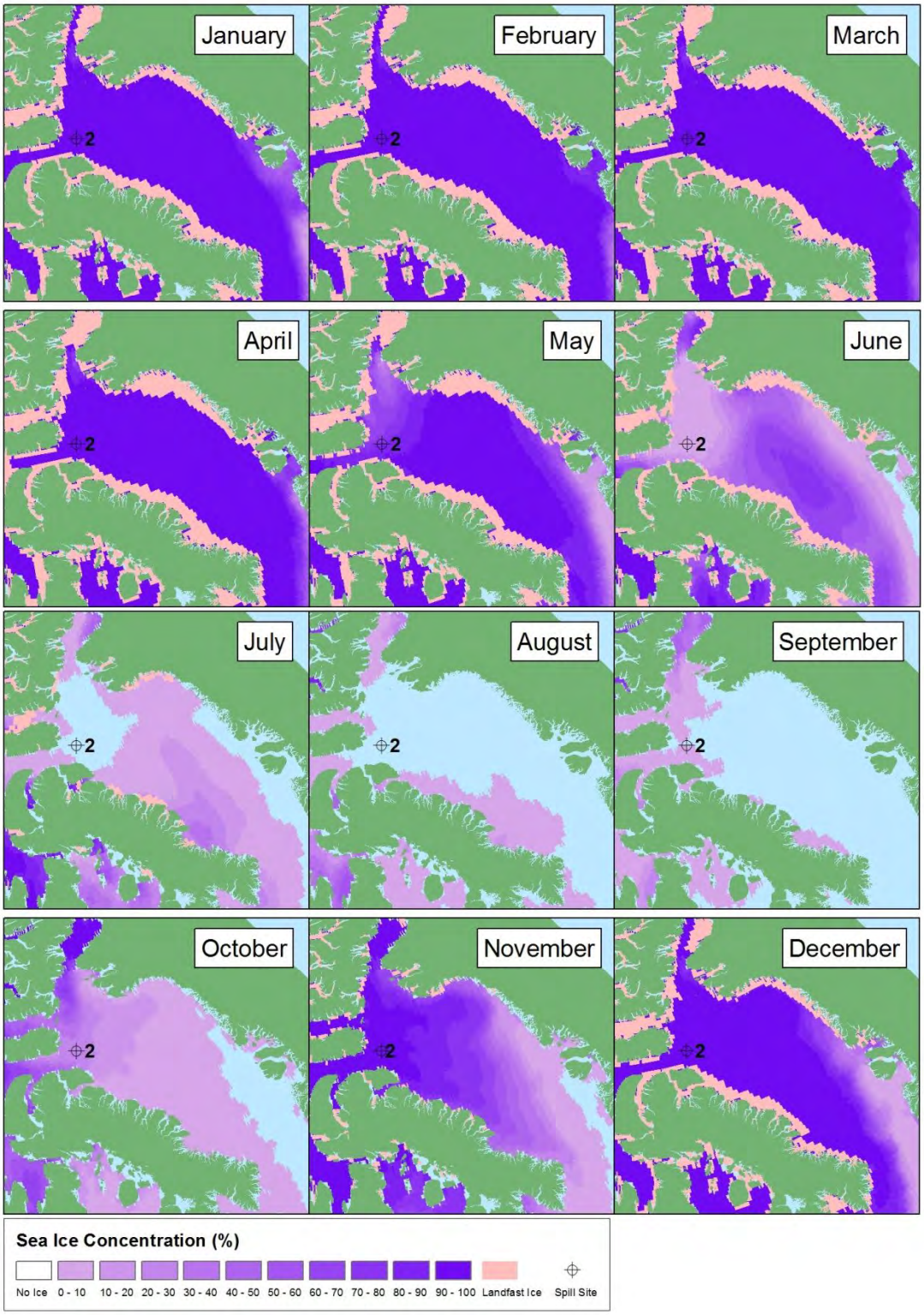

Figure 45. Average monthly cover of sea ice and landfast ice near the Baffin Bay spill site.

Figure 46 shows the monthly ECMWF wind speeds at the Baffin Bay spill site throughout the year. January through March, wind speed is primarily west-northwesterly, and becomes more variable and weaker in late spring through summer. In June, direction shifts to predominantly easterly, while July and August have no real dominant direction evident. During fall, wind direction transitions back to primarily northwesterly with higher wind speeds.

Average monthly ECMWF wind speeds at the Baffin Bay spill site range from around 8 to 13 knots (Figure 47). July has the minimum monthly average around 7 knots, subsequently increasing to around 12 knots in September and remaining high throughout winter. Wind speeds begin to decrease in April to the minimum in July.

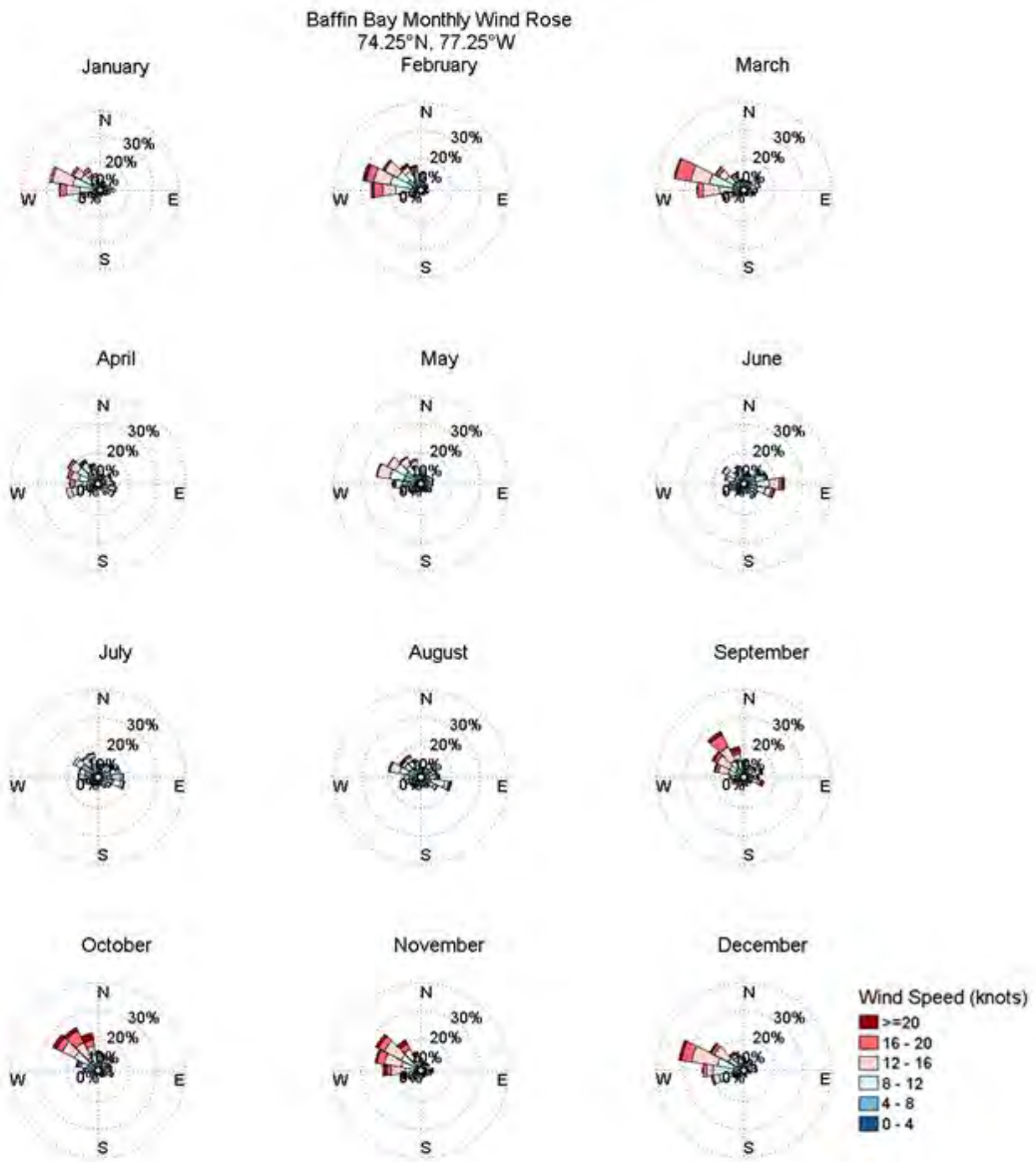

Figure 46. ECMWF monthly averaged wind roses near the Baffin Bay spill site, averaged over the period of 2011-2015. Wind speeds are in knots, using meteorological convention (i.e., direction wind is coming from).

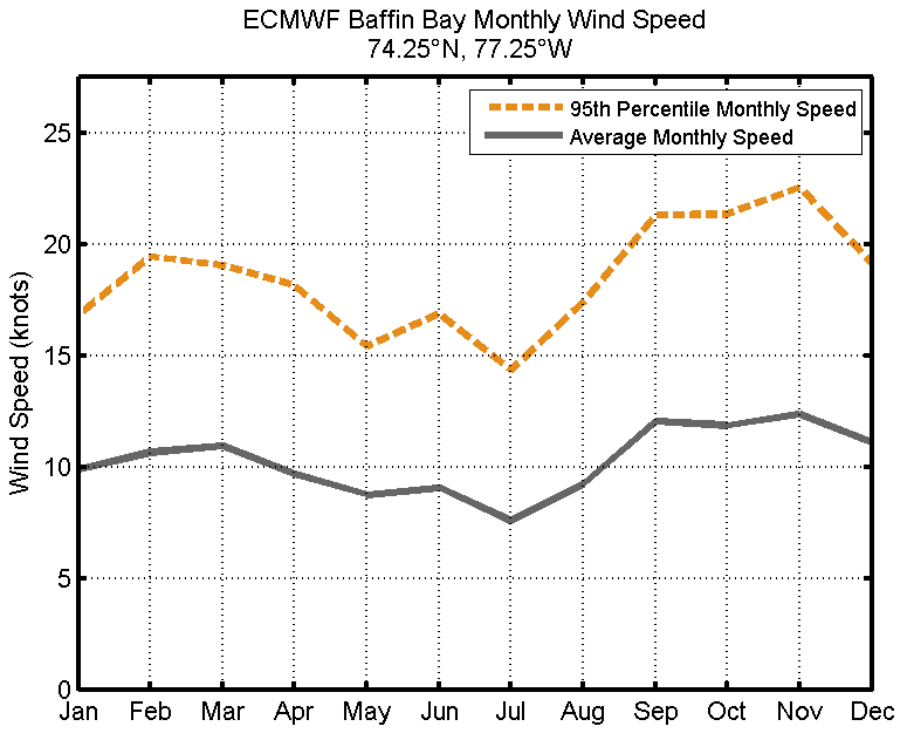

Figure 47. ECMWF wind statistics: monthly average (grey solid) and 95th percentile (orange dash) wind speed near the Baffin Bay spill site for 2011-2015.

The vertical profile of temperature, salinity, and density at the Baffin Bay spill site for June through October is shown in Figure 48. Salinity is approximately 32.3 psu at the surface and increases to 34.5 psu near the sea floor. Temperature at the surface is approximately 1.4 ºC and decreases to a minimum of -1.3 ºC at 80 m before increasing gradually to 1.2 ºC at 700 m. Density at the surface is 25.9 kg/m^3 and increases to 27.6 kg/m^3 near the sea floor.

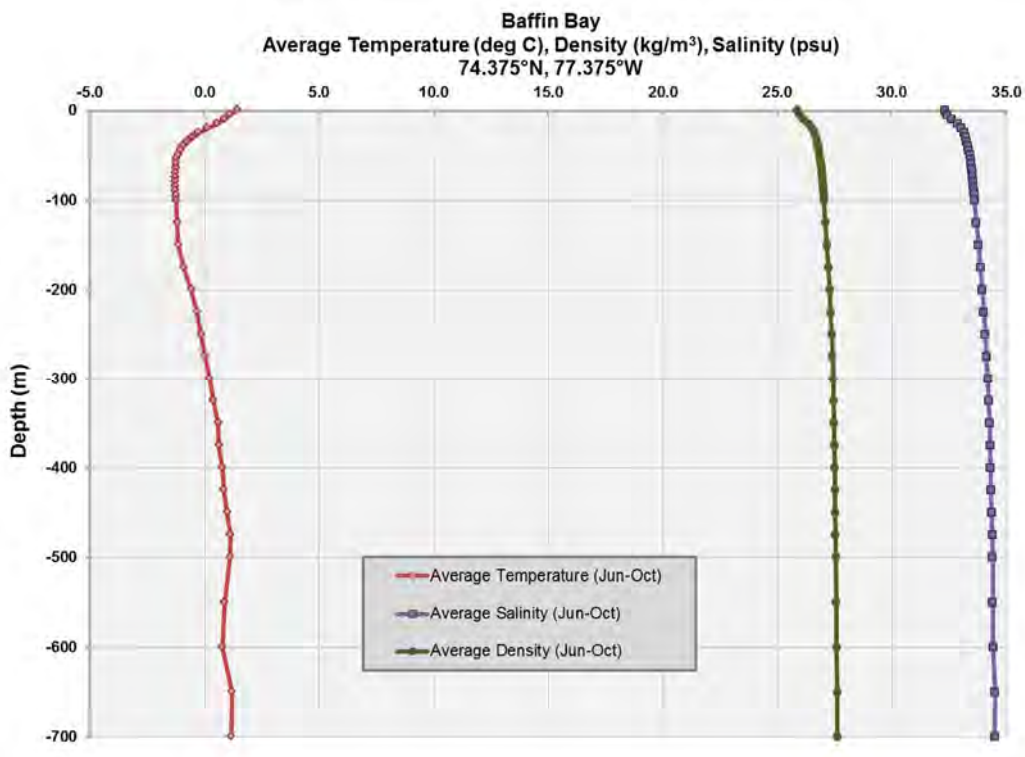

Figure 48. Vertical profile of average temperature (red), salinity (purple), and density (green) near the Baffin Bay spill site for June to October. Data from the World Ocean Atlas 2013.

6.3 Near-field Modeling

The key inputs to the near-field model include flow rate, gas-to-oil ratio, aperture or pipe diameter, and a vertical profile of water temperature and density. For both scenarios 2A and 2B, the gas-to-oil ratio was assumed to be 1,000 scf/stb (standard cubic feet per stock tank barrel), and the pipe diameter was assumed to be 38.1 cm. In the absence of site-specific information for the area of interest, these values are considered to be reasonable proxy values based on past modeling experience.

The near-field modeling results provide a description of the plume characteristics, including the plume location (namely plume trap height), plume geometry, and the release droplet size distribution. The results of the near-field model are then used to provide the initial conditions for the stochastic and deterministic far-field modeling in SIMAP, including:

- Termination height (trap height) of the plume;
- Diameter of the plume; and
- Oil droplet size distribution.

Figure 49 and Figure 50 present the OILMAP Deep modeling results for scenarios 2A and 2B. Despite the difference in duration between the two scenarios (1-day vs. 34-days), plume formation and behavior as well as droplet formation are identical.

Figure 49 shows the plume radius plotted as a function of the height above the sea floor (wellhead), and plume velocity along the centerline of the blowout as a function of the height above the seafloor. Plume centerline velocity defines the vertical movement of the mixture of gas, oil, and water along the center of the plume. The model indicates that the velocity of the plume decreases quickly at heights further from the discharge point as it entrains heavier ambient seawater. As the plume continues to rise and entrain more ambient seawater, the centerline velocity gradually decreases, and approaches zero at about 258 m above the wellhead (a depth of 429 m below the water surface). From this termination height, gas and oil droplets will ascend to the water surface under free rise velocities determined by Stokes law. The plume is expected to reach a maximum radius of approximately 54 m.

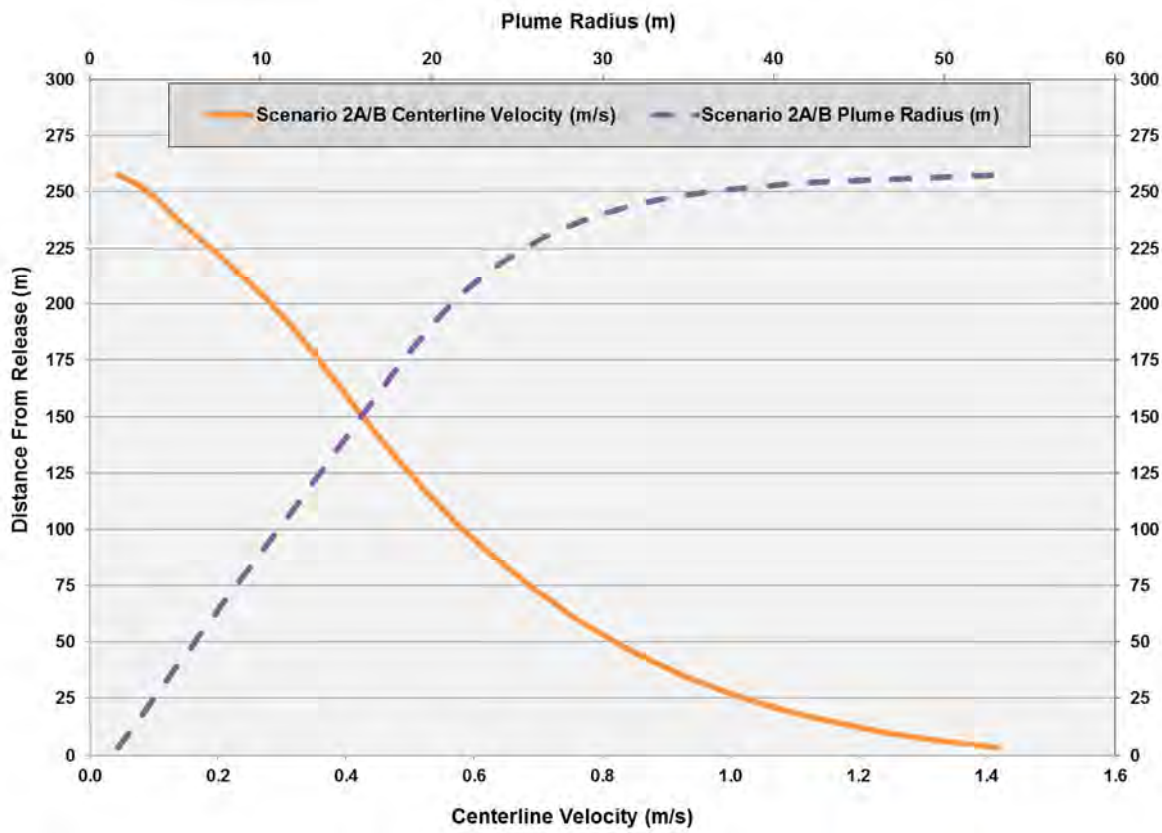

Figure 49. Predicted blowout plume centerline velocity and plume radius versus elevation above release point for the Baffin Bay blowout events (scenarios 2A and 2B).

The near-field modeling results also provide a characterization of the oil droplet size distribution generated by the blowout. This distribution has a profound effect on how oil is transported after the initial plume, as the droplet size dictates how long the oil droplet will remain suspended in the water column. Figure 50 shows the model-estimated droplet size distribution and droplet rise times to the surface for scenarios 2A and 2B. The oil droplet sizes for these scenarios are relatively large, and would tend to reach the surface quickly. The minimum droplet size was 500 µm; a droplet this size would be expected to surface in about 11.1 hours. The maximum droplet size was 10,000 µm, which would surface in about 1.0 hours.

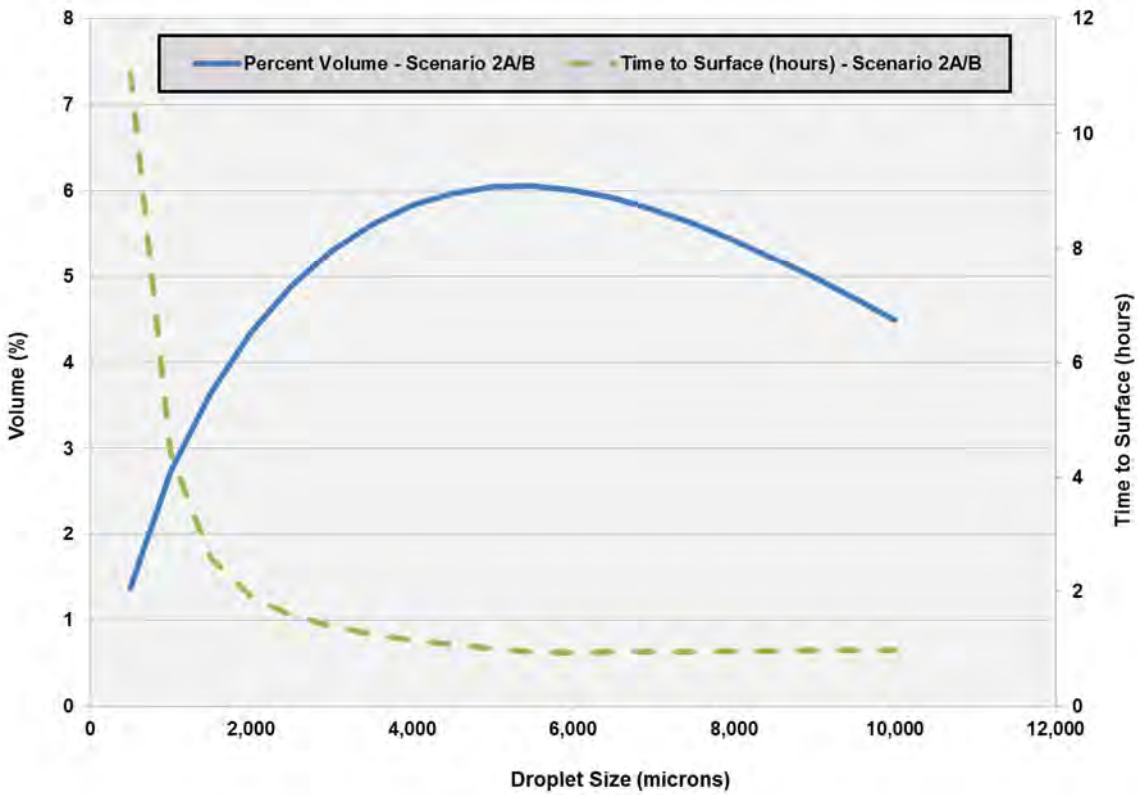

Figure 50. Predicted droplet size distribution and droplet rise times to the surface for the Baffin Bay blowout events (scenarios 2A and 2B).

6.4 Stochastic Modeling

Using the near-field model results as initial conditions for the far-field modeling, the SIMAP stochastic model was used to predict the statistical footprint of oiling associated with the blowout scenarios.

6.4.1 Stochastic Scenario Parameters

The stochastic scenario input parameters developed for 2A and 2B (see Section 6.1) are summarized in Table 13 below. Each scenario was simulated (tracked) for 45 days beyond the end of the blowout release. No spill response measures were included in the stochastic simulations for these scenarios.

Table 13. Stochastic scenario input parameters for scenarios 2A and 2B.

ID #	Spill Type	Location	Release Depth (m)	Oil Type	Spill Rate	Spill Duration (days)	Total Volume (m^3)	Season	Simulation Duration (days)
2A	Subsurface blowout	74.401196°N, 77.467675°W	687	Medium crude	3,340 m^3/day	1	3,340	June to October	46
2B	Subsurface blowout	74.401196°N, 77.467675°W	687	Medium crude	3,340 m^3/day	34	113,560	June to October	79

6.4.2 Stochastic Results

The results of the stochastic model simulations for scenarios 2A and 2B are shown in Table 14 and Table 15.

Table 14 presents shoreline oiling statistics for both scenarios, including the percentage of simulations reaching shore, time to shore, peak volume of oil ashore, and the shoreline length oiled above the ecological threshold of 100 g/m^2. The percentage of simulations reaching shore indicates the likelihood that a particular spill event will reach nearby coastal areas with a level of shoreline oiling greater than 100 g/m^2. The percentage of simulations reaching shore is based on the total number of trajectories out of the ensemble of 100+ individual runs that reached the coast in the stochastic analysis. Note that a spill event with high probability of shoreline oiling does not imply that a particular section of the coast will be oiled, only that there is a high probability of oil reaching the coastline *at some location*.

Both scenarios had a high probability of causing shoreline oiling above 100 g/m^2, with 71% of trajectories reaching shore for scenario 2A, and 82% of trajectories reaching shore for scenario 1B. As expected, the volume of oil ashore and the shoreline length oiled was substantially higher for the longer duration, larger volume blowout (scenario 2B). On average, the peak volume of oil ashore for scenario 2A is about 26% of the total volume spilled, and about 14% of the total volume spilled for scenario 2B. The minimum time for oil to first reach shore was similar between the two scenarios, at about 3 days.

Table 14. Scenarios 2A and 2B stochastic results – shoreline oiling statistics.

ID	Spill Event	Total Volume Spilled (m^3)	Simulations Reaching Shore (%)[1]	Time to Reach Shore (days)		Peak Volume of Oil Ashore (m^3)		Shoreline Length Oiled Above 100 g/m^2 (km)	
				Min.	Avg.	Max.	Avg.	Max.	Avg.
2A	Baffin Bay – 1-Day Blowout	3,340	71	3.1	20.6	1,787	877	472	164
2B	Baffin Bay – 34-Day Blowout	113,560	82	3.2	23.2	33,756	15,511	1,916	1,034

[1] Percentage of simulations reaching shore is calculated based on the number of individual trajectories that resulted in shoreline oiling above a threshold of 100 g/m^2 of oil.

Table 15 presents surface oiling and water column oiling statistics. The 1-day blowout (scenario 2A) resulted in a water surface footprint of, on average, about 71 km^2 oiled above the ecological threshold of 10 g/m^2. The water surface oiling footprint for the 34-day blowout (scenario 1B) was approximately 1,334 km^2 oiled on average. Because of the relatively large size of the oil droplets from the blowouts (Section 6.3), the droplets tend to surface quickly and the residence time in the water column is relatively short. As such, entrainment of oil in the water column was relatively low for both scenarios. On average, the peak volume of oil entrained in the water column was about 18% of the total volume for scenario 2A, and about 4% of the total volume for scenario 2B.

Table 15. Scenarios 2A and 2B Stochastic results – surface oiling and water column oiling statistics.

ID	Spill Event	Total Volume Spilled (m^3)	Water Surface Area Oiled Above 0.01 g/m^2 (km^2)		Water Surface Area Oiled Above 10 g/m^2 (km^2)		Volume of Oil in Water Column (m^3)	
			Max.	Avg.	Max.	Avg.	Max.	Avg.
2A	Baffin Bay – 1-Day Blowout	3,340	17,602	3,937	88	71	2,069	591
2B	Baffin Bay – 34-Day Blowout	113,560	87,032	38,535	2,244	1,334	10,029	4,089

The following figures (Figure 51 through Figure 54) illustrate the spatial extent of water surface oiling and shoreline oiling probabilities for scenarios 2A and 2B. For each scenario, three figures are presented:

1. **Probability of Water Surface Oiling Above 0.01 g/m^2**: The map defines the area in which water surface oiling above the socioeconomic threshold of 0.01 g/m^2 may be expected and the associated probability of oiling (based on analysis of the 200 or 120[6] individual trajectories run for each spill scenario). The map does not imply that the entire contoured area would be covered with oil in the event of a spill. The map also does not provide any information about the quantity of oil in a given area.

2. **Probability of Water Surface Oiling Above 10 g/m^2**: The map defines the area in which water surface oiling above the ecological threshold of 10 g/m^2 may be expected and the associated probability of oiling (based on analysis of the 200 or 120 individual trajectories run for each spill scenario). The map does not imply that the entire contoured area would be covered with oil in the event of a spill. The map also does not provide any information about the quantity of oil in a given area.

3. **Probability of Shoreline Oiling Exceeding 100 g/m^2**: This map shows the probability of shoreline oiling above the ecological threshold of 100 g/m^2 (based on analysis of the 200 or 120 individual trajectories run for each spill scenario). The map does not imply that the entire shoreline extent would be oiled in the event of a spill. The map also does not provide any information about the quantity of oil in a given area.

A brief summary of each stochastic simulation follows the figures for each case.

[6] For the 34-day blowout scenario, 120 individual model runs were simulated instead of 200 due to file size and computational limitations.

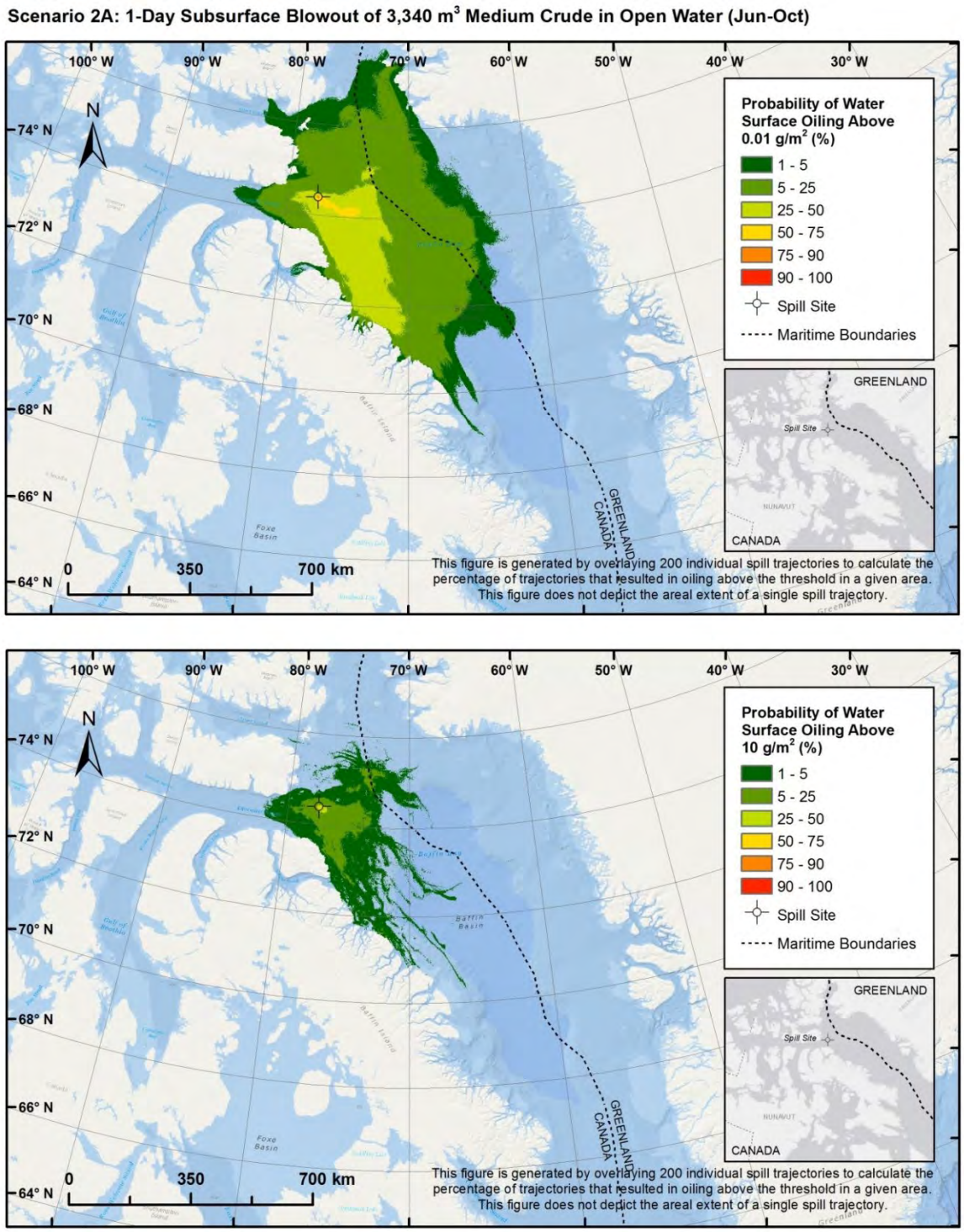

Figure 51. Scenario 2A (1-day blowout of 3,340 m^3 crude oil) stochastic results – Probability of water surface oiling above the socioeconomic threshold of 0.01 g/m^2 (top panel) and probability of water surface oiling above the ecological threshold of 10 g/m^2 (bottom panel).

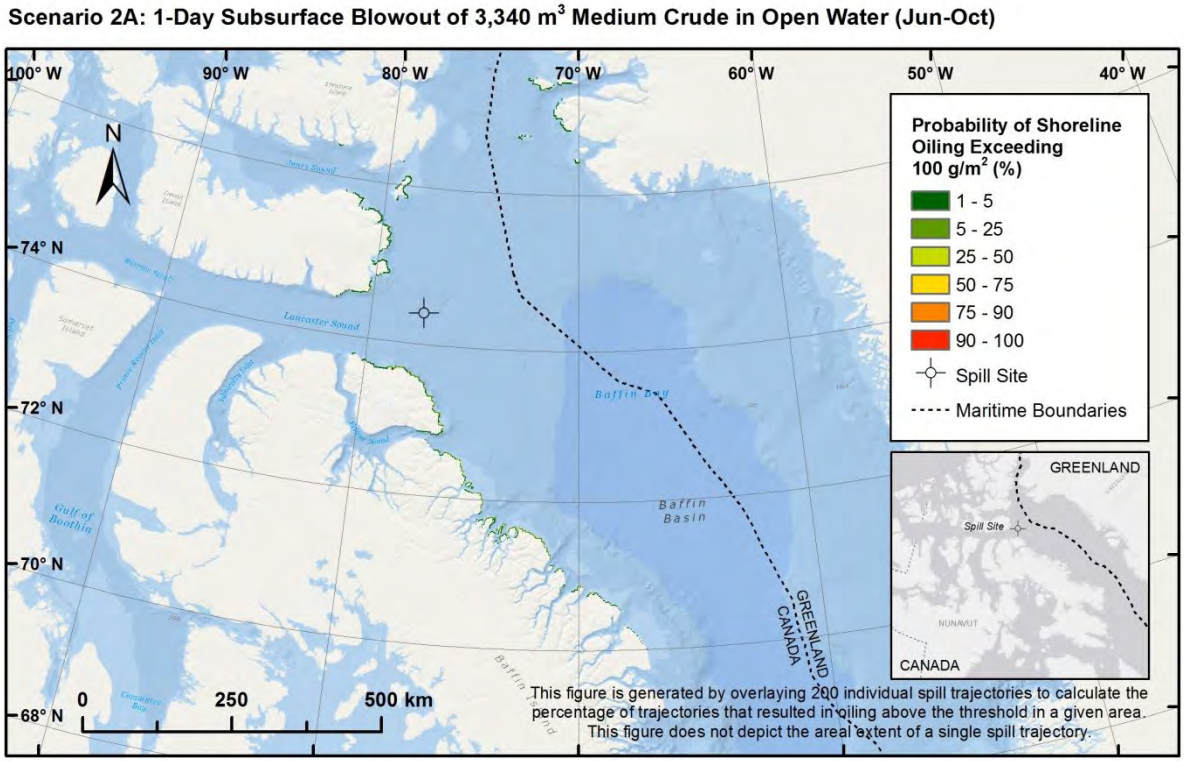

Figure 52. Scenario 2A (1-day blowout of 3,340 m^3 crude oil) stochastic results – Probability of shoreline oiling above the ecological threshold of 100 g/m^2.

As shown in Figure 51, the stochastic water surface oiling footprint was for scenario 2A was relatively variable. For the socioeconomic threshold of 0.01 g/m^2, the zone of highest probability was oriented to the east and southeast of the spill site. There is a low (<25%) probability of surface oil above the threshold being transported to the north into the North Water Polynya area. There is also a low to moderate probability of water surface oiling within Greenlandic territorial waters. For the ecological threshold of 10 g/m^2, the stochastic surface oiling footprint is much smaller, with lower overall probabilities.

There is an approximately 71% chance that shoreline oiling above 100 g/m^2 will occur at some location in the study area (Table 14). However, because the locations of potential shoreline oiling are variable and widespread, the highest probability of any individual segment of the coastline being oiled above the threshold is 24% (Figure 52). Areas that could potentially be oiled above the threshold include Greenlandic shoreline near Kap Atholl, Kap Parry, Carey Islands, and Northumberland Island; and Canadian shorelines along Ellesmere, Coburg, Devon, Bylot, and Baffin Islands.

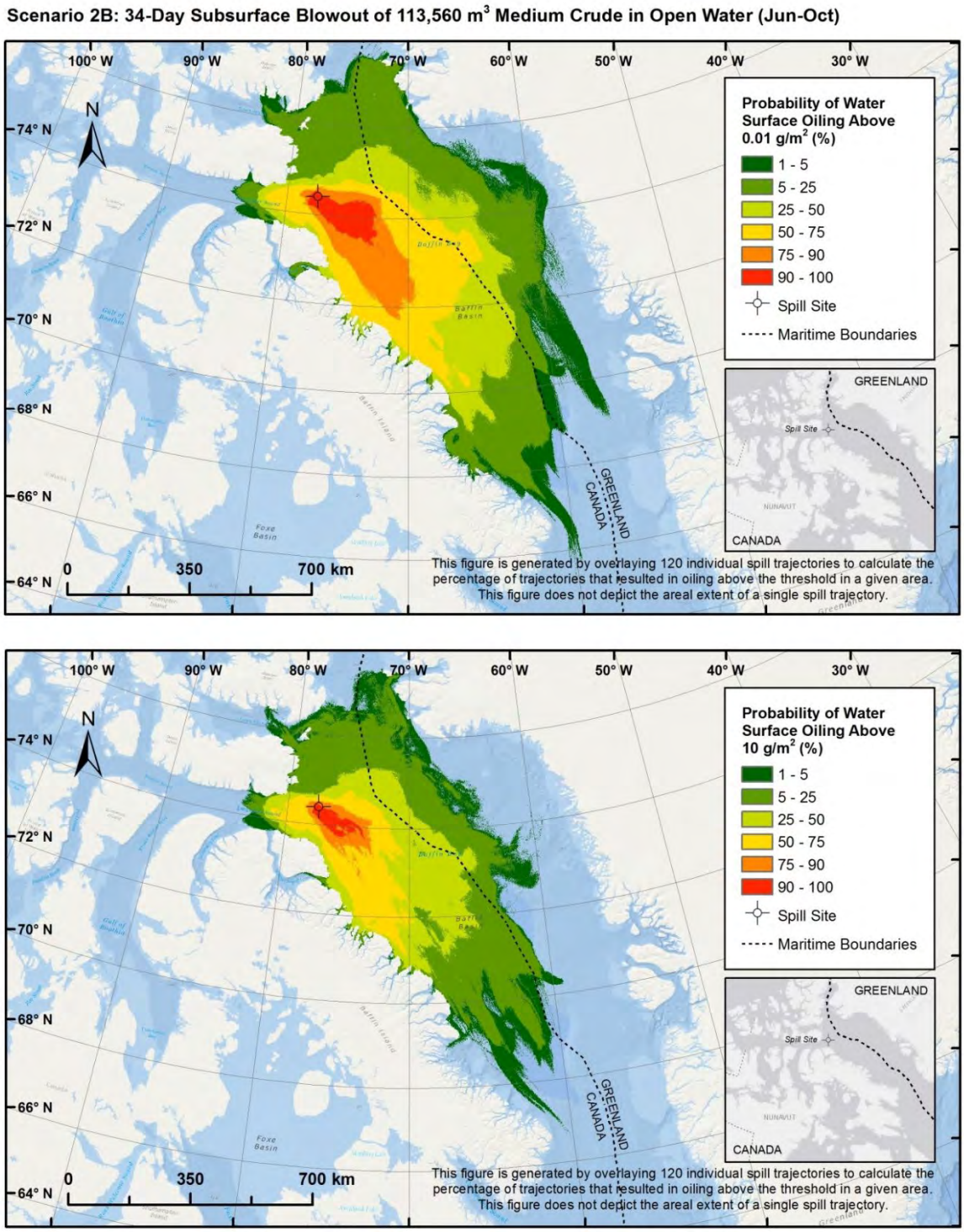

Figure 53. Scenario 2B (34-day blowout of 113,560 m^3 crude oil) stochastic results – Probability of water surface oiling above the socioeconomic threshold of 0.01 g/m^2 (top panel) and probability of water surface oiling above the ecological threshold of 10 g/m^2 (bottom panel).

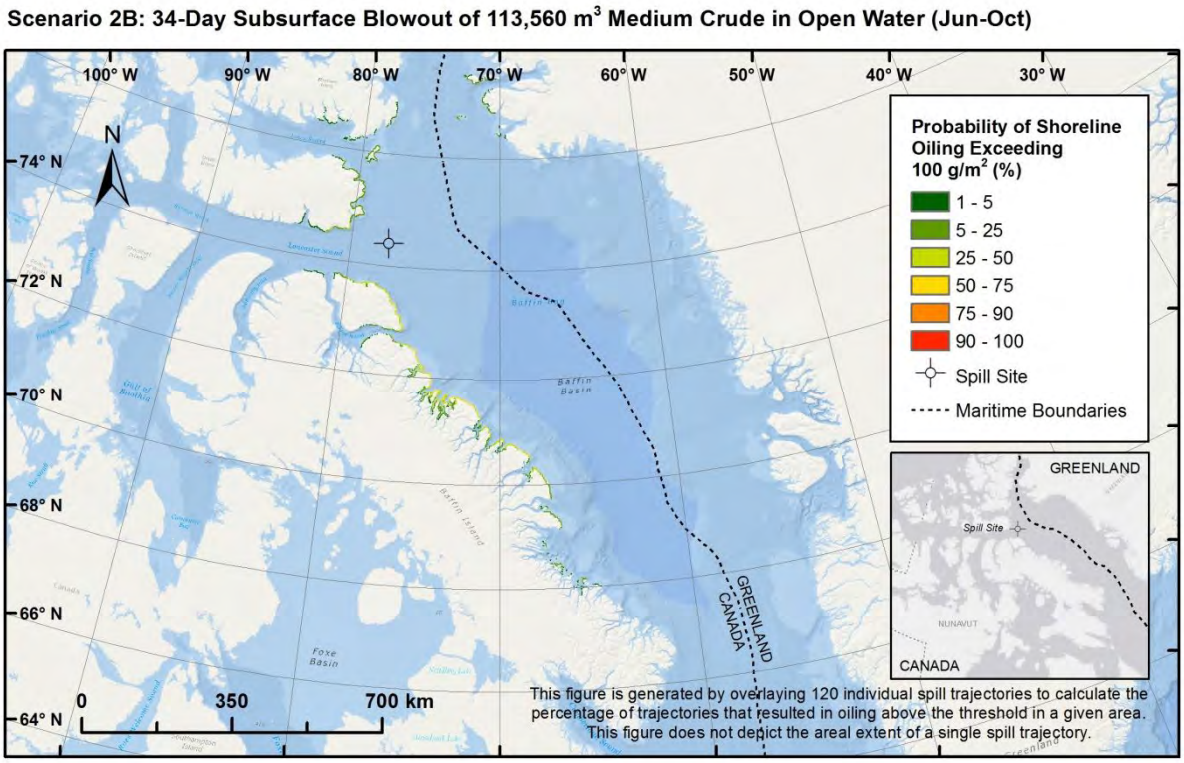

Figure 54. Scenario 2B (34-day blowout of 113,560 m^3 crude oil) stochastic results – Probability of shoreline oiling above the ecological threshold of 100 g/m^2.

Like scenario 2A, the stochastic water surface oiling footprint for scenario 2B is predominately oriented to the east and southeast of the spill site, towards Baffin Island (Figure 53). There is a low to moderate probability of surface oil above the threshold being transported to the north into the North Water Polynya area. There is also a high probability of water surface oiling within Greenlandic territorial waters above the socioeconomic threshold. For the ecological threshold, the stochastic surface oiling footprint is somewhat restricted in size compared to the lower socioeconomic threshold, but still very large. Probabilities of water surface oiling remain low to moderate at this threshold for the North Water Polynya, and the probability of oiling within Greenlandic waters is moderate.

There is an approximately 82% chance that shoreline oiling above 100 g/m^2 will occur at some location in the study area (Table 14). The locations of potential shoreline oiling are variable and widespread, and the highest probability of any individual segment of the coastline being oiled above the threshold is 67% (Figure 54). Areas that could potentially be oiled above the threshold include Greenlandic shoreline near Kap Atholl, Kap Parry, Carey Islands, and Northumberland Island; and Canadian shorelines along Ellesmere, Coburg, Devon, Bylot, and Baffin Islands. The highest probability of oiling is for the shorelines to the south of the spill site along Bylot and Baffin Islands.

6.5 Deterministic Modeling

The deterministic trajectory and fate simulations provide an estimate of the 3-D trajectory (movement) and fate (weathering) for a particular individual spill event.

6.5.1 Deterministic Scenario Parameters

Trajectories were selected from the stochastic scenario based on pre-defined criteria. Different parameters or criteria can be used to select individual trajectories for deterministic analysis. For example, deterministic trajectories can be "representative" or "worst-case" for a variety of consequence metrics (e.g., shoreline length oiled, time to shore, volume of oil ashore, water column contamination, water surface area swept). The selected deterministic cases for scenario 2B are summarized in Table 16. At the request of WWF-Canada, the deterministic scenarios were simulated (tracked) for longer than the corresponding stochastic scenario in order to provide more information about the ultimate fate of the spilled oil. These durations were based on test simulations and were selected to reflect either:

- The point at which zero or minimal oil remains on the water surface;
- The point beyond which oil begins to leave the extent of the environmental input data (e.g., currents, winds); or
- The point beyond which the duration begins to reduce the credibility of model results (due to increasing uncertainly with longer post-spill durations).

One of the deterministic cases included simulation of a hypothetical spill response, described in Section 6.5.1.1 below.

Table 16. Selected deterministic cases for scenario 2B.

ID	Spill Event	Type of Deterministic Case[1]	Spill Response Type	Spill Start Date	Simulation Duration (Days)
2B	Baffin Bay – 34-Day Blowout	Worst-case Shoreline Length Oiled	None	12 September 2014	100
2B	Baffin Bay – 34-Day Blowout	Worst-case Shoreline Length Oiled	Subsurface dispersant injection at wellhead	12 September 2014	100
2B	Baffin Bay – 34-Day Blowout	Worst-case Water Surface Area Oiled	None	16 October 2014	100
2B	Baffin Bay – 34-Day Blowout	Worst-case Volume of Oil in the Water Column	None	2 September 2013	100

[1] The "worst case" for a given consequence metric was defined as the trajectory with the 95th percentile value for oiling above the ecological threshold (i.e., 100 g/m^2 for the shoreline, and 10 g/m^2 for the water surface).

6.5.1.1 Response Parameters

The license area in which the Baffin Bay spill site is located has not been developed or explored. As such, there are no oil spill contingency plans in place on which to base the response simulation for scenario 2B. In consultation with WWF-Canada, a highly effective response method, subsurface dispersant injection, was selected for the response simulation to illustrate a hypothetical "best case" response.

Subsurface dispersants were applied for the first and only time in history during the 2010 Macondo MC252 (Deepwater Horizon) well blowout in the Gulf of Mexico. As the result of the measured success of those operations, U.S. regulatory agencies and industry operators are currently incorporating subsurface dispersant application into offshore well spill response plan strategies, including for Arctic operations. The subsurface injection of dispersants is theoretically one of the most effective response strategies for deep water blowouts.

The response assumptions applied in the modeling are summarized in Table 17. Subsurface injection of dispersants at the wellhead was assumed to begin 72 hours after the onset of the spill and continue through the remaining duration of the 34-day blowout. Based on expert opinion and research studies conducted for the U.S. Bureau of Safety and Environmental Enforcement, it takes about 72 hours to begin subsurface dispersants operations. The model simulations assumed that the blowout plume was 100% treated at a dispersant-to-oil ratio (DOR) of 1:100 (which corresponds to high dispersability). To carry out this response, a supply of 273,524 gallons (1,035,401 liters or 1,035.4 m^3) of dispersants would be required. There were no limitations applied for operational time periods or weather-related down-times.

Table 17. Subsurface dispersant injection modeling assumptions for scenario 2B.

ID #	Response Start	Response End	Dispersant-to-Oil Application Ratio	Fraction of Plume Treated (%)	Location of Treatment	Daily Volume of Dispersant Applied (gallons)	Total Volume of Dispersant Applied (gallons)	Pump Rate Assuming Constant Operation (gpm)
2B	72 hrs post-spill start	Day 34 post-spill start	1:100	100	wellhead	8,823	273,524	6.1

To model the response, the subsurface dispersant injection is applied in the near-field modeling. OILMAP Deep includes a subsurface dispersant algorithm to account for the interfacial tension (IFT) reduction that results from treating subsurface oil with dispersant. The model allows for a variable fraction of the plume to be treated and takes inputs defining the volume of dispersant applied to determine the DOR of the treated fraction.

Note that “dispersant to oil ratio” terminology for subsea dispersant applications differs from surface dispersant applications:

- The DOR for surface dispersant application refers to the ratio of volume of oil to be potentially removed per volume of dispersant being applied. Thus, a larger DOR (e.g., 1:40 vs. 1:20) implies a more “efficient” dispersant type (or application method) that will reduce the amount of floating oil by fractioning it into small oil droplets.
- In subsea dispersant treatments, the objective is to reduce the interfacial tension of the oil and create smaller oil droplets that remain permanently dispersed in the water column. Unlike the application of surface dispersants, the DOR for subsea application refers to the volumetric ratio of dispersant to oil, such that a larger DOR (e.g., 1:150) reduces the droplet size distribution more than a smaller DOR (e.g., 1:100).

The dispersant treatment algorithm employs a modified Weber number calculation based on an adjusted IFT determined by the relationship between IFT and DOR. This relationship is based on findings from laboratory experiments (Khelifa and So, 2009). The empirical findings from the different studied oil/dispersant mixtures were averaged to develop a singular proxy for the IFT reduction function; this relationship (shown in Figure 55) is nonlinear and highly sensitive (both axes use a logarithmic scale). At lower dosage (DOR ~1:1000), by increasing the amount of dispersant being used, the IFT initially reduces relatively slowly as a function of DOR and then decreases sharply before leveling off (DOR between 1:100 and 1:10). Interestingly, beyond a certain optimal (DOR greater than approximately 1:20), increasing the dispersant actually increases the IFT; beyond this ratio, the increase in dispersant usage becomes counter-productive. Also shown for reference in this figure are the IFT of untreated oil and a commercial dispersant; interestingly the mixture of oil and dispersant can have an IFT less than that of the dispersant. Dispersant application can lower interfacial tension to values orders of magnitude smaller than those typically associated with untreated/unweathered oil.

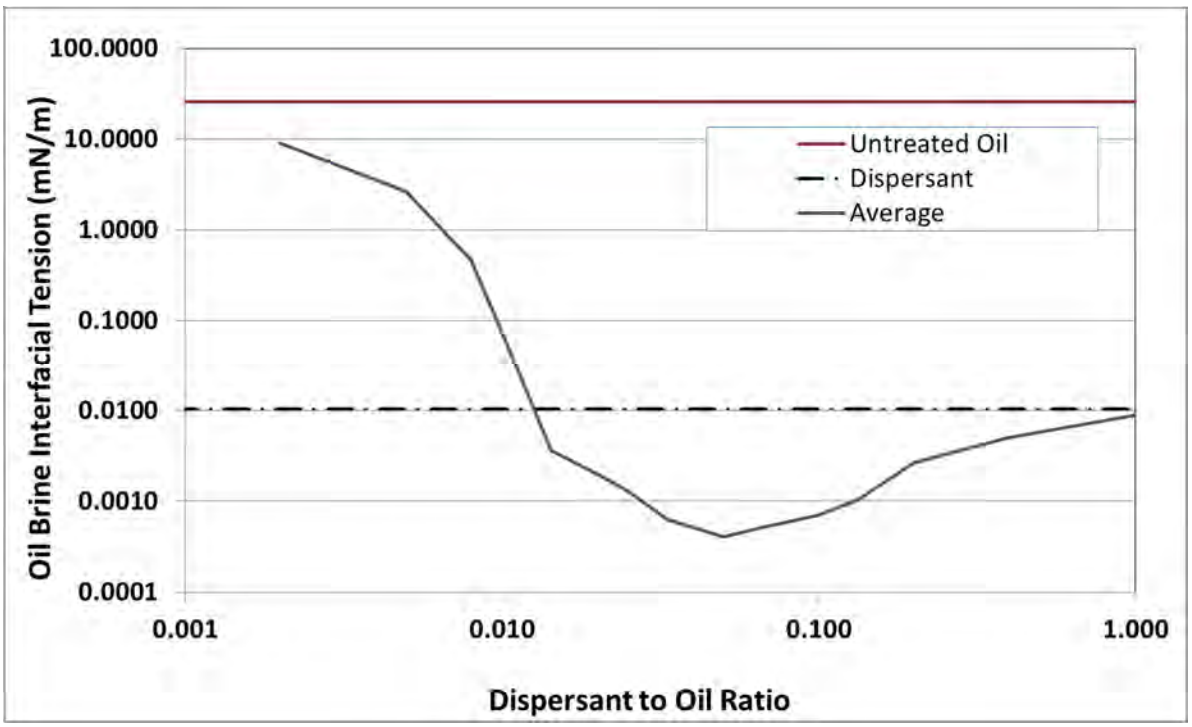

Figure 55. Oil-brine interfacial tension as a function of Dispersant to Oil Ratio (DOR) (1 mN/m = 1 dyne/cm). The plot is using logarithmic scales in both axis.

Figure 56 illustrates the effect of subsurface dispersant injection on the droplet size distribution for scenario 2B. The untreated (no dispersant) simulation predicts droplets sizes ranging from 500 µm to 10,000 µm (Section 6.3). By reducing the IFT, the dispersant treatment reduces the oil droplet size range dramatically, with droplets sizes ranging from 27 µm to a maximum of 540 µm.

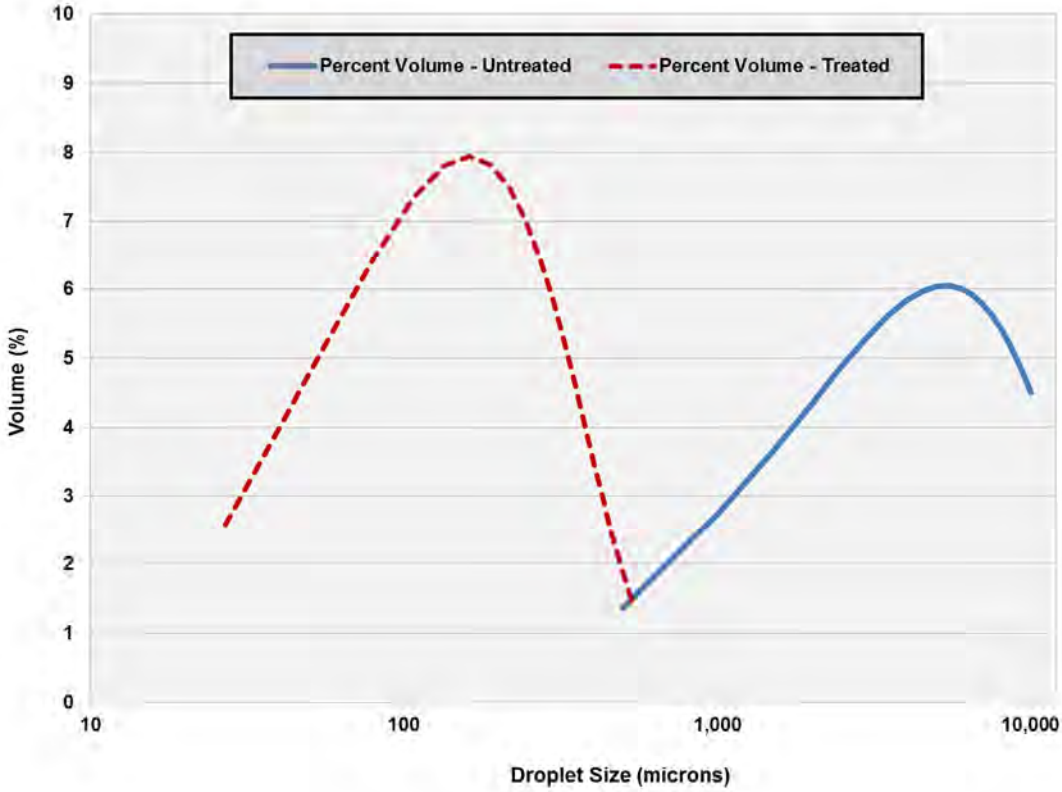

Figure 56. Predicted droplet size distribution for scenario 2B, with and without subsurface dispersant treatment (DOR 1:100). Note: the x-axis is logarithmic.

Droplet rise velocity is a function of droplet diameter and therefore is always the same for a given oil droplet diameter. Figure 57 shows the time it would take oil droplets of varying sizes to reach the water surface based on free rise velocities only (i.e., not taking into account dispersion or vertical currents) and the vertical rise distance between the trap height and the water surface (i.e., 429 m, see Section 6.3). This figure illustrates the large differences in free rise time to surface for the treated and untreated scenarios. The untreated scenario has droplets that would surface in less than 1 to approximately 11 hours, and the 1:100 DOR treatment scenario has droplets that would surface in approximately 10 to 2,771 hours. Lower rise velocities of the oil particles correspond to longer residence times of oil suspended in the water column and thus a larger volume of affected water. In the far-field modeling in SIMAP, it is assumed that droplets smaller than 50 µm in diameter would remain permanently entrained in the water column.

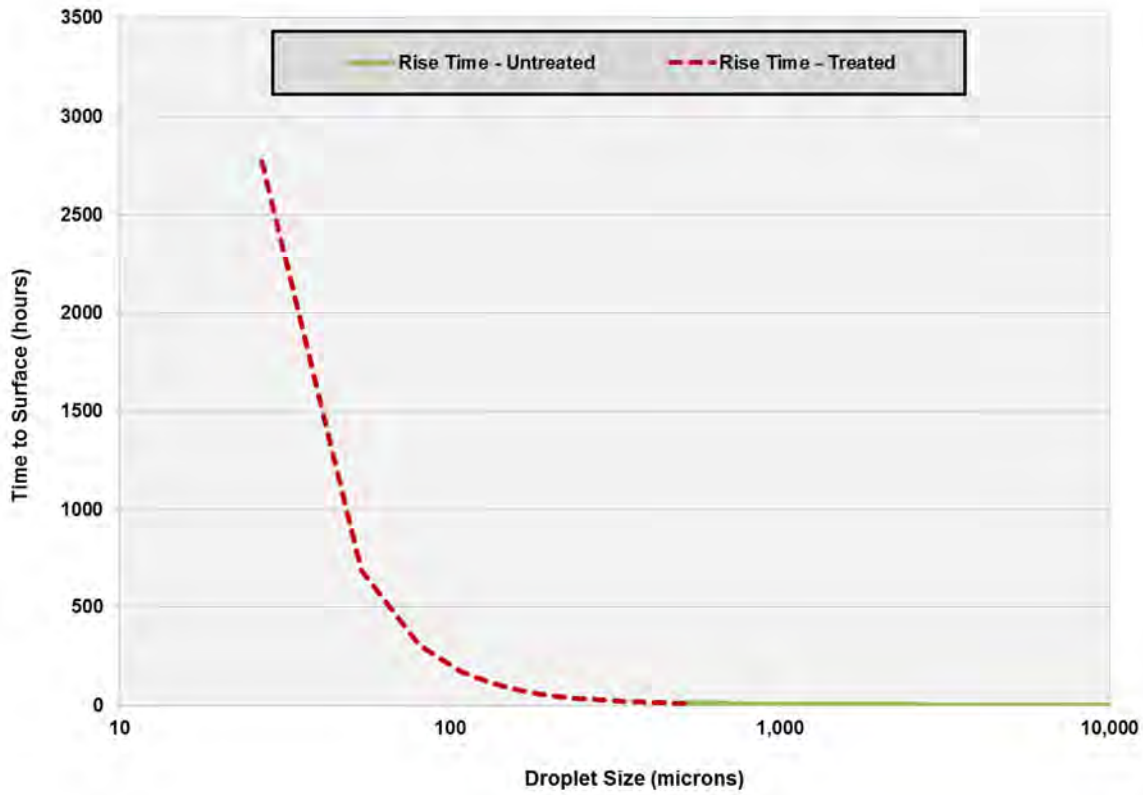

Figure 57. Predicted rise time to the surface based on free rise velocity for the droplet size distributions associated with the untreated and treated (DOR 1:100) simulations for scenario 2B. Note: the x-axis is logarithmic.

6.5.2 Deterministic Results

Note: Because the deterministic simulations for this spill site were run longer than the corresponding stochastic simulation (i.e., 100 vs. 79 days for scenario 2B), the deterministic results presented herein are not directly comparable to the stochastic results reported in Section 6.4.2. Similarly, the selection criteria used to identify the deterministic cases from the stochastic analysis should be interpreted with caution. For example, the worst case shoreline length oiled trajectory in the stochastic analysis (79-day simulation) may no longer be the worst case shoreline length oiled trajectory when simulated for 100 days in the deterministic analysis.

Key results from the deterministic simulations for the Baffin Bay 34-day blowout scenario (2B) are summarized in Table 18, including volume of water exceeding 1 ppb of dissolved aromatics (the most toxic components of oil), water surface area oiled, shoreline length oiled, time to first reach shore, and peak volume of oil ashore.

Table 18. Summary of deterministic results for the Baffin Bay 34-day blowout scenarios.

ID	Deterministic Case	Volume of Water Exceeding 1 ppb of Dissolved Aromatics (m^3)	Water Surface Area Oiled Above 0.01 g/m^2 (km^2)	Water Surface Area Oiled Above 10 g/m^2 (km^2)	Shoreline Length Oiled Above 100 g/m^2 (km)	Time to Shore (Days)	Peak Volume of Oil Ashore (m^3)
2B	Worst-case Shoreline Length Oiled	1.5×10^{10}	8,615.1	948.1	1,427.9	6.4	26,076.8
2B	Worst-case Shoreline Length Oiled, with Response	5.0×10^{10}	14,161.5	513.0	1,325.6	6.3	22,184.2
2B	Worst-case Water Surface Area Oiled	2.8×10^{11}	5,651.1	1,786.1	111.5	13.5	636.7
2B	Worst-case Volume of Oil in the Water Column [1]	1.1×10^{10}	19,978.7	976.5	1,323.6	13.1	25,963.1

[1] Note: This case was selected from the stochastic analysis based on the 95th percentile case for total hydrocarbons in the water column, which is used as a proxy for evaluating water column contamination. The detailed deterministic modeling provides more specific water column contamination metrics, namely the volume of water contaminated above 1 ppb of dissolved aromatics (a screening threshold for impacts on sensitive water column organisms). The worst case volume of total hydrocarbons in the water column does not necessarily result in the worst case volume of water contaminated above 1 ppb of dissolved aromatics, as many factors are involved (including simulation length).

The following figures (Figure 58 through Figure 65) the results of the deterministic simulations for scenario 2B. Three figures are shown for each deterministic case:

4. **Maximum Floating Oil Concentration**: This map shows the maximum concentration (g/m^2) of floating oil that passed through a given area at some point during the simulation. This map also displays the approximate subsurface area swept by dissolved aromatic concentrations greater than 1 ppb. This concentration is used as a screening threshold for potential impacts on sensitive water column organisms (based on French McCay, 2009).

5. **Shoreline Oil Concentration**: This map shows the concentration (g/m^2) of oil on the shoreline at the end of the simulation.

6. **Mass Balance**: This graph shows a time history of the fate and weathering of the spilled oil during the simulation. Components of the oil tracked over time include amount of oil on the sea surface, on the shoreline, in the water column (subsurface), in subsea sediments, evaporated into the atmosphere, and decayed (e.g., by photo-oxidation, biodegradation).

A brief description of each deterministic simulation follows the figures for each case.

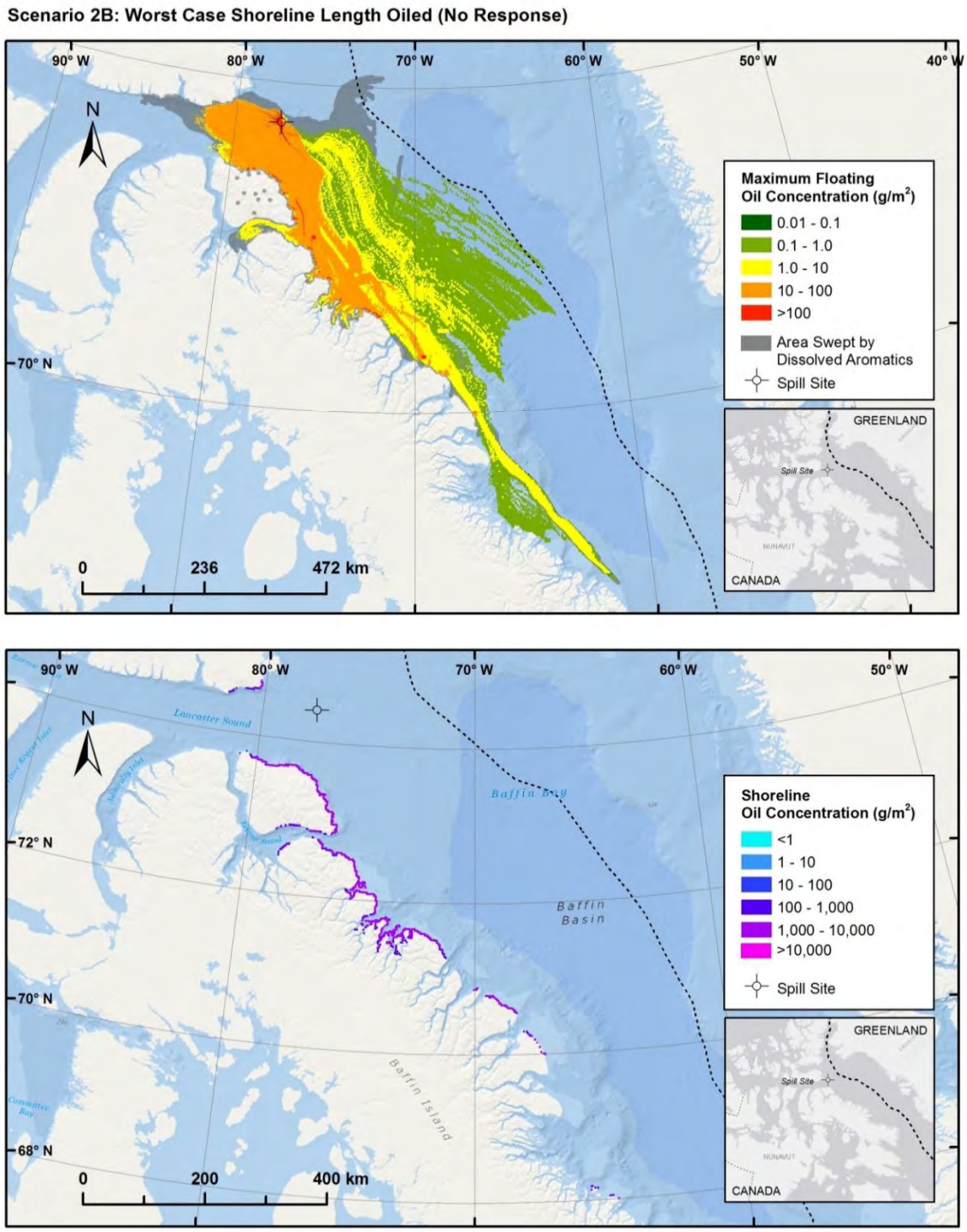

Figure 58. Scenario 2B: Worst-case (95th percentile) trajectory for shoreline length oiled above 100 g/m^2, with no spill response – Maximum concentration (g/m^2) of floating oil that passed by a given area during the simulation and the subsurface area swept by dissolved aromatics (top panel); and total concentration (g/m^2) of oil on the shoreline at the end of the simulation (bottom panel).

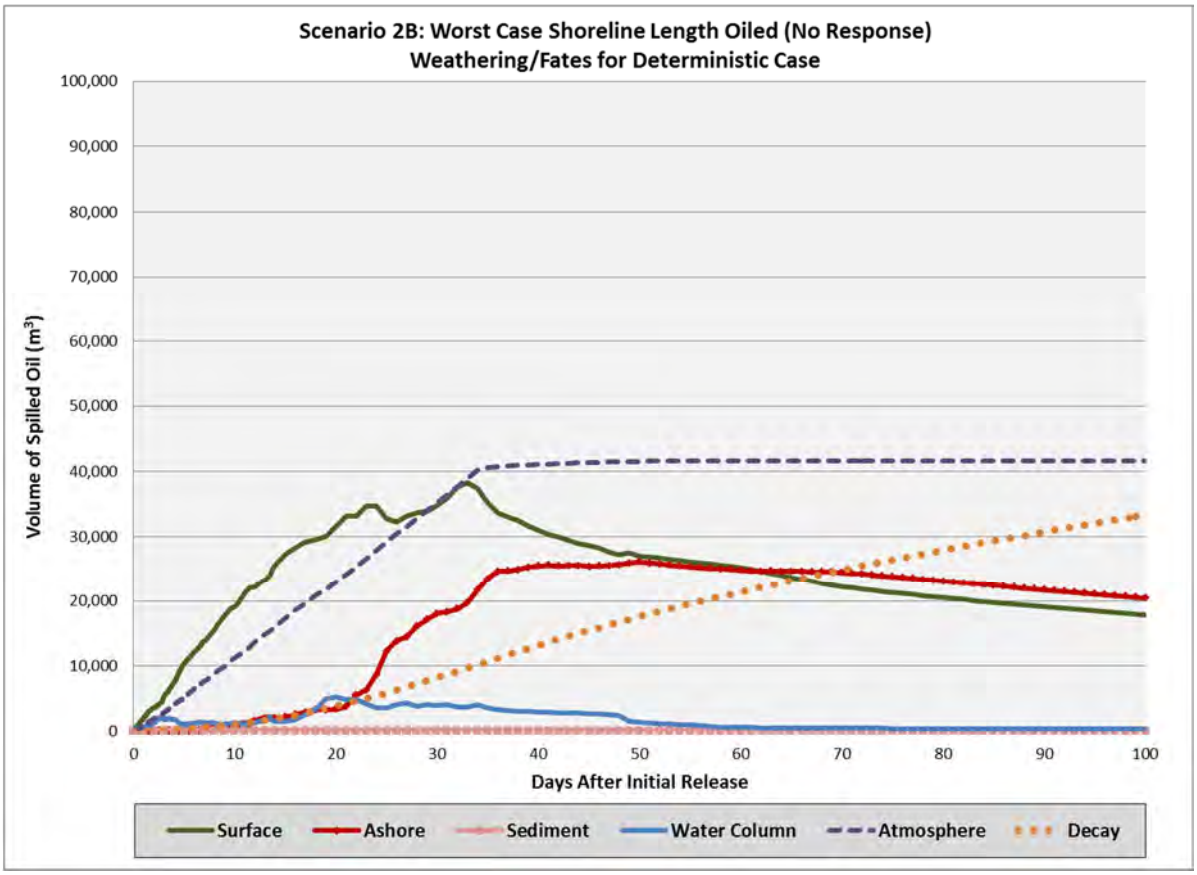

Figure 59. Scenario 2B: Worst-case (95th percentile) trajectory for shoreline length oiled above 100 g/m^2, with no spill response – Mass balance graph.

For scenario 2B, the worst-case trajectory for shoreline length oiled was modeled without spill response (Figure 58 and Figure 59) and with the subsurface injection of dispersants (Figure 60 and Figure 61).

For the no-response scenario, the spill trajectory heads to the north of the spill site for the first day of the spill, then turns to the west, reaching the shoreline of Devon Island at 6.4 days into the simulation, and north Bylot Island at about 9 days into the simulation. The floating oil then turns to the south and southeast and travels along Bylot Island, oiling the coast. At 18 days into the simulation, the oil has begun to reach the shoreline of Baffin Island. At about 28 days into the simulation, the floating oil not retained on shore begins to travel westward, entering Pond Inlet and the mouth of Lancaster Sound and causing further shoreline oiling along the associated coastlines. By 35 days, the trajectory has mainly turned southeastward again and travels along the coastline of Baffin Island, causing shoreline oiling nearly as far south as Kivitoo. At the end of the 100-day simulation, 17,878.4 m^3 of oil (about 16% of the volume spilled) remains on the water surface in Baffin Bay, the vast majority of which is trapped in landfast ice or bound in floating sea ice and moving with the ice currents.

Evaporation plays a major role in removal, with about 37% of the spilled volume evaporated, most of which occurred during the first 34 days. Natural decay processes also play a large role, with about 29% of the spilled volume removed by natural decay processes such as

biodegradation and photo-oxidation by the end of the simulation. The peak volume of oil on the shoreline was 26,076.8 m^3, at 50 days after the spill start. At the end of the simulation, 20,443.8 m^3 of oil remains on shore, with a total of 1,427.9 km of shoreline oiled above the ecological threshold of 100 g/m^2.

In general, the subsurface area swept by dissolved aromatics (the most toxic components of oil) followed the same trajectory as the surface oil, extending somewhat beyond the surface oil footprint to the north, east, and west. The peak volume of water exceeding 1 ppb of dissolved aromatics (a screening threshold for impacts on sensitive water column organisms) was 1.5×10^{10} m^3. At the end of the simulation, about 265.5 m^3 of oil remains entrained in the water column and over time will tend to move with the prevailing subsurface currents.

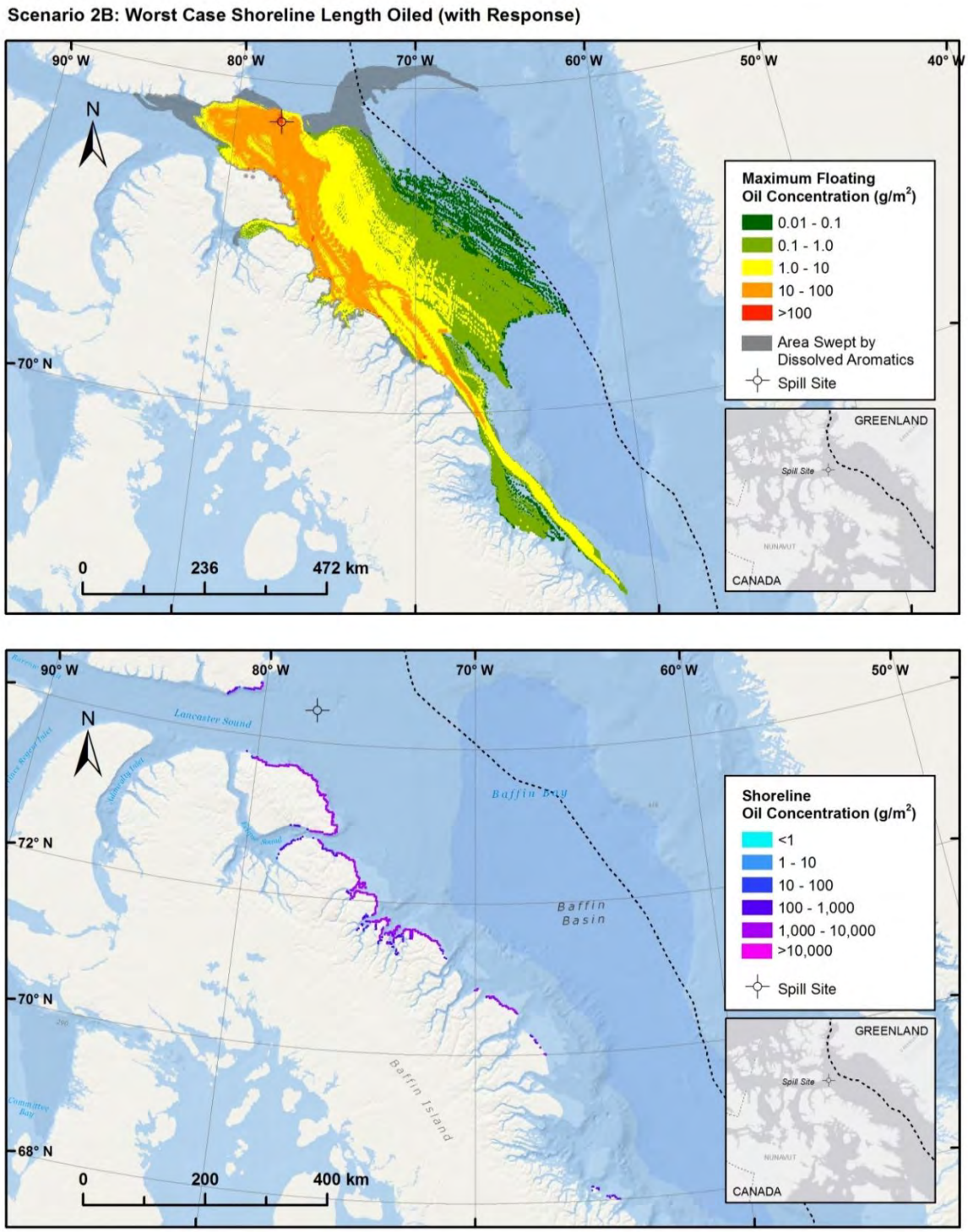

Figure 60. Scenario 2B: Worst-case (95th percentile) trajectory for shoreline length oiled above 100 g/m^2, with spill response (subsurface dispersant injection) – Maximum concentration (g/m^2) of floating oil that passed by a given area during the simulation and the subsurface area swept by dissolved aromatics (top panel); and total concentration (g/m^2) of oil on the shoreline at the end of the simulation (bottom panel).

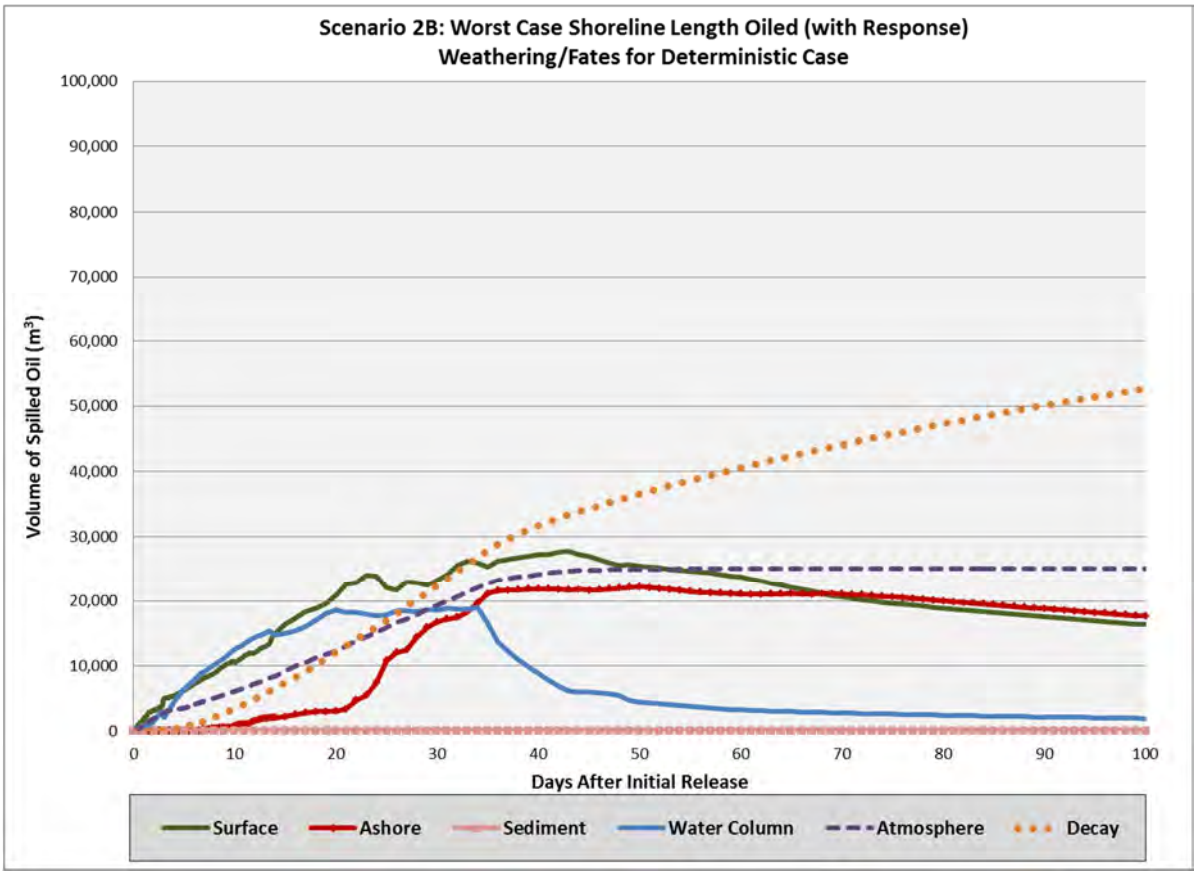

Figure 61. Scenario 2B: Worst-case (95th percentile) trajectory for shoreline length oiled above 100 g/m^2, with spill response (subsurface dispersant injection) – Mass balance graph.

For the scenario 2B, the worst-case trajectory for shoreline length oiled with the subsurface injection of dispersants (Figure 60 and Figure 61), the floating oil follows the same general trajectory described for the no-response scenario in the previous paragraphs. The spill trajectory heads to the north of the spill site for the first day of the spill, then turns to the west, reaching the shoreline of Devon Island at about 6.3 days into the simulation, and north Bylot Island at about 9 days into the simulation. The floating oil then turns to the south and southeast and travels along Bylot Island, oiling the coast. At about 18 days into the simulation, the oil has begun to reach the shoreline of Baffin Island. At about 28 days into the simulation, the floating oil not retained on shore begins to travel westward, entering Pond Inlet and the mouth of Lancaster Sound and causing further shoreline oiling along the associated coastlines. By 35 days, the trajectory has mainly turned southeastward again and travels along the coastline of Baffin Island, causing shoreline oiling nearly as far south as Kivitoo.

Though the trajectory is similar between the response and no-response scenarios, the volume of oil on the water surface and on the shore is reduced when response (beginning 3 days post-spill start) is applied. At the end of the 100 day simulation, 16,352.3 m^3 of oil (about 14% of the volume spilled) remains on the water surface in Baffin Bay, the vast majority of which is trapped in landfast ice or bound in floating sea ice and moving with the ice currents. This surface volume is reduced from 17,878.4 m^3 (about 16% of the volume spilled) in the no-response case. The peak volume of oil on the shoreline is 22,184.2 m^3, at 50 days after the spill start, compared to 26,076.8

m^3 in the no-response case. At the end of the simulation, 17,633.5 m^3 of oil remains on shore, with a total of 1,325.6 km of shoreline oiled above the ecological threshold of 100 g/m^2 (reduced from 1,427.9 km in the no-response scenario).

The subsurface injection of dispersants resulted in a smaller size distribution of oil droplets (see Section 6.5.1.1) that are slow to rise to the surface and thus have a long residence time in the water column. While this reduces the amount of oil on the surface and shoreline, it increases the amount of oil in the water column and leads to a larger affected volume of water. For the response scenario, the volume of oil entrained in the water column at the end of simulation was 1,908.7 m^3, compared to 265.5 m^3 in the no-response case. The peak volume of water exceeding 1 ppb of dissolved aromatics (a screening threshold for impacts on sensitive water column organisms) was 5.0×10^{10} m^3 (compared to 1.5×10^{10} m^3 in the no-response case).

Like the no-response case, evaporation plays a role in removal, with about 22% of the spilled volume evaporated, most of which occurred during the first 34 days. Natural decay processes also play a large role, with about 46% of the spilled volume removed by natural decay processes such as biodegradation and photo-oxidation by the end of the simulation.

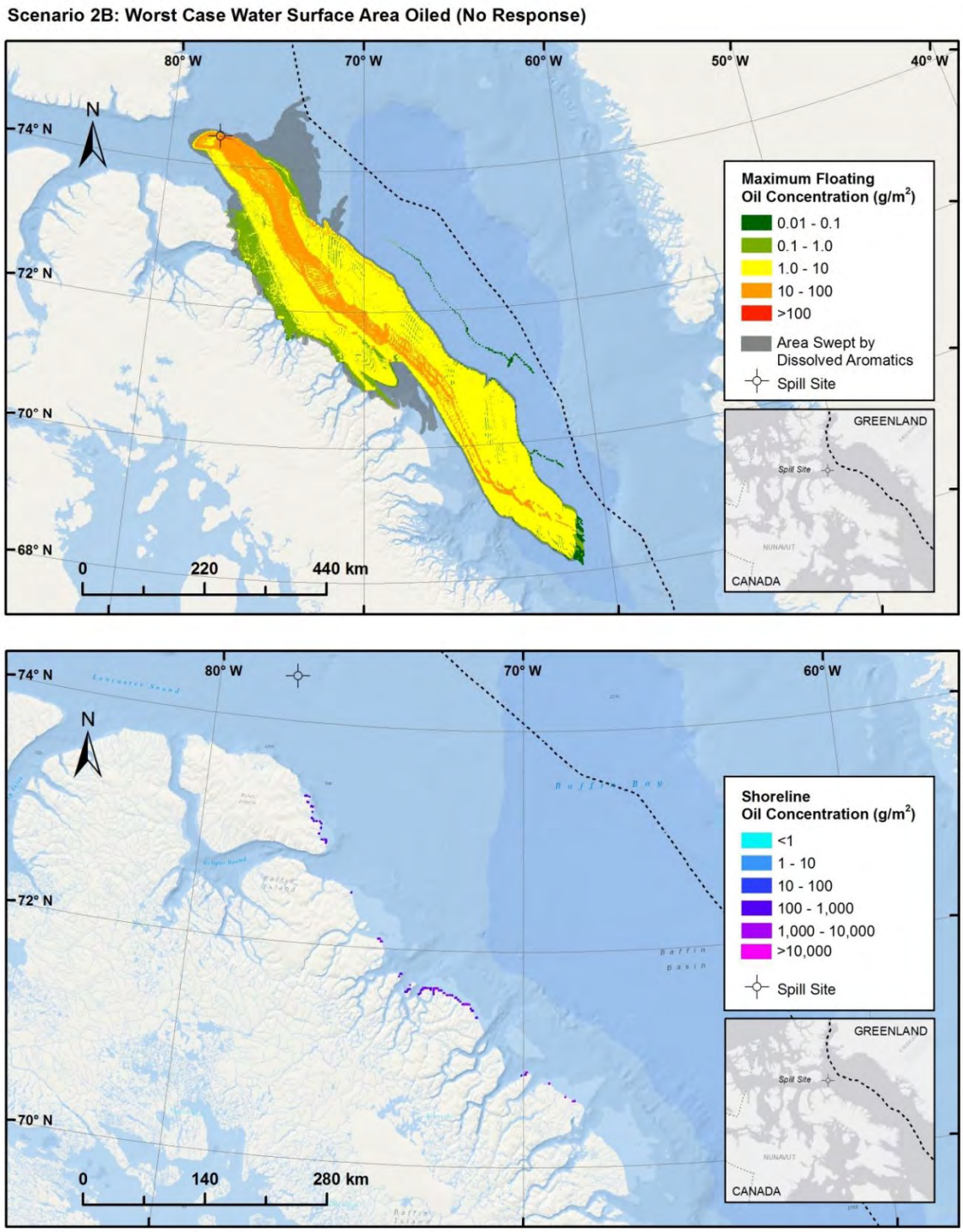

Figure 62. Scenario 2B: Worst-case (95th percentile) trajectory for water surface area oiled above 10 g/m^2, with no spill response – Maximum concentration (g/m^2) of floating oil that passed by a given area during the simulation and the subsurface area swept by dissolved aromatics (top panel); and total concentration (g/m^2) of oil on the shoreline at the end of the simulation (bottom panel).

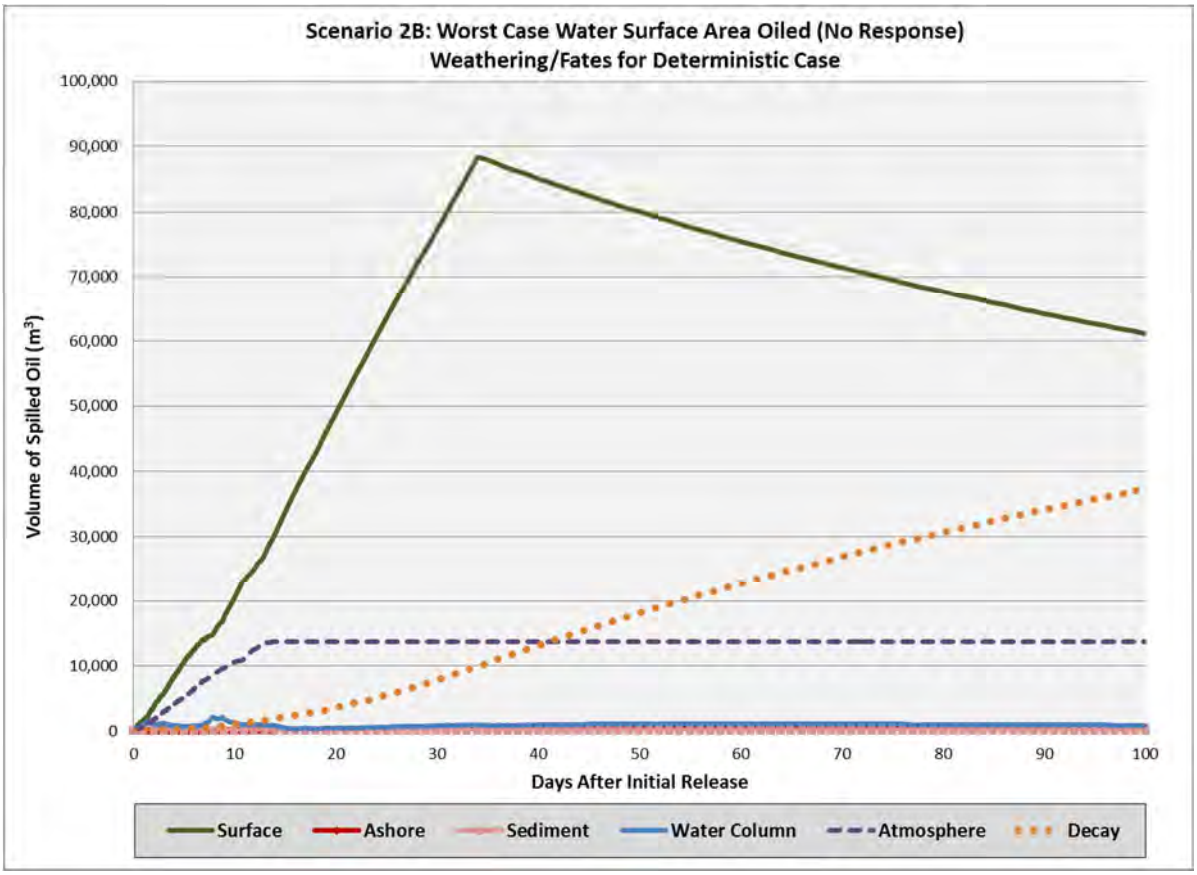

Figure 63. Scenario 2B: Worst-case (95th percentile) trajectory for water surface area oiled above 10 g/m^2, with no spill response – Mass balance graph.

For scenario 2B, the worst-case trajectory for water surface area oiled was modeled without spill response (Figure 62 and Figure 63).

The spill trajectory initially heads primarily to the southeast of the spill site, turning more to the west approximately 12 days after the spill start, and reaching the shoreline of Bylot Island at 13.5 days into the simulation. The floating oil trajectory continues to travel southeastward along the Canadian coast, and begins to oil the shoreline of Baffin Island at about 16 days into the simulation. By this point in the simulation, the majority of floating oil not retained on shore is bound in sea ice and moving with the ice currents. The oil continues to travel southwestward along the coast of Baffin Island, oiling areas nearly as far south as the Clyde River area. At the end of the 100-day simulation, 61,138.8 m^3 of oil (about 54% of the volume spilled) remains on the water surface in Baffin Bay, the vast majority of which is trapped in landfast ice, or bound in sea ice. Over time, this oil would continue to move with the ice currents, potentially oiling other areas.

Because the oil becomes trapped in sea ice beginning at about 16 days into the simulation, evaporation is reduced and plays less of a role in removal, with about 12% of the spilled volume evaporated. Natural decay processes still play a large role (as much of the decay occurs in subsurface waters, unaffected by the presence of ice), with about 33% of the spilled volume removed by natural decay processes such as biodegradation and photo-oxidation by the end of the simulation. The peak volume of oil on the shoreline was 636.7 m^3, at 43 days after the spill start. At

the end of the simulation, 453.0 m^3 of oil remains on shore, with a total of 111.5 km of shoreline oiled above the ecological threshold of 100 g/m^2.

In general, the subsurface area swept by dissolved aromatics (the most toxic components of oil) followed the same trajectory as the surface oil, extending somewhat beyond the surface oil footprint to the east and southwest. The peak volume of water exceeding 1 ppb of dissolved aromatics (a screening threshold for sensitive water column organisms) was 2.8×10^{11} m^3. At the end of the simulation, about 855.2 m^3 of oil remains entrained in the water column and over time will tend to move with the prevailing subsurface currents.

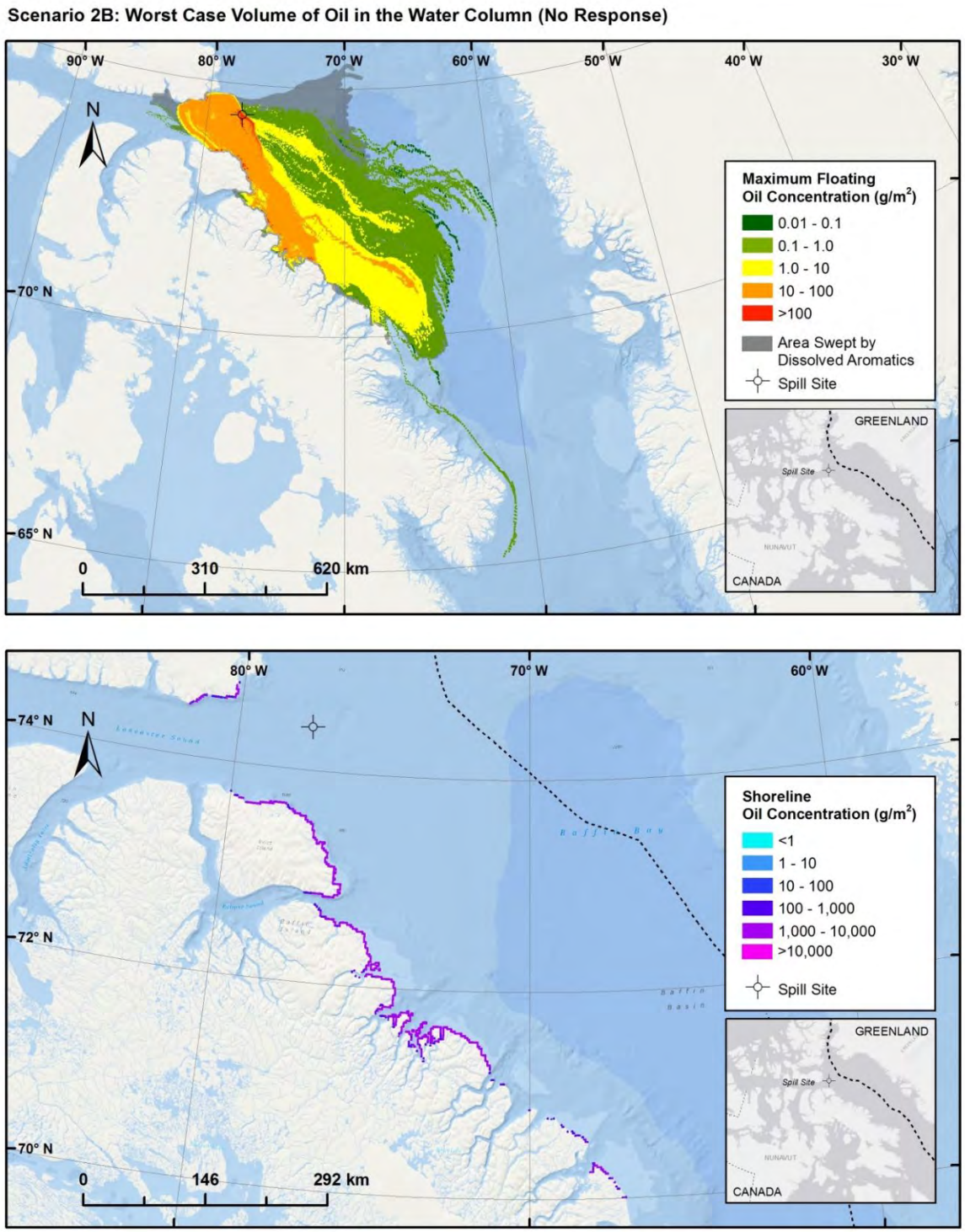

Figure 64. Scenario 2B: Worst-case (95th percentile) trajectory for volume of oil in the water column, with no spill response – Maximum concentration (g/m^2) of floating oil that passed by a given area during the simulation and the subsurface area swept by dissolved aromatics (top panel); and total concentration (g/m^2) of oil on the shoreline at the end of the simulation (bottom panel).

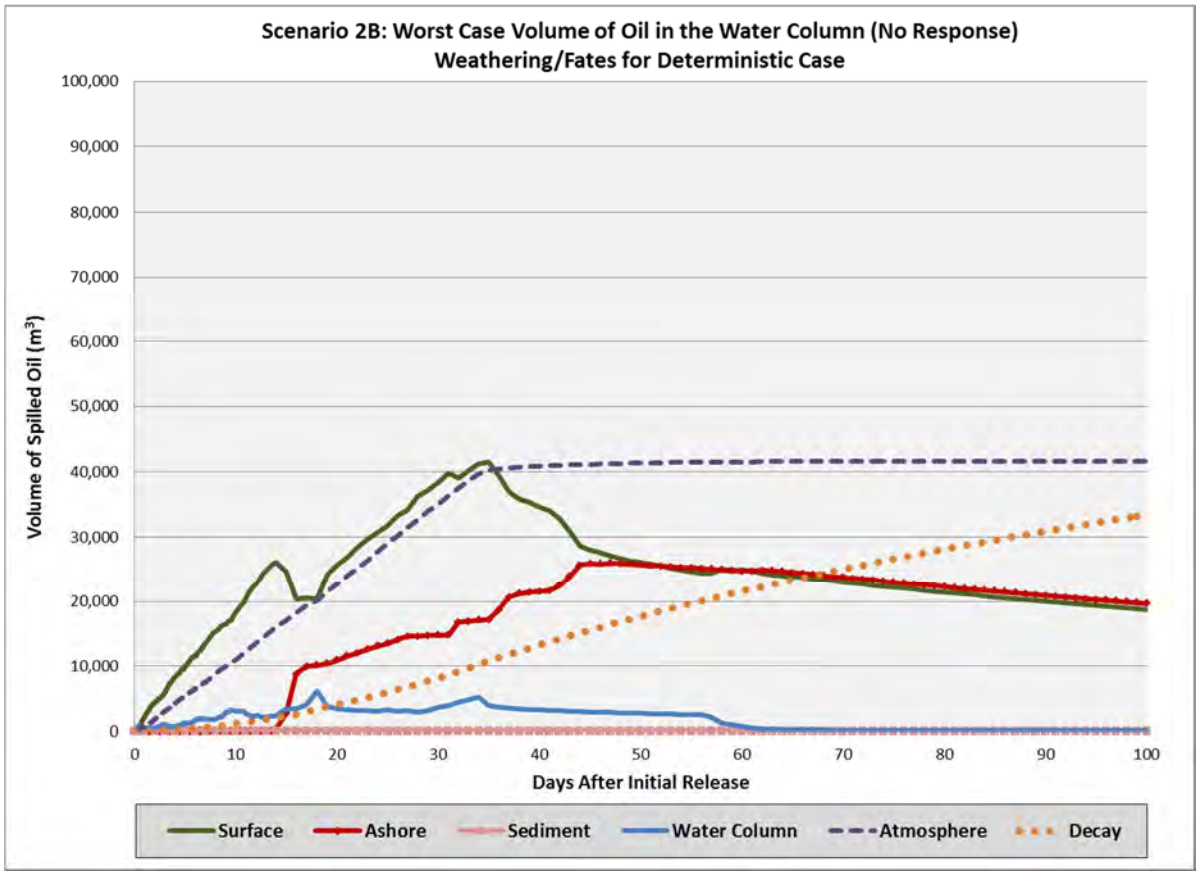

Figure 65. Scenario 2B: Worst-case (95th percentile) trajectory for volume of oil in the water column, with no spill response – Mass balance graph.

For scenario 2B, the worst-case trajectory for volume of oil in the water column was modeled without spill response (Figure 64 and Figure 65).

The spill trajectory initially heads to the west of the spill site, turning southeastward after about 2 days. The floating oil continues to travel southwestward offshore of Bylot and Baffin Islands until about 12 days into the simulation, when the floating moves west, first making landfall on Bylot Island at 13.1 days into the simulation, and then subsequently oiling a large swath of the shoreline of Baffin Island and Bylot Island. At about 23 days after the start of the spill, the floating oil moves north-northwest and reaches the shoreline of Devon Island at about 24 days into the simulation. Floating oil also travels into the mouth of Lancaster Sound before turning southeastward again and traveling along Bylot and Baffin Islands, causing additional shoreline oiling. By about 60 days into the simulation, the majority of floating oil not retained on shore is bound in sea ice and moving with the ice currents southeastward through Baffin Bay. At the end of the 100-day simulation, 18,706.1 m^3 of oil (about 16% of the volume spilled) remains on the water surface in Baffin Bay, the vast majority of which is trapped in landfast ice, or bound in sea ice. Over time, this oil would continue to move with the ice currents, potentially oiling other areas.

Evaporation plays a major role in removal, with about 37% of the spilled volume evaporated, most of which occurred during the first 34 days. Natural decay processes also play a large role, with about 29% of the spilled volume removed by natural decay processes such as

biodegradation and photo-oxidation by the end of the simulation. The peak volume of oil on the shoreline was 25,963.1 m^3, at 47 days after the spill start. At the end of the simulation, 19,659.3 m^3 of oil remains on shore, with a total of 1,323.6 km of shoreline oiled above the ecological threshold of 100 g/m^2.

In general, the subsurface area swept by dissolved aromatics (the most toxic components of oil) followed the same trajectory as the surface oil, extending somewhat beyond the surface oil footprint to the west and northeast towards the North Water Polynya area. The peak volume of water exceeding 1 ppb of dissolved aromatics (a screening threshold for impacts on sensitive water column organisms) was 1.1×10^{10} m^3. At the end of the simulation, about 26.5 m^3 of oil remains entrained in the water column and over time will tend to move with the prevailing subsurface currents.

6.6 Conclusions

The hypothetical scenario 2B blowout (34 days of flow for a total spill volume of 113,560 m^3), if it were to occur, would be the fourth largest well blowout ever in the world, based on current records. Only 0.5% of blowouts have ever been of this size or larger. The smaller scenario 2A (1 day of flow for a total spill volume of 3,340 m^3) – would be the 15th largest well blowout incident worldwide. Only 2% of blowouts have ever been this size or larger. Both of these scenarios represent relatively extreme volumes for blowouts, with a very low likelihood of occurrence.[7]

Based on the stochastic analysis, both of the scenarios are highly likely to cause shoreline oiling above the ecological threshold of 100 g/m^2 at some location, with 71% of trajectories reaching shore for the 1-day blowout (scenario 2A), and 82% of trajectories reaching shore for the 34-day blowout scenario (scenario 2B). The potential shoreline oiling locations are widespread and include Greenlandic coastline near Kap Atholl, Kap Parry, Carey Islands, and Northumberland Island; and Canadian coastline along Ellesmere, Coburg, Devon, Bylot, and Baffin Islands. Because of the large geographic range of shorelines potentially affected, oil spill contingency and response planning for these blowout scenarios could be challenging.

For both of the blowout scenarios, the stochastic analysis indicated that there is a low to moderate probability of water surface oiling above the ecological threshold of 10 g/m^2 within the North Water Polynya area. Because of the relatively large size of the oil droplets from the blowouts (as indicated by the near-field modeling), the droplets tend to surface quickly and the residence time in the water column is relatively short. As such, entrainment of oil in the water column was relatively low for both scenarios.

In the deterministic analysis, the response strategy (i.e., subsurface dispersant injection) simulated for the 34-day blowout scenario (scenario 2B) reduced the peak amount of oil on the water surface by 28% and the peak amount of oil on the shoreline by about 15%. The shoreline length oiled above the ecological threshold of 100 g/m^2 was also reduced by about 7%. However, though the dispersant reduced the volume of oil ashore, shore length oiled, and the volume of oil on the water surface, it does not remove oil from the environment, but rather displaces it. As such, the peak volume of oil in the water column was increased by 265% and the volume of water

[7] See Appendix A for additional discussion of benchmarking blowout flow rates, durations, and total volumes, as well as a discussion of blowout likelihood.

exceeding 1 ppb of dissolved aromatics (a screening threshold for impacts on sensitive water column organisms) was increased by 233% when subsurface dispersant injection was included in the simulation.

Subsurface dispersants reduce the interfacial tension of oil, dramatically reducing the droplet size distribution of the blowout plume. This leads to more oil in the water column, increased dissolution rates of soluble hydrocarbons (mostly aromatics), and enhanced biodegradation rates. Application of dispersants can reduce the effects of shoreline oil and surface floating oil on birds and other wildlife, but the trade-off is increased risks to fish and invertebrates in the water column.

It should also be noted that even with the application of a highly effective spill response strategy for the 34-day blowout (scenario 2B), the environmental consequences of such a large volume blowout would be substantial.

7.0 SCENARIO 3 – GREENLAND COAST CRUISE SHIP SPILL

7.1 Scenario Development

One scenario (scenario 3) was developed for the western Greenland coast near Disko Island to simulate a hypothetical spill from a large cruise ship. The selected spill site location (Figure 66) is off Disko Island in Disko Bay at 69.074430°N, 53.500040°W. The site was selected because of its credibility as a potential accidental cruise ship spill site, as this is a popular route for cruise ships. The specific location was chosen based on its proximity to the shipping lane and the presence of rock pinnacles that would typically be the type of location at which a grounding accident might occur.

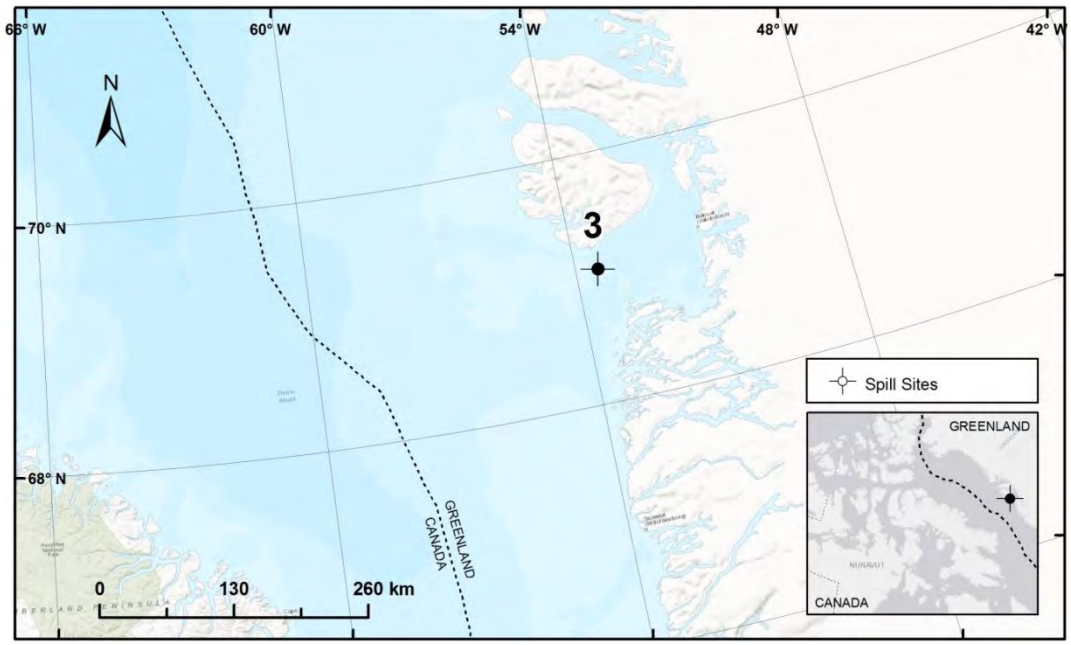

Figure 66. Location of the selected spill site off the Greenland coast near Disko Island (scenario 3).

The spill site location is about 15 km south of the location of the Quest grounding in June 2007 (Joint Division for Investigation of Maritime Accidents et al., 2008). The master of the Quest took the vessel off-course in that case to allow the small number of passengers to view icebergs and whales. The Quest was also smaller than the larger cruise ship being considered in this scenario. A larger cruise ship is less likely to deliberately go off course.

In addition, the selected modeling site also has particular significance with respect to ecological sensitivity. It is within the Priority 1 marine area in Disko Bay and Store Hellefiskebanke (Christensen et al., 2012). The region is a hotspot for tourism, whale spotting, seabird colonies, and an important fishery for Greenland halibut. In addition, the islands of Grønne Ejeland/Kitsissunnguit are protected by law because of their status as an important site for Arctic tern (Egevang et al., 2005). The Disko Bay area has also been named a potential Super-EBSA (Ecologically or Biologically Significant Marine Area) by the IUCN.

The location was also selected as one that could potentially cause impacts to sensitive areas outside of Disko Bay that are of particular concern with respect to marine mammals. The area serves as a key wintering area for species including bowhead and beluga whales and narwhal. The area is also an important recruitment area for shrimp and sand eels, which are a key forage fish for seals and whales. It is a vital wintering area for king eider (more than 50% of the flyway populations), common eider, and thick-billed murre, as well as other seabirds. Recent unpublished information indicates that the entire area between Disko Bay, south to Cape Farewell and west to the mouth of Hudson Strait, appears to be a winter hotspot for seabirds (Speer and Laughlin, 2011). There is a significant concentration of bearded seals on the ice at Store Hellefiskebanke and winter occurrences of walrus and seals, making it an important hunting area. In addition, the shrimp and Greenland halibut fisheries in this area are quite important to the Greenland economy.

The season defined for the hypothetical cruise ship spill scenario was July through September, which corresponds with the scheduled cruises through Disko Bay to Ilulissat. This time period also corresponds to open water conditions.

The oil type selected for modeling was an intermediate fuel oil, IFO 180, which is typical for a larger cruise ship. Cruise ships will use diesel fuel closer in to port, because of air emissions concerns, but will use an intermediate or heavy fuel oil while underway at sea. If a vessel uses IFO 180 while at sea, it would have some on board even while in port burning diesel. The IFO 180 was chosen for modeling because it would tend to have greater environmental consequences on the water surface and shorelines if spilled and would pose a greater challenge for cleanup response operations than diesel.

The spill volume for scenario 3 is based on a 68,000 GT (gross tonnage) cruise ship, such as the *Crystal Serenity*, which has regularly-scheduled cruises to Ilulissat during August and September. This is most likely to be the largest cruise ship to transit the waters of Disko Bay. Being the largest vessel, it would also have the correspondingly largest bunker fuel tanks. The bunker fuel volume for a 68,000 GT-cruise ship like the *Crystal Serenity* is about 2,800 m^3 (17,610 bbl), which would be divided amongst a number of smaller tanks. The release volume assumed for the scenario 3 was 280 m^3 (1,761 bbl), which would represent 10% of the bunker fuel. To put that in perspective, this volume would generally be considered a “maximum most-probable” discharge for a vessel of this size and type under current U.S. Coast Guard regulations. In the modeling, it was assumed that the oil would flow out of the bunker tank(s) involved over the course of about 12 hours.

Determining the probability of vessel oil spills due to accidents such as groundings and collisions involves determining the probability that there will be an accident and the probability that the accident will actually result in oil spillage. Not all accidents result in the spillage of oil. Collisions are unlikely to occur in this area since the transit routes are not particularly busy, but groundings are a distinct possibility.

There are about 15 to 20 trips per week with five ships during the cruise season of July to September for Disko Lines and one trip annually for the *Crystal Serenity* – or about 240 trips in the area per year. To develop a conservative estimate of a grounding related-spill, the accident rate from a study for Cook Inlet, Alaska (Etkin, 2012) was applied to the 240 transits to derive an estimate of accidents of 0.408 or 1 in 2.4 years. Assuming that the cruise ships have a double-hull on their bunker tanks, the probability that a grounding accident would result in a spill is 0.02. This

would mean that the likelihood of a grounding-related spill is conservatively about 0.0082 – or once in 122 years. Note that this is the chance of a spill of *some volume* of oil, not a particular volume. The likelihood of a grounding resulting in the spill volume modeled for this study would be even smaller.

See Appendix A for additional discussion regarding the development of spill scenario parameters and vessel spill likelihood.

7.2 Environmental Analysis

Monthly TOPAZ4 surface current roses for the Greenland coast spill site are shown in Figure 67. The directionality of surface currents is fairly consistent throughout the year, but there is seasonal variability evident. The primary direction is west-northwestward with average speeds ranging from 2-6 cm/s. During winter through early spring (December to April), surface current flow has a more northern component, while summer and fall indicates a more southern component.

Monthly TOPAZ4 surface current speed statistics (average and 95th percentile) show the variability in intensity throughout the year at the site of interest (Figure 68). Speeds are lowest in spring and early summer and highest during fall and winter. Monthly average surface current speeds are generally low, and range from a minimum of 2 cm/s in July, to a maximum of 6 cm/s in November.

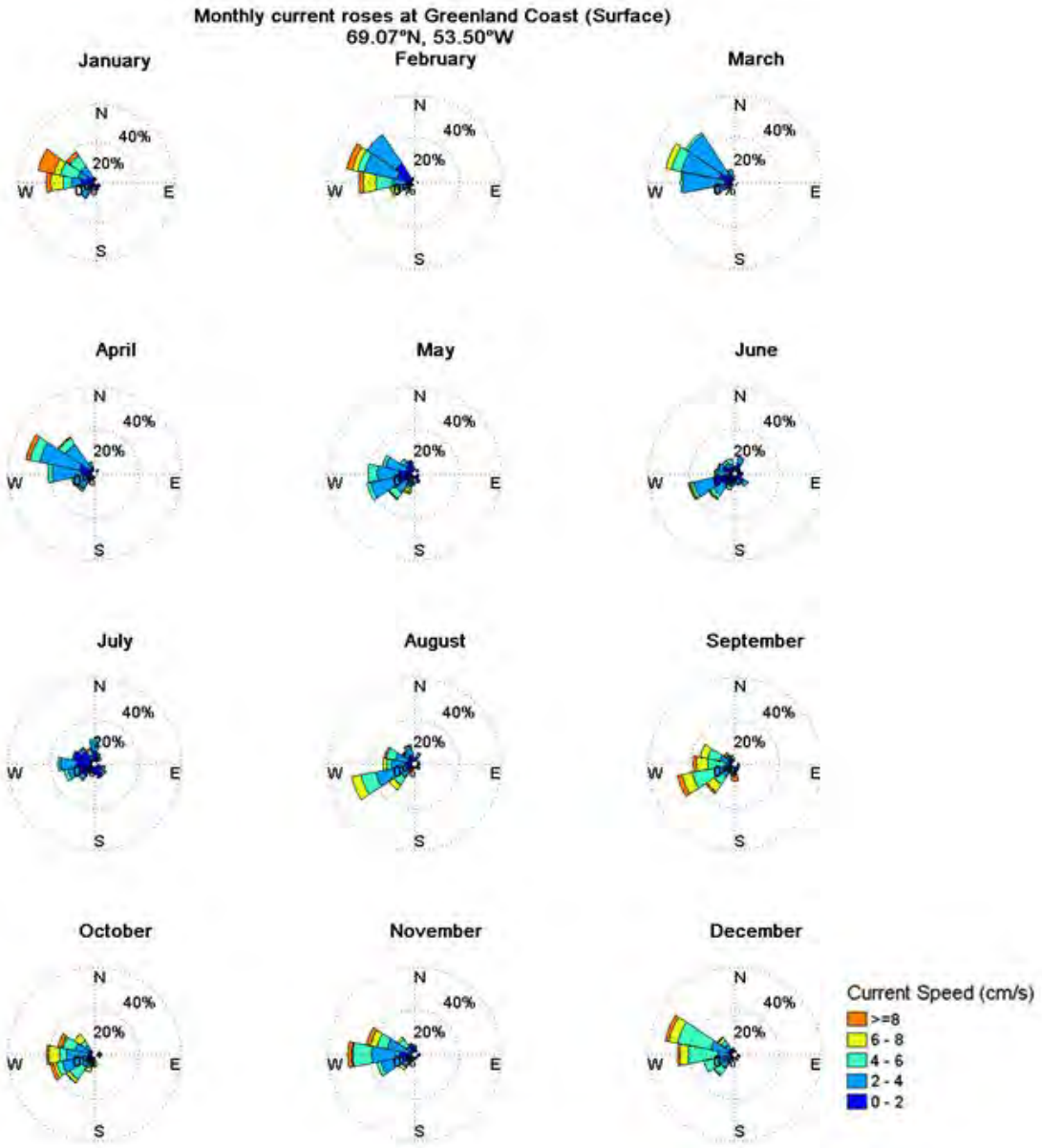

Figure 67. TOPAZ4 monthly averaged surface current roses near the Greenland coast spill site averaged over the period of 2011-2015. Direction convention is standard (i.e., direction currents are moving to).

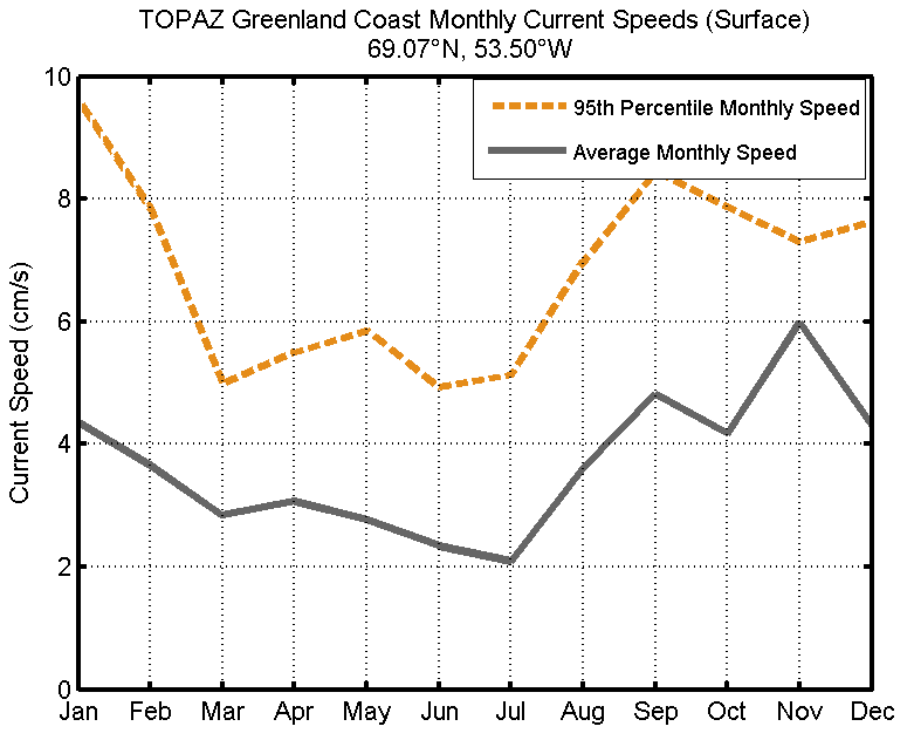

Figure 68. TOPAZ4 current statistics: monthly average (grey solid) and 95th percentile (orange dash) current speed at the surface near the Greenland coast spill site for 2011-2015.

Figure 69 presents the monthly ECMWF wind roses for the Greenland coast spill site. Wind speed is highest in winter months and can exceed 20 knots. Direction is variable, but overall exhibits a predominantly north-northwesterly wind.

The average monthly wind speeds statistics at the Greenland coast spill site are presented in Figure 70. The average monthly speeds range between 5-10 knots, with the lowest speeds occurring in summer (June-August). Wind intensity increases in September and reaches a maximum in December that lasts through January before declining steadily to a minimum in June-July.

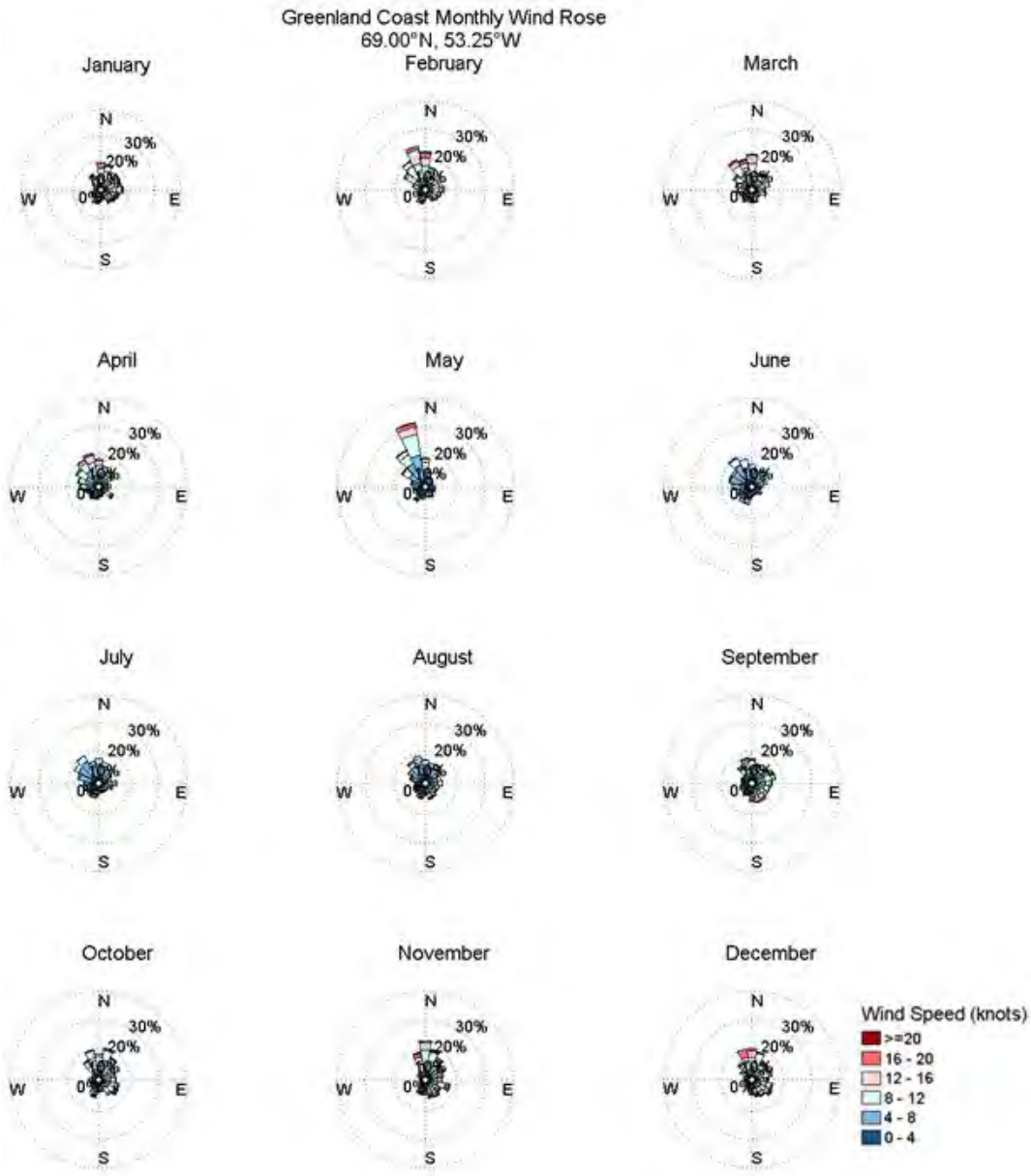

Figure 69. ECMWF monthly averaged wind roses near the Greenland coast spill site, averaged over the period of 2011-2015. Wind speeds are in knots, using meteorological convention (i.e., direction wind is coming from).

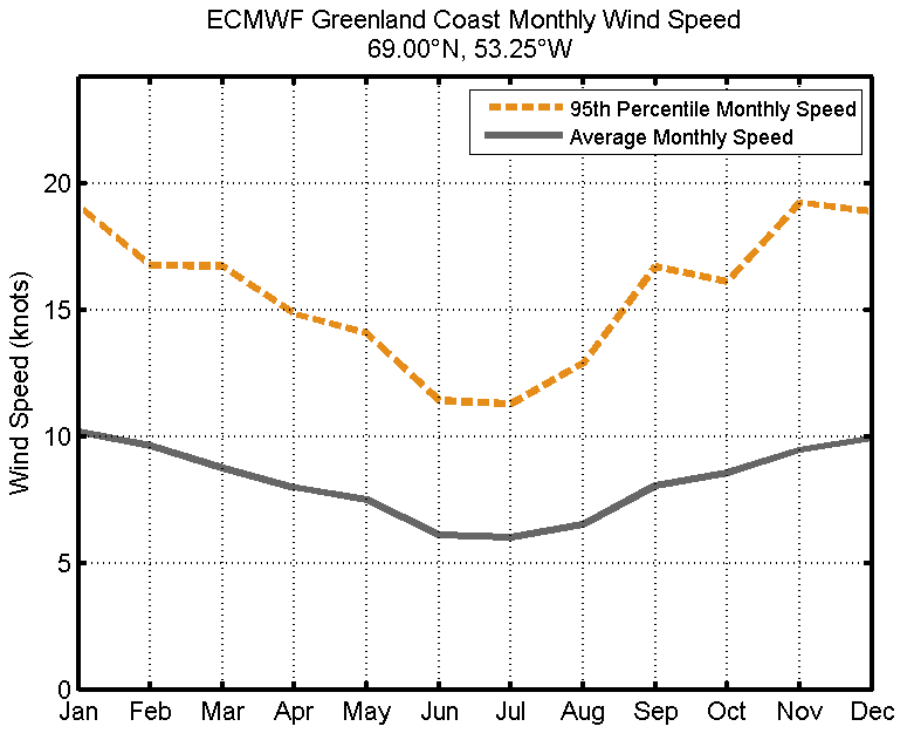

Figure 70. ECMWF wind statistics: monthly average (grey solid) and 95th percentile (orange dash) wind speed near the Greenland coast spill site for 2011-2015.

Monthly average sea ice and landfast ice cover near the spill site during the period of interest are shown in Figure 71. Sea ice coverage is based on data from TOPAZ4 (2011-2015) and landfast ice coverage is based on data from the National Snow and Ice Data Center (1991 through 1998).

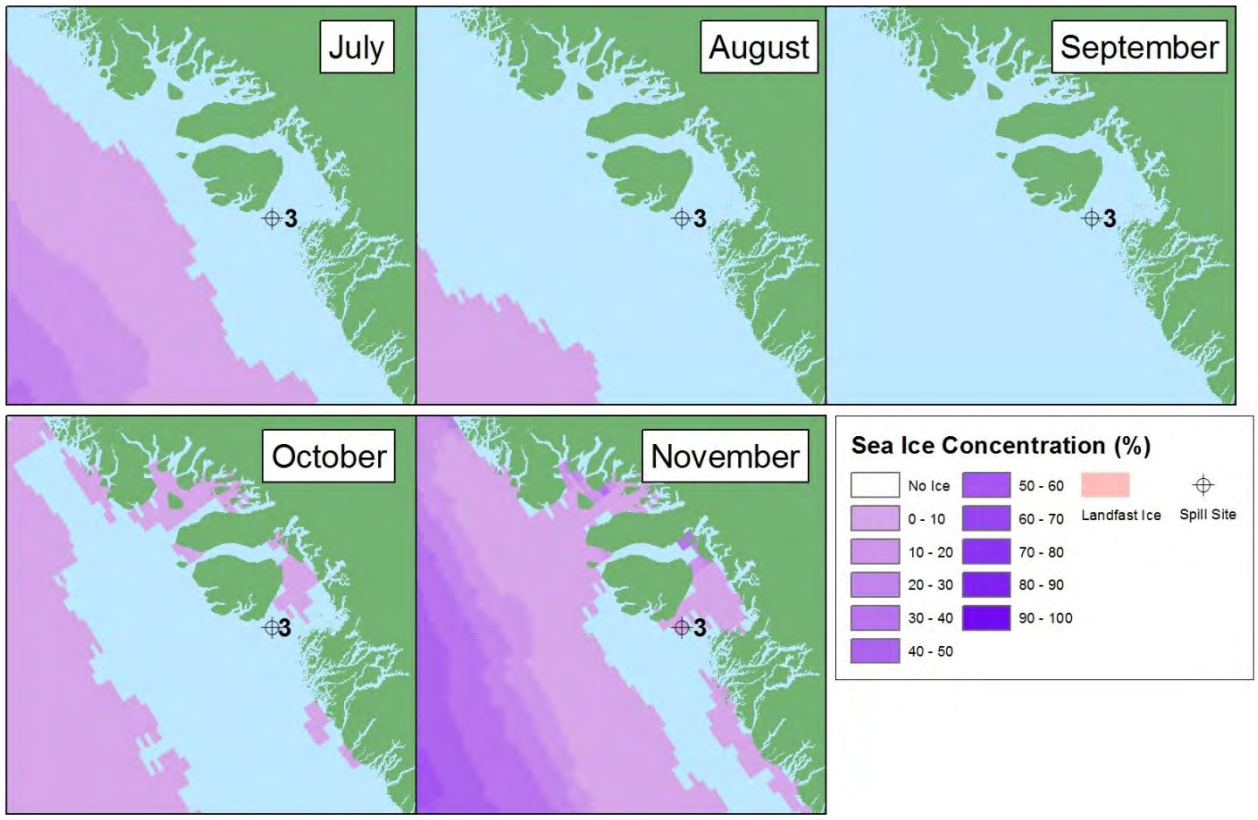

Figure 71. Average monthly cover of sea ice and landfast ice near the Greenland coast spill site during the period of interest.

The vertical profile of temperature, salinity, and density at the Greenland coast spill site for July through September is shown in Figure 72. Salinity is approximately 32.6 psu at the surface and increases to 34.1 psu near the sea floor. Temperature at the surface is about 5.3 ºC, decreasing to 1.7 ºC near the sea floor. Density at the surface is 25.7 kg/m^3 and increases to 27.2 kg/m^3 at depth.

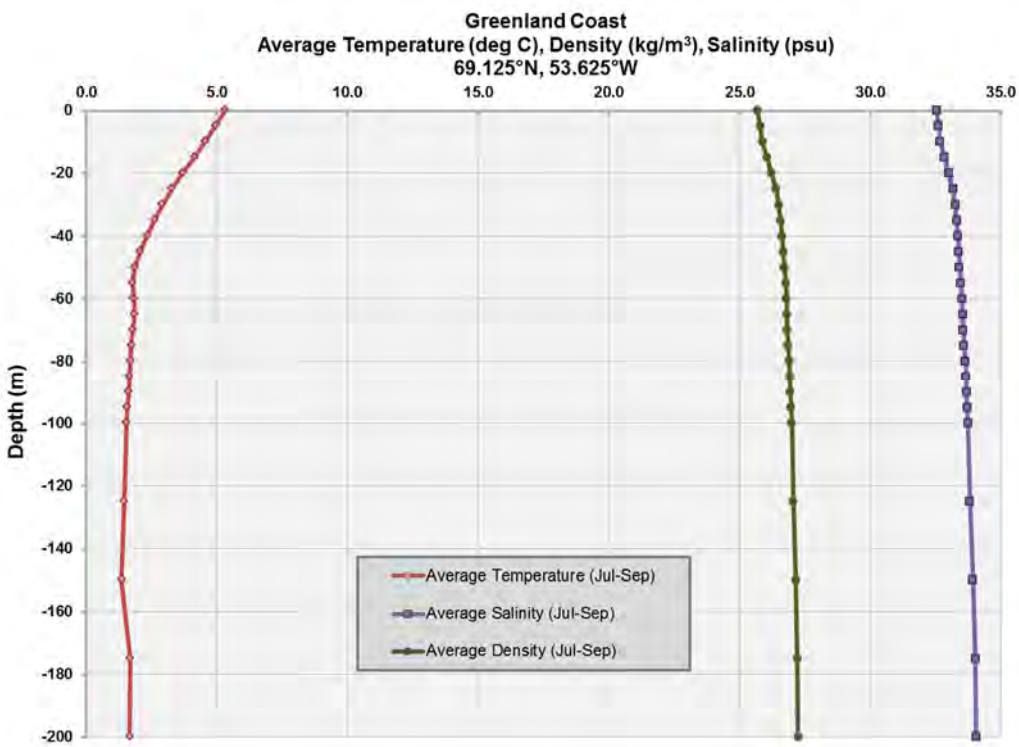

Figure 72. Vertical profile of average temperature (red), salinity (purple), and density (green) near the Greenland coast spill site for July to September. Data from the World Ocean Atlas 2013.

7.3 Stochastic Modeling

The SIMAP stochastic model was used to predict the statistical footprint of oiling associated with the cruise ship spill scenario.

7.3.1 Stochastic Scenario Parameters

The stochastic scenario input parameters developed for scenario 3 (see Section 7.1) are summarized in Table 19 below. The scenario was simulated (tracked) for 30 days after the initial release. No spill response measures were included in the stochastic simulation for this scenario.

Table 19. Stochastic scenario input parameters for scenario 3.

ID #	Spill Type	Location	Oil Type	Spill Duration (days)	Total Volume (m^3)	Season	Simulation Duration (days)
3	Cruise ship surface spill	69.074430°N, 53.500040°W	IFO 180	0.5	280	July to September	30

7.3.2 Stochastic Results

The results of the stochastic model simulation for scenario 3 are shown in Table 20 and Table 21.

Table 20 presents shoreline oiling statistics, including the percentage of simulations reaching shore, time to shore, peak volume of oil ashore, and the shoreline length oiled above the ecological threshold of 100 g/m^2. The percentage of simulations reaching shore indicates the likelihood that a particular spill event will reach nearby coastal areas with a level of shoreline oiling greater than 100 g/m^2. The percentage of simulations reaching shore is based on the total number of trajectories out of the ensemble of 200 individual runs that reached the coast in the stochastic analysis. Note that a spill event with high probability of shoreline oiling does not imply that a particular section of the coast will be oiled, only that there is a high probability of oil reaching the coastline *at some location*.

Scenario 3 had a high probability of causing shoreline oiling above 100 g/m^2, with 95% of trajectories reaching shore. The average shoreline length oiled above 100 g/m^2 was relatively high given the relatively small spill volume, with an average of 49 km oiled. On average, the peak volume of oil ashore is approximately 66% of the total volume spilled. This is attributable to the persistent nature of the IFO 180. The minimum time for oil to first reach shore was 12 hours, which could make for a challenging response effort.

Table 20. Scenario 3 stochastic results – shoreline oiling statistics.

ID	Spill Event	Total Volume Spilled (m^3)	Simulations Reaching Shore (%)[1]	Time to Reach Shore (days)		Peak Volume of Oil Ashore (m^3)		Shoreline Length Oiled Above 100 g/m^2 (km)	
				Min.	Avg.	Max.	Avg.	Max.	Avg.
3	Greenland Coast – Cruise Ship	280	95	0.5	4.4	245	186	119	49

[1] Percentage of simulations reaching shore is calculated based on the number of individual trajectories that resulted in shoreline oiling above a threshold of 100 g/m^2 of oil.

Table 21 presents surface oiling and water column oiling statistics. Scenario 3 resulted in a water surface footprint of, on average, about 12 km^2 oiled above the ecological threshold of 10 g/m^2. On average, the peak volume of oil entrained in the water column was about 0.1% of the total volume spilled. Again, this is attributable to the properties of IFO 180, which does not readily entrain into the water column.

Table 21. Scenario 3 stochastic results – surface oiling and water column oiling statistics.

ID	Spill Event	Total Volume Spilled (m^3)	Water Surface Area Oiled Above 0.01 g/m^2 (km^2)		Water Surface Area Oiled Above 10 g/m^2 (km^2)		Volume of Oil in Water Column (m^3)	
			Max.	Avg.	Max.	Avg.	Max.	Avg.
3	Greenland Coast – Cruise Ship	280	2,158	344	14	12	0.8	0.4

The following figures (Figure 73 and Figure 74) illustrate the spatial extent of water surface oiling and shoreline oiling probabilities for scenario 3. Three figures are presented for the scenario:

1. **Probability of Water Surface Oiling Above 0.01 g/m^2**: The map defines the area in which water surface oiling above the socioeconomic threshold of 0.01 g/m^2 may be expected and the associated probability of oiling (based on analysis of the 200 individual trajectories run for the spill scenario). The map does not imply that the entire contoured area would be covered with oil in the event of a spill. The map also does not provide any information about the quantity of oil in a given area.

2. **Probability of Water Surface Oiling Above 10 g/m^2**: The map defines the area in which water surface oiling above the ecological threshold of 10 g/m^2 may be expected and the associated probability of oiling (based on analysis of the 200 individual trajectories run for the spill scenario). The map does not imply that the entire contoured area would be covered with oil in the event of a spill. The map also does not provide any information about the quantity of oil in a given area.

3. **Probability of Shoreline Oiling Exceeding 100 g/m^2**: This map shows the probability of shoreline oiling above the ecological threshold of 100 g/m^2 (based on analysis of the 200 individual trajectories run for the spill scenario). The map does not imply that the entire shoreline extent would be oiled in the event of a spill. The map also does not provide any information about the quantity of oil in a given area.

A brief summary of the stochastic simulation follows the figures.

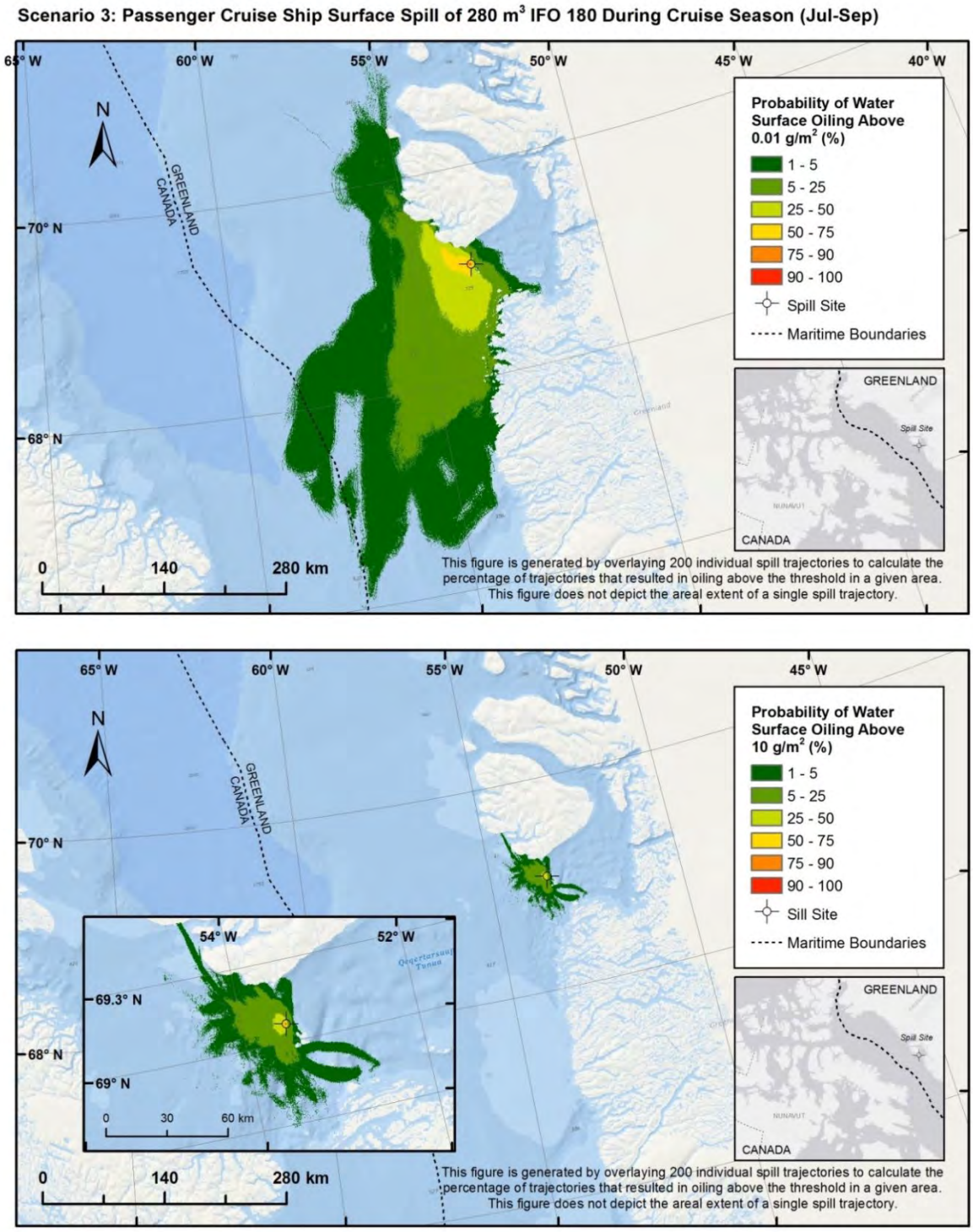

Figure 73. Scenario 3 (surface spill of 280 m^3 IFO 180) stochastic results – Probability of water surface oiling above the socioeconomic threshold of 0.01 g/m^2 (top panel) and probability of water surface oiling above the ecological threshold of 10 g/m^2 (bottom panel).

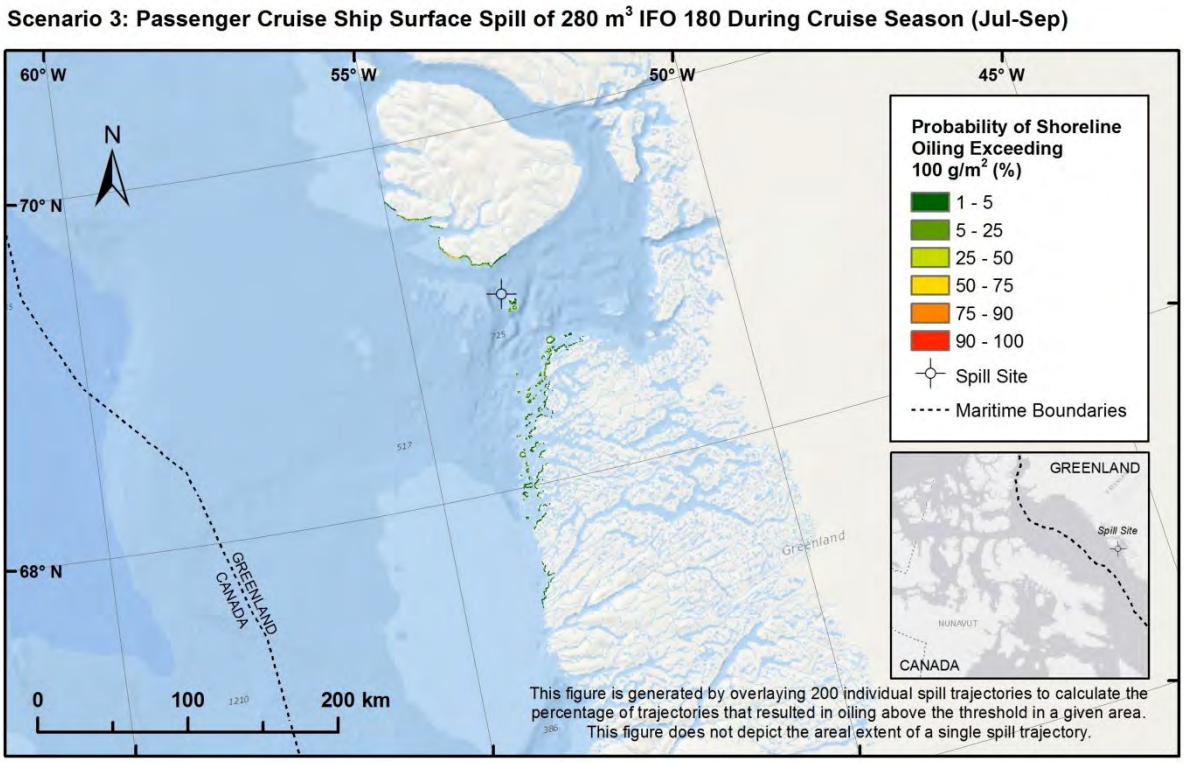

Figure 74. Scenario 3 (surface spill of 280 m^3 IFO 180) stochastic results – Probability of shoreline oiling above the ecological threshold of 100 g/m^2.

For the socioeconomic threshold of 0.01 g/m^2, the stochastic water surface oiling footprint for scenario 3 is variable in direction, but the zone of highest probabilities is oriented to the northwest of the spill site towards Disko Island (Figure 73). There is also a low to moderate probability of water surface oiling to the south of the spill site, and a very low (<5%) probability of oiling above the threshold in Canadian territorial waters. For the ecological threshold of 10 g/m^2, the stochastic surface oiling footprint is much smaller, with lower overall probabilities. The footprint is restricted to Greenlandic waters at the mouth of Disko Bay. For this threshold, areas of moderate or high probability are limited to within a few kilometers of the spill site.

There is an approximately 95% chance that shoreline oiling above 100 g/m^2 will occur at some location in the study area (Table 20). However, the highest probability of any individual segment of the coastline being oiled above the threshold is 31% (Figure 74). The highest probability of oiling is for shorelines to the northwest of the spill site on south Disko Island (west of Qeqertasuaq). There is also a low probability of shoreline oiling along the complex coastline from near Aasiaat to south of Attu.

7.4 Deterministic Modeling

The deterministic trajectory and fate simulations provide an estimate of the 3-D trajectory (movement) and fate (weathering) for a particular individual spill event.

7.4.1 Deterministic Scenario Parameters

Trajectories were selected from the stochastic scenario based on pre-defined criteria. Different parameters or criteria can be used to select individual trajectories for deterministic analysis. For example, deterministic trajectories can be "representative" or "worst-case" for a variety of consequence metrics (e.g., shoreline length oiled, time to shore, volume of oil ashore, water column contamination, water surface area swept). The selected deterministic cases for scenario 3 are summarized in Table 22. At the request of WWF-Canada, the deterministic scenarios were simulated (tracked) for longer than the corresponding stochastic scenario in order to provide more information about the ultimate fate of the spilled oil. These durations were based on test simulations and were selected to reflect the point at which zero or minimal oil remains on the water surface.

No spill response measures were included in the deterministic simulations for this scenario.

Table 22. Selected deterministic cases for scenario 3.

ID	Spill Event	Type of Deterministic Case[1]	Spill Response Type	Spill Start Date	Simulation Duration (Days)
3	Greenland Coast – Cruise Ship	Worst-case Shoreline Length Oiled	None	25 July 2015	35
3	Greenland Coast – Cruise Ship	Worst-case Water Surface Area Oiled	None	24 August 2013	35

[1] The "worst case" for a given consequence metric was defined as the trajectory with the 95th percentile value for oiling above the ecological threshold (i.e., 100 g/m^2 for the shoreline, and 10 g/m^2 for the water surface).

7.4.2 Deterministic Results

Note: Because the deterministic simulations for this spill site were run longer than the corresponding stochastic simulation (i.e., 35 vs. 30 days), the deterministic results presented herein are not directly comparable to the stochastic results reported in Section 7.3.2. Similarly, the selection criteria used to identify the deterministic cases from the stochastic analysis should be interpreted with caution. For example, the worst case shoreline length oiled trajectory in the stochastic analysis (30-day simulation) may no longer be the worst case shoreline length oiled trajectory when simulated for 35 days in the deterministic analysis.

Key results from the deterministic simulations for the cruise ship spill scenario are summarized in Table 23, including volume of water exceeding 1 ppb of dissolved aromatics (the most toxic components of oil), water surface area oiled, shoreline length oiled, time to first reach shore, and peak volume of oil ashore.

Table 23. Summary of deterministic results for the Greenland coast cruise ship scenarios.

ID	Deterministic Case	Volume of Water Exceeding 1 ppb of Dissolved Aromatics (m^3)	Water Surface Area Oiled Above 0.01 g/m^2 (km^2)	Water Surface Area Oiled Above 10 g/m^2 (km^2)	Shoreline Length Oiled Above 100 g/m^2 (km)	Time to Shore (Days)	Peak Volume of Oil Ashore (m^3)
3	Worst-case Shoreline Length Oiled	7.4×10^7	262.0	17.4	103.7	3.5	188.8
3	Worst-case Water Surface Area Oiled	5.2×10^7	48.2	18.2	27.7	2.2	226.0

The following figures (Figure 75 through Figure 78) present the results of the deterministic simulations for each scenario. Three figures are shown for each deterministic case:

7. **Maximum Floating Oil Concentration**: This map shows the maximum concentration (g/m^2) of floating oil that passed through a given area at some point during the simulation. This map also displays the approximate subsurface area swept by dissolved aromatic concentrations greater than 1 ppb. This concentration is used as a screening threshold for potential impacts on sensitive water column organisms (based on French McCay, 2009).

8. **Shoreline Oil Concentration**: This map shows the concentration (g/m^2) of oil on the shoreline at the end of the simulation.

9. **Mass Balance**: This graph shows a time history of the fate and weathering of the spilled oil during the simulation. Components of the oil tracked over time include amount of oil on the sea surface, on the shoreline, in the water column (subsurface), in subsea sediments, evaporated into the atmosphere, and decayed (e.g., by photo-oxidation, biodegradation).

A brief description of each deterministic simulation follows the figures for each case.

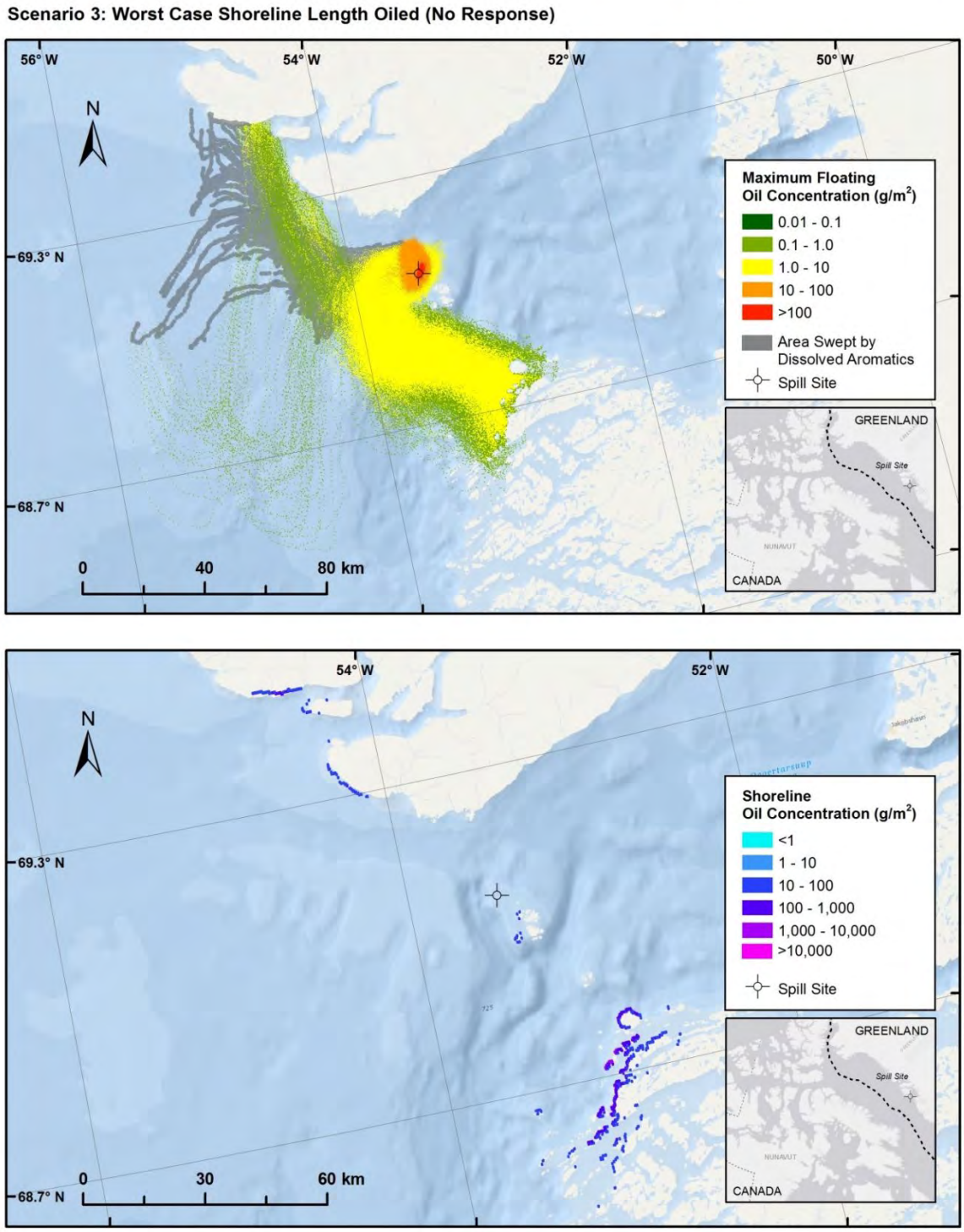

Figure 75. Scenario 3: Worst-case (95th percentile) trajectory for shoreline length oiled above 100 g/m^2, with no spill response – Maximum concentration (g/m^2) of floating oil that passed by a given area during the simulation and the subsurface area swept by dissolved aromatics (top panel); and total concentration (g/m^2) of oil on the shoreline at the end of the simulation (bottom panel).

Figure 76. Scenario 3: Worst-case (95th percentile) trajectory for shoreline length oiled above 100 g/m^2, with no spill response – Mass balance graph.

For scenario 3, the worst-case trajectory for shoreline length oiled was modeled without spill response (Figure 75 and Figure 76).

The spill trajectory initially heads mainly to the north of the spill site, and the floating slick spreads and expands at the mouth of Disko Bay for several days, first reaching shore at the islands to the southeast of the spill site at 3.5 days after the spill. The floating oil then spreads to the west and southeast, reaching the shoreline near Aasiaat beginning at about 13 days into the simulation. Floating oil not retained on shore turns north and reaches the shoreline of Disko Island by 23 days into in the simulation. By 27 days post-spill, about 1% of the volume spilled remains on the water surface and travels to the southwest towards Baffin Bay. At the end of the 35-day simulation, about 3.0 m^3 (1% of the volume spilled) remains on the water surface, and would continue to be transported by winds and currents.

Evaporation plays a role in removal, with about 18% of the spilled volume evaporated, most of which occurred during the first few days after the spill. Natural decay processes also play a role, with about 21% of the spilled volume removed by natural decay processes such as biodegradation and photo-oxidation by the end of the simulation. The peak volume of oil on the shoreline was 188.8 m^3, at 19 days after the spill start. At the end of the simulation, 170.4 m^3 of oil remains on shore, with a total of 103.7 km of shoreline oiled above the ecological threshold of 100 g/m^2. IFO

180 does not readily entrain into the water column and entrainment of oil was very low for the simulation. At the end of the simulation, no oil remains entrained in the water column.

Despite the low volume of oil entrained in the water column, there is still the potential for water column impacts from aromatics (the most toxic components of oil) dissolving into the water column from the surface slick. In general, the subsurface area swept by dissolved aromatics followed the same trajectory as the surface oil, extending somewhat beyond the surface oil footprint to the west. The peak volume of water exceeding 1 ppb of dissolved aromatics (a screening threshold for impacts on sensitive water column organisms) was 7.4×10^7 m^3.

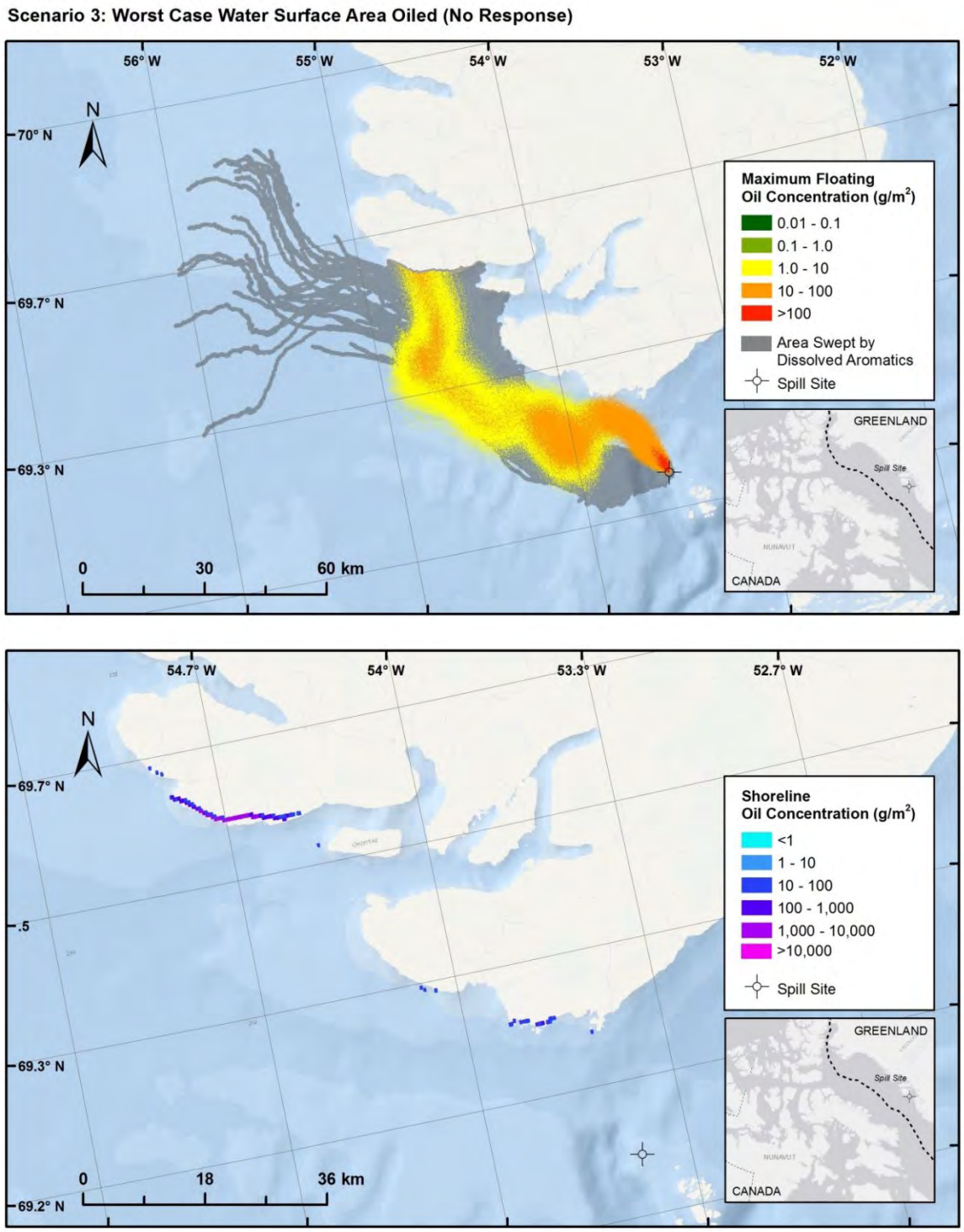

Figure 77. Scenario 3: Worst-case (95th percentile) trajectory for water surface area oiled above 10 g/m^2, with no spill response – Maximum concentration (g/m^2) of floating oil that passed by a given area during the simulation and the subsurface area swept by dissolved aromatics (top panel); and total concentration (g/m^2) of oil on the shoreline at the end of the simulation (bottom panel).

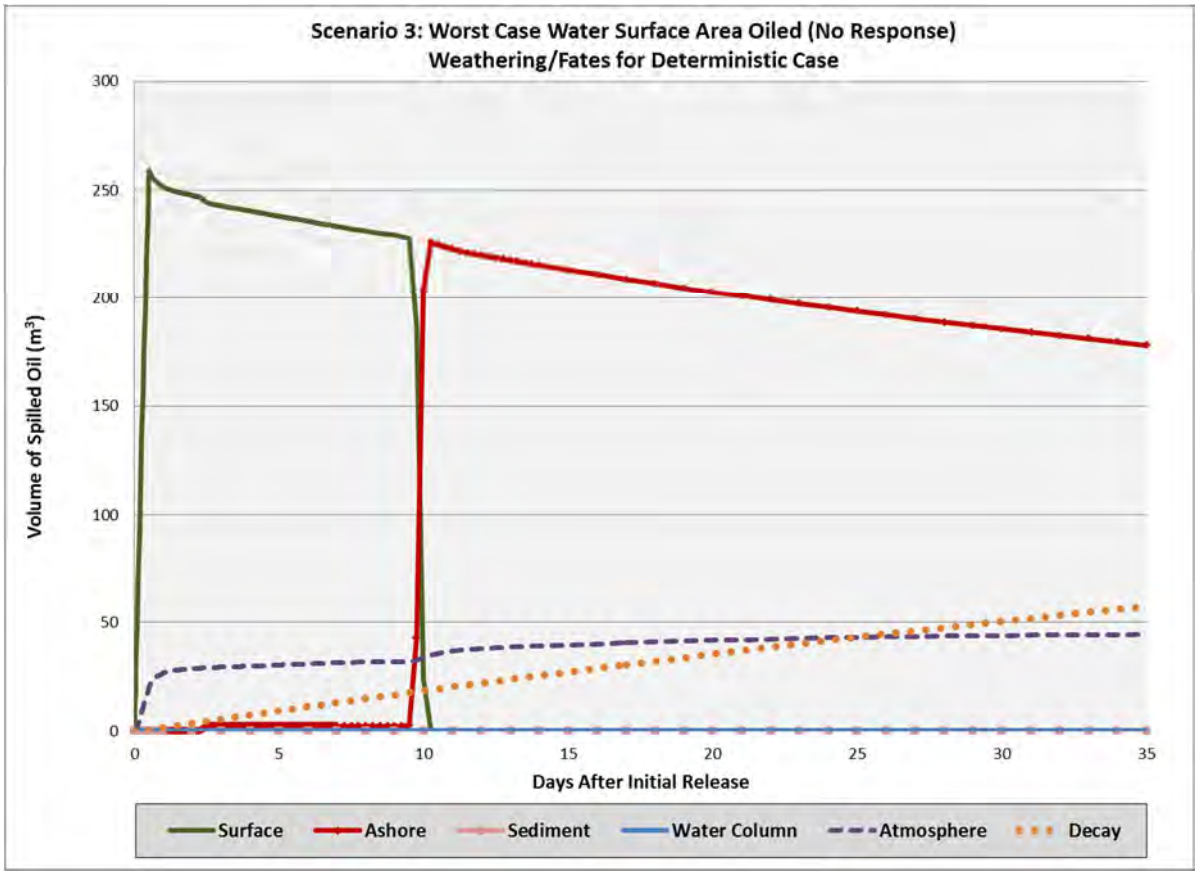

Figure 78. Scenario 3: Worst-case (95th percentile) trajectory for water surface area oiled above 10 g/m^2, with no spill response – Mass balance graph.

For scenario 3, the worst-case trajectory for water surface area oiled was modeled without spill response (Figure 77 and Figure 78).

The spill trajectory initially heads to the north-northwest of the spill site, first reaching shore along southwest coast of Disko Island near Qeqertarsuaq with a small amount of oil (<1% of the total volume spilled) at 2.2 days after the spill. The floating oil then travels to the west before turning northwestward and oiling additional areas of west Disko Island starting at about 9.4 days after the spill. During this shoreline oiling event, all of the remaining floating oil is deposited on the shoreline and by 10.5 days post-spill, no oil remains on the water surface.

Evaporation plays a role in removal, with about 16% of the spilled volume evaporated, most of which occurred during the first few days after the spill. Natural decay processes also play a role, with about 21% of the spilled volume removed by natural decay processes such as biodegradation and photo-oxidation by the end of the simulation. The peak volume of oil on the shoreline was 226.0 m^3, at 10.3 days after the spill start. At the end of the simulation, 178.0 m^3 of oil remains on shore, with a total of 27.7 km of shoreline oiled above the ecological threshold of 100 g/m^2. IFO 180 does not readily entrain into the water column and entrainment of oil was very low for the simulation. At the end of the simulation, no oil remains entrained in the water column.

Despite the low volume of oil entrained in the water column, there is still the potential for water column impacts from aromatics (the most toxic components of oil) dissolving into the water column from the surface slick. In general, the subsurface area swept by dissolved aromatics followed the same trajectory as the surface oil, extending somewhat beyond the surface oil footprint to the west. The peak volume of water exceeding 1 ppb of dissolved aromatics (a screening threshold for impacts on sensitive water column organisms) was 5.2 x 10^7 m^3.

7.5 Conclusions

Based on the stochastic analysis, the cruise ship spill scenario (scenario 3) had a high probability of causing shoreline oiling above the ecological threshold of 100 g/m^2, with 95% of trajectories reaching shore at some location. The highest probability of oiling is for shorelines to the northwest of the spill site on south Disko Island, but there are also low probabilities of shoreline oiling along the complex coastline from near Aasiaat to south of Attu.

The average shoreline length oiled above 100 g/m^2 was relatively high given the relatively small spill volume, with an average of 49 km oiled. On average, the peak volume of oil ashore was approximately 66% of the total volume spilled. This is attributable to the high viscosity of IFO 180, which makes it difficult to disperse and highly persistent. For the same spill volume, a spill of a heavier oil type like IFO 180 is more likely to oil shorelines and wildlife at sea than other oil types like crudes and light oils. In the stochastic analysis, the minimum time for oil to reach shore was 12 hours, which could make for a challenging response effort.

IFO 180 does not readily entrain into the water column, and the volume of oil entrained in the water column was relatively low. Despite the low volume of oil entrained in the water column, there is still the potential for water column impacts from aromatics (the most toxic components of oil) dissolving into the water column from the surface slick. For the two deterministic scenarios (which did not include the worst case for water column oiling), the volume of water exceeding 1 ppb of dissolved aromatics (a screening threshold for sensitive water column organisms) was 52 million and 74 million m^3.

The persistence of IFO 180 on the water surface and shoreline was evident in the deterministic analysis. For the worst-case surface area oiled deterministic simulation, the maximum concentration of floating oil exceeded 10 g/m^2 (the threshold for impacts on birds and wildlife associated with the water surface) for the majority of the trajectory. Even though the spill volume is relatively small compared to other types of scenarios modeled, an unmitigated cruise ship spill of IFO 180 could substantially impact biota associated with this ecologically-sensitive area.

8.0 SCENARIO 4 – LANCASTER SOUND PRODUCT TANKER SPILL

8.1 Scenario Development

One scenario (scenario 4) was developed for a hypothetical spill from a product tanker in Lancaster Sound. The selected spill site location is near Wollaston Island to the west of Bylot Island at the entrance to Navy Board Inlet (Figure 79). The specific location is 73.731023°N, 81.010920°W. The reasoning behind the selection of this specific site is that it is a plausible grounding location due to the presence of shallower water and rocks surrounding Wollaston Island. It is also potentially near the route of a tanker delivering fuel to communities such as Resolute or Arctic Bay. This location was selected as *representative* for spill sites. Spills from product tankers may occur in various locations in the region from tankers taking somewhat different routes.

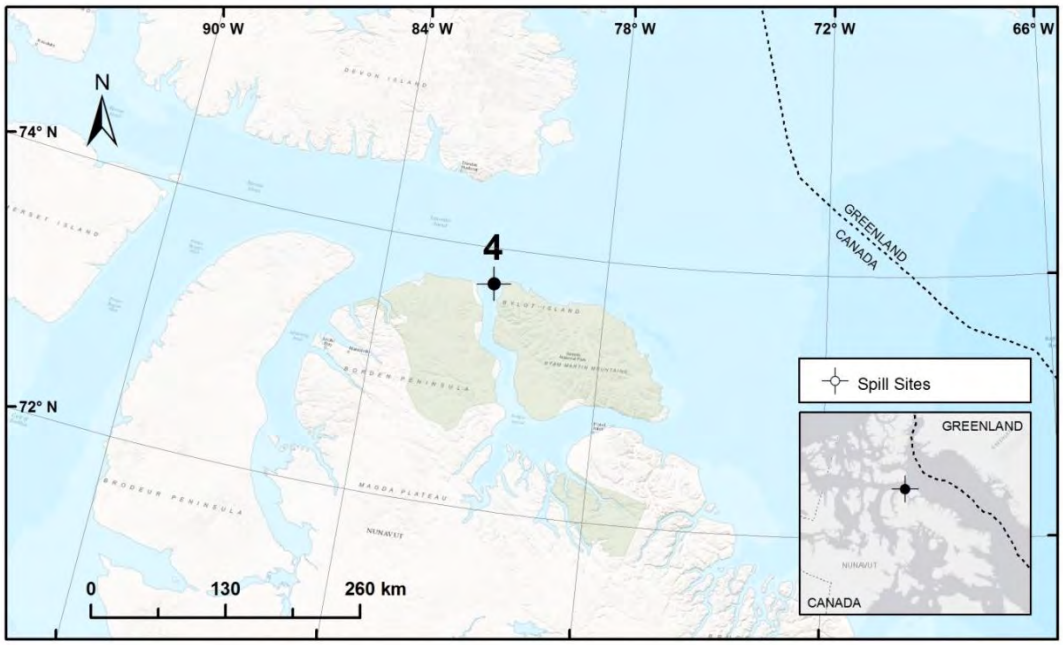

Figure 79. Location of the selected spill site in Lancaster Sound (scenario 4).

The season evaluated for scenario 4 corresponds to “open water” conditions, and was based on analysis of average monthly ice coverage data from TOPAZ4 at the spill site (2011-2015). Average ice cover of less than 30% was defined as “open water.” This time period corresponded to June through September.

The oil type selected for modeling was Arctic diesel, which may be expected to be transported as cargo for deliveries to Resolute or other Arctic communities, as well as to mining operations at Baffinland Mines.

The source of the hypothetical spill was assumed to be a product tanker of about 13,000 DWT (deadweight tonnage), such as the *T/V Maria Desgagnés.* This representative tanker has a deadweight tonnage of 13,199 DWT, with a total cargo capacity of 15,171.1 m^3 (95,422 bbl). Normally, the tanks would not be filled over 98% capacity to allow for vapor expansion, so that the

actual loaded bunker tank volume would be 14,867.9 m^3 (93,515 bbl). The largest cargo tank on board holds approximately 2,400 m^3 (15,096 bbl). The hypothetical spill scenario involves the full release of 2,400 m^3 (15,096 bbl) from this largest tank, or about 16% of the total load. In the modeling, it was assumed that the oil would flow out of the tank(s) involved over the course of about 12 hours.

Tanker traffic varies from year to year, and the specific routes taken also vary. This study did not include a specific vessel traffic study to determine the probabilities of tanker groundings or other accidents at specific locations, including the spill site selected for modeling. However, the tanker traffic that could transit the general study area was considered in developing a spill probability estimate for tanker spills.

The probability that an oil tanker will have a serious grounding is about 0.000007 groundings per day per vessel (Det Norske Veritas, 2011). Based on data for the year 2013, there are about 24 tanker trips through the region annually. These tanker trips include those associated with supplying Arctic communities with fuel, as well as those supplying mining activity (Mariport Group Ltd., 2012; Curran, 2015). If one assumes that each voyage takes about 10 days, this would mean that there may be, at most, 0.0018 groundings per year, or a 1 in 556 chance that a serious grounding accident would occur in any year.

However, not all accidents result in the spillage of oil, and the probability that a product tanker grounding will result in a spill is estimated to be 0.18 (Yip et al., 2011; Rawson et al., 1998; NRC, 1998; NRC, 2001; IMO, 1995; Etkin et al., 2002). This means that the probability that there would be a spill associated with a product tanker grounding accident is about 1 in 3,086. Note that this is the chance of a spill of *some volume* of oil, not a particular volume. The likelihood of a grounding resulting in the large spill volume modeled for this study would be even smaller. Also, this is not the probability that a tanker spill would occur in this specific location or even only in Lancaster Sound, but rather the probability that there would be a tanker spill in the general region. With more tanker traffic, there would be a higher probability of spills, with less traffic, a lower probability.

See Appendix A for additional discussion regarding the development of spill scenario parameters and vessel spill likelihood.

8.2 Environmental Analysis

Monthly TOPAZ4 current roses at the Lancaster Sound spill site are presented in Figure 80. The primary direction is east-northeastward with little directional variability. Currents are weaker in winter and spring (December to May), and higher during summer and fall (June to November). The strongest currents exceed 15 cm/s and are directed to the east.

At the Lancaster Sound spill site, the average monthly current speeds vary between around 3-10 cm/s (Figure 81). The lowest current speeds occur in the early part of the year and increase quickly after May to a maximum monthly average speed of 10 cm/s in September. Current speeds subsequently decrease to a monthly minimum average of around 3 cm/s in April.

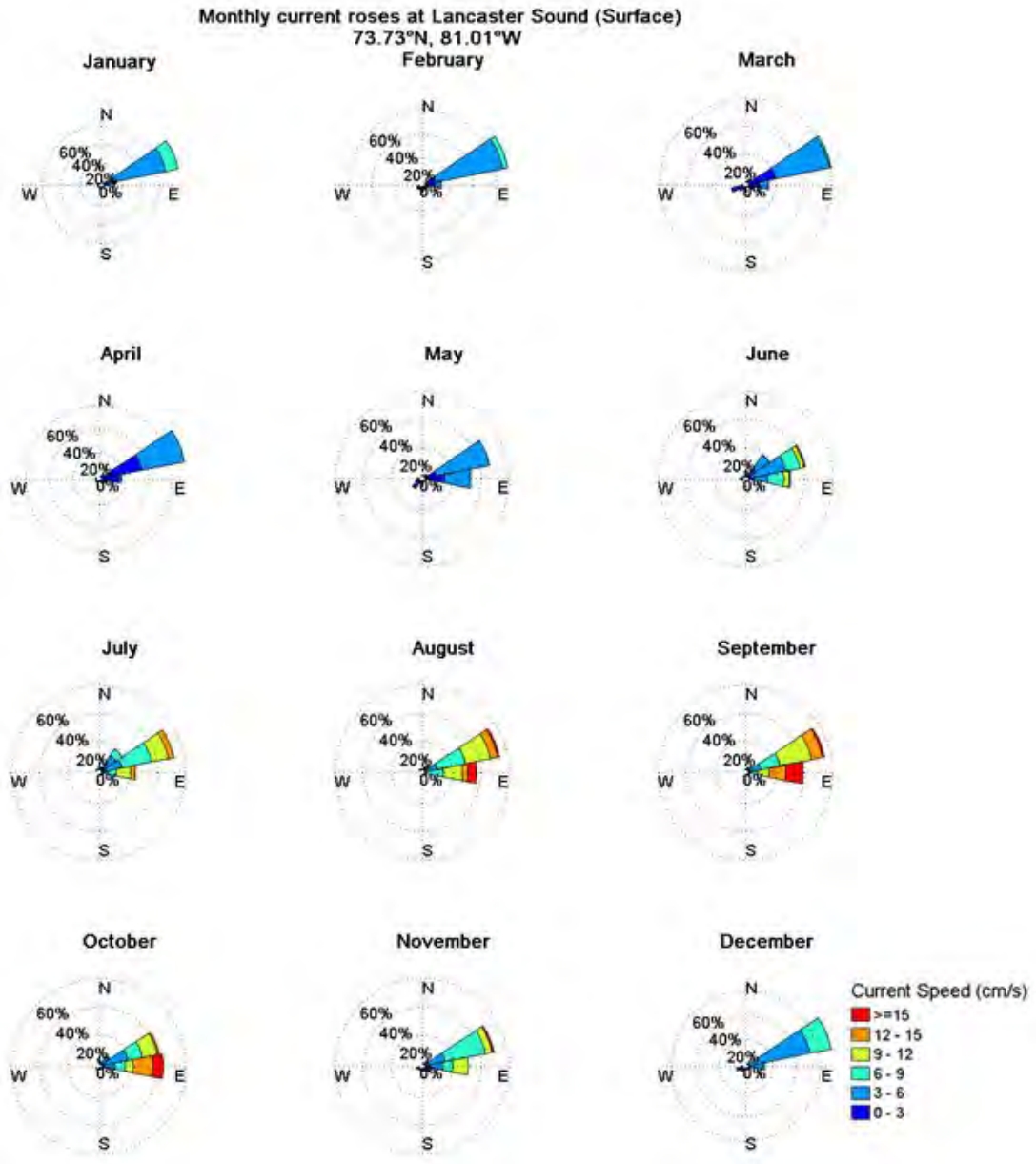

Figure 80. TOPAZ4 monthly averaged surface current roses near the Lancaster Sound spill site averaged over the period of 2011-2015. Direction convention is standard (i.e., direction currents are moving to).

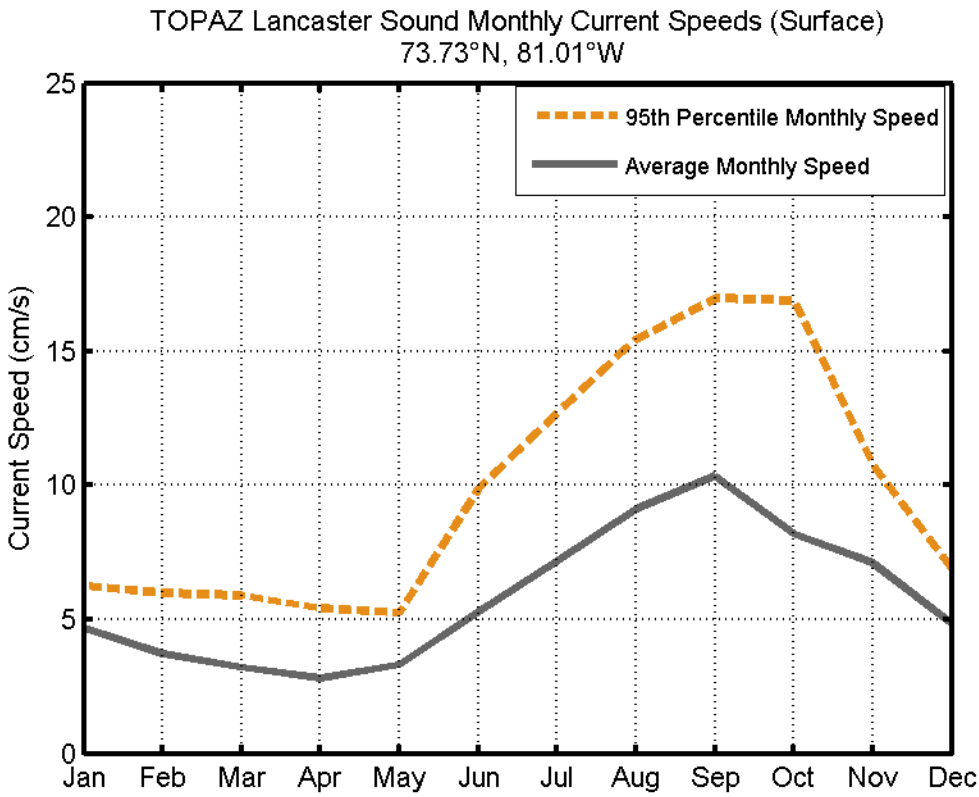

Figure 81. TOPAZ4 current statistics: monthly average (grey solid) and 95th percentile (orange dash) current speed at the surface near the Lancaster Sound spill site for 2011-2015.

Figure 82 shows ECMWF monthly wind roses at the Lancaster Sound spill site. During winter, wind is primarily from the west-southwest. In spring, wind direction begins to have an easterly component, and shifts to primarily easterly from June through August. In September, wind direction starts to transition to more westerly, but easterly winds are still present. Wind speeds can exceed 20 knots.

Figure 83 presents monthly wind speed statistics (average and 95th percentile) at the Lancaster Sound spill site. Wind speed fluctuates throughout the year with monthly average speeds ranging between 6-9 knots. The highest monthly average speed occurs in September, and the minimum is in January and lasts through February.

Figure 82. ECMWF monthly averaged wind roses near the Lancaster Sound spill site, averaged over the period of 2011-2015. Wind speeds are in knots, using meteorological convention (i.e., direction wind is coming from).

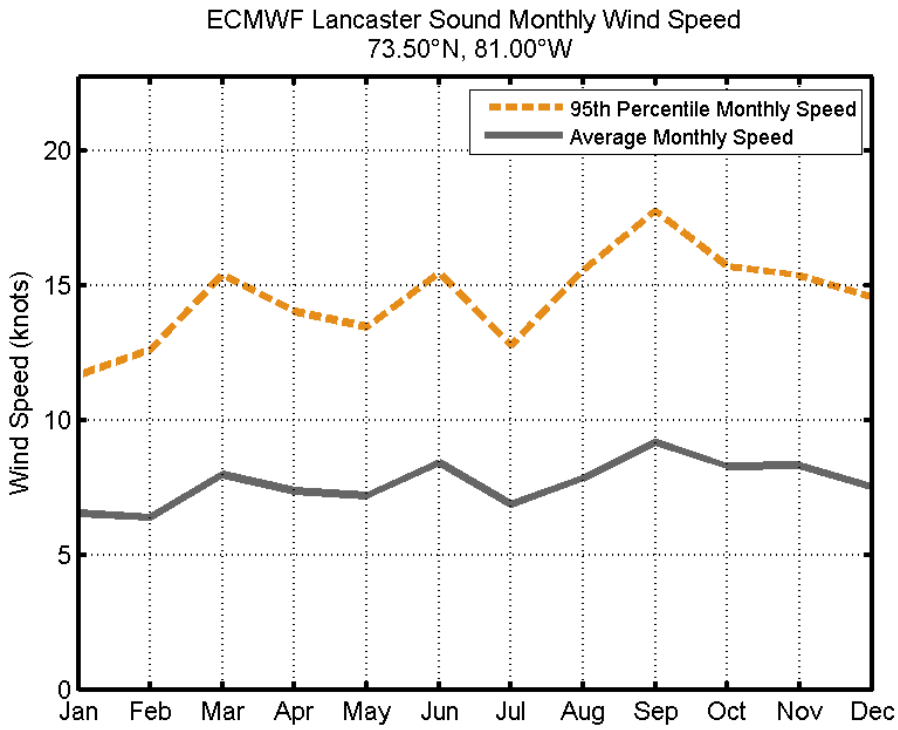

Figure 83. ECMWF wind statistics: monthly average (grey solid) and 95th percentile (orange dash) wind speed near the Lancaster Sound spill site for 2011-2015.

Monthly average sea ice and landfast ice cover near the spill site are shown in Figure 84. Sea ice coverage is based on data from TOPAZ4 (2011-2015) and landfast ice coverage is based on data from the National Snow and Ice Data Center (1991 through 1998).

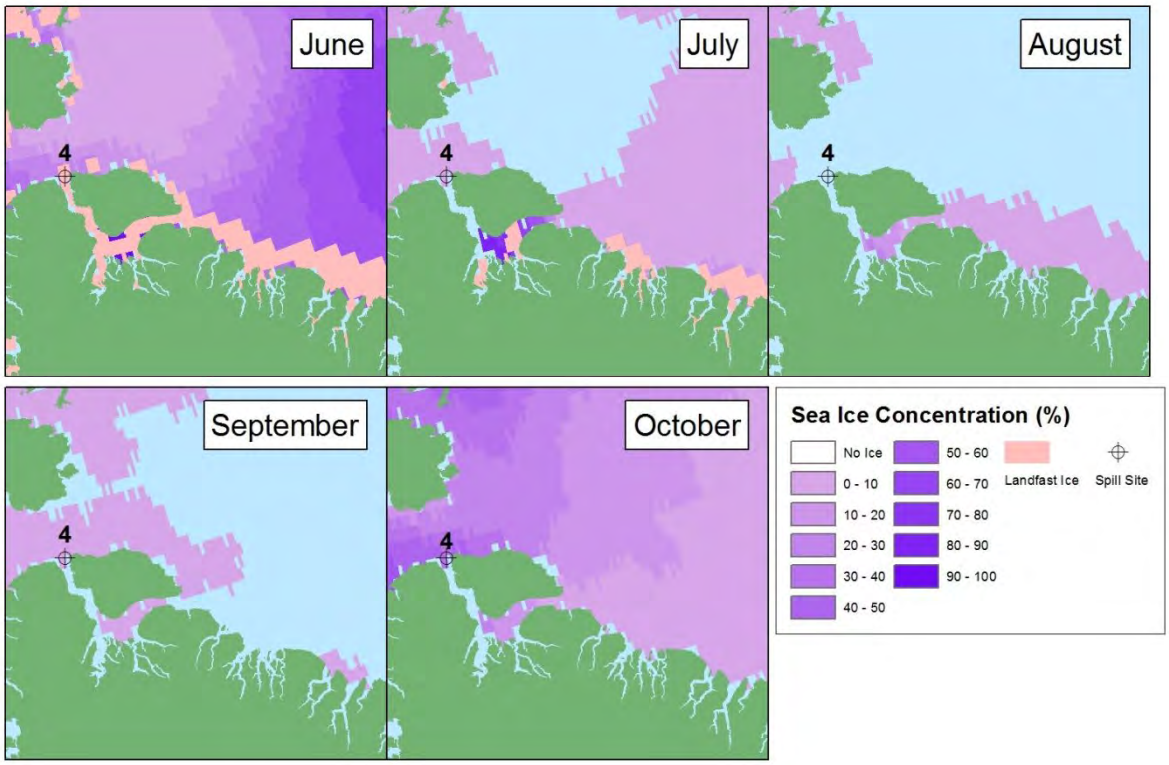

Figure 84. Average monthly cover of sea ice and landfast ice near the Lancaster Sound spill site during the period of interest.

The vertical profile of temperature, salinity, and density at the Lancaster Sound spill site for June through September is shown in Figure 85. Salinity is about 31.8 psu at the surface and increases to 34.2 psu at the sea floor. Temperature at the surface is approximately 0.9 ºC and decreases to a minimum of -1.2 ºC at 125 m, before increasing to 0.4 ºC near the sea floor. Density at the surface is 25.5 kg/m^3 and increases to 27.4 kg/m^3 at depth.

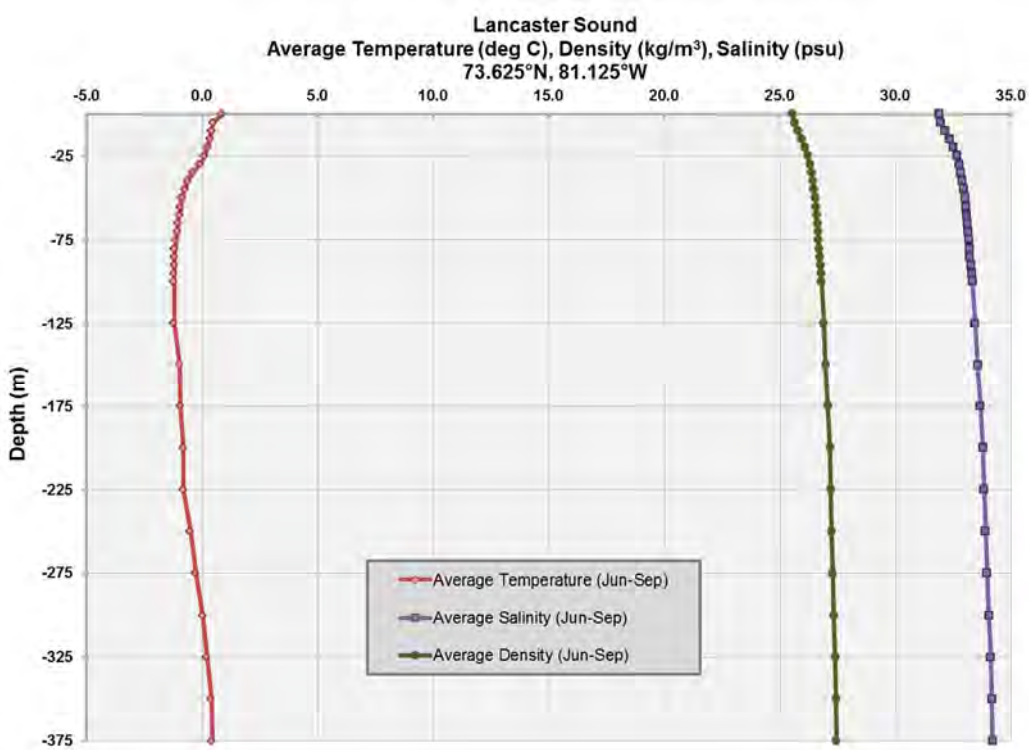

Figure 85. Vertical profile of average temperature (red), salinity (purple), and density (green) near the Lancaster Sound spill site for June to September. Data from the World Ocean Atlas 2013.

8.3 Stochastic Modeling

The SIMAP stochastic model was used to predict the statistical footprint of oiling associated with the product tanker spill scenario. Note: no deterministic analysis was conducted for this scenario.

8.3.1 Stochastic Scenario Parameters

The stochastic scenario input parameters developed for scenario 4 (see Section 8.1) are summarized in Table 24 below. The scenario was simulated (tracked) for 30 days after the initial release. No spill response measures were included in the stochastic simulation for this scenario.

Table 24. Stochastic scenario input parameters for scenario 4.

ID #	Spill Type	Location	Oil Type	Spill Duration (days)	Total Volume (m^3)	Season	Simulation Duration (days)
4	Product tanker surface spill	73.731023°N, 81.010920°W	Arctic diesel	0.5	2,400	June to September	30

8.3.2 Stochastic Results

The results of the stochastic model simulation for scenario 4 are shown in Table 25 and Table 26 below.

Table 25 presents shoreline oiling statistics, including the percentage of simulations reaching shore, time to shore, peak volume of oil ashore, and the shoreline length oiled above the ecological threshold of 100 g/m^2. The percentage of simulations reaching shore indicates the likelihood that a particular spill event will reach nearby coastal areas with a level of shoreline oiling greater than 100 g/m^2. The percentage of simulations reaching shore is based on the total number of trajectories out of the ensemble of 200 individual runs that reached the coast in the stochastic analysis. Note that a spill event with high probability of shoreline oiling does not imply that a particular section of the coast will be oiled, only that there is a high probability of oil reaching the coastline *at some location*.

Scenario 4 had a high probability of causing shoreline oiling above 100 g/m^2, with 93% of trajectories reaching shore. The average shoreline length oiled above 100 g/m^2 was, on average, approximately 27 km. On average, the peak volume of oil ashore is approximately 21% of the total volume spilled. Due to the close proximity of the spill site to shore, the minimum time for oil to first reach shore was less than 1 hour.

Table 25. Scenario 4 stochastic results – shoreline oiling statistics.

ID	Spill Event	Total Volume Spilled (m^3)	Simulations Reaching Shore (%)[1]	Time to Reach Shore (days)		Peak Volume of Oil Ashore (m^3)		Shoreline Length Oiled Above 100 g/m^2 (km)	
				Min.	Avg.	Max.	Avg.	Max.	Avg.
4	Lancaster Sound – Product Tanker	2,400	93	<0.1	5.9	1,121	496	74	27

[1] Percentage of simulations reaching shore is calculated based on the number of individual trajectories that resulted in shoreline oiling above a threshold of 100 g/m^2 of oil.

Table 26 presents surface oiling and water column oiling statistics. Scenario 4 resulted in a water surface footprint of, on average, about 12 km^2 oiled above the ecological threshold of 10 g/m^2. On average, the peak volume of oil entrained in the water column was relatively high, at about 41% of the total volume spilled. This is attributable to the light nature of diesel oil, which entrains easily into the water column.

Table 26. Scenario 4 stochastic results – surface oiling and water column oiling statistics.

ID	Spill Event	Total Volume Spilled (m^3)	Water Surface Area Oiled Above 0.01 g/m^2 (km^2)		Water Surface Area Oiled Above 10 g/m^2 (km^2)		Volume of Oil in Water Column (m^3)	
			Max.	Avg.	Max.	Avg.	Max.	Avg.
4	Lancaster Sound – Product Tanker	2,400	2,193	210	36	12	1,749	980

The following figures (Figure 86 and Figure 87) illustrate the spatial extent of water surface oiling and shoreline oiling probabilities for scenario 4. Three figures are presented for the scenario:

1. **Probability of Water Surface Oiling Above 0.01 g/m^2**: The map defines the area in which water surface oiling above the socioeconomic threshold of 0.01 g/m^2 may be expected and the associated probability of oiling (based on analysis of the 200 individual trajectories run for the spill scenario). The map does not imply that the entire contoured area would be covered with oil in the event of a spill. The map also does not provide any information about the quantity of oil in a given area.

2. **Probability of Water Surface Oiling Above 10 g/m^2**: The map defines the area in which water surface oiling above the ecological threshold of 10 g/m^2 may be expected and the associated probability of oiling (based on analysis of the 200 individual trajectories run for the spill scenario). The map does not imply that the entire contoured area would be covered with oil in the event of a spill. The map also does not provide any information about the quantity of oil in a given area.

3. **Probability of Shoreline Oiling Exceeding 100 g/m^2**: This map shows the probability of shoreline oiling above the ecological threshold of 100 g/m^2 (based on analysis of the 200 individual trajectories run for the spill scenario). The map does not imply that the entire shoreline extent would be oiled in the event of a spill. The map also does not provide any information about the quantity of oil in a given area.

A brief summary of the stochastic simulation follows the figures.

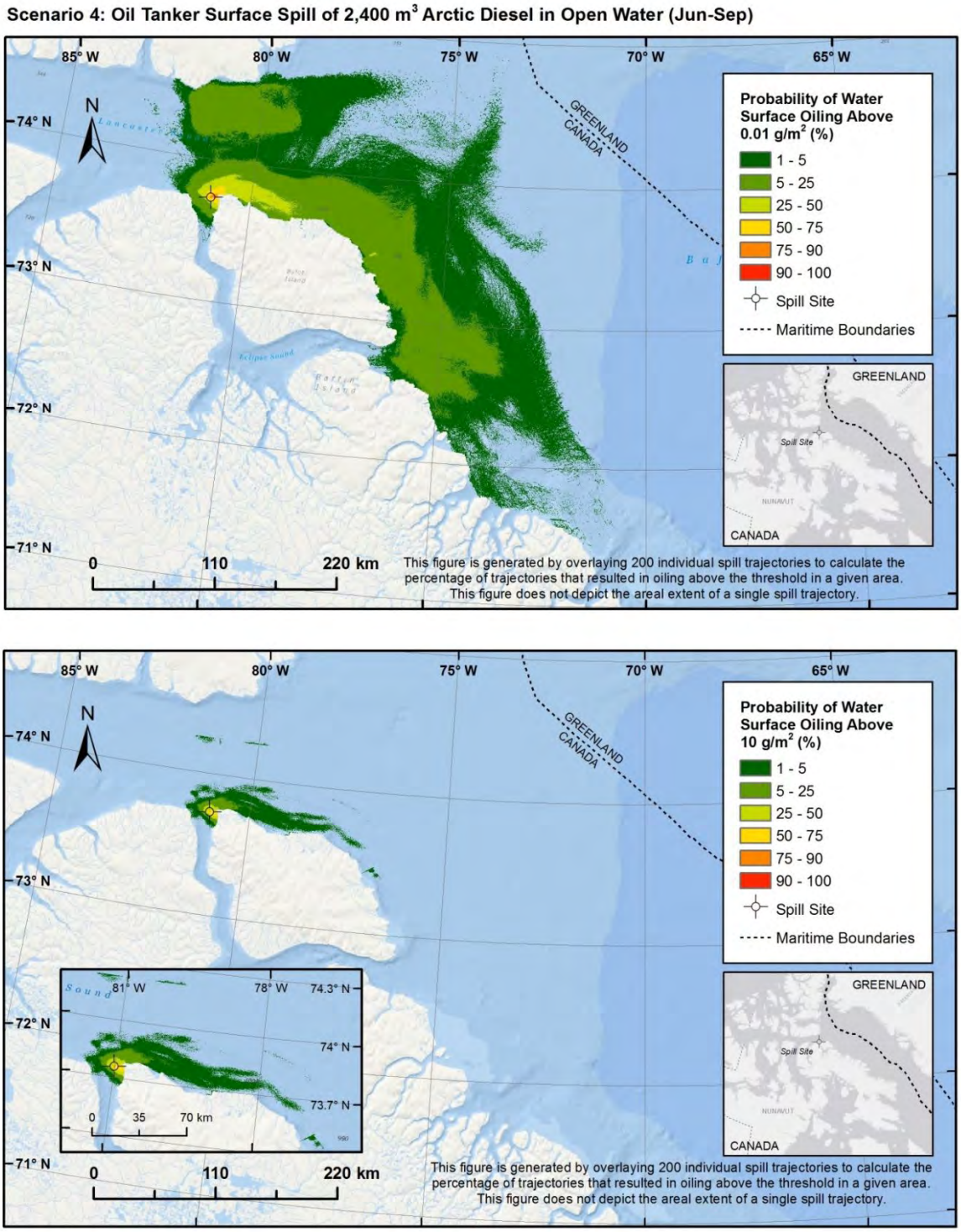

Figure 86. Scenario 4 (surface spill of 2,400 m^3 Arctic diesel) stochastic results – Probability of water surface oiling above the socioeconomic threshold of 0.01 g/m^2 (top panel) and probability of water surface oiling above the ecological threshold of 10 g/m^2 (bottom panel).

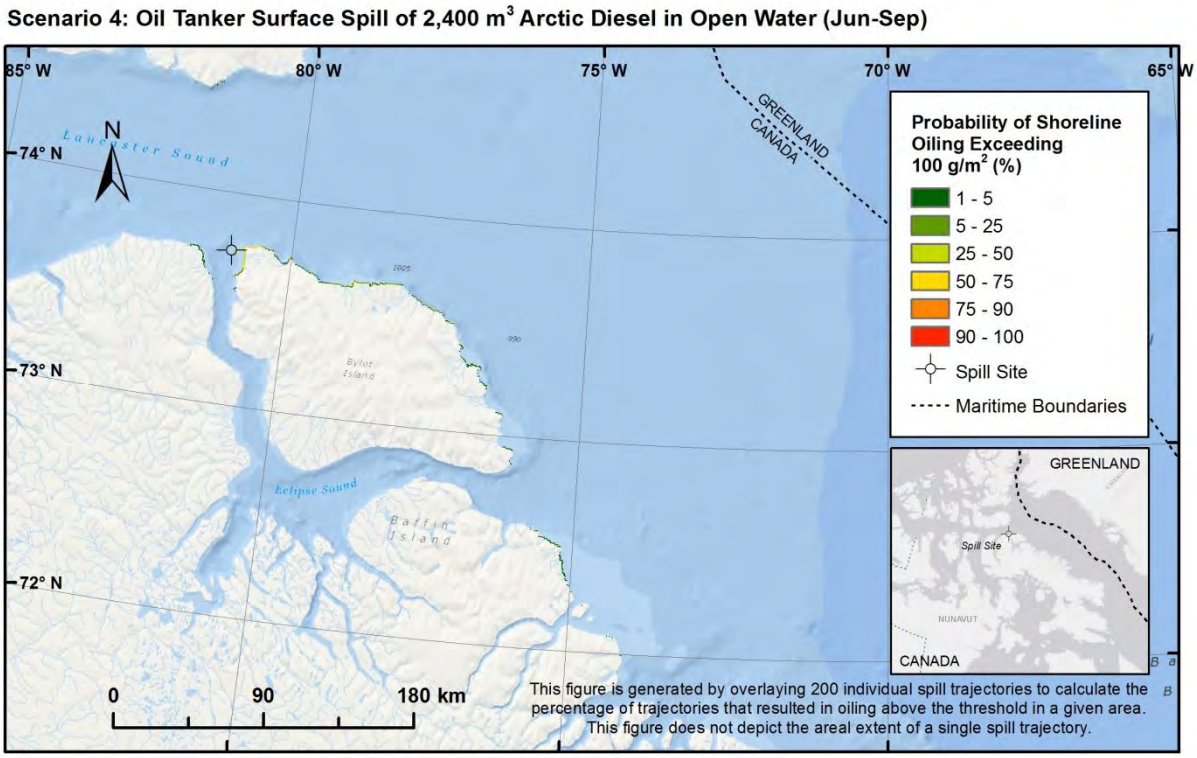

Figure 87. Scenario 4 (surface spill of 2,400 m^3 Arctic diesel) stochastic results – Probability of shoreline oiling above the ecological threshold of 100 g/m^2.

For the socioeconomic threshold of 0.01 g/m^2, the stochastic surface oiling footprint for scenario 4 is variable in direction, but generally oriented to the east of spill site and southeast along Bylot Island (Figure 86). There is also a low (<25%) probability of water surface oiling to the north of the spill site due to some trajectories becoming entrained in the water column and resurfacing offshore of Devon Island. For the ecological threshold of 10 g/m^2, the stochastic water surface oiling footprint is much smaller, with lower overall probabilities. The footprint is restricted to the waters just offshore of north Bylot Island. For this threshold, areas of moderate or high probability are limited to within a few kilometers of the spill site.

There is an approximately 93% chance that shoreline oiling above 100 g/m^2 will occur at some location in the study area (Table 20). The highest probability of any individual segment of the coastline being oiled above the threshold is about 82% (Figure 87). The highest probability of oiling is for shorelines to the east of the spill site on the northwest tip of Bylot Island and Wollaston Island, which are in close proximity to the spill site. There are also low probabilities of oiling along the northern and eastern sides of Bylot Island, and very low probabilities of oiling on Baffin Island and Devon Island.

8.4 Conclusions

The stochastic analysis indicated that scenario 4 had a high probability of causing shoreline oiling above 100 g/m^2, with 93% of trajectories reaching shore at some location. The highest probability of oiling is for shorelines to the east of the spill site on the northwest tip of Bylot Island and Wollaston Island. The high probability of shoreline oiling for this spill scenario was mainly due to the close proximity of the spill site to shore. If a product tanker spill of the same volume were to occur in a different location in Lancaster Sound (farther from shore), the probability of shoreline oiling would likely be reduced. However, the predominant direction of transport of the spilled oil would likely still be to the east and southeast along Bylot and Baffin Islands.

In general, light oils like diesel oil tend to rapidly spread to sheens and are easily dispersed into the water column by winds and waves, because of the low viscosities characteristic of these oils. Diesel oils that become dispersed into the water column can be quite toxic to water column organisms because of their high volatile content. This high content of volatiles can also promote the rapid evaporation of much of the spilled oil's mass from the water surface and shoreline.

As a result, a product tanker spill of Arctic diesel would typically have less impact on the water surface and shoreline, and more impact on the water column relative to a similar spill of a heavier oil type (like crude or heavy fuel oil). The results for scenario 4 were consistent with this general pattern, with a relatively small footprint (and low probabilities) of surface oil exceeding the ecological threshold of 10 g/m^2. On average, the peak volume of oil entrained in the water column for scenario 4 was relatively high, at about 41% of the total volume spilled. The shoreline impacts for scenario 4 were moderate, but as mentioned earlier, this was mainly due to the close proximity of the spill site to shore.

9.0 SCENARIOS 5A AND 5B – ECLIPSE SOUND BULK CARRIER SPILLS

9.1 Scenario Development

Two spill scenarios were developed for Eclipse Sound (scenarios 5A and 5B), based on a hypothetical bunker fuel spill from a bulk carrier in two seasons: open water and ice-covered. The selected spill site is near the entrance to Milne Inlet about 4.7 km east of Pisiktarfik Island (Figure 88). The specific location is 72.559040°N, 80.256612°W. The location was selected because it is en route to the Baffinland Mines (Figure 14) and is in a location that would likely cause significant oiling of the surrounding shorelines.

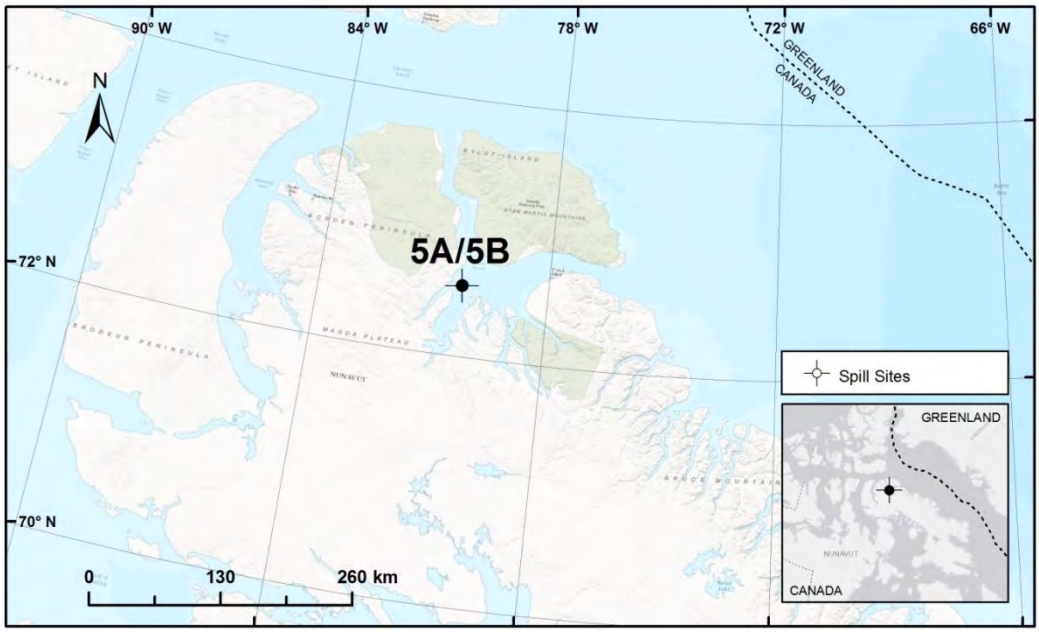

Figure 88. Location of the selection spill site in Eclipse Sound (scenarios 5A and 5B).

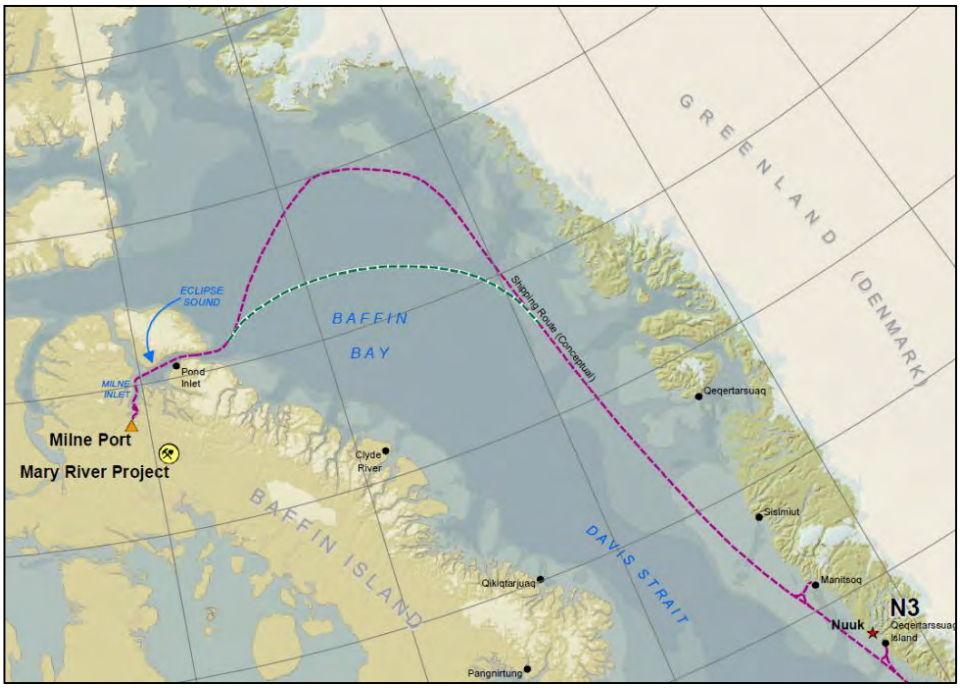

Figure 89. Shipping routes to Milne Port, Baffinland Mines (Baffinland Iron Mines Corporation, 2015). The purple line shows the shipping route in the open water season; the green line shows the route during the ice-covered season.

Baffinland Iron Mines Corporation's proposed shipping season is from June 25 through March 7. Ice and open water seasons were defined based on analysis of average monthly ice coverage data from TOPAZ4 at the spill site (2011-2015). Average ice cover of less than 30% was defined as "open water." Average ice cover of more than 30% was defined as "ice-covered". The two resulting seasons used for modeling were:

- Case 5A: Open water (August through October); and
- Case 5B: Ice (June 25 through July 31, and November 1 through March 7).

The oil type selected for scenarios 5A and 5B was an intermediate fuel oil, IFO 380. This would be the expected bunker fuel for a bulk carrier.

The source of the hypothetical spill was assumed to be an 85,000 DWT (Panamax) Polar Class 4 (PC4-DNV ICE 17) bulk carrier or iron ore carrier that may transit to and from the Baffinland Mines. A vessel of this type would be expected to have about 5,500 m^3 of IFO bunker fuel and 750 m^3 of diesel fuel. The fuel tanks are located in the central part of the stern, which provides protection as with a double-hull. The spill volume used in the modeling assumes the release of 1,000 m^3 from one bunker tank over the course of 12 hours, i.e., the entire contents of that single tank (about 18% of the total bunker fuel load).

The iron ore bulk carrier selected for the hypothetical spill scenario is expected to make 12 transits during January and February of each year (Baffinland Iron Mines Corporation, 2015). The probability of a serious grounding with a bulk carrier is about 0.000012 per day per ship (Det Norske Veritas, 2011). Assuming the transits take about 10 days (an over-estimate), one might expect a 1 in 694 chance of a serious grounding in a particular year from a bulk carrier transiting to

or from the Baffinland Mines. However, not all groundings result in the spillage of oil, and the probability that the grounding would result in spillage of bunker fuel is estimated to be 0.02 (Etkin and Michel 2003; Michel and Winslow 1999, 2000; Barone et al. 2007; Herbert Engineering et al. 2003). The probability of a grounding-related spill from a bulk carrier is 1 in 35,000. Note that this is the chance of a spill of *some volume* of oil, not a particular volume. The likelihood of a grounding resulting in the large spill volume modeled for this study would be even smaller. Also, this probability is specific to the traffic associated with Baffinland Mines. With additional non-tank vessel traffic through this area, the probability of spills would increase.

See Appendix A for additional discussion regarding the development of spill scenario parameters and vessel spill likelihood.

9.2 Environmental Analysis

Figure 90 presents the TOPAZ4 monthly surface current roses at the Eclipse Sound spill site. Seasonality is evident in both direction and amplitude. During winter, surface currents are weaker with average speeds typically between 1-1.5 cm/s and directed to the northwest. Surface speeds begin to increase in late spring with west-northwestward flow. Speeds from June through September are variable with speeds exceeding 2 cm/s. The predominant direction varies from month to month, ranging from southwestward to eastward to northwestward.

The TOPAZ4 monthly surface current speed statistics (average and 95th percentile) are presented in Figure 91. Monthly average surface current speeds are relatively low and vary between slightly under 1 cm/s to less than 2 cm/s. There are two main peaks in monthly surface speed that occur in May and September. The lowest average speed occurs in November and remains low through winter.

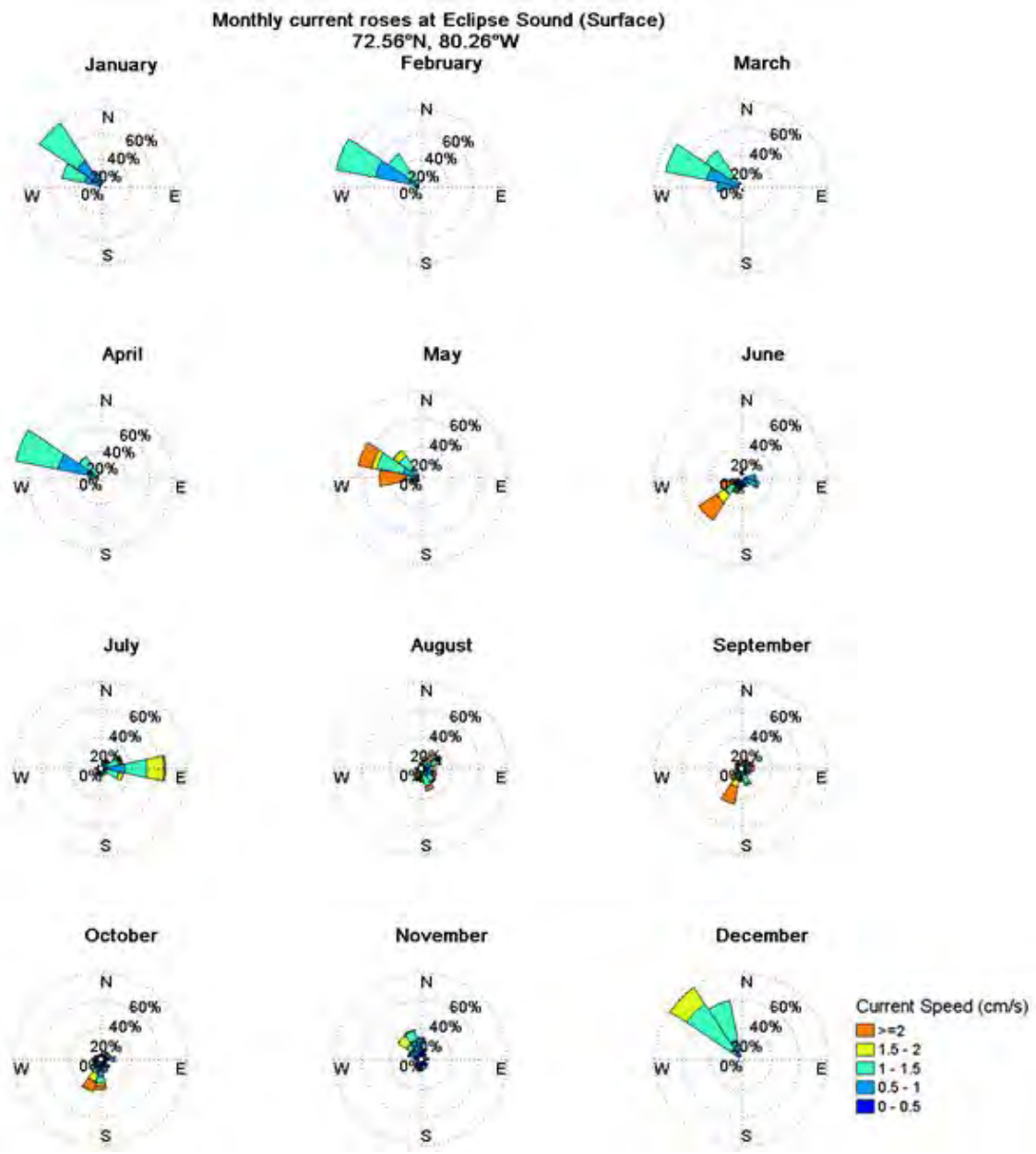

Figure 90. TOPAZ4 monthly averaged surface current roses near the Eclipse Sound spill site, averaged over the period of 2011-2015. Direction convention is standard (i.e., direction currents are moving to).

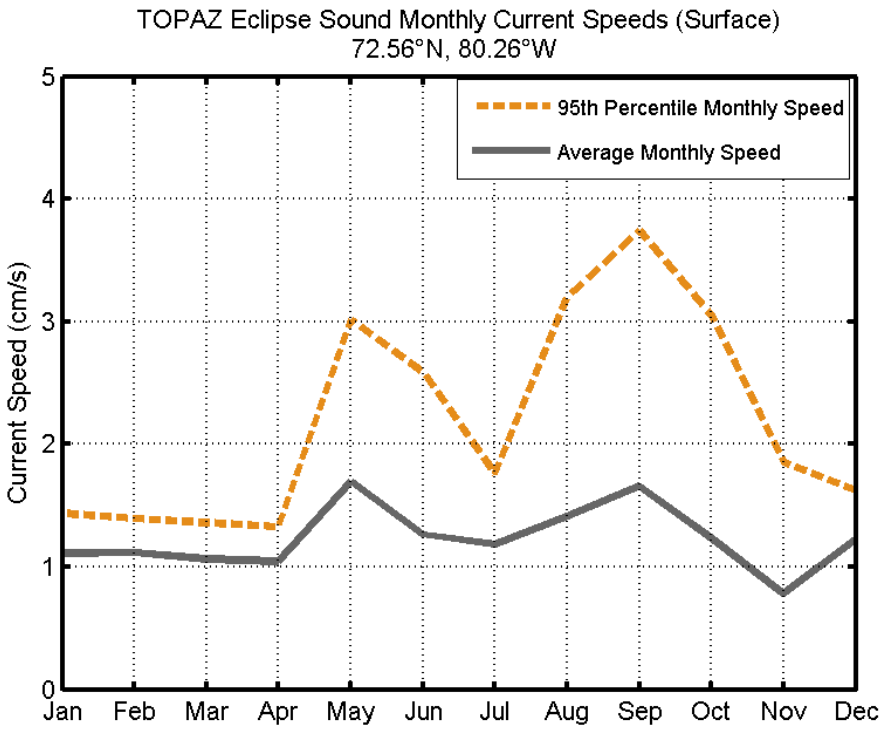

Figure 91. TOPAZ4 current statistics: monthly average (grey solid) and 95th percentile (orange dash) current speed at the surface near the Eclipse Sound spill site for 2011-2015.

Figure 92 displays average monthly ice roses at the Eclipse Sound spill site. Ice coverage is variable and inconsistent throughout the year. At the spill site, there is no TOPAZ4 ice velocity data in January and February, but data exist the rest of the year. When present, ice is directed westward from March to June, and becomes more variable the remaining months.

Monthly average sea ice and landfast ice cover near the spill site are shown in Figure 93. Sea ice coverage is based on data from TOPAZ4 (2011-2015) and landfast ice coverage is based on data from the National Snow and Ice Data Center (1991 through 1998). To incorporate sea ice in areas lacking complete TOPAZ4 data coverage (namely Milne Inlet, Navy Board Inlet, and Tremblay Sound), GIS polygons were created in these data gap areas to represent average sea ice coverage. The coverage values for these polygons were based on the monthly average sea ice coverage from nearby TOPAZ4 data.

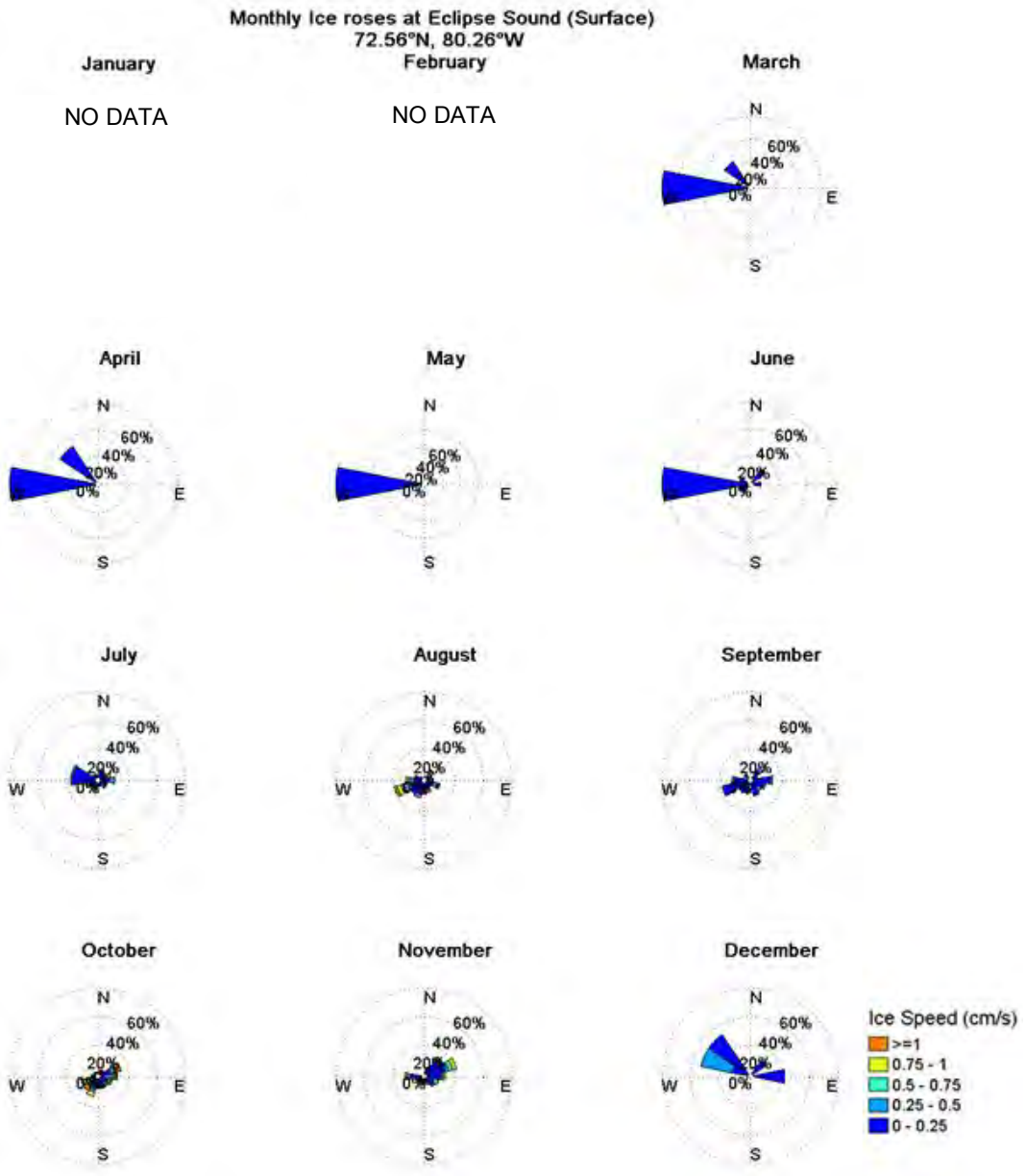

Figure 92. TOPAZ4 monthly averaged ice roses near the Eclipse Sound spill site, averaged over the period of 2011-2015. Ice roses are presented for the surface. Direction convention is standard (i.e., direction ice is moving to). TOPAZ4 ice velocity data are not available for the spill site during January and February.

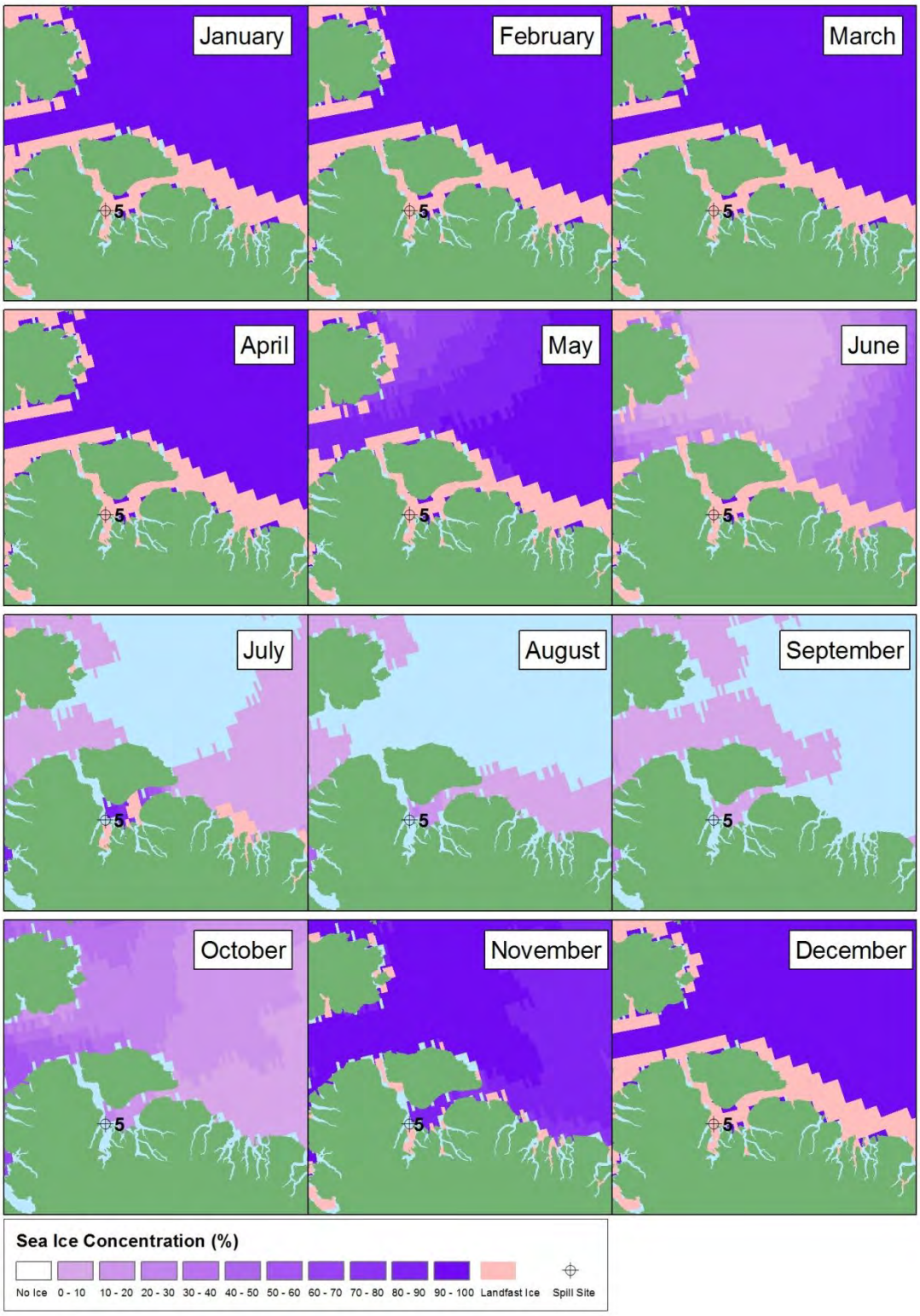

Figure 93. Average monthly cover of sea ice and landfast ice near the spill site for the Eclipse Sound spill site.

Figure 94 presents a HYDROMAP tidal current rose for the Eclipse Sound spill site. The direction is divided between northeastward and southwestward. Figure 95 presents a HYDROMAP stick plot for the Eclipse Sound spill site for a representative 26-day period. The tidal signature is evident with the nearly equal division of northeastward and southwestward current direction and cyclical pattern of high and low speeds.

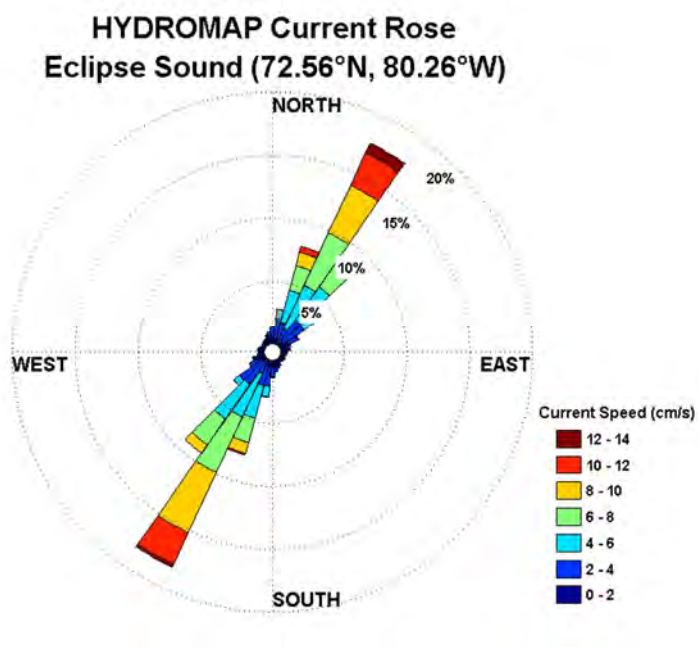

Figure 94. Time-averaged HYDROMAP surface current rose near the Eclipse Sound spill site. Direction convention is standard (i.e., direction currents are moving to).

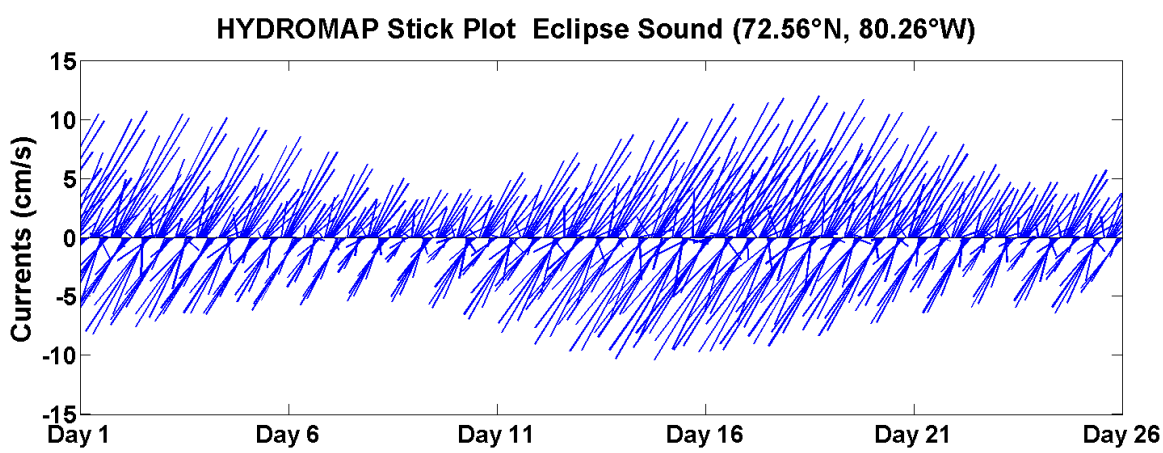

Figure 95. HYDROMAP tidal current stick plot for the Eclipse Sound spill site.

Figure 96 presents monthly ECMWF wind roses for the Eclipse Sound spill site. Wind direction is generally variable throughout the year. From December to March, the wind is primarily northerly and becomes more variable in April and May before transitioning to primarily northeasterly in June-August. Wind is variable from September through November as the seasons transition.

Monthly wind speed statistics at the Eclipse Sound spill site are presented in Figure 97. The typical monthly average speeds range from 5 to 8 knots with the highest speeds during summer and fall, and the lowest speeds in winter and spring.

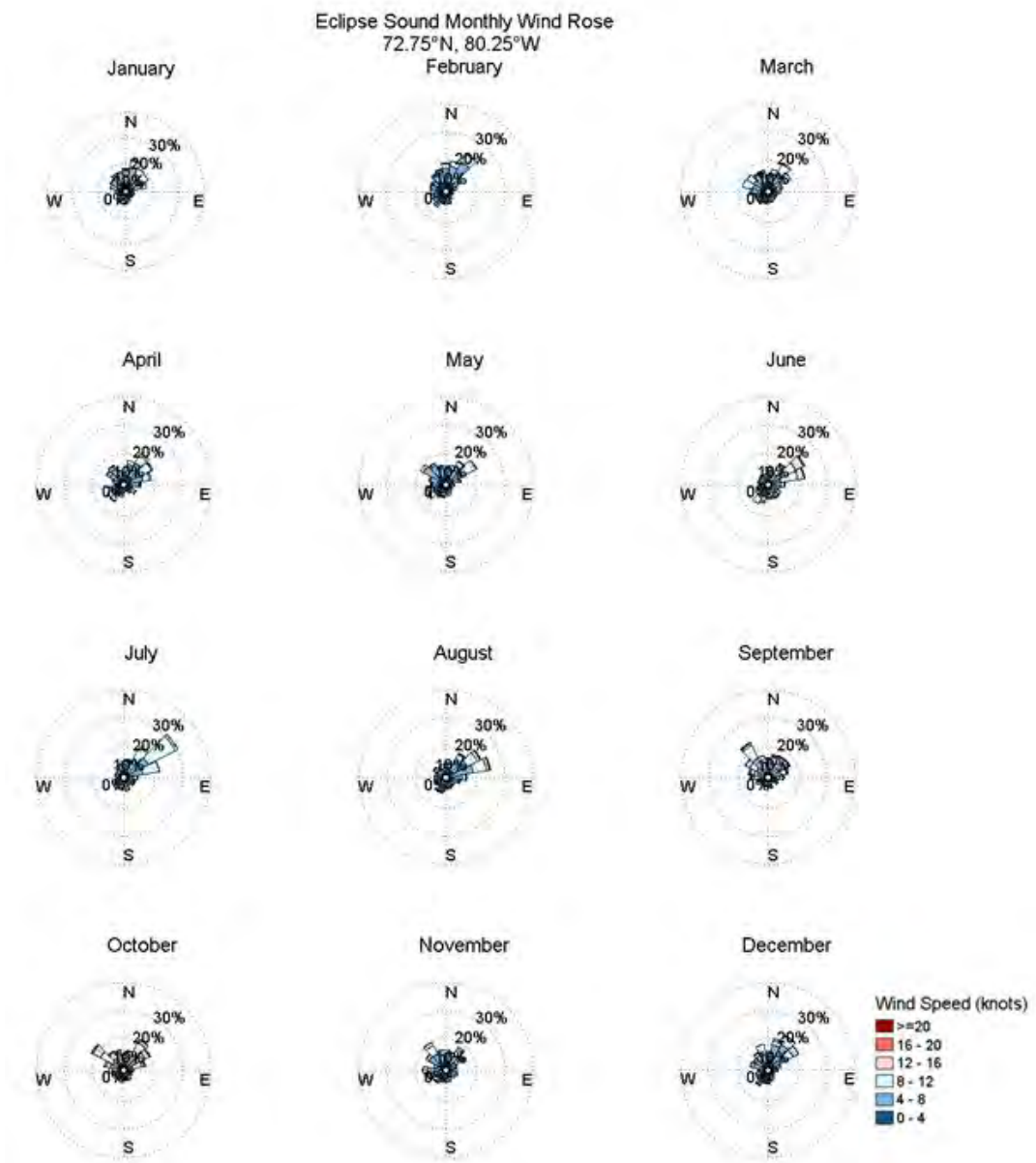

Figure 96. ECMWF monthly averaged wind roses near the Eclipse Sound spill site averaged over the period of 2011-2015. Wind speeds are in knots, using meteorological convention (i.e., direction wind is coming from).

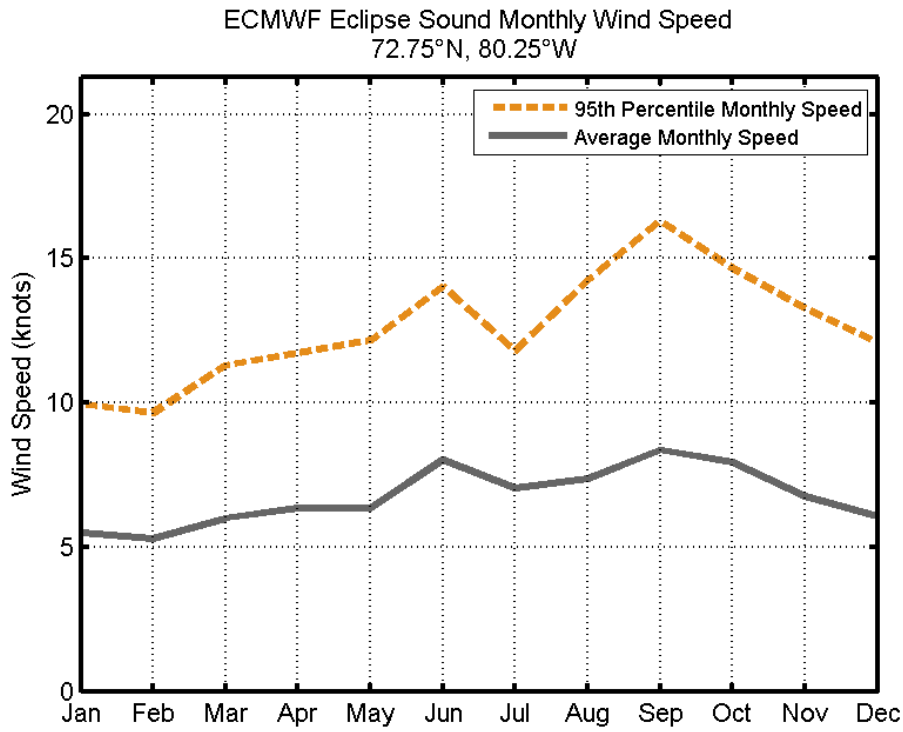

Figure 97. ECMWF wind statistics: monthly average (grey solid) and 95th percentile (orange dash) wind speed near the Eclipse Sound spill site for 2011-2015.

Figure 98 displays the vertical profile of temperature, salinity, and density for the two time periods used in the spill scenarios (June to July and November to March [ice period] and August to October [open water period]). Throughout periods of ice coverage, water temperature values are lower with increased salinity and density values. During the ice period, salinity is about 32.6 psu at the surface and increases to 33.8 psu near the sea floor. Temperature at the surface is approximately -0.8 ºC and increases to -0.7 ºC near the sea floor. Density at the surface is about 26.2 kg/m^3 and increases to 27.2 kg/m^3 at depth. During the open water period, salinity is about 31.0 psu at the surface and increases to 33.6 psu near the sea floor. Temperature at the surface is about 0.7 ºC and decreases to -0.4 ºC near the sea floor. Density at the surface is about 24.8 kg/m^3, decreasing to 27.0 kg/m^3 at depth.

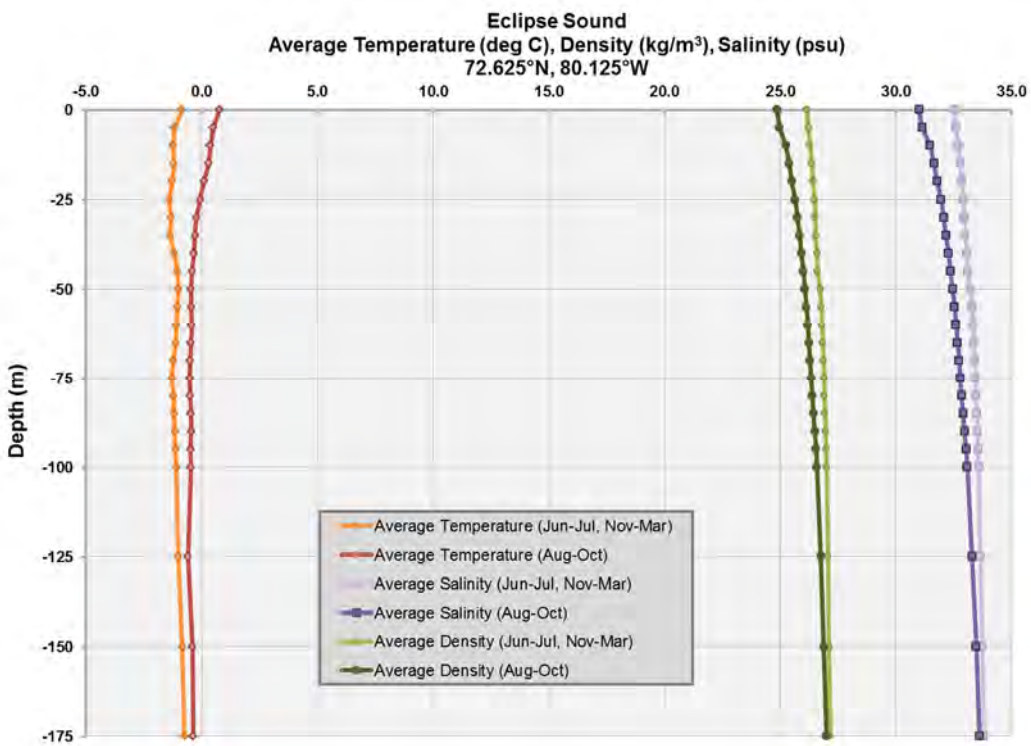

Figure 98. Vertical profile of average temperature (red), salinity (purple), and density (green) near the Eclipse Sound spill site for ice-covered (June-July, November-March) and open water (August-October) periods. Data from the World Ocean Atlas 2013.

9.3 Stochastic Modeling

The SIMAP stochastic model was used to predict the statistical footprint of oiling associated with the bulk carrier spill scenarios.

9.3.1 Stochastic Scenario Parameters

The stochastic scenario input parameters developed for scenarios 5A and 5B (see Section 9.1) are summarized in Table 27 below. Both scenarios were simulated (tracked) for 30 days after the initial release. No spill response measures were included in the stochastic simulations for these scenarios.

Table 27. Stochastic scenario input parameters for scenarios 5A and 5B.

ID #	Spill Type	Location	Oil Type	Spill Duration (days)	Total Volume (m^3)	Season	Simulation Duration (days)
5A	Bulk carrier surface spill	72.559040°N, 80.256612°W	IFO 380	0.5	1,000	Open water (August to October)	30
5B	Bulk carrier surface spill	72.559040°N, 80.256612°W	IFO 380	0.5	1,000	Ice (June 25 to July 31, November 1 to March 7)	30

9.3.2 Stochastic Results

The results of the stochastic model simulations for scenarios 5A and 5B are shown in Table 28 and Table 29.

Table 28 presents shoreline oiling statistics for both scenarios, including the percentage of simulations reaching shore, time to shore, peak volume of oil ashore, and the shoreline length oiled above the ecological threshold of 100 g/m^2. The percentage of simulations reaching shore indicates the likelihood that a particular spill event will reach nearby coastal areas with a level of shoreline oiling greater than 100 g/m^2. The percentage of simulations reaching shore is based on the total number of trajectories out of the ensemble of 200 individual runs that reached the coast in the stochastic analysis. Note that a spill event with high probability of shoreline oiling does not imply that a particular section of the coast will be oiled, only that there is a high probability of oil reaching the coastline *at some location*.

In open water conditions (scenario 5A), there was a high probability of shoreline oiling above 100 g/m^2, with 98% of trajectories reaching shore. In ice-covered conditions (scenario 5B), the probability of shoreline oiling is greatly reduced, with only 23% of trajectories reaching shore above the threshold during the simulation. However, oil trapped in ice for the winter may oil shorelines following the breakup and melt of ice in the summer.

For the trajectories that did reach shore, the peak volume of oil ashore and the shoreline length oiled were similar between the two cases, with slightly lower values in scenario 5B. Peak volumes oil of ashore for both scenarios, on average, were relatively high, with 83% of the total volume spilled for scenario 5A, and 73% of the total volume spilled for scenario 5B. The minimum time for oil to first reach shore was similar between the two scenarios, at <1 day. However, the average time to shore was much longer for scenario 5B (14.2 days versus 1.2 days for scenario 5A), due to the presence of ice.

Table 28. Scenarios 5A and 5B stochastic results – shoreline oiling statistics.

ID	Spill Event	Total Volume Spilled (m^3)	Simulations Reaching Shore (%)[1]	Time to Reach Shore (days)		Peak Volume of Oil Ashore (m^3)		Shoreline Length Oiled Above 100 g/m^2 (km)	
				Min.	Avg.	Max.	Avg.	Max.	Avg.
5A	Eclipse Sound – Open Water	1,000	98	0.2	1.2	965	833	99	43
5B	Eclipse Sound – Ice	1,000	23	0.6	14.2	908	731	54	32

[1] Percentage of simulations reaching shore is calculated based on the number of individual trajectories that resulted in shoreline oiling above a threshold of 100 g/m^2 of oil.

Table 29 presents surface oiling and water column oiling statistics. In open water conditions (scenario 5A), the resulting water surface footprint was, on average, about 16 km^2 oiled above the ecological threshold of 10 g/m^2. The water surface oiling footprint in ice-covered conditions (scenario 5B) was approximately 4 km^2 oiled on average. On average, the peak volume of oil entrained in the water column was less than 0.01% of the total volume spilled. This is attributable to the properties of IFO 380, which does not readily entrain into the water column.

Table 29. Scenarios 5A and 5B stochastic results – surface oiling and water column oiling statistics.

ID	Spill Event	Total Volume Spilled (m^3)	Water Surface Area Oiled Above 0.01 g/m^2 (km^2)		Water Surface Area Oiled Above 10 g/m^2 (km^2)		Volume of Oil in Water Column (m^3)	
			Max.	Avg.	Max.	Avg.	Max.	Avg.
5A	Eclipse Sound – Open Water	1,000	165	20	47	16	0.1	<0.1
5B	Eclipse Sound – Ice	1,000	45	4	37	4	0.1	<0.1

The following figures (Figure 99 through Figure 102) illustrate the spatial extent of water surface oiling and shoreline oiling probabilities for scenarios 5A and 5B. For each scenario, three figures are presented:

1. **Probability of Water Surface Oiling Above 0.01 g/m^2**: The map defines the area in which water surface oiling above the socioeconomic threshold of 0.01 g/m^2 may be expected and the associated probability of oiling (based on analysis of the 200 individual trajectories run for each spill scenario). The map does not imply that the entire contoured area would be covered with oil in the event of a spill. The map also does not provide any information about the quantity of oil in a given area.

2. **Probability of Water Surface Oiling Above 10 g/m^2**: The map defines the area in which water surface oiling above the ecological threshold of 10 g/m^2 may be expected and the associated probability of oiling (based on analysis of the 200 individual trajectories run for each spill scenario). The map does not imply that the entire contoured area would be covered with oil in the event of a spill. The map also does not provide any information about the quantity of oil in a given area.

3. **Probability of Shoreline Oiling Exceeding 100 g/m^2**: This map shows the probability of shoreline oiling above the ecological threshold of 100 g/m^2 (based on analysis of the 200 individual trajectories run for each spill scenario). The map does not imply that the entire shoreline extent would be oiled in the event of a spill. The map also does not provide any information about the quantity of oil in a given area.

A brief summary of each stochastic simulation follows the figures for each case.

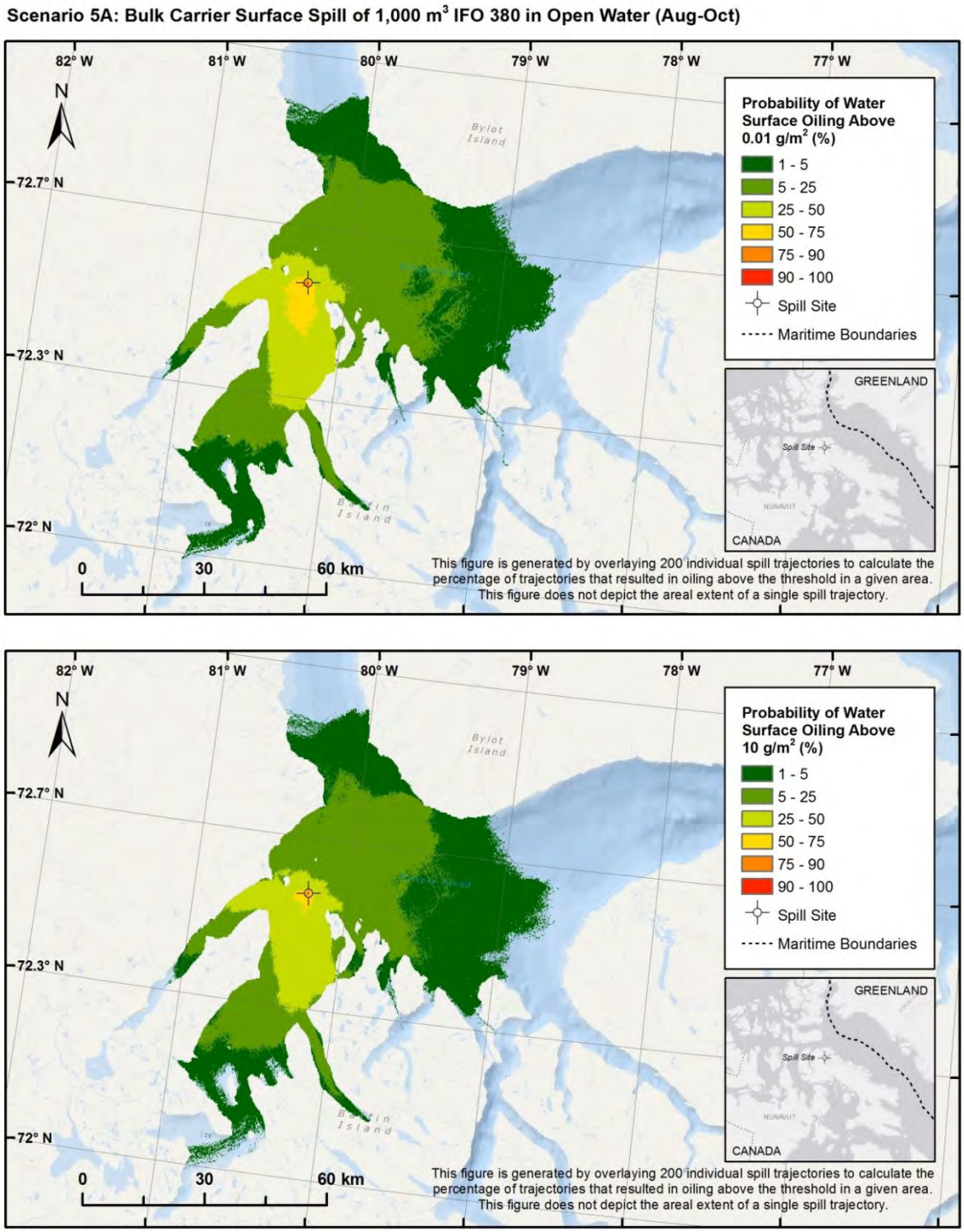

Figure 99. Scenario 5A (surface spill of 1,000 m^3 IFO 380 in open water conditions) stochastic results – Probability of water surface oiling above the socioeconomic threshold of 0.01 g/m^2 (top panel) and probability of water surface oiling above the ecological threshold of 10 g/m^2 (bottom panel).

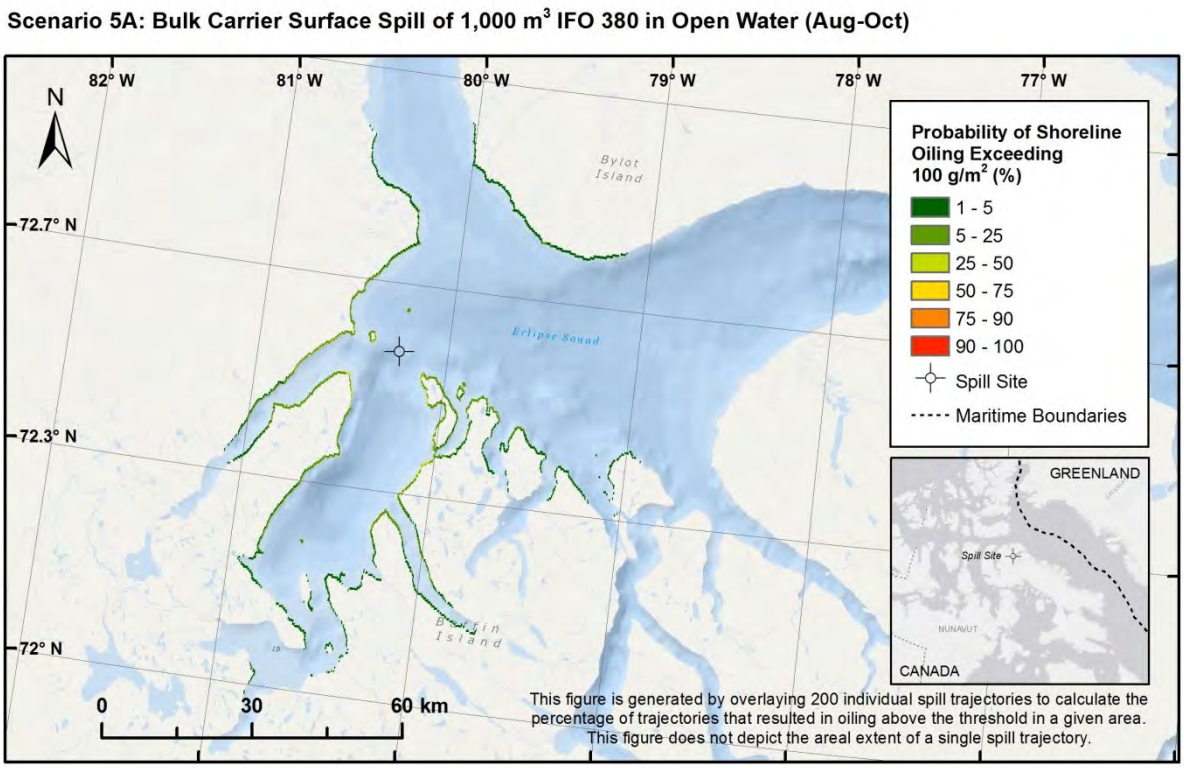

Figure 100. Scenario 5A (surface spill of 1,000 m^3 IFO 380 in open water conditions) stochastic results – Probability of shoreline oiling above the ecological threshold of 100 g/m^2.

For the socioeconomic threshold of 0.01 g/m^2, the stochastic water surface oiling footprint for scenario 5A is variable in direction, but the zone of highest probabilities is oriented mainly to the south of the spill site into Milne Inlet and to the west into Tremblay Sound (Figure 99). There is also a low (<25%) probability of water surface oiling to the north and east of the spill site in the main body of Eclipse Sound. For the ecological threshold of 10 g/m^2, the stochastic surface oiling footprint is very similar, with slightly reduced probabilities.

There is an approximately 98% chance that shoreline oiling above 100 g/m^2 will occur at some location (Table 29). However, the highest probability of any individual segment of the coastline being oiled above the threshold is 41% (Figure 100). The highest probability of oiling is for shorelines to the south of the spill site along the shorelines of the mouth of upper Milne Inlet, and to the west-northwest on the shoreline of Pisiktarfik Island. There are also lower probabilities of shoreline oiling farther south into Milne Inlet, to the southwest along Tremblay south, to the north on Bylot Island, as far east as Emmerson Island, and to the north along the southern shorelines of Navy Board Inlet.

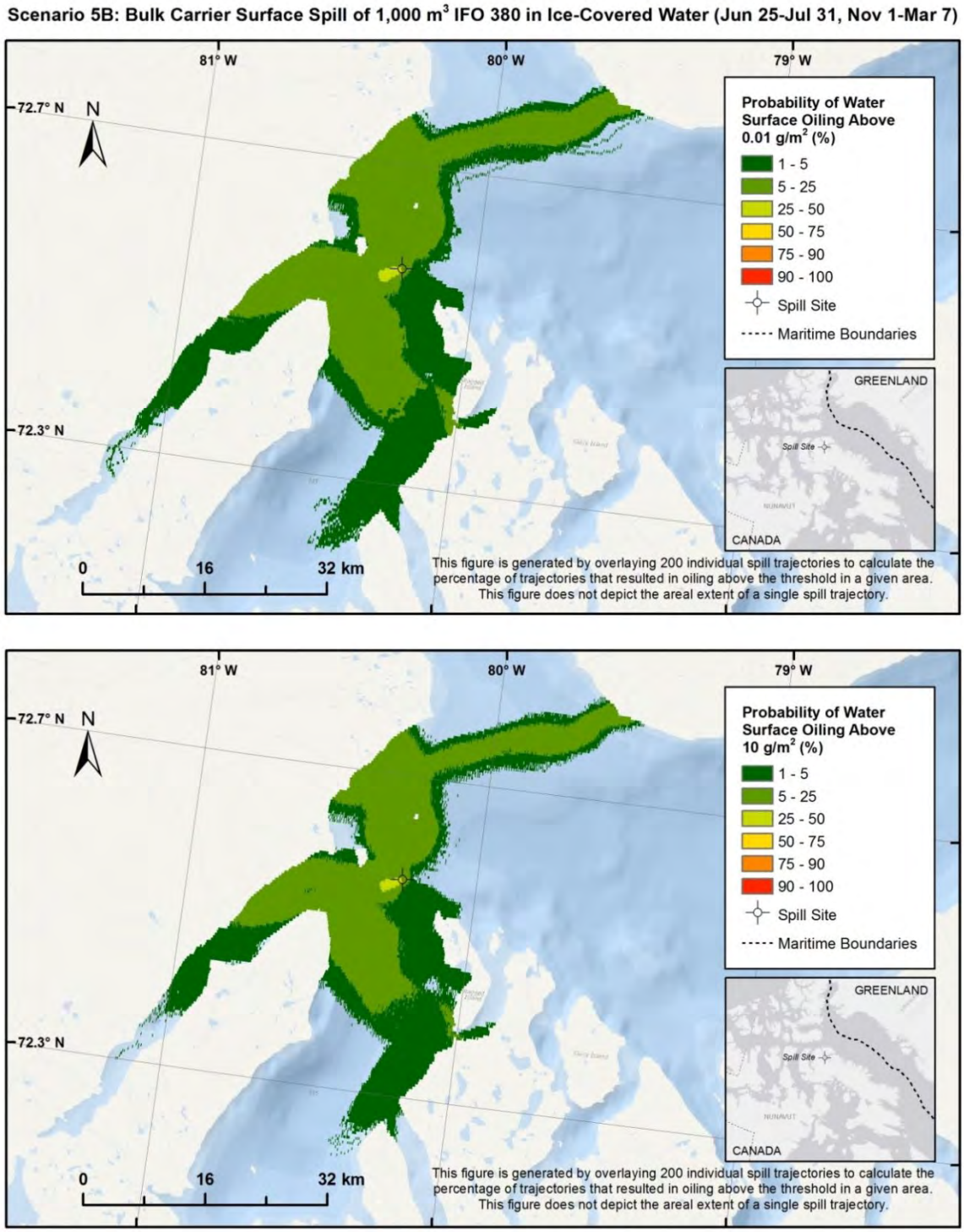

Figure 101. Scenario 5B (surface spill of 1,000 m^3 IFO 380 in ice conditions) stochastic results – Probability of water surface oiling above the socioeconomic threshold of 0.01 g/m^2 (top panel) and probability of water surface oiling above the ecological threshold of 10 g/m^2 (bottom panel).

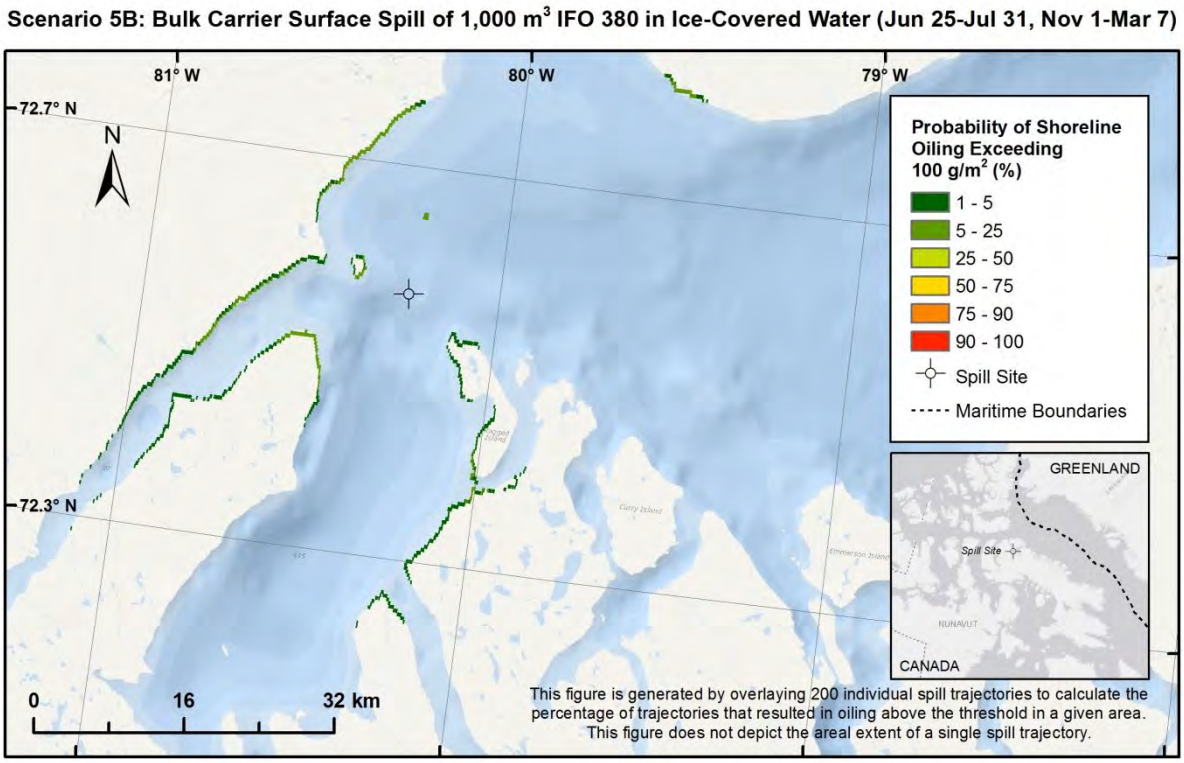

Figure 102. Scenario 5B (surface spill of 1,000 m^3 IFO 380 in ice conditions) stochastic results – Probability of shoreline oiling above the ecological threshold of 100 g/m^2.

For the socioeconomic threshold of 0.01 g/m^2, the stochastic water surface oiling footprint for scenario 5B is variable in direction, with the zone of highest probabilities is restricted to within a few kilometers of the spill site and oriented to the south (Figure 101). There is also a low (<25%) probability of water surface oiling to the north of the spill site into Eclipse Sound, to the south into Milne Inlet, and to the southwest into Tremblay Sound. For the ecological threshold of 10 g/m^2, the stochastic surface oiling footprint is very similar, with slightly reduced probabilities.

There is an approximately 23% chance that shoreline oiling above 100 g/m^2 will occur at some location during the model simulation (Table 29). However, the highest probability of any individual segment of the coastline being oiled above the threshold is 12% (Figure 102). The highest probability of oiling is for shorelines to the southwest of the spill site along the western shoreline of the mouth of Milne Inlet, and to the west-northwest on the shoreline of Pisiktarfik Island. There are also lower probabilities of shoreline oiling to the southwest along Tremblay Sound, to the north on Bylot Island, and farther south into Milne Inlet.

9.4 Deterministic Modeling

The deterministic trajectory and fate simulations provide an estimate of the 3-D trajectory (movement) and fate (weathering) for a particular individual spill event.

9.4.1 Deterministic Scenario Parameters

Trajectories were selected from the stochastic scenarios based on pre-defined criteria. Different parameters or criteria can be used to select individual trajectories for deterministic analysis. For example, deterministic trajectories can be "representative" or "worst-case" for a variety of consequence metrics (e.g., shoreline length oiled, time to shore, volume of oil ashore, water column contamination, water surface area swept). The selected deterministic cases for scenario 5 are summarized in Table 30. The three representative cases for water surface oiling were selected to demonstrate the release of ice-bound oil following ice melt and breakup (July case), open water conditions (August case), and the capture of floating oil in ice during the transition to ice-covered conditions (October case). The fourth deterministic case is the worst case for surface area oiled at any point during the June 25 to March 7 Baffinland Mines operating season.

No spill response measures were included in the deterministic simulations.

Table 30. Selected deterministic cases for scenario 5.

ID	Spill Event	Type of Deterministic Case[1]	Spill Response Type	Spill Start Date	Simulation Duration (Days)
5	Eclipse Sound – Bulk Carrier	Representative Water Surface Area Oiled in July	None	16 July 2013	30
5	Eclipse Sound – Bulk Carrier	Representative Water Surface Area Oiled in August	None	27 August 2014	30
5	Eclipse Sound – Bulk Carrier	Representative Water Surface Area Oiled in October	None	30 October 2012	30
5	Eclipse Sound – Bulk Carrier	Worst-case Water Surface Area Oiled	None	10 August 2014	30

[1] The "worst case" was defined as the trajectory with the 95th percentile value for water surface oiling above the ecological threshold of 10 g/m^2. The "representative" case for a given month was defined as the trajectory with the 50th percentile value for oiling above the ecological threshold of 10 g/m^2.

9.4.2 Deterministic Results

Key results from the deterministic simulations for the Eclipse Sound bulk carrier spill scenarios are summarized in Table 12, including volume of water exceeding 1 ppb of dissolved aromatics (the most toxic components of oil), water surface area oiled, shoreline length oiled, time to first reach shore, and peak volume of oil ashore.

Table 31. Summary of deterministic results for the Eclipse Sound bulk carrier scenarios.

ID	Deterministic Case	Volume of Water Exceeding 1 ppb of Dissolved Aromatics (m^3)	Water Surface Area Oiled Above 0.01 g/m^2 (km^2)	Water Surface Area Oiled Above 10 g/m^2 (km^2)	Shoreline Length Oiled Above 100 g/m^2 (km)	Time to Shore (Days)	Peak Volume of Oil Ashore (m^3)
5	Representative Water Surface Area Oiled in July	2.0×10^6	4.7	4.7	40.0	15.0	759.9
5	Representative Water Surface Area Oiled in August	3.9×10^6	6.0	6.0	36.3	0.8	860.1
5	Representative Water Surface Area Oiled in October	1.1×10^7	5.5	5.5	1.3	1.3	55.3
5	Worst-case Water Surface Area Oiled	8.5×10^6	12.5	12.5	40.4	1.3	888.6

The following figures (Figure 103 through Figure 110) present the results of the deterministic simulations for each scenario. Three figures are shown for each deterministic case:

10. **Maximum Floating Oil Concentration**: This map shows the maximum concentration (g/m^2) of floating oil that passed through a given area at some point during the simulation. This map also displays the approximate subsurface area swept by dissolved aromatic concentrations greater than 1 ppb. This concentration is used as a screening threshold for potential impacts on sensitive water column organisms (based on French McCay, 2009).

11. **Shoreline Oil Concentration**: This map shows the concentration (g/m^2) of oil on the shoreline at the end of the simulation.

12. **Mass Balance**: This graph shows a time history of the fate and weathering of the spilled oil during the simulation. Components of the oil tracked over time include amount of oil on the sea surface, on the shoreline, in the water column (subsurface), in subsea sediments, evaporated into the atmosphere, and decayed (e.g., by photo-oxidation, biodegradation).

A brief description of each deterministic simulation follows the figures for each case.

Scenario 5: Representative Water Surface Area Oiled in July (No Response)

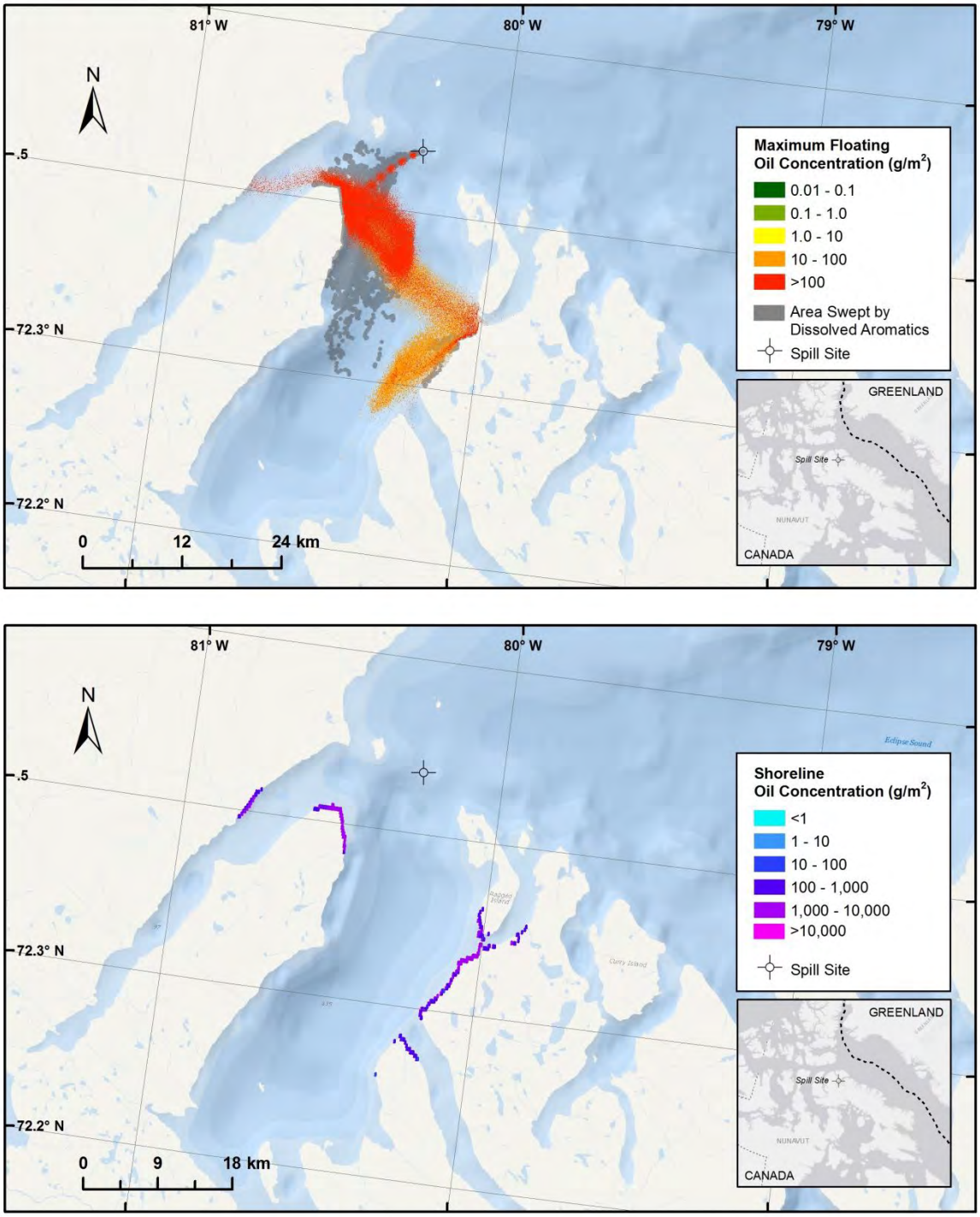

Figure 103. Scenario 5: Representative (50th percentile) trajectory for water surface area oiled above 10 g/m^2 for spills originating in the month of July, with no spill response – Maximum concentration (g/m^2) of floating oil that passed by a given area during the simulation and the subsurface area swept by dissolved aromatics (top panel); and total concentration (g/m^2) of oil on the shoreline at the end of the simulation (bottom panel).

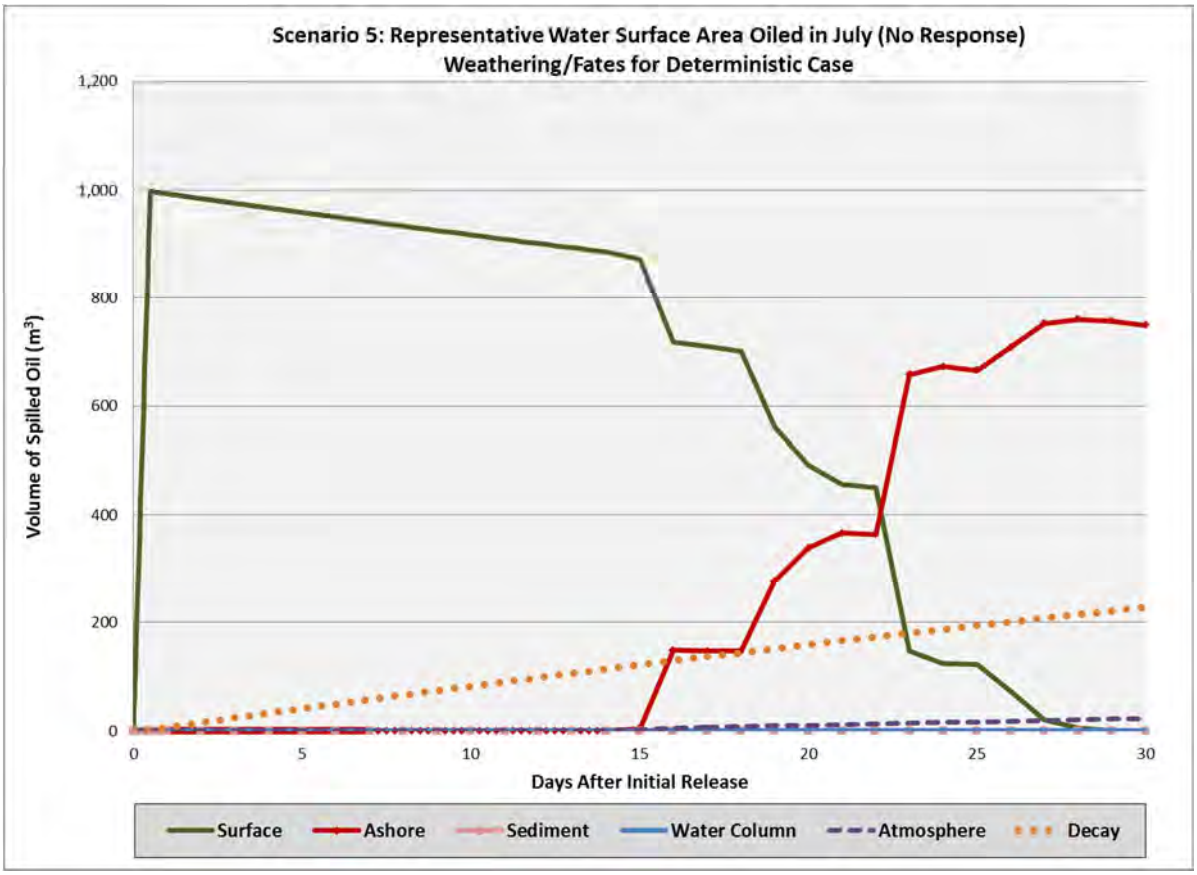

Figure 104. Scenario 5: Representative (50th percentile) trajectory for water surface area oiled above 10 g/m^2 for spills originating in the month of July, with no spill response – Mass balance graph.

The representative case for water surface oiling for spills beginning in the month of July was selected to demonstrate the release of ice-bound oil following ice melt and breakup (Figure 103 and Figure 104). This scenario was modeled without response.

At the beginning of the spill, the ice cover is high, and the oil is trapped on the surface at the spill site, with some oil removed over time due to nature decay processes. At about 14 days into the simulation, the ice-bound oil is released as floating oil and travels to the southwest of the spill site, reaching shore at the west coast of upper Milne Inlet at 15 days following the spill. Floating oil not retained on shore then travels briefly to the east-southeast before turning to the north and west and entering Tremblay Sound at about 18 days after the spill and causing shoreline oiling in this area. The remaining floating oil then travels east-southeast again into Milne Inlet, oiling the eastern coastline of upper Milne Inlet beginning at about 22 days after the spill. By 23 days post-spill, less than 15% of the volume spilled remains on the water surface. At the end of the 30-day simulation, no oil remains on the water surface.

Natural decay processes play a role in the removal of oil, with about 23% of the spilled volume removed by natural decay processes such as biodegradation and photo-oxidation by the end of the simulation. Evaporation plays a very small role in removal, with about 2% of the spilled volume evaporated by the end of the simulation. The peak volume of oil on the shoreline was 759.9 m^3, at 28 days after the spill start. At the end of the simulation, 749.6 m^3 (about 75% of the

total volume spilled) remain on shore, with a total of 40.0 km of shoreline oiled above the ecological threshold of 100 g/m^2. IFO 380 does not readily entrain into the water column and there was virtually no entrainment of oil in the water column during the simulation.

Despite the lack of oil entrained in the water column, there is still the potential for water column impacts from aromatics (the most toxic components of oil) dissolving into the water column from the surface slick. In general, the subsurface area swept by dissolved aromatics followed the same trajectory as the thickest surface oil, extending somewhat beyond the surface oil footprint to the south. The peak volume of water exceeding 1 ppb of dissolved aromatics (a screening threshold for impacts on sensitive water column organisms) was 2.0 million m^3.

Scenario 5: Representative Water Surface Area Oiled in August (No Response)

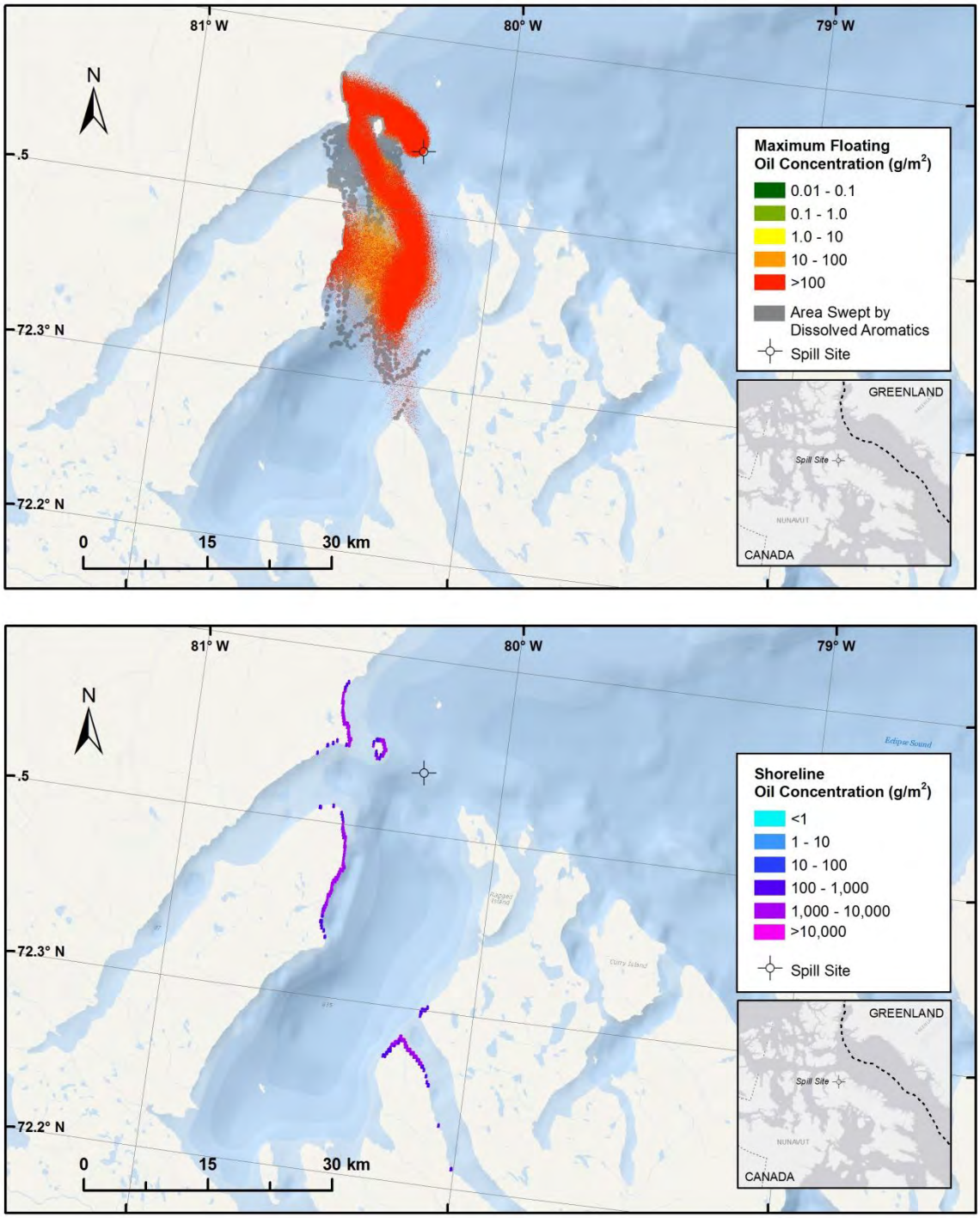

Figure 105. Scenario 5: Representative (50th percentile) trajectory for water surface area oiled above 10 g/m^2 for spills originating in the month of August, with no spill response – Maximum concentration (g/m^2) of floating oil that passed by a given area during the simulation and the subsurface area swept by dissolved aromatics (top panel); and total concentration (g/m^2) of oil on the shoreline at the end of the simulation (bottom panel).

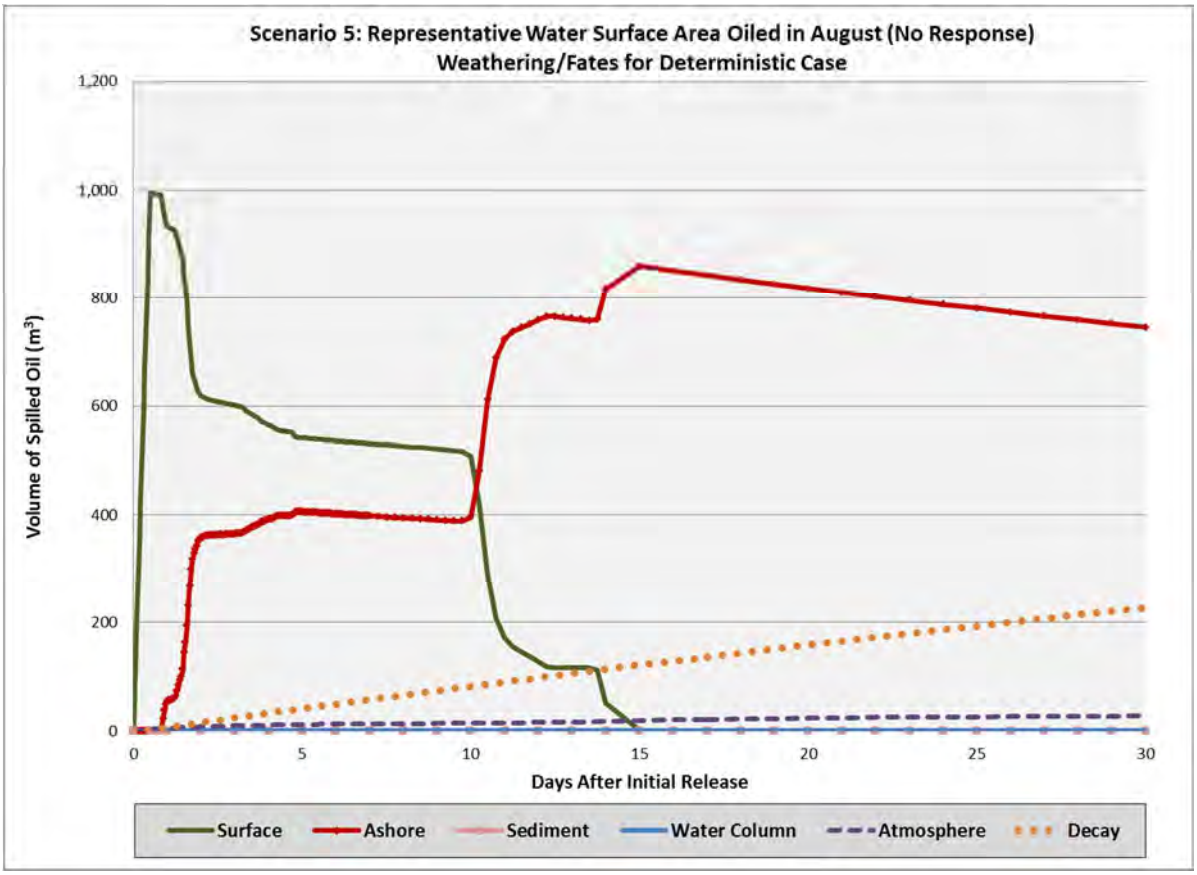

Figure 106. Scenario 5: Representative (50th percentile) trajectory for water surface area oiled above 10 g/m^2 for spills originating in the month of August, with no spill response – Mass balance graph.

The representative case for water surface oiling for spills beginning in the month of August was selected to demonstrate the movement of oil in open water conditions (Figure 105 and Figure 106). This scenario was modeled without response.

The floating oil trajectory heads generally to the northwest of the spill site for the first few days after the spill, first reaching shore at Pisiktarfik Island at about 18 hours after the start of the spill. The floating oil continues to travel northwest, oiling the shoreline to the west of Pisiktarfik Island, before traveling generally south-southeast into Milne Inlet, oiling associated shorelines beginning at about 9.7 days into the simulation. By 11 days post-spill, about 17% of the volume spilled remains on the water surface. At the end of the 30-day simulation, no oil remains on the water surface.

Natural decay processes play a role in the removal of oil, with about 23% of the spilled volume removed by natural decay processes such as biodegradation and photo-oxidation by the end of the simulation. Evaporation plays a very small role in removal, with about 3% of the spilled volume evaporated by the end of the simulation. The peak volume of oil on the shoreline was 860.1 m^3, at 15 days after the spill start. At the end of the simulation, 745.0 m^3 (about 75% of the total volume spilled) remain on shore, with a total of 36.3 km of shoreline oiled above the ecological threshold of 100 g/m^2. IFO 380 does not readily entrain into the water column and there was virtually no entrainment of oil in the water column during the simulation.

Despite the lack of oil entrained in the water column, there is still the potential for water column impacts from aromatics (the most toxic components of oil) dissolving into the water column from the surface slick. In general, the subsurface area swept by dissolved aromatics followed the same trajectory as the surface oil, extending somewhat beyond the surface oil in the area to the west of the spill site. The peak volume of water exceeding 1 ppb of dissolved aromatics (a screening threshold for impacts on sensitive water column organisms) was 3.9 million m^3.

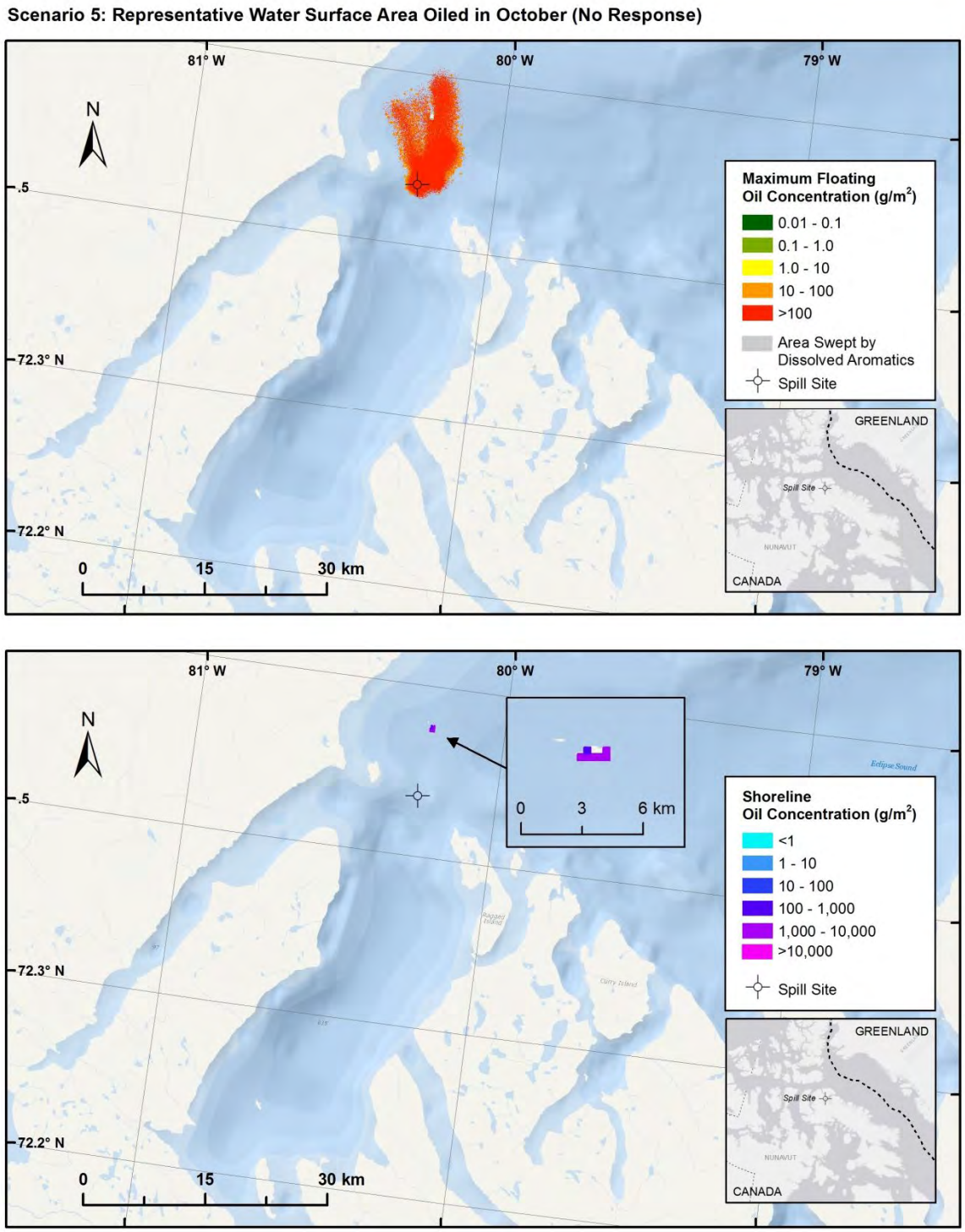

Figure 107. Scenario 5: Representative (50th percentile) trajectory for water surface area oiled above 10 g/m^2 for spills originating in the month of October, with no spill response – Maximum concentration (g/m^2) of floating oil that passed by a given area during the simulation and the subsurface area swept by dissolved aromatics (top panel); and total concentration (g/m^2) of oil on the shoreline at the end of the simulation (bottom panel).

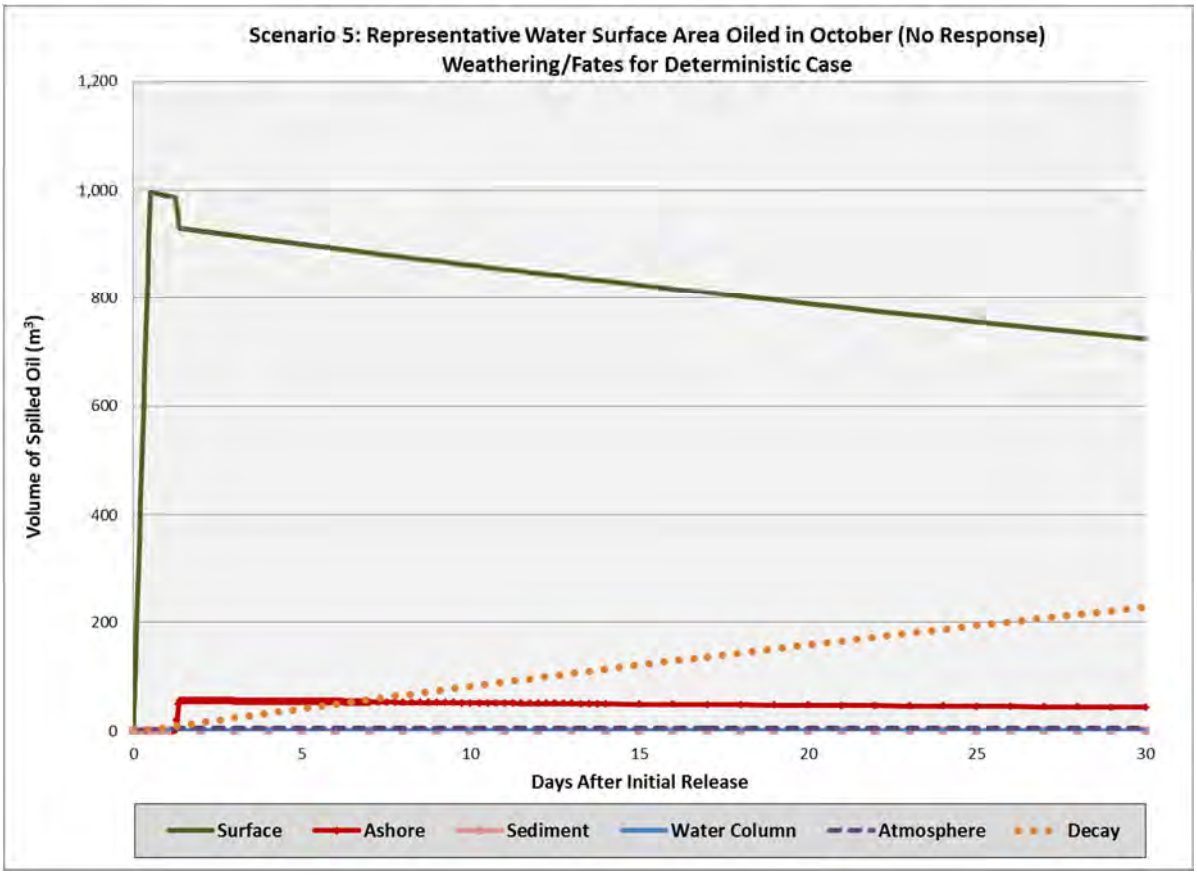

Figure 108. Scenario 5: Representative (50th percentile) trajectory for water surface area oiled above 10 g/m^2 for spills originating in the month of October, with no spill response – Mass balance graph.

The representative case for water surface oiling for spills beginning in the month of October was selected to demonstrate the capture of floating oil in ice during the transition to ice-covered conditions (Figure 107 and Figure 108). This scenario was modeled without response.

At the beginning of the spill, the floating oil travels generally to the north and north-northwest of the spill site, first reaching shore about 1.3 days into the simulation at a small island to the north of the spill site. Shortly thereafter, the sea ice concentration increases and the floating oil becomes trapped in immobile sea ice (pack ice) for the remainder of the simulation. Some of the trapped oil is removed over time due to natural decay processes. At the end of the 30-day simulation, 723.8 m^3 (about 72% of the volume spilled) is trapped in pack ice on the water surface. This oil could potentially oil other areas upon breakup and melt of the ice. The ultimate fate of this oil is unknown, and would be dependent on the environmental conditions at the time of release from the ice. However, during open water conditions, the fate of the oil released from ice would likely be consistent with the results of the stochastic scenario 5A.

Natural decay processes play a role in the removal of oil, with about 23% of the spilled volume removed by natural decay processes such as biodegradation and photo-oxidation by the end of the simulation. Evaporation contributes little to removal, with less than 0.5% of the spilled volume evaporated by the end of the simulation. The peak volume of oil on the shoreline was 55.3 m^3, at about 1.4 days after the spill start. At the end of the simulation, 43.1 m^3 of oil remains on

shore, with a total of 1.3 km of shoreline oiled above the ecological threshold of 100 g/m^2. IFO 380 does not readily entrain into the water column and there was virtually no entrainment of oil in the water column during the simulation.

Despite the lack of oil entrained in the water column, there is still the potential for water column impacts from aromatics (the most toxic components of oil) dissolving into the water column from the surface slick. The subsurface area swept by dissolved aromatics was entirely contained within the surface oiling footprint. The peak volume of water exceeding 1 ppb of dissolved aromatics (a screening threshold for impacts on sensitive water column organisms) was 11 million m^3.

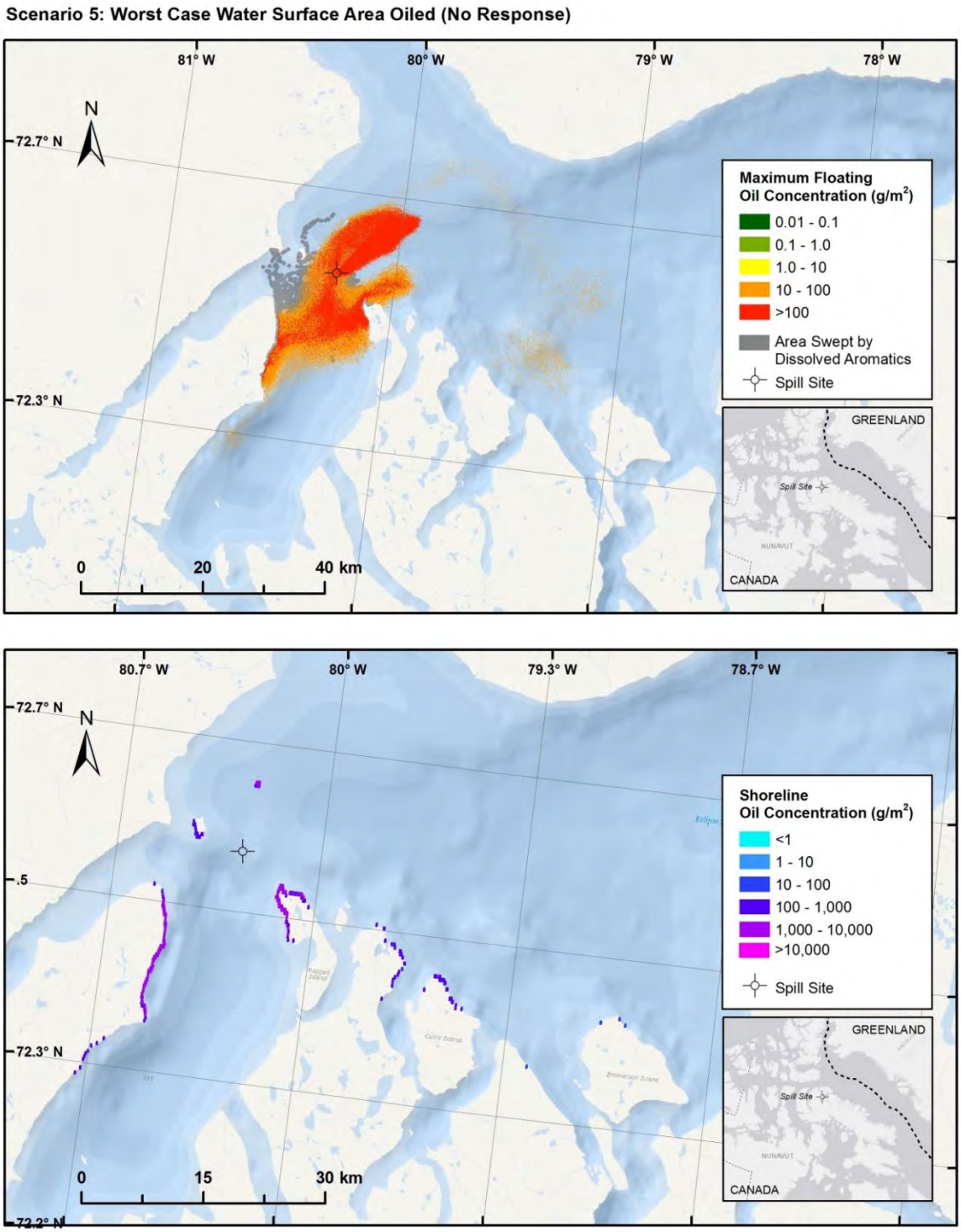

Figure 109. Scenario 5: Worst-case (95th percentile) trajectory for water surface area oiled above 10 g/m^2, with no spill response – Maximum concentration (g/m^2) of floating oil that passed by a given area during the simulation and the subsurface area swept by dissolved aromatics (top panel); and total concentration (g/m^2) of oil on the shoreline at the end of the simulation (bottom panel).

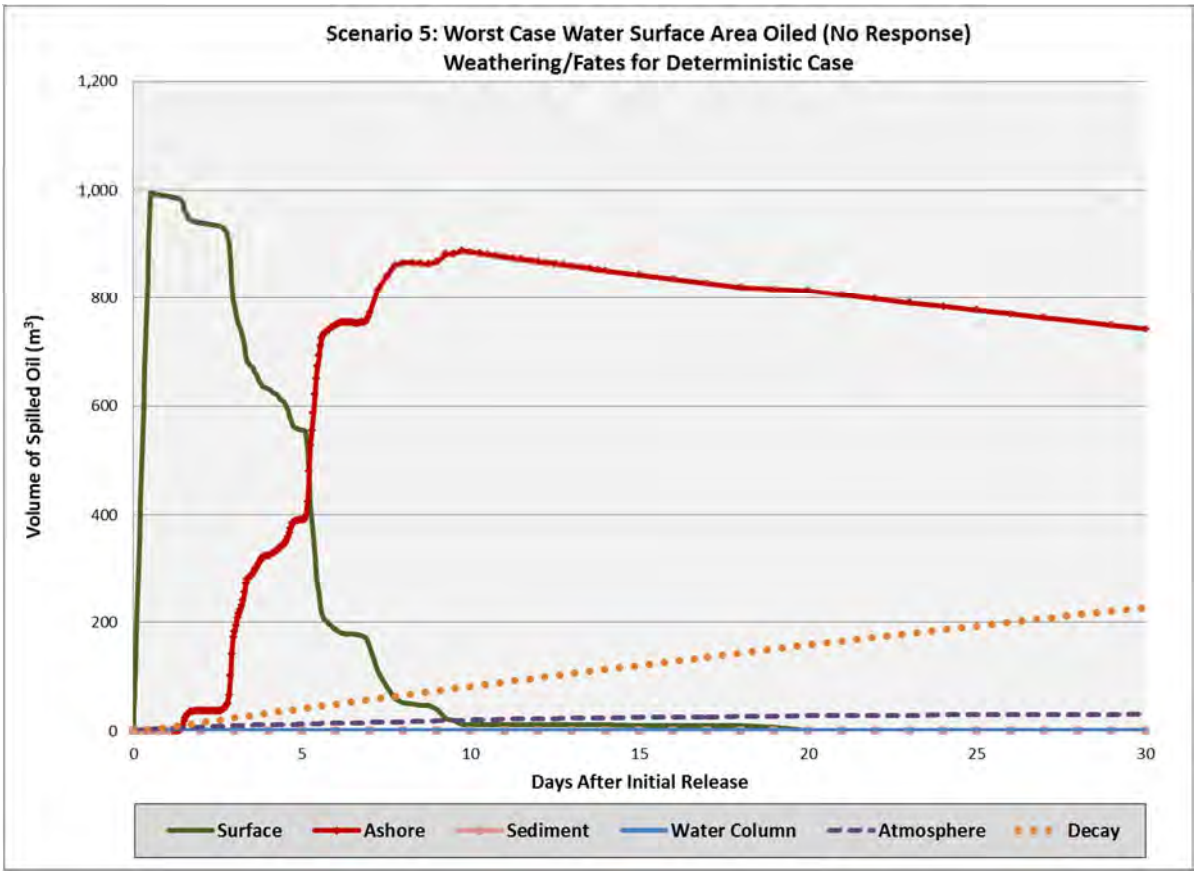

Figure 110. Scenario 5: Worst-case (95th percentile) trajectory for water surface area oiled above 10 g/m^2, with no spill response – Mass balance graph.

The worst-case for surface area oiled at any point during the June 25 to March 7 Baffinland Mines operating season, was modeled without response (Figure 109 and Figure 110).

The spill trajectory initially travels mainly to the northeast of the spill site for approximately the first day after the spill, before turning briefly to the west. Oil first comes ashore at about 1.3 days into the simulation at a small island to the north of the spill site. The floating oil then travels southward into upper Milne Inlet, oiling the shoreline of Ragged Island beginning at about 2.7 days into the simulation and the western shoreline of upper Milne Inlet beginning at about 5.1 days. Floating oil not retained on shore then travels to the north, oiling Pisiktarfik Island at about 9.7 days after the spill. After this shoreline oiling event, very little floating oil (11.3 m^3, about 1% of the total volume spilled) remains on the water surface and travels roughly eastward through Eclipse Sound, oiling additional shoreline areas as far east as Emmerson Island. At the end of the 30-day simulation, no oil remains on the water surface.

Natural decay processes play a role in the removal of oil, with about 23% of the spilled volume removed by natural decay processes such as biodegradation and photo-oxidation by the end of the simulation. Evaporation plays a very small role in removal, with about 3% of the spilled volume evaporated by the end of the simulation. The peak volume of oil on the shoreline was 888.6 m^3, at about 10 days after the spill start. At the end of the simulation, 742.1 m^3 (about 74% of the total volume spilled) remain on shore, with a total of 40.4 km of shoreline oiled above the

ecological threshold of 100 g/m^2. IFO 380 does not readily entrain into the water column and there was virtually no entrainment of oil in the water column during the simulation.

Despite the lack of oil entrained in the water column, there is still the potential for water column impacts from aromatics (the most toxic components of oil) dissolving into the water column from the surface slick. In general, the subsurface area swept by dissolved aromatics followed the same trajectory as the thickest surface oil, extending somewhat beyond the surface oil footprint to the west and east of the spill site. The peak volume of water exceeding 1 ppb of dissolved aromatics (a screening threshold for impacts on sensitive water column organisms) was 8.5 million m^3.

9.5 Conclusions

Based on the stochastic analysis, the bulk carrier spill in open water conditions (scenario 5A) had a high probability of causing shoreline oiling above the ecological threshold of 100 g/m^2, with 98% of trajectories reaching shore at some location. The highest probability of oiling is for shorelines to the south of the spill site along the mouth of upper Milne Inlet, and to the west-northwest on the shoreline of Pisiktarfik Island. However there are lower probabilities of shoreline oiling farther south into Milne Inlet, to the southwest along Tremblay Sound, to the north on Bylot Island, as far east as Emmerson Island, and to the north along the southern shorelines of Navy Board Inlet. In ice-covered conditions (scenario 5B), the probability of shoreline oiling is greatly reduced, with only 23% of trajectories reaching shore above the threshold during the simulation. However, oil trapped in ice for the winter may oil shorelines following the breakup of ice in the summer.

Peak volumes oil of ashore for both scenarios, on average, were relatively high, with 83% of the total volume spilled for scenario 5A, and 73% of the total volume spilled for scenario 5B. This is attributable to the very high viscosity of IFO 380, which makes it difficult to disperse and highly persistent. For the same spill volume, a spill of a heavier oil type like IFO 380 is more likely to oil shorelines and wildlife at sea than other oil types like crudes and light oils. In the stochastic analysis, the minimum time for oil to reach shore was about 5 hours in open water conditions (scenario 5A) and 15 hours in ice-covered conditions (scenario 5B), which could make for a challenging response effort.

IFO 380 does not readily entrain into the water column, and the volume of oil entrained in the water column was relatively low. On average, the peak volume of oil entrained in the water column in the stochastic analysis was less than 0.01% of the total volume spilled. Despite the low volume of oil entrained in the water column, there is still the potential for water column impacts from aromatics (the most toxic components of oil) dissolving into the water column from the surface slick. For the deterministic scenarios (which did not include the worst case for water column oiling), the volume of water exceeding 1 ppb of dissolved aromatics (a screening threshold for impacts on sensitive water column organisms) ranged between 2 million and 11 million m^3.

The persistence of IFO 380 on the water surface and shoreline was evident in the deterministic analysis. For all of the deterministic simulations of the bulk carrier spill, the maximum concentration of floating oil exceeded 10 g/m^2 (the threshold for impacts on birds and wildlife associated with the water surface) for the entire trajectory, and typically exceeded 100 g/m^2. An unmitigated bulk carrier spill of IFO 380 in this area could substantially impact biota associated with the water surface.

10.0 REFERENCES

Baffinland Iron Mines Corporation. 2015. Terms of Reference for the Social Impact Assessment: Baffinland Iron Mines Corporation Trans-Shipping of Iron Ore in Greenland Waters. March 2015. 73 pp.

Barone, M., A. Campanile, F. Caprio, and E. Fasano. 2007 The impact of new MARPOL regulations on Bulker design: A case study. In: *Proceedings of the 2nd International Conference on Marine Research and Transportation*, 10 pp.

Bentsen, M., G. Evensen, H. Drange, and A.D. Jenkins. 1999. Coordinate transformation on a sphere using conformal mapping. Monthly Weather Review 127: 2733–2740.

Bleck, R. 2002. An oceanic general circulation model framed in hybrid isopycnic-cartesian coordinates. Ocean Modelling 4: 55-88.

Boyer, T.P., J.I. Antonov, O.K. Baranova, C. Coleman, H.E. Garcia, A. Grodsky, D.R. Johnson, R.A. Locarnini, A.V. Mishonov, T.D. O'Brien, C.R. Paver, J.R. Reagan, D. Seidov, I.V. Smolyar, and M.M. Zweng. 2013. World Ocean Database 2013. Sydney Levitus, Ed.; Alexey Mishonov, Technical Ed.; NOAA Atlas NESDIS 72, 209 pp.

Cairn Energy. 2011. Oil Spill Prevention and Contingency Plan: Exploration Drilling Programme 2011 – Greenland. Report No. ED/GRL/RSK/29/10/2071. 214 pp.

Christensen, T., K. Falk, T. Boye, F. Ugarte, D. Boertmann, and A. Mosbech. 2012. Identifikation af sårbare marine områder i den grønlandske/danske del af Arktis. Aarhus Universitet, DCE – Nationalt Center for Miljø og Energi. 72 pp.

Curran, O. 2015. Shipping and Marine Wildlife Management Plan. BAF-PH1-830-P16-0024 Rev 5. Baffinland Iron Mines Corporation, Sustainable Development, Health, Safety & Environment. Appendix J10. 9 March 2015. 198 pp.

Dale, D. 2011a. Response Options Calculator (ROC) Users Guide. Genwest Systems, Inc. May 2011. 72 pp.

Dale, D. 2011b. Response Options Calculator (ROC) Technical Documentation. Genwest Systems, Inc. May 2011. 45 pp.

DeCola, E., T. Robertson, and S. Fletcher. 2006. Offshore Oil Spill Response in Dynamic Ice Conditions: A Report to WWF on Considerations for the Sakhalin II Project. Prepared for WWF UK and WWF Germany by Nuka Research and Planning Group LLC, Alaska, USA. 74 pp.

Det Norske Veritas. 2011. Ship Oil Spill Risk Models. Det Norske Veritas Project No. PP002916. Prepared for Australian Maritime Safety Authority. December 2011. 50 pp.

Drozdowski, A., S. Nudds, C.G. Hannah, H. Niu, I. Peterson, and W. Perrie. 2011. Review of oil spill trajectory modelling in the presence of ice. Canadian Technical Report of Hydrography and Ocean Sciences 274: vi + 84 pp.

Dyb, K., L. Thorsen, and L. Nielsen. 2012. Technical Report: Blowout Risk Evaluation in the Labrador Sea. Report No. AFT-2011-0444-02.3. March 2012.Prepared by Acona Flow Technology AS for Denmark Bureau of Minerals and Petroleum. 72 p.

Egbert, G.D. and S.Y. Erofeeva. 2002. Efficient inverse modeling of barotropic ocean tides. Journal of Atmospheric and Oceanic Technology, 19:183204.

Egevang, C., D. Boertmann, and O. Stenderup Kristensen. 2005. Monitering af havternebestanden på Kitsissunnguit (Grøne Ejland) og den sydlige del af Disko Bugt, 2002–2004. Teknisk rapport nr. 62. Pinngortitaleriffik, Grønlands Naturinstitut. 41 pp.

Etkin, D.S. 2012. Cook Inlet Maritime Risk Assessment: Spill Baseline and Accident Casualty Study – Spill Scenarios and Impacts. Prepared by Environmental Research Consulting and The Glosten Associates for Cook Inlet Risk Assessment, Anchorage, AK. March 2012. 142 pp.

Etkin, D.S., D. French McCay, N. Whittier, S. Subbayya, and J. Jennings. 2002. Modeling of response, socioeconomic, and natural resource damage costs for hypothetical oil spill scenarios in San Francisco Bay. In: *Proceedings of the 25th Arctic & Marine Oilspill Program (AMOP) Technical Seminar*: 1,075-1,102.

Etkin, D.S., and K. Michel. 2003. Bio-Economic Modeling of Oil Spills from Tanker/Freighter Groundings on Rock Pinnacles in San Francisco Bay. Vol. II: Spill Volume Report. Prepared for US Army Corps of Engineers, Sacramento District. Contract DACW07-01-C-0018). 42 p.

Evensen, G. 1994. Sequential data assimilation with nonlinear quasi-geostrophic model using Monte Carlo methods to forecast error statistics. Journal of Geophysical Research 99(10): 143-10,162.

Evers, K-U., K.R. Sørheim, and I. Singsaas. 2006. Oil Spill Contingency Planning in the Arctic: Recommendations. ARCOP Growth Project GRD2-2000-30112. Prepared by Hamburgische Schiffbay-Versuchsanstalt GmBH (HVSA), Hamburg, Germany, and SINTEF, Trondheim, Norway. 47 pp.

Fanneløp, T.K. and K. Sjøen. 1980. Hydrodynamics of underwater blowouts. AIAA 8th Aerospace Sciences Meeting, January 14-16, Pasadena, California. AIAA paper, pp. 80-0219.

Fingas, M. 2001. The Basics of Oil Spill Cleanup. Second Edition. Lewis Publishers, CRC Press LLC, Boca Raton, Florida. 233 pp.

Fingas, M. 2011. Physical Spill Countermeasures. In: *Oil Spill Science and Technology: Prevention, Response, and Cleanup*, edited by M. Fingas. Elsevier, Inc. pp. 303–338.

French, D., M. Reed, K. Jayko, S. Feng, H. Rines, S. Pavignano, T. Isaji, S. Puckett, A. Keller, F. W. French III, D. Gifford, J. McCue, G. Brown, E. MacDonald, J. Quirk, S. Natzke, R. Bishop, M. Welsh, M. Phillips and B.S. Ingram. 1996. The CERCLA type A natural resource damage assessment model for coastal and marine environments (NRDAM/CME), Technical Documentation, Vol. I-V. Final Report, submitted to the Office of Environmental

Policy and Compliance, U.S. Dept. of the Interior, Washington, DC. Available from National Technical Information Service, 5285 Port Royal Road, Springfield, VA 22161, PB96-501788.

French, D.P., H. Rines, and P. Masciangioli. 1997. Validation of an orimulsion spill fates model using observations from field test spills. In: *Proceedings of 20th Arctic and Marine Oil Spill Program (AMOP) Technical Seminar*. Vancouver, Canada, June 10-13, 1997, Emergencies Science Division, Environment Canada, Ottawa, ON, Canada, pp. 933-961.

French McCay, D.P. 2003. Development and Application of Damage Assessment Modeling: Example Assessment for the *North Cape* Oil Spill. Marine Pollution Bulletin 47(9-12): 341-359.

French McCay, D.P. 2004. Oil spill impact modeling: development and validation. Environmental Toxicology and Chemistry 23(10): 2441-2456.

French McCay, D.P. 2009. State-of-the-art and research needs for oil spill impact assessment modeling. In: *Proceedings of the 32nd AMOP Technical Seminar on Environmental Contamination and Response*, Emergencies Science Division, Environment Canada, Ottawa, ON, Canada, pp. 601-653.

French McCay, D.P., and J.J. Rowe. 2004. Evaluation of bird impacts in historical oil spill cases using the SIMAP oil spill model. In: *Proceedings of the 27th Arctic and Marine Oil Spill Program (AMOP) Technical Seminar*, Emergencies Science Division, Environment Canada, Ottawa, ON, Canada, pp. 421-452.

General Bathymetric Chart of the Oceans (GEBCO). 2009. Centenary Edition of the GEBCO Digital Atlas, published on behalf of the Intergovernmental Oceanographic Commission (IOC) and the International Hydrographic Organization (IHO) as part of the General Bathymetric Chart of the Oceans; British Oceanographic Data Centre (BODC), Liverpool.

General Bathymetric Chart of the Oceans (GEBCO). 2014. Gridded bathymetry data. <http://www.gebco.net/data_and_products/gridded_bathymetry_data/>

Hamilton, J., and Y. Wu. 2013. Synopsis and trends in the physical environment of Baffin Bay and Davis Strait. Canadian Technical Report of Hydrography and Ocean Sciences.

Herbert Engineering Corp. and Designers & Planners, Inc. 2003. Evaluation of Accidental Oil Spills from Bunker Tanks (Phase 1). Prepared for US Coast Guard Ship Structure Committee and Research, Washington, DC, and US Coast Guard Development Center, Groton, Connecticut. Report No. SSC-424. 54 pp.

Holand, P. 2013. Blowout and Well Release Characteristics and Frequencies, 2013. SINTEF Report F25705. SINTEF Technology and Society, Trondheim, Norway. 114 pp.

Hunke, E.C. and J.K. Dukowicz. 1997. An Elastic-Viscous-Plastic model for sea ice dynamics. Journal of Physical Oceanography 27: 1849-1867.

International Maritime Organization (IMO). 1995. Interim Guidelines for Approval of Alternative Methods of Design and Construction of Oil Tankers under Regulation 13F(5) of Annex I of MARPOL 73/78. Resolution MEPC.66(37). Adopted September 14, 1995.

Isaji, T., E. Howlett, C. Dalton, and E.L. Anderson. 2001a. Stepwise continuous-variable-rectangular grid hydrodynamics model. In: *Proceedings of the Twenty-fourth Arctic and Marine Oilspill Program (AMOP) Technical Seminar*, Edmonton (Alberta) Canada, pp. 597-610, June 12, 2001.

Isaji, T., E. Howlett, C. Dalton, and E.L. Anderson. 2001b. Stepwise continuous-variable-rectangular grid hydrodynamics model. In *Proceedings of the 7th International Conference on Estuarine and Coastal Modeling*, St. Pete Beach, FL, November 5-7, 2001.

IUCN and UNEP-WCMC. 2016. The World Database on Protected Areas (WDPA) [On-line]. Cambridge, UK: UNEP-WCMC. Available at: www.protectedplanet.net. Accessed June, 2016.

Joint Division for Investigation of Maritime Accidents & Bahamas Maritime Authority Report. 2008. Marine Accident Report: Quest Grounding on 27 June 2007. Danish Maritime Authority Case No. 200708695. Bahamas Maritime Authority Case No. 80011365/2007/5545/ 15 pp.

Jokuty, P., Whiticar, S., Wang, Z., Fingas, M., Fieldhouse, B., Lambert, P., Mullin, J. 1999. Properties of Crude Oils and Oil Products. Manuscript Report EE-165, Environmental Protection Service, Environment Canada, Ottawa, ON, Canada, 13pp. + appendices.

Khelifa, A and L. So. 2009. Effects of Chemical Dispersants on Oil-Brine Interfacial Tension and Droplet Formation. In: *Proceedings of the 32nd AMOP Technical Seminar on Environmental Contamination and Response*.

Konig Beatty, C.S. 2007. Arctic Landfast Sea Ice. PhD Thesis, Center for Atmosphere Ocean Science, Department of Mathematics, New York University.

Konig Beatty, C.S. 2012. Arctic Landfast Sea Ice 1953-1998. Version 1. Boulder, Colorado USA. NSIDC: National Snow and Ice Data Center. doi: http://dx.doi.org/10.7265/N5ZW1HV4.

Levitus, S. 1982. Climatological Atlas of the World Ocean, NOAA/ERL GFDL Professional Paper 13, Princeton, N.J., 173 pp. (NTISPB83-184093).

Mahoney, A.R., H. Eicken, L.H. Shapiro, R. Gens, T. Heinrichs, F.J. Meyer, and A. Graves Gaylord. 2012. Mapping and Characterization of Recurring Spring Leads and Landfast Ice in the Beaufort and Chukchi Seas. U.S. Dept. of the Interior, Bureau of Ocean Energy Management, Alaska Region, Anchorage, AK. OCS Study BOEM 2012-067. 179 pp.

Mariport Group Ltd. 2012. Arctic Shipping Developments for World Wildlife Canada. Prepared for World Wildlife Fund Canada, by The Mariport Group, Ltd., Digby, Nova Scotia, Canada. 72 pp.

McDougall, T.J. 1978. Bubble plumes in stratified environments. Journal of Fluid Mechanics 85(4): 655-672.

Melling, H., Y. Grattno, and G. Ingram. 2001. Ocean circulation within the North Water Polynya of Baffin Bay. Atmosphere-Ocean 39(3): 301-325. DOI: 10.1080/07055900.2001.9649683.

Michel, K., and T.S. Winslow. 1999. Cargo ship bunker tanks: Designing to mitigate oil spillage. Society for Naval Architects and Marine Engineers (SNAME) Joint California Sections Meeting. 14 May 1999. 13 pp.

Michel, K., and T.S. Winslow. 2000. Cargo ship bunker tanks: Designing to mitigate oil spillage. Marine Technology 37(4): 191-199.

Mosbech, A., D. Boertmann, and M. Jespersen. 2007. Strategic Environmental Impact Assessment of Hydrocarbon Activities in the Disko West Area. National Environmental Research Institute, University of Aarhus, Denmark. NERI Technical Report No. 618. 192 p.

Mueller, H., Y. Gratton, and G. Ingram. 2010. Ocean circulation within the North Water polynya of Baffin Bay. Atmosphere-Ocean 39(3): 301-325. DOI:10.1080/07055900.2001.9649683

Münchow, A., K.K. Falkner, and H. Melling. 2013. Baffin Island and West Greenland Current systems in the Northern Baffin Bay. Preprint submitted to Progress in Oceanography.

National Research Council (NRC). 1998. Double-Hull Tanker Legislation: An Assessment of the Oil Pollution Act of 1990. National Academy Press, Washington, DC. 266 pp.

National Research Council (NRC). 2001. Environmental Performance of Tanker Designs in Collision and Grounding: Method for Comparison. National Academies Marine Board/Transportation Research Board Special Report No. 259. National Academy Press, Washington, DC. 136 pp., plus appendices.

Nuka Research and Planning Group. 2014. Estimating an Oil Spill Response Gap for the US Arctic Ocean. Prepared for US Bureau of Safety and Environmental Enforcement (BSEE), US Department of the Interior (Contract E13PC00024), by Nuka Research and Planning Group LLC, Alaska, USA.86 p.

Owen, A. 1980. A three-dimensional model of the Bristol Channel. Journal of Physical Oceanography 10: 1290-1302.

Perry, J. and R. Bright. 2010. Capricorn Greenland Exploration 1: Capricorn Sigguk Exploration Drilling Environmental Impact Assessment Exploration Drilling Programme, Sigguk Block, Disko West, Greenland. Prepared by Environmental Resources Management Ltd. for Cairn Energy. Reference No. 0108885. March 2010. 501 p.

Peterson, I.K., S. Prinsenberg, and J.S. Holladay. 2008. Observations of sea ice thickness, surface roughness and ice motion in Amundsen Gulf. Journal of Geophysical Research (113) doi: 10.1029/2007JC004456.

Rawson, C., K. Crake, and A. Brown. 1998. Assessing the environmental performance of tankers in accidental grounding and collision. SNAME Transactions Vol. 106: 41-58.

Reed, M., D.P. French, S.Feng, F.W. French III, E. Howlett, K, Jayko, W.Knauss, J. McCue, S. Pavignano, S. Puckett, H. Rines, R. Bishop, M. Welsh, and J. Press. 1996. The CERCLA type A natural resource damage assessment model for the Great Lakes environments (NRDAM/GLE), Vol. I-III. Final report, submitted to Office of Environmental Policy and Compliance, U.S. Department of the Interior, Washington, DC, by Applied Science Associates, Inc., Narragansett, RI, April 1996, Contract No. 14-01-0001-88-C-27.

Sadler, H.E. 1976. Water, heat, and salt transports through Nares Strait, Ellesmere Island. Journal of the Fisheries Research Board of Canada 33: 2286–2295.

Sakov, P., F. Counillon, L. Bertino, K.A. Lisaeter, P.R. Oke, and A Korablev. 2012. TOPAZ4: an ocean-sea ice data assimilation system for the North Atlantic and Arctic. Ocean Sci. 8: 633–656.

Samuelson, A. and L. Bertino. 2013. Lofoten and versteralen currents, Mid-term Report. NERSC Technical Report no. 312. Nansen Environmental and Remote Sensing Center.

Schroeder Gearon, M., D. French McCay, E. Chaite, S. Zamorski, D. Reich, J. Rowe, and D.S. Etkin. 2014. SIMAP Modelling of hypothetical oil spills in the Beaufort Sea for World Wildlife Fund. RPS ASA report for WWF-Canada, Canadian Arctic Program. 310 pp.

Sørstrøm, S.E., P.J. Brandvik, I. Buist, P. Daling, D. Dickins, L.G. Faksness, S. Potter, J. Fritt Rasmussen, and I. Singsaas. 2010. Joint industry program on oil spill contingency for Arctic and ice covered waters. SINTEF report.

Spaulding, M.L. 1982. User's manual for a simple gas blowout plume model. Continental Shelf Institute, Trondheim, Norway.

Spaulding, M.L. 1988. A state-of-the-art review of oil spill trajectory and fate modelling. Oil and Chemical Pollution (4): 39-55.

Speer, L., and T.L. Laughlin. 2011. IUCN/NRDC Workshop to Identify Areas of Ecological and Biological Significance or Vulnerability in the Arctic Marine Environment: Workshop Report. 40 pp.

Steiner, R. 2011. Review of Cairn Oil Spill Prevention and Contingency Plan (OSCP), Exploration Drilling Programme – 2011 Greenland. 7 pp.

Sterling, I. 1980. The biological importance of polynyas in the Canadian Arctic. Arctic 33(2): 303-315.

Tang, C.C.L., C.K. Ross, T. Yao, B. Petrie, B.M. DeTracey, and E. Dunlap. 2004. The circulation, water masses and sea-ice of Baffin Bay. Bedford Institute of Oceanography, Ocean Sciences Division, Fisheries and Oceans Canada.

Valeur, H.H., C. Hansen, K.Q. Hansen, L. Rasmussen, and N. Thingvad. 1996. Weather, sea and ice conditions in eastern Baffin Bay, offshore northwest Greenland, a review. Danish Meteorological Institute Technical Report, Number 96-12.

Venkatesh, S., H. El-Tahan, G. Comfort, and R. Abdelnour. 1990. Modelling the behaviour of oil spills in ice-infested waters. Atmosphere-Ocean. Canadian Meteorological and Oceanographic Society 28(3): 303-329.

Yapa, P.D., L. Zheng, and F.H. Chen. 2001. A model for deepwater oil/gas blowouts. Marine Pollution Bulletin 43: 234–241.

Yip, T.L., W.K. Talley, and D. Jin. 2011. The effectiveness of double hulls in reducing vessel-accident oil spillage. Marine Pollution Bulletin 62(11): 2,427-2,432.

APPENDIX A

Appendix A: Modeling Oil Spill Trajectories in Baffin Bay and Lancaster Sound:

Spill Scenario Development
Spill Probability Analysis
Spill Response Development

Final Report

Prepared by:

Dagmar Schmidt Etkin, PhD
Environmental Research Consulting
41 Croft Lane
Cortlandt Manor, NY 10567-1160

Submitted to:

Danielle Ameen Reich
Shoal's Edge Consulting

Paul Crowley, Vice-President, Arctic
WWF-Canada

13 June 2016

WWF®

ENVIRONMENTAL RESEARCH CONSULTING

Contents

Contents **1**

List of Figures **2**

List of Tables **3**

Executive Summary **4**

Part I: Spill Scenario Development **7**

Melville Bay Well Blowout Scenarios 7
Baffin Bay Well Blowouts 10
Cruise Ship Spill along West Greenland Coast 12
Product Tanker Spill in Lancaster Sound 16
Bulk Carrier Spills in Eclipse Sound 18
Summary of Spill Scenarios 21

Part II: Spill Probability Analysis: Well Blowouts **22**

Historical Well Blowouts 22
Probabilities of Well Blowouts 23
Benchmarking of Blowout Flow Rates 25
Benchmarking of Blowout Durations 26
Benchmarking of Total Blowout Volumes 28
Conclusions on Well Blowout Probabilities 29

Part III: Spill Probability Analysis: Vessel Spills **31**

Cruise Ship Scenario 31
Product Tanker Scenario 32
Bulk Carrier Scenarios 33
Overall Conclusions on Vessel Spill Probabilities 33

Part IV: Spill Response Development **35**

SIMAP Response Modeling Basics 35
Overall Daily Surface Operational Assumptions (Cases 1A and 1B) 35
Parameters and Thresholds for Mechanical Response (Cases 1A and 1B) 36
Parameters and Thresholds for Surface Dispersant Response (Cases 1A and 1B) 39
Parameters and Thresholds for *In Situ* Burning Response (Cases 1A and 1B) 40
Sub-Surface Dispersant Operations (Case 2B) 41
Summary of Spill Response Scenarios 42

References **44**

List of Figures

Figure 1: Site Selected for Hypothetical Well Blowout Scenarios in Melville Bay 8
Figure 2: Oil Exploration Blocks in Baffin Bay 8
Figure 3: Resource Areas of Concern in Melville Bay 9
Figure 4: Site Selected for Hypothetical Well Blowout Scenarios in Baffin Bay 11
Figure 5: Hypothetical Cruise Ship Spill Location off Disko Island 13
Figure 6: Map of Cruise Destinations near Disko Island 13
Figure 7: Resource Areas of Concern near Disko Bay 14
Figure 8: IUCN Environmentally or Biologically Significant Marine Areas Showing Disko Bay 15
Figure 9: Crystal Serenity Cruise Ship 16
Figure 10: Location for Hypothetical Product Tanker Spill in Lancaster Sound 17
Figure 11: T/V Maria Desgagnés 17
Figure 12: Tank Configuration in T/V Maria Desgagnés 18
Figure 13: Location of Hypothetical Spill Site near Milne Inlet (Cases 5A and 5B) 18
Figure 14: Shipping Routes to Milne Port, Baffinland Mines 19
Figure 15: Iron Ore Bulk Carrier Proposed for Trans-Shipping from Baffinland Mines 20
Figure 16: Configuration of Iron Ore Carrier Proposed for Trans-Shipping from Baffinland Mines 20
Figure 17: Blowout Flow Rate Benchmarking 26
Figure 18: Benchmarking of Blowout Durations 28
Figure 19: Total Blowout Volume Benchmarking 28
Figure 20: Cairn Blocks for 2011 Exploration 30
Figure 21: Nearshore and Offshore Response Operation Zones 37
Figure 22: Expected Operational Limits of Spill Response by Ice Coverage 37
Figure 23: Factors that Affect Skimmer Efficiency 38

List of Tables

Table 1: Summary of Hypothetical Oil Spill Scenarios for Modeling 4
Table 2: Summary of Inputs and Assumptions for Spill Response Modeling 6
Table 3: Basic Spill Scenarios for Development..... 7
Table 4: Summary of Hypothetical Oil Spill Scenarios for Modeling 21
Table 5: Largest Historical Offshore Well Blowouts 22
Table 6: Summary of Hypothetical Well Blowout Scenarios for Modeling..... 23
Table 7: Estimates of Probabilities of Well Blowouts..... 24
Table 8: Spill Volume Distribution of US Oil Well Blowouts 24
Table 9: Reported Blowout Flow Rates for Benchmarking..... 25
Table 10: Distribution Blowout/Well Release Duration until Natural Bridging..... 27
Table 11: Blowout Durations Relative to Ixtoc I and Macondo MC-252..... 27
Table 12: Total Blowout Volumes Relative to Largest Incidents 29
Table 13: Summary of Hypothetical Vessel Oil Spill Scenarios for Modeling 31
Table 14: Summary of Inputs and Assumptions for Spill Response Modeling 42

Modeling Oil Spill Trajectories in Baffin Bay and Lancaster Sound: Spill Scenario Development, Spill Probability Analysis, and Spill Response Development

Executive Summary

Eight scenarios were developed to analyze the oil trajectories, fates, and effects of hypothetical oil spills in the western and eastern parts of Baffin Bay and Lancaster Sound. The scenarios selected are summarized in Table 1. The scenarios were selected and defined to represent scenarios from offshore oil activity and vessels. The specific parameters of each spill were based on oil types and volumes that reasonably represented credible spill scenarios. The locations and seasons were selected for both credibility and in relation to effects on particularly sensitive environmental resources that had been identified.

Table 1: Summary of Hypothetical Oil Spill Scenarios for Modeling

Case #	Location	Spill Source	Oil Type	Spill Rate	Spill Duration (days)	Volume (m^3)	Season(s)
1A	Melville Bay license areas	Exploratory Well Blowout	Medium Crude	3,340 m^3/day	1	3,340	Open water: July to October
1B				3,340 m^3/day	34	113,560	
2A	Baffin Bay license areas (entrance to Lancaster Sound)	Exploratory Well Blowout	Medium Crude	3,340 m^3/day	1	3,340	Open water: June to October
2B				3,340 m^3/day	34	113,560	
3	Greenland coast Off Disko Island	Cruise Ship 68,000 GT IFO 180: 2,800 m^3	IFO 180	-	0.5	280	Cruise Season: July to September
4	Lancaster Sound	Product Tanker ≈13,000 DWT Arctic Diesel: 15,000 m^3	Arctic Diesel	-	0.5	2,400	Open water: June to September
5A	Eclipse Sound Milne Inlet	Bulk Carrier 85,000 DWT Polar Class 4 Panamax IFO 380: 6,250 m^3	IFO 380	-	0.5	1,000	Open water: August to October
5B							Ice: June 25 to July 31; Nov. 1 to March 7

A comprehensive analysis of the probability of the selected spill scenarios, or of spills in general in this region, was outside the scope of the study. However, a brief analysis of probabilities was conducted to provide a perspective on risk. Since major oil spills are relatively infrequent events, the probability that a

major spill would happen in any of these locations is very low. This analysis did not determine the probability that the specific scenario (i.e., incident location and circumstances) would occur, but rather the probability that a spill of this type could occur in the region of the study.

The scenarios were benchmarked against other historical incidents for comparison. The well blowout scenarios modeled represent relatively extreme cases. The larger of the hypothetical blowout scenarios (34 days of flow for a total of 113,560 m^3) would be the fourth largest well blowout ever worldwide, based on current records. Only 0.5% of blowouts have ever been of this size or larger. The smaller scenario – 1 day of flow for a total of 3,340 m^3 – would be the 15th largest incident worldwide. Only 2% of blowouts have ever been this size or larger. Both of these scenarios represent relatively extreme volumes for blowouts. The probability that there would be a well blowout of 113,560 m^3 from any particular well is about 1 in 60,000 to 1 in 1.6 million (0.000000625 to 0.000017). If one assumes that there are a total of about 15 wells in the blocks in total, the probability would increase to 1 in 4,000 to 1 in 107,000 (0.0000094 to 0.00025).

The probability of a cruise ship spill is about 1 in 122 to 1 in 1,013 per year. This probability is based only on current cruise vessel traffic. Increased cruise ship traffic could change probabilities.

The probability of a product tanker spill is estimated to be about 1 in 3,086, based on current tanker traffic supplying Arctic communities and mining operations. This may increase to 1 in 1,736 by the year 2030, based on traffic projections.[1] The probability of a bunker spill from a bulk carrier spill is about 1 in 35,000.

Any increases in vessel traffic may increase these probabilities.[2] Likewise, decreases in traffic may reduce probabilities. Specific navigational hazards and extreme weather conditions in the region may increase these probabilities. Changes in vessel routes may also change probabilities.

Note that the probabilities of spills may not necessarily be for the volume selected for modeling.

To evaluate the potential effectiveness of oil spill response operations, three well blowout scenarios were selected for simulations (modeling) of response operations – two with a three-pronged approach to on-water response (mechanical containment and recovery, surface dispersants, and *in situ* burning), and one with sub-surface dispersants. The input parameters and assumptions for spill response applied in the modeling are summarized in Table 2.

[1] Mariport Group Ltd. 2012.
[2] Étienne et al. 2013.

Table 2: Summary of Inputs and Assumptions for Spill Response Modeling				
Response Strategy	**Input or Assumption[3]**	**Scenario**		
		Case 1A	**Case 1B**	**Case 2B**
		Melville Bay 1-day blowout of 3,340 m^3/day	**Melville Bay 34-day blowout of 3,340 m^3/day**	**Baffin Bay 34-day blowout of 3,340 m^3/day**
Mechanical Containment & Recovery	**Maximum Wind Speed**	55.6 km/h (30 kts)	55.6 km/h (30 kts)	--
	Maximum Current Speed	0.36 m/s (0.7 kts)	0.36 m/s (0.7 kts)	--
	Sea State (Max. Wave Height)	1.07 meters	1.07 meters	--
	Ice Coverage	<20%	<20%	--
	Minimum Oil Thickness	8 µm	8 µm	--
	Max. Oil Viscosity- Offshore	15,000 cP	15,000 cP	--
	Max. Oil Viscosity- Nearshore	80 cP	80 cP	--
	Daily Removal - Offshore	90 m^3	90 m^3	--
	Daily Removal - Nearshore	30 m^3	30 m^3	--
	Arctic Conditions Adjustment	62.5%	62.5%	--
Surface Dispersants	**Dispersant:Oil Ratio**	1:20	1:20	--
	Daily Oil Treated	888 m^3	888 m^3	--
	Maximum Oil Viscosity	20,000 cP	20,000 cP	--
	Minimum Oil Thickness	8 µm	8 µm	--
	Minimum Wind Speed	5.6 km/h (3.0 kts)	5.6 km/h (3.0 kts)	--
	Maximum Wind Speed	50 km/h (27 kts)	50 km/h (27 kts)	--
	Ice Coverage	<30%	<30%	--
	Arctic Conditions Adjustment	62.5%	62.5%	--
	Minimum Water Depth	10 meters	10 meters	--
	On-Scene Response Time	48 hours after spill	48 hours	--
In Situ Burning	**Maximum Water Content**	60%	60%	--
	Minimum Oil Thickness	8 µm	8 µm	--
	Maximum Wind Speed	55.6 km/h (30 kts)	55.6 km/h (30 kts)	--
	Sea State (Max. Wave Height)	0.3 meters	0.3 meters	--
	Maximum Current Speed	0.36 m/s (0.7 kts)	0.36 m/s (0.7 kts)	--
	Ice Coverage	<30%, >70%	<30%, >70%	--
	Distance from Shore	10 km	10 km	--
	Daily Oil Burned	878 m^3	878 m^3	--
	Arctic Conditions Adjustment	62.5%	62.5%	--
Subsurface Dispersants	**Dispersant:Oil Ratio**	--	--	1:100
	Daily Application	--	--	33.4 m^3
	On-Scene Response Time	--	--	72 hours

[3] Daily removals shown are theoretical maximum removal rates before the application of the Arctic condition adjustment factor.

Part I: Spill Scenario Development

To determine the trajectory, fate, and effects of hypothetical oil spill scenarios in Baffin Bay and Lancaster Sound, and to evaluate the potential effectiveness of response measures to mitigate environmental damages, scenarios needed to be selected and developed for further analysis. The goals were to establish credible scenarios for these regions that would adequately represent the range of oil types, spill volumes, locations, and seasonal timing that may reasonably be expected in Baffin Bay and Lancaster Sound.

Working with representatives from WWF-Canada, WWF-Denmark, Greenland Institute of Natural Resources, Greenland Department of Environment and Mineral Resources, Transport Canada, Qikiqtani Inuit Association, Baffinland Mines, and other interested stakeholders, a total of eight scenarios (outlined in Table 3) were developed to represent the five base cases requested by WWF-Canada.

Table 3: Basic Spill Scenarios for Development

Case #	Location	Spill Type	# of Oil Types	# of Spill Volumes/ Durations	# of Seasons	Total # of Scenarios
1	Melville Bay license areas	Subsurface blowout	1	2	1	2
2	Baffin Bay license areas (near entrance of Lancaster Sound)	Subsurface blowout	1	2	1	2
3	Greenland coast off Disko Island	Surface spill (cruise ship grounding)	1	1	1	1
4	Lancaster Sound	Surface spill (product tanker)	1	1	1	1
5	Eclipse Sound	Surface spill (bulk carrier)	1	1	2	2
TOTAL						**8**

Melville Bay Well Blowout Scenarios

The two Melville Bay, Greenland, well blowout scenarios (Case 1A and Case 1B) – two volumes with one oil type in one season – were developed for modeling.

Location: The site selected for the hypothetical well blowouts in Melville Bay was within Pitu Block (also called Block 6) in Cairn Energy's exploration license areas, as shown in Figure 1 and Figure 2. The specific location was: latitude 75.231740, longitude -60.645321 (decimal degrees).

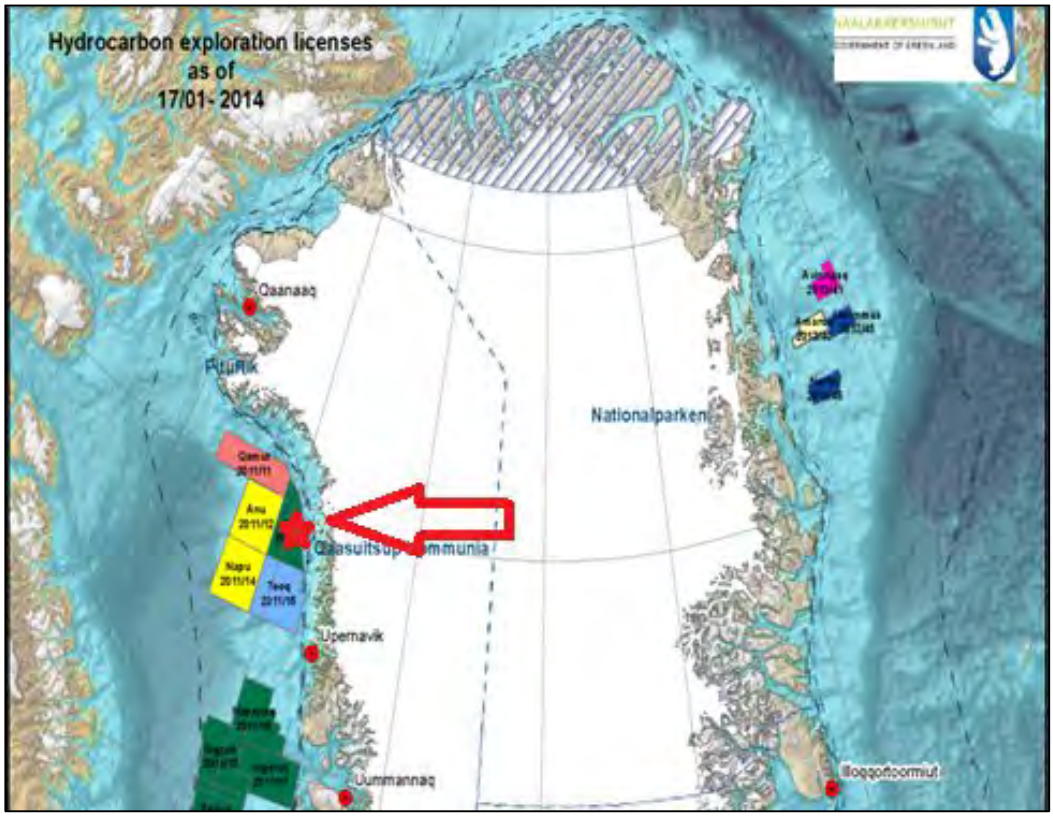

Figure 1: Site Selected for Hypothetical Well Blowout Scenarios in Melville Bay

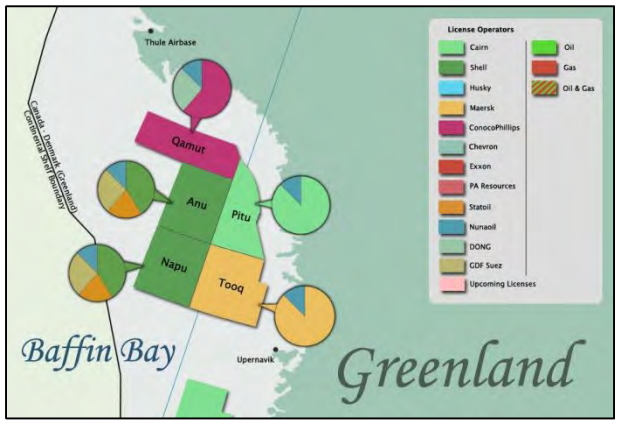

Figure 2: Oil Exploration Blocks in Baffin Bay

The site was selected to be within Cairn Energy's license area for credibility as a potential blowout location, but also because of its relative proximity to shore and to several sensitive resources of concern to stakeholders, particularly the Priority 1 region North Water Polynya (shown as V1 in Figure 3), and the Melville Bay Nature Preserve (shown as V2 in Figure 3). The latter is protected because of its importance as a habitat for polar bears, narwhal, and beluga.

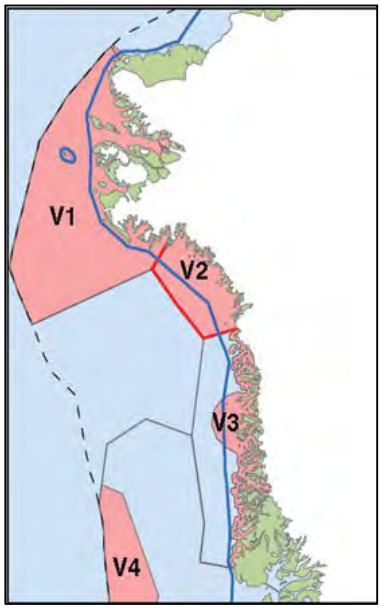

Figure 3: Resource Areas of Concern in Melville Bay

Season: The season defined for the scenarios was open water. The season is based on analysis of average monthly ice coverage data from TOPAZ at the spill site (2011-2015). Average ice cover of less than 30% was defined as "open water." This corresponded to July through October. [See Figure 18 in main report.]

Oil Type: The oil type selected was similar to Statfjord (medium) crude (886.3 kg/m^3, 28.25 °API), which is a crude oil that represents the characteristics of crudes found in other exploration wells in the region.[4] The precise characteristics of crude oil from a particular well can only be known after direct sampling from that well, which is not possible in this case, as the Pitu Block has not yet been explored or developed.

Flow rate: The rate of flow from a particular well is dependent on the characteristics of the well itself, particularly the reservoir pressure, but also the type of well (development, exploratory, etc.). The actual flow rate of a well can often not be predicted in advance and will be determined only when the actual well is drilled. Flow rates can vary during the course of oil extraction, including variations in the amount of crude oil versus water or brine in the flow. The flow rates that are described for wells are generally the *average* flow rate. [*A more complete discussion of flow rates, including benchmarking of the flow rates selected for this analysis, are included in Part II of this report.*]

The flow rate assumed for the modeling of the hypothetical well blowouts from the Pitu Block was 3,340 m^3 per day, which corresponds to 21,008 barrels (bbl) per day. These flow rates were assumed in other studies conducted in the region, [5] and were deemed to be reasonable approximations of the magnitude of flow rate that might be expected for a well in this license area.

[4] Based on Mosbech et al. 2007; Perry and Bright 2010.
[5] Mosbech et al. 2007; Perry and Bright 2010.

Duration of flow: Given an [average] flow rate for a particular well, the total volume will depend on the duration of flow – the length of time that the well continues to release crude oil to the environment. The duration of flow is determined by the length of time that it takes for the well to either bridge naturally (fill in with enough sediment to naturally stop flowing without any human intervention), to be capped and contained, or to be intercepted by a relief well(s) to stop the flow. [*A more complete discussion of durations of flow, including benchmarking of the durations assumed for this analysis, are included in Part II of this report.*]

In the case of the Pitu Block well blowout scenarios, two durations of flow were assumed. The first assumed that there would be natural bridging that occurs within one day; the second assumed that a relief well operation successfully stopped the flow at the end of the 34th day of flow, as per the Cairn Oil Spill Contingency Plan (OSCP).[6,7] For these scenarios, capping and containment was not considered. Generally, as explained further in Part II of this report, relief well operations take longer than capping and containment operations, and would represent the worst case with respect to flow duration and ultimate spill volume.

The two flow durations that were assumed differentiated the two scenarios or cases for the Melville Bay blowouts:

- **Case 1A:** 3,340 m^3 per day for 1 day (natural bridging)[8] for a total of 3,340 m^3 (21,008 bbl) spilled; and
- **Case 1B:** 3,340 m^3 per day for 34 days (relief well)[9] for a total of 113,560 m^3 (714,271 bbl) spilled.

Baffin Bay Well Blowouts

Two scenarios (Case 2A and Case 2B) were developed for the Baffin Bay license area – two spill volumes of the same oil type, in one season.

Location: The location selected for the Baffin Bay scenario was at the entrance to Lancaster Sound near the Hope Structure (Figure 4). The precise location was: latitude 74.401196, longitude -77.467675 (decimal degrees). This location is in the Shell license area and close to the Hope Structure, which is at the entrance to Lancaster Sound. The location was selected with respect to credibility as being in the Shell license area, as well as being near an upwelling feature near the mouth of Lancaster Sound, which was mentioned by some stakeholders as being of concern with respect to the way in which the spilled oil might be transported.[10]

---

[6] Based on the Cairn Energy Oil Spill Contingency Plan 2011 (Cairn Energy 2011).
[7] The Cairn Oil Spill Contingency Plan (Cairn Energy, 2011) was developed for activities in a different license area of West Greenland, located well to the south of Pitu Block. However, it is the best available information, as no contingency plans are currently available for the Pitu Block area.
[8] Based on the Cairn Energy Oil Spill Contingency Plan 2011 (Cairn Energy 2011).
[9] Based on the Cairn Energy Oil Spill Contingency Plan 2011 (Cairn Energy 2011).
[10] Shell announced June 8, 2016 that it was relinquishing its exploration permits for this license area. The permits were relinquished to the Nature Conservancy of Canada for use in marine conservation efforts in the Arctic (http://www.cbc.ca/news/canada/north/shell-lancaster-sound-permits-1.3620681).

Season: The season defined for the scenarios was open water. The season is based on analysis of average monthly ice coverage data from TOPAZ at the spill site (2011-2015). Average ice cover of less than 30% was defined as "open water." This corresponded to June through October for the Baffin Bay area. [See Figure 45 in main report.]

Oil Type: The oil type selected was similar to Statfjord (medium) crude (886.3 kg/m^3, 28.25 °API), which is a crude oil that represents the characteristics of crudes found in other exploration wells in the region.[11] The precise characteristics of crude oil from a particular well can only be known after direct sampling from that well, which is not possible in this case, as the license area has not yet been explored or developed.

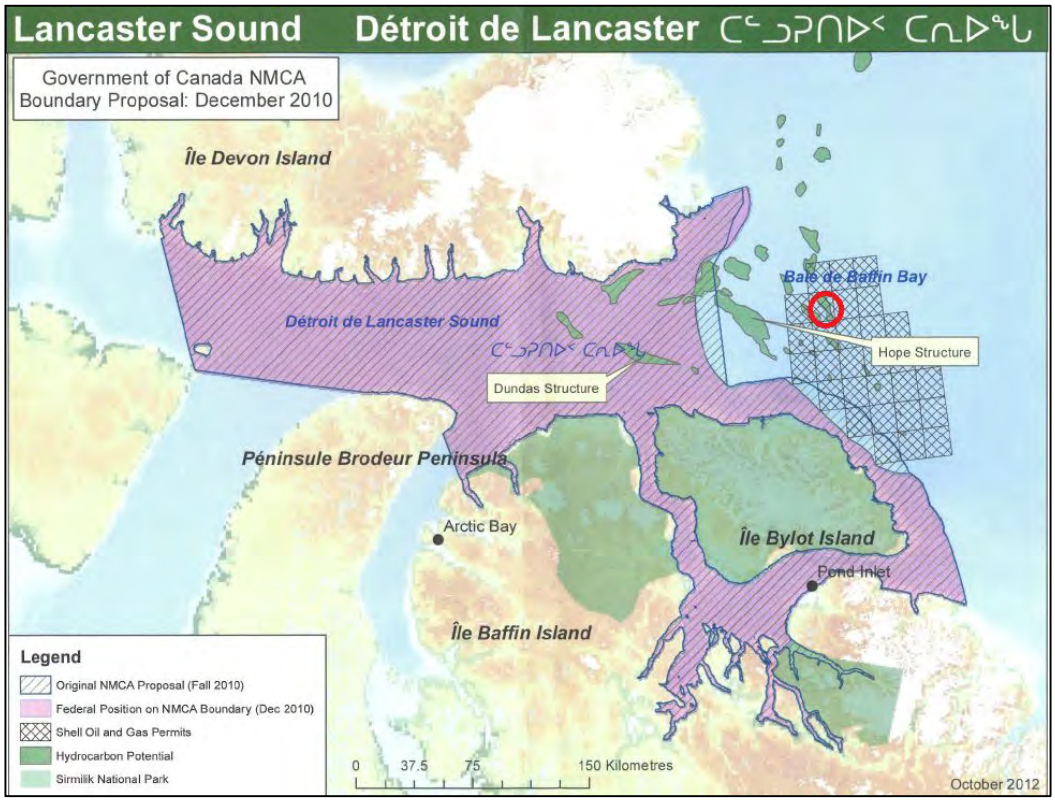

Figure 4: Site Selected for Hypothetical Well Blowout Scenarios in Baffin Bay

Flow rate: The rate of flow from a particular well is dependent on the characteristics of the well itself, particularly the reservoir pressure, but also the type of well (development, exploratory, etc.). The actual flow rate of a well can often not be predicted in advance and will be determined only when the actual well is drilled. Flow rates can vary during the course of oil extraction, including variations in the amount of crude oil versus water or brine in the flow. The flow rates that are described for wells are generally the *average* flow rate. [*A more complete discussion of flow rates, including benchmarking of the flow rates selected for this analysis, are included in Part II of this report.*]

[11] Based on Mosbech et al. 2007; Perry and Bright 2010.

The flow rate assumed for the modeling of the hypothetical well blowouts from the Baffin Bay well was 3,340 m^3 per day, which corresponds to 21,008 barrels (bbl) per day. These flow rates were assumed in other studies conducted in the region, [12] and were deemed to be reasonable approximations of the magnitude of flow rate that might be expected for a well in this license area.

Duration of flow: Given an [average] flow rate for a particular well, the total volume will depend on the duration of flow – the length of time that the well continues to release crude oil to the environment. The duration of flow is determined by the length of time that it takes for the well to either bridge naturally (fill in with enough sediment to naturally stop flowing without any human intervention), to be capped and contained, or to be intercepted by a relief well(s) to stop the flow. [*A more complete discussion of durations of flow, including benchmarking of the durations assumed for this analysis, are included in Part II of this report.*]

In the case of the Baffin Bay well blowout scenarios, two durations of flow were assumed. The first assumed that there would be natural bridging that occurs within one day; the second assumed that a relief well operation successfully stopped the flow at the end of the 34th day of flow. For these scenarios, capping and containment was not considered. Generally, as explained further in Part II of this report, relief well operations take longer than capping and containment operations, and would represent the worst case with respect to flow duration and ultimate spill volume.

The two flow durations that were assumed differentiated the two scenarios or cases for the Baffin Bay blowouts:

- **Case 2A:** 3,340 m^3 per day for 1 day (natural bridging)[13] for a total of 3,340 m^3 (21,008 bbl) spilled; and
- **Case 2B:** 3,340 m^3 per day for 34 days (relief well)[14] for a total of 113,560 m^3 (714,271 bbl) spilled.

Cruise Ship Spill along West Greenland Coast

One scenario (Case 3) was developed for the Greenland coast near Disko Island to simulate a hypothetical spill from a large cruise ship.

Location: The selected location for the cruise ship spill was off Disko Island in Disko Bay at: latitude 69.074430, longitude -53.500040 (decimal degrees), as shown in Figure 5. The site was selected because of its credibility as one at which a cruise ship might have an accidental spill, as this is a popular route for cruise ships (Figure 6). The specific location was chosen as it is near the shipping lane and has rock pinnacles that would typically be locations at which a grounding accident might occur. The location is about 15 km south of the location of the Quest grounding in June 2007.[15] The master of the Quest took the vessel off-course in that case to allow the small number of passengers to view icebergs and whales. That vessel was also smaller than the larger cruise ship being considered in this scenario. A larger cruise ship is less likely to *deliberately* go off course.

[12] Mosbech et al. 2007; Perry and Bright 2010.
[13] Based on the Cairn Energy Oil Spill Contingency Plan 2011.
[14] Based on the Cairn Energy Oil Spill Contingency Plan 2011.
[15] Joint Division for Investigation of Maritime Accidents et al. 2008.

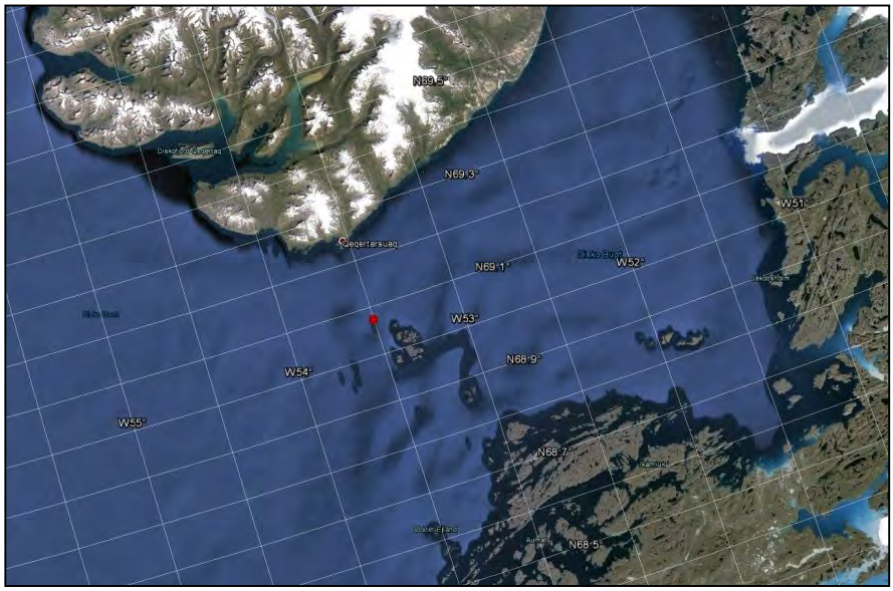

Figure 5: Hypothetical Cruise Ship Spill Location off Disko Island

Figure 6: Map of Cruise Destinations near Disko Island[16]

[16] http://diskoline.dk/en/

The location was also selected as one that could potentially cause impacts to sensitive areas outside of Disko Bay that are of particular concern with respect to potential impacts to marine mammals in the event of a spill.

In addition, the selected modeling site also has particular significance with respect to ecological sensitivity. It is within the Priority 1 marine area in Disko Bay and Store Hellefiskebanke.[17] The region is a hotspot for tourism, whale spotting, seabird colonies, and an important fishery for Greenland halibut. In addition, the islands of Grønne Ejeland/Kitsissunnguit (V5 in Figure 7) are protected by law because of their status as an important site for Arctic tern.[18] The Disko Bay area has also been named a potential Super-EBSA by the IUCN[19] (Figure 8).

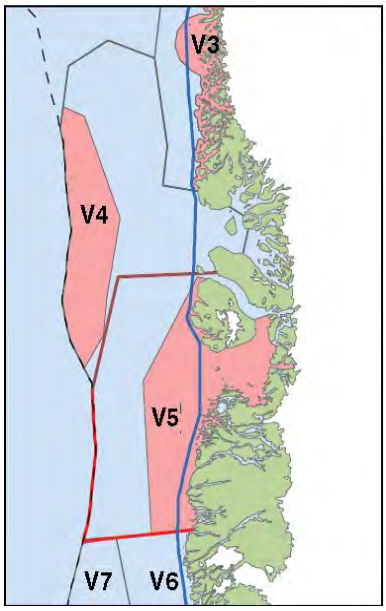

Figure 7: Resource Areas of Concern near Disko Bay

The area is an important recruitment area for shrimp and sand eels, an important forage fish for seals and whales. It is a vital wintering area for king eider (more than 50% of the flyway populations), common eider, and thick-billed murre, as well as other seabirds. It includes a very large colony of Arctic tern (over 20,000 pairs). The area serves as a key wintering area for IUCN red-listed species including bowhead and beluga whales and narwhal. There is a significant concentration of bearded seals on the ice at Store Hellefiskebanke and winter occurrences of walrus and seals, making the area an important hunting area. In addition, the shrimp and Greenland halibut fisheries in this area are quite important to the Greenland economy. Recent unpublished information indicates that the entire area between Disko Bay, south to Cape Farewell and west to the mouth of Hudson Strait, appears to be a winter hotspot for seabirds.[20]

[17] Christensen et al. 2012.
[18] Egevang et al. 2005.
[19] Ecologically or biologically significant marine areas.
[20] Speer and Laughlin 2011.

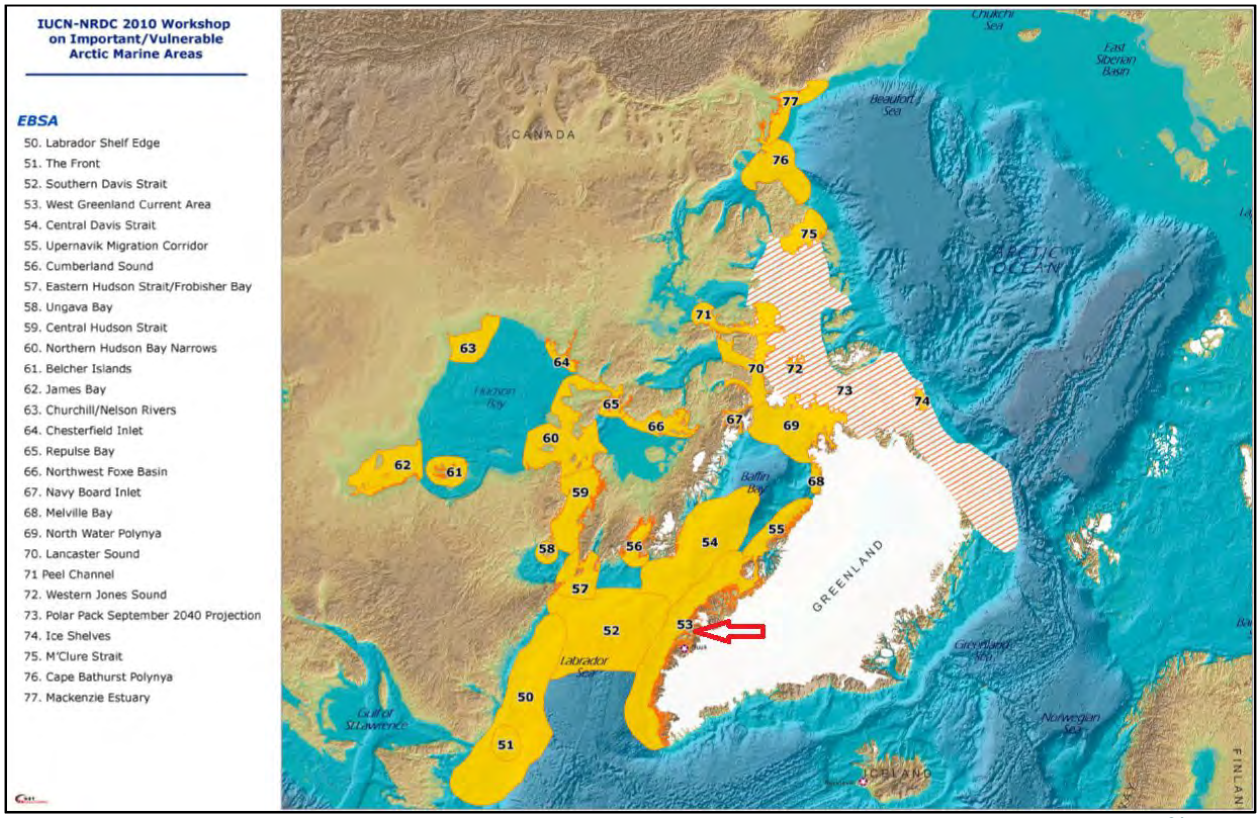

Figure 8: IUCN Environmentally or Biologically Significant Marine Areas Showing Disko Bay[21]

Season: The season defined for the hypothetical cruise ship spill scenario was July through September, which corresponds with the scheduled cruises through Disko Bay to Ilulissat.[22] This time period also corresponds to open water conditions. [See Figure 71 in main report.]

Oil Type: The oil type selected for modeling was an intermediate fuel oil, IFO 180, which is typical for a larger cruise ship. Many ships will use diesel fuel closer in to port, because of air emissions concerns, but will use an intermediate or heavy fuel oil while underway at sea. If a vessel uses IFO 180 while at sea, it would have some on board even while in port burning diesel. The IFO 180 was chosen for modeling because it would tend to have greater environmental consequences on the water surface and shorelines if spilled and would pose a greater challenge for cleanup response operations than diesel.

Spill Source and Volume: The spill volume is based on a 68,000 GT (gross tonnage) cruise ship, such as the *Crystal Serenity* (Figure 9),[23] which has regularly-scheduled cruises to Ilulissat during August and September. This is most likely to be the largest cruise ship to transit the waters of Disko Bay. Being the largest vessel, it would also have the correspondingly largest bunker fuel tanks.

[21] Egevang et al. 2005.
[22] http://www.cruisetimetables.com/cruises-to-ilulissat-greenland-2016.html
[23] IMO 9243667

Figure 9: Crystal Serenity Cruise Ship[24]

The bunker fuel volume for a 68,000 GT-cruise ship, like the *Crystal Serenity,* is about 2,800 m^3 (17,610 bbl), which would be divided amongst a number of smaller tanks. The release volume assumed for the hypothetical spill scenario was 280 m^3 (1,761 bbl), which would represent 10% of the bunker fuel. To benchmark this volume, it should be considered that this volume would generally be considered a "maximum most-probable" discharge for a vessel of this size and type under US Coast Guard regulations.

In the modeling, it was assumed that the oil would flow out of the bunker tank(s) involved over the course of about 12 hours.

Product Tanker Spill in Lancaster Sound

One spill scenario (Case 4) was developed for a hypothetical spill from a product tanker in Lancaster Sound.

Location: The location selected for the hypothetical tanker oil spill in Lancaster Sound is near Wollaston Island to the west of Bylot Island at the entrance to Navy Board Inlet (Figure 10). The specific location was: latitude 73.731023, longitude -81.010920 (decimal degrees).

The reasoning behind the selection of this specific site is that it is a plausible grounding location due to the presence of shallower water and rocks surrounding Wollaston Island. It is also potentially near the route of a tanker delivering fuel to communities such as Resolute or Arctic Bay. This location was selected as *representative* for spill sites. Spills from product tankers may occur in various locations in the region from tankers taking somewhat different routes.

[24] Photo from: http://maritime-connector.com/ship/crystal-serenity-9243667/

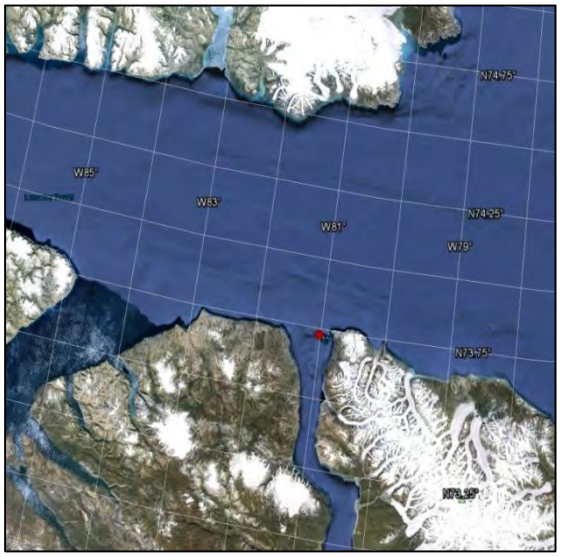

Figure 10: Location for Hypothetical Product Tanker Spill in Lancaster Sound

Season: The season selected was the open water season – June through September, based on analysis of average monthly ice coverage data from TOPAZ at the spill site (2011-2015). Average ice cover of less than 30% was defined as "open water." [See Figure 84 in the main report.]

Oil Type: The oil type selected was Arctic diesel, which may be expected to be transported as cargo for deliveries to Resolute or other communities, as well as to mining operations at Baffinland Mines, though the route taken may be slightly different in the latter.

Spill Source and Volume: The source of the hypothetical spill was assumed to be a product tanker of about 13,000 DWT (deadweight tonnage), such as the *T/V Maria Desgagnés* (Figure 11).

Figure 11: T/V Maria Desgagnés [25]

The representative tanker, *T/V Maria Desgagnés*, has a deadweight tonnage of 13,199 DWT, with a total cargo capacity of 15,171.1 m^3 (95,422 bbl). Normally, the tanks would not be filled over 98% capacity to

[25] Photo from: www.fleetmon.com (IMO 9163752)

allow for vapor expansion, so that the actual loaded bunker tank volume would be 14,867.9 m^3 (93,515 bbl). The largest cargo tank on board holds approximately 2,400 m^3 (15,096 bbl). The hypothetical spill scenario involves the full release of 2,400 m^3 (15,096 bbl) from this largest tank (Tank 5 in Figure 12), or about 16% of the entire cargo load.

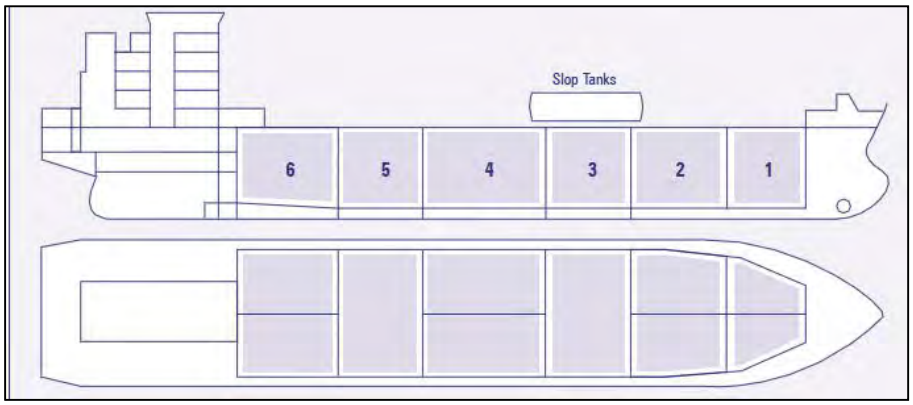

Figure 12: Tank Configuration in T/V Maria Desgagnés[26]

For the modeling, the release was assumed to occur over the course of 12 hours.

Bulk Carrier Spills in Eclipse Sound

Two spill scenarios were developed for Eclipse Sound (Case 5A and Case 5B), based on the hypothetical bunker fuel spill from a bulk carrier in two seasons – open water and ice.

Location: The site for the hypothetical spill in Eclipse Sound was near the entrance to Milne Inlet about 4.7 km east of Pisiktarfik Island (Figure 13). The specific location was: latitude 72.559040, longitude -80.256612 (decimal degrees).

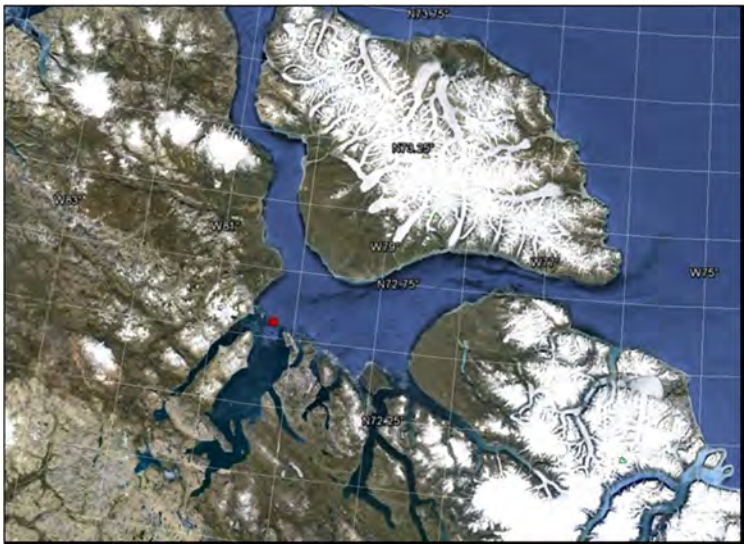

Figure 13: Location of Hypothetical Spill Site near Milne Inlet (Cases 5A and 5B)

[26] Information from Desgagnés Tanker, Inc. (www.desgagnes.com)

The location was selected because it is en route to the Baffinland Mines (Figure 14) and is in a location that would likely cause significant oiling of surrounding islands.

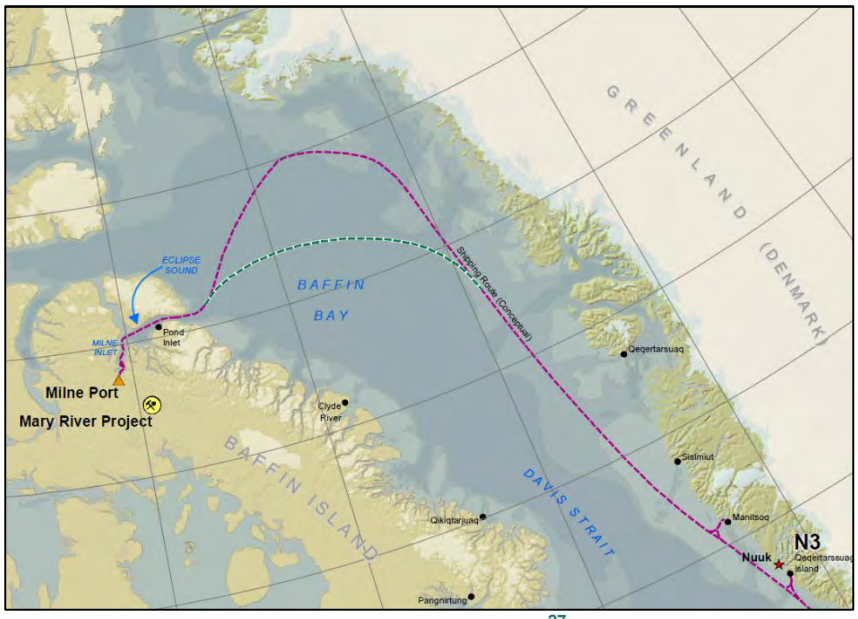

Figure 14: Shipping Routes to Milne Port, Baffinland Mines[27]

Season: Baffinland Iron Mines Corporation's proposed shipping season is from 25 June through 7 March. Ice and open water seasons were based on analysis of average monthly ice coverage data from TOPAZ at the spill site (2011-2015). [See Figure 93 in main report.] Average ice cover of less than 30% was defined as "open water." The two seasons selected for the modeling of the hypothetical spills were:

- **Case 5A:** Open water (August through October)
- **Case 5B:** Ice (25 June through 31 July, and 1 November through 7 March).

Oil Type: The oil type selected for the hypothetical spills was an intermediate fuel oil, IFO 380. This would be the expected bunker fuel for a bulk carrier.

Spill Source and Volume: The source for the hypothetical spill scenarios was an 85,000 DWT (Panamax) Polar Class 4 (PC4-DNV ICE 17) bulk carrier or iron ore carrier that may transit to and from the Baffinland Mines. For the month of January or February, it is assumed that there will be two PC4 vessels each making three round trips from Milne Port to Greenland for a total of six shipments of ore from Milne Port to Greenland. This equates to a PC4 vessel passing through Eclipse Sound approximately 12 times (in both directions) in the month of January or February. The vessel would be similar to the one shown in foreground of Figure 15.

[27] Purple line shows shipping route in open water season; green line shows route in winter months (ice season). From: Baffinland 2015.

Figure 15: Iron Ore Bulk Carrier Proposed for Trans-Shipping from Baffinland Mines[28]

A vessel of this type would be expected to have about 5,500 m^3 of IFO bunker fuel and 750 m^3 of diesel fuel. The fuel tanks are located in the central part of the stern (left side of Figure 16), which provides protection as with a double-hull. The spill volume used in the modeling assumes the release of 1,000 m^3 from one bunker tank over the course of 12 hours, i.e., the entire contents of that single tank, or about 18% of the total bunker fuel load.

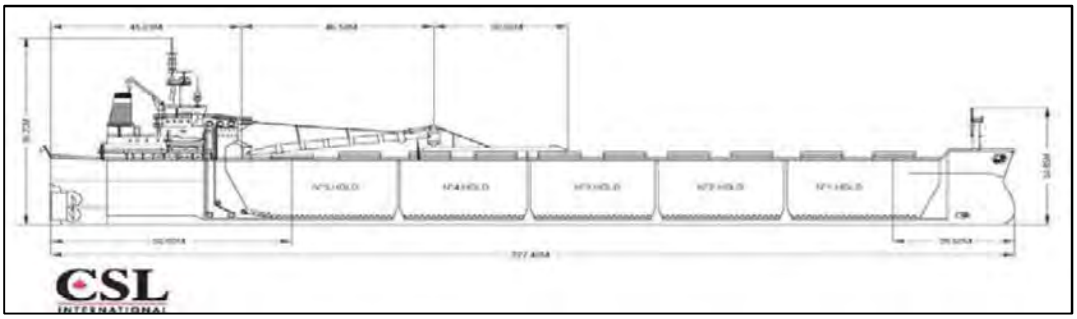

Figure 16: Configuration of Iron Ore Carrier Proposed for Trans-Shipping from Baffinland Mines[29]

[28] Baffinland 2015.
[29] Baffinland 2015.

Summary of Spill Scenarios

The eight hypothetical oil spill scenarios modeled are summarized in Table 4.

Table 4: Summary of Hypothetical Oil Spill Scenarios for Modeling

Case #	Location	Spill Source	Oil Type	Spill Rate	Spill Duration (days)	Volume (m^3)	Season(s)
1A	Melville Bay license areas Lat: 75.231740 Lon: -60.645321	Exploratory Well Blowout	Medium Crude	3,340 m^3/day	1	3,340	Open water: July to October
1B				3,340 m^3/day	34	113,560	
2A	Baffin Bay license areas (entrance to Lancaster Sound) Lat: 74.401196 Lon:-77.467675	Exploratory Well Blowout	Medium Crude	3,340 m^3/day	1	3,340	Open water: June to October
2B				3,340 m^3/day	34	113,560	
3	Greenland coast Off Disko Island Lat: 69.074430 Lon: -53.500040	Cruise Ship 68,000 GT IFO 180: 2,800 m^3	IFO 180	-	0.5	280	Cruise Season: July to September
4	Lancaster Sound Lat: 73.731023 Lon: -81.010920	Product Tanker ≈13,000 DWT Arctic Diesel: 15,000 m^3	Arctic Diesel	-	0.5	2,400	Open water: June to September
5A	Eclipse Sound Milne Inlet Lat: 72.559040 Lon: -80.256612	Bulk Carrier 85,000 DWT Polar Class 4 Panamax IFO 380: 6,250 m^3	IFO 380	-	0.5	1,000	Open water: August to October
5B							Ice: June 25 to July 31; Nov. 1 to March 7

Part II: Spill Probability Analysis: Well Blowouts

The hypothetical oil spill scenarios developed for modeling are all relatively unlikely events, though if they were to occur, the consequences could be significant. In order to provide a perspective on the probability and relative frequency of oil spills and these types of spills in particular, a brief probability analysis was conducted.

Historical Well Blowouts

There have been about 607 well blowouts worldwide since the mid-1950s – or about 10 incidents per year worldwide.[30] Blowouts do not necessarily result in the release of oil, and those that do are usually of short duration and involve a low volume of spillage. Major or "catastrophic" blowout incidents, such as Macondo MC252 or Ixtoc I, are, fortunately, rare events. Historical offshore well blowouts of 10,000 bbl (1,590 m^3) or more are shown in Table 5 in descending order of total volume.

Table 5: Largest Historical Offshore Well Blowouts

Well	Start Date	Location	m^3 Spilled	Flow Rate (m^3/day)			Duration (days)
				Peak	Average	Low	
Ixtoc I[31]	6/3/1979	Bahia del Campeche, Mexico	524,685 to 1,629,080	4,770	3,190 to 5,565	1,590	290
Macondo MC252[32]	4/20/2010	Gulf of Mexico, USA	389,519 to 667,747	5,708 to 9,539	4,579 to 7,854	-	85
Bull Run/Atwood Oceanics[33]	1/1/1973	Dubai, UAE	317,975	-	-	-	-
Abkatun 91[34]	10/1/1986	Bahia del Campeche, Mexico	39,270	-	-	-	-
Montara[35]	9/21/2009	Timor Sea, Australia	4,547 to 34,071	318	62 to 64	64	74
Ekofisk Bravo B-14[36]	4/20/1977	North Sea, Norway	32,176	-	4.464	-	7
Funiwa 5[37]	1/17/1980	Forcados, Nigeria	31,797	-	1,987	-	16
Hasbah 6[38]	10/2/1980	Gulf, Saudi Arabia	16,694	-	1,855	-	9
Alpha Well 21 A[39]	1/28/1969	Pacific, off California	15,899	-	1,445	-	11
Iran Marine Intl.[40]	12/1/1971	Gulf, Iran	15,899	795	-	-	-

[30] Holand 2013.
[31] Dokken 2011; Boehm and Fiest 1982.
[32] Hauck et al 2013; McNutt et al. 2012a; 2012b; Oldenburg et al. 2012; Fitch et al. 2013.
[33] Etkin 2009.
[34] Etkin 2009.
[35] Comm. Australia 2011.
[36] Etkin 2009.
[37] Etkin 2009.
[38] vanOudenhoven. 1983.
[39] Etkin 2009.

Table 5: Largest Historical Offshore Well Blowouts							
Well	**Start Date**	**Location**	**m^3 Spilled**	**Flow Rate (m^3/day)**			**Duration (days)**
				Peak	**Average**	**Low**	
Main Pass Block 41-C[41]	3/1/1970	Gulf of Mexico	10,334	477	350	159	30
Yum II/ Zapoteca[42]	10/10/1987	Bahia del Campeche, Mexico	9,323	-	4,770	-	51
South Timbalier B-26[43]	12/1/1970	Gulf of Mexico	8,441	-	-	-	-
Trinimar Marine 327[44]	8/8/1973	Gulf of Paria, Venezuela	5,827	-	318	-	5
Greenhill Timbalier Bay 251[45]	9/29/1992	Gulf of Mexico	1,828	496	229	19	14

Probabilities of Well Blowouts

This project involved four blowout scenarios, as summarized in Table 6.

Table 6: Summary of Hypothetical Well Blowout Scenarios for Modeling				
Case #	**Location**	**Spill Rate**	**Duration (days)**	**Volume (m^3)**
1A	Melville Bay license areas	3,340 m^3/day	1	3,340
1B		3,340 m^3/day	34	113,560
2A	Baffin Bay license areas (Lancaster Sound)	3,340 m^3/day	1	3,340
2B		3,340 m^3/day	34	113,560

The likelihood of a well blowout depends on a large number of factors related to location, well characteristics, and operating conditions. For regions for which there are few, if any, offshore exploration and production wells, historical data from other regions are the only benchmarks. Estimates of the probability of well blowouts, measured as the frequency or rate per well, have varied by region, time period, and other factors. Various studies have investigated the probability of well blowouts per well as summarized in Table 7.

Estimates of blowout probabilities *per exploratory well* vary from 0.000123 to 0.00337, or about 1 in 8,000 to 1 in 300. Note that these are probabilities that there will be a blowout of some kind, not necessarily a blowout of the magnitude of the incidents in Table 6.

Blowouts are defined as losses of well control. While the term "blowout" conjures up an image of a major catastrophic release of oil, in reality, most blowouts are very small and result in the release of very little oil, as, for example, in Table 8.

---

[40] Etkin 2009.
[41] Alpine Geophysical 1971.
[42] Etkin 2009.
[43] Etkin 2009.
[44] Etkin 2009.
[45] Etkin 2009.

Table 7: Estimates of Probabilities of Well Blowouts[46]			
Location/Well Type	**Mean Blowout Probability per Well**		**Data Source**
	Probability	**Return Years**	
Gulf of Mexico/North Sea Exploratory	0.00250	400	Holand 2006
Worldwide Exploration Deepwater High Pressure	0.00190	526	
Worldwide Exploration Deepwater "Normal"	0.00031	3,226	
Worldwide Exploration Appraisal Well Deep (Substrate)	0.00128	781	Holand 2013
Worldwide Exploration Appraisal Well Shallow (Substrate)	0.00154	649	
Worldwide Exploration Wildcat Well Deep (Substrate)	0.00154	649	
Worldwide Exploration Wildcat Well Shallow (Substrate)	0.00210	476	
Worldwide Exploration Well	0.00337	297	
Beaufort Sea	0.00082	1,220	Bercha 2010
East Coast Canada	0.00150	667	
Beaufort Sea Exploratory	0.00250	400	
Danish Labrador Sea Exploration "Normal"	0.000123	8,130	Dyb et al. 2012
Danish Labrador Sea Exploration High Pressure	0.000765	1,307	
Worldwide Exploration Well	0.0015	667	Etkin 2015

Table 8: Spill Volume Distribution of US Oil Well Blowouts			
Volume		**Number**	**% Total**
Barrels (bbl)	**Cubic meters (m^3)**		
1 – 9 bbl	**0.2 – 1.99 m^3**	1	3%
10 – 99 bbl	**2 – 15.99 m^3**	10	32%
100 – 999 bbl	**16 – 158.99 m^3**	10	32%
1,000 – 9,999 bbl	**159 – 1,589.99 m^3**	5	16%
10,000 – 99,999 bbl	**1,590 – 15,898.99 m^3**	4	13%
100,000 – 999,999 bbl	**15,899 – 158,987.99 m^3**	0	0%
1,000,000+ bbl	**159,988 m^3 +**	1	3%
Total		**31**	**100%**

Another approach to estimating the probability of a catastrophic well blowout is the application of extreme value theory (EVT). This approach has been widely used in studying rare events, such as stock market crashes and earthquakes. A study conducted by US Bureau of Ocean Energy Management (BOEM) researchers[47] applied EVT to catastrophic oil well blowouts of one million barrels or more (160,000 m^3) in the US Gulf of Mexico. Incorporating 49 years of Gulf of Mexico oil spill data (1964 – 2012), the mean return period was estimated to be 165 years.[48] This means that it is expected that a well blowout of more than one million barrels (160,000 m^3) would occur roughly once in 165 years amongst all the wells in the Gulf of Mexico.

[46] Adapted from Etkin 2015.
[47] Ji et al. 2014.
[48] The 95% confidence interval was 41 years to more than 500 years.

For the Melville Bay and Baffin Bay (Lancaster Sound) areas, it can be expected that a well blowout of some type may occur once in 300 to 8,000 years per well, based on the estimates of blowout probabilities *per exploratory well* that vary from 0.000123 to 0.00337. Data on the number of wells planned for these areas were not available. But, if there were to be a well blowout, it would likely be very small.

Benchmarking of Blowout Flow Rates

The release rate or flow rate for a well blowout is dependent on the specific characteristics of the well involved, most notably the reservoir pressure. The actual flow during an incident can vary over time and fluctuate over the course of a single day. The flow rate assumed for the study scenarios is 3,340 m^3 per day (21,008 bbl per day). According to the most comprehensive international data,[49] blowout release or flow rates are poorly documented. Flow-rate figures exist for some blowouts, but not for most. Often flow rates are calculated after the fact based on the estimated total volume and the duration of flow. This limits the degree to which the modeling scenario flow rates can be benchmarked. The assumed study flow rates were compared with the peak and average flow rates for the historical well blowouts shown in Table 9 and Figure 17.

Table 9: Reported Blowout Flow Rates for Benchmarking[50]

Scenario	Average Flow	
	bbl/day	m^3/day
Macondo MC-252-Oldenburg Estimate[51]	56,000	8,903
Macondo MC-252-McNutt Estimate[52]	50,000	7,949
Macondo MC-252-High Estimate	49,400	7,854
Ixtoc I-High Estimate	35,000	5,565
Ixtoc I-Low Estimate	30,000	4,770
Yum II/Zapoteca	30,000	4,770
Ekofisk Bravo B-14	28,080	4,464
Baffin Bay/Melville Bay Study Scenarios	**21,008**	**3,340**
Hasbah 6	11,667	1,855
Alpha 21-A (Santa Barbara)	9,090	1,445
Macondo MC-252-Low Estimate	2,880	458
Main Pass 41-C	2,200	350
Trinimar Marine 327	2,000	318
Greenhill TB-251	1,440	229
Montara-High Estimate	400	64
Montara-Low Estimate	390	62

These are representative flow rates and do not represent all potential flow rates. Note that there are some estimated potential flow rates reported to be as high as 449,000 bbl/day (71,385 m^3) for some wells in the

[49] Holand 2006, 2013.
[50] Holand 2006, 2013
[51] Oldenburg et al. 2012.
[52] McNutt et al. 2012a; McNutt et al. 2012b.

US Gulf of Mexico. These flow rates have never been seen in an actual well blowout to date, however. They are estimated based on characteristics of the specific wells and reservoirs.

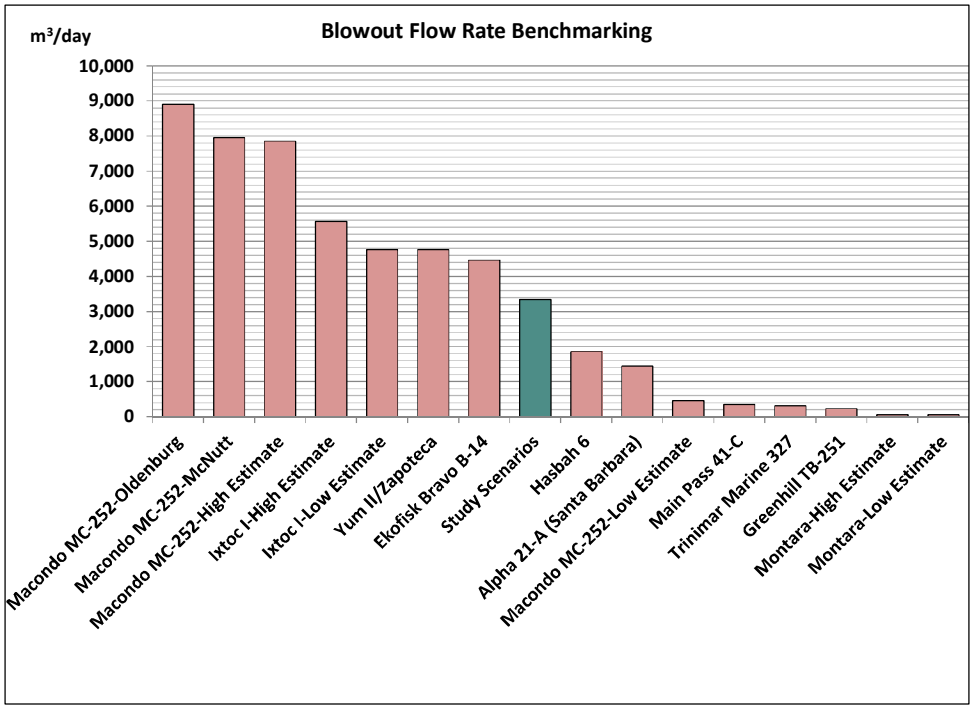

Figure 17: Blowout Flow Rate Benchmarking

The study flow rate is about 38% of the maximum flow rate estimated for the 2010 Macondo MC-252 spill in the Gulf of Mexico, and about 80% of the average flow rate reported for that incident.

Benchmarking of Blowout Durations

The duration of flow – that is, the length of time that the well continues to release oil – is the other factor that determines the total volume of spillage. The durations for the study scenarios are assumed to be one day and 34 days. The one-day duration is based on an assumption of natural bridging, and the 34-day duration assumes that a relief well needs to be drilled to stop the flow.

Studies indicate that about 84% of well blowouts bridge naturally, *i.e.*, the flow is stopped as sediment naturally fills in the wellbore without any intervention in 0.5 to 5 days, as shown in Table 10.[53] Generally, the duration of flow is relatively short, which would limit the total volume of spillage. In the other 16% of cases, human intervention in the form of relief wells and/or containment and capping is required to stop the flow of oil.

In the event of a blowout, well operators do not wait until natural bridging occurs, but rather immediately begin the necessary intervention operations, as per the relevant contingency plans. Frequently, however, the blowout bridges naturally before the intervention operation is completed. This is the scenario that is represented by Cases 1A and 2A – flow for one day. Worldwide, about 10% of blowouts have been stopped with relief wells, and 6% by capping and containment operations. The *maximum* time for relief

[53] Dyb et al. 2012; Holand 2013.

well operations is 75 days.[54] Fifty percent of relief well operations took less than five days, 75% less than 10 days, and 90% less than 25 days. The 34-day relief well operation assumed in Cases 1B and 2B represent the estimated 95th percentile case.

Table 10: Distribution Blowout/Well Release Duration until Natural Bridging[55]

Operation Phase	Flow Duration							
	≤10 min	10 min - ≤40 min	40 min - ≤ 2 hrs	2 hrs - ≤12 hrs	12 hrs - ≤2 days	2 days - ≤5 days	> 5 days	Unknown
Development Deep	0%	0%	13%	25%	13%	13%	13%	25%
Development Shallow	0%	0%	13%	9%	17%	17%	17%	26%
Exploration Deep	0%	0%	4%	8%	21%	13%	29%	25%
Exploration Shallow	0%	3%	6%	13%	6%	22%	25%	25%
Completion	0%	0%	0%	10%	20%	0%	60%	10%
Workover	0%	4%	0%	17%	38%	8%	21%	13%
Production	0%	0%	0%	0%	44%	22%	22%	11%

The blowout durations modeled in this study relative to the two longest recorded durations of flow are shown in Table 11 and Figure 18.

Table 11: Blowout Durations Relative to Ixtoc I and Macondo MC-252

Scenario	Days	Relative Duration Comparison	
		Macondo MC-252	Ixtoc I
Ixtoc I	290	3.412	1.000
Macondo MC-252	85	1.000	0.293
Labrador Relief Well	75	0.882	0.259
Montara	74	0.871	0.255
Yum II/Zapoteca	51	0.600	0.176
Study Scenario (Longer Duration)	**34**	**0.400**	**0.117**
Main Pass 41-C	30	0.353	0.103
Labrador Cap	25	0.294	0.086
Funiwa 5	16	0.188	0.055
Greenhill TB-251	14	0.165	0.048
Alpha 21-A	11	0.129	0.038
Hasbah 6	9	0.106	0.031
Ekofisk Bravo B-14	7	0.082	0.024
Trinimar Marine 327	5	0.059	0.017
Study Scenario (Shorter Duration)	**1**	**0.012**	**0.003**

[54] Dyb et al. 2012.
[55] Based on data in Holand 2013.

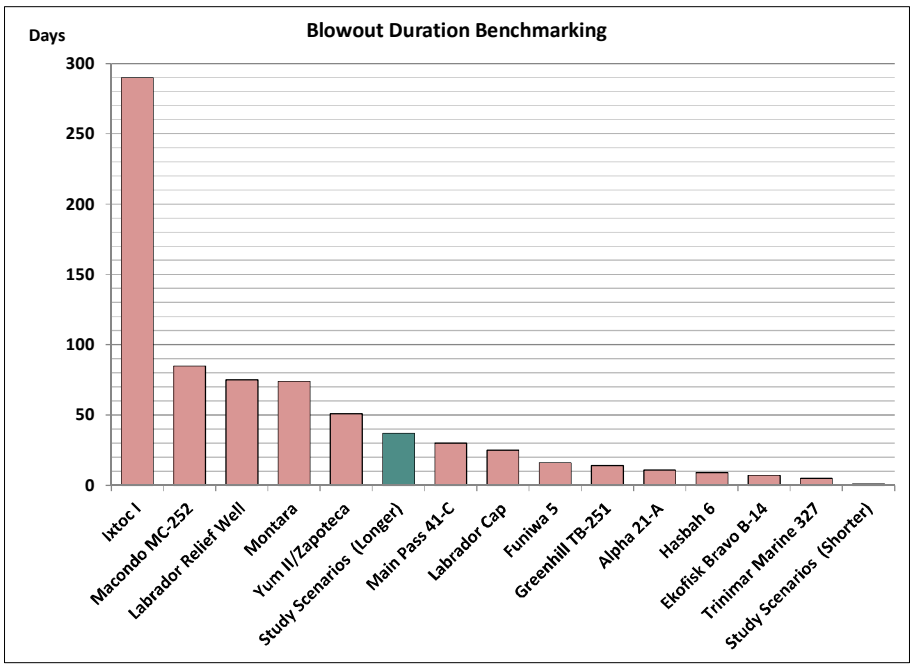

Figure 18: Benchmarking of Blowout Durations

Benchmarking of Total Blowout Volumes

The total volumes of the study blowout scenarios were benchmarked against the total volumes of the largest well blowouts (from Table 5). The benchmarking results are shown in Figure 19 and Table 12.

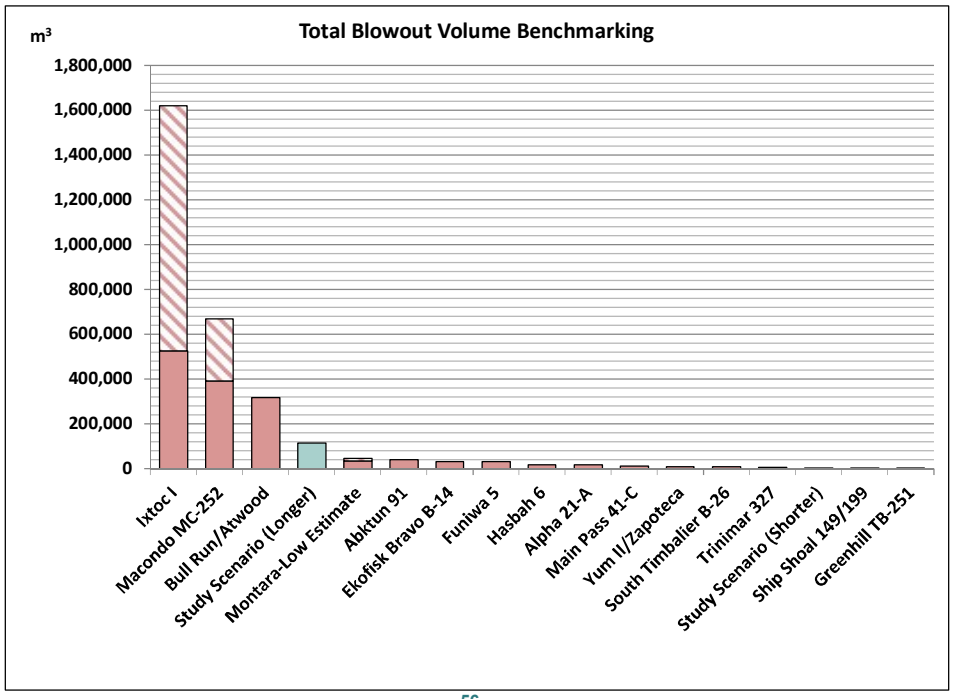

Figure 19: Total Blowout Volume Benchmarking[56]

[56] The hashed areas in the bar chart indicate the higher estimated volumes of spillage.

Table 12: Total Blowout Volumes Relative to Largest Incidents			
Scenario	**Volume Released (m^3)**	**Relative Volume Comparison**	
		Macondo MC-252 Higher Estimate	**Ixtoc I Higher Estimate**
Ixtoc I (Higher Estimate)	1,620,078	2.4262	1.0000
Macondo MC-252 (Higher Estimate)	667,745	1.0000	0.4122
Ixtoc I (Lower Estimate)	524,657	0.7857	0.3238
Macondo MC-252 (Lower Estimate)	389,518	0.5833	0.2404
Bull Run/Atwood	317,974	0.4762	0.1963
Study Scenario (34-Day)	**113,560**	**0.1701**	**0.0701**
Montara (Higher Estimate)	45,470	0.0681	0.0281
Montara (Lower Estimate)	34,071	0.0510	0.0210
Abktun 91	39,270	0.0588	0.0242
Ekofisk Bravo B-14	32,176	0.0482	0.0199
Funiwa 5	31,797	0.0476	0.0196
Hasbah 6	16,694	0.0250	0.0103
Alpha 21-A	15,899	0.0238	0.0098
Main Pass 41-C	10,334	0.0155	0.0064
Yum II/Zapoteca	9,323	0.0140	0.0058
South Timbalier B-26	8,441	0.0126	0.0052
Trinimar 327	5,827	0.0087	0.0036
Study Scenario (1-Day)	**3,340**	**0.0050**	**0.0021**

The larger of the hypothetical blowout scenarios (34 days of flow for a total of 113,560 m^3), if it were to occur, would be the fourth largest well blowout ever worldwide, based on current records. Only 0.5% of blowouts have ever been of this size or larger. The smaller scenario – 1 day of flow for a total of 3,340 m^3 – would be the 15th largest incident worldwide. Only 2% of blowouts have ever been this size or larger. Both of these scenarios represent relatively extreme volumes for blowouts.

Conclusions on Well Blowout Probabilities

Based on the brief analysis presented, one can conclude that:

- The probability that there would be a well blowout of any kind from an individual well is about 1 in 300 to 1 in 8,000 (0.000123 to 0.00337);
- Most well blowouts are small; only 0.5% of well blowouts have ever been the magnitude of the 34-day blowout scenarios developed for this study;
- The probability that there would be a well blowout of 113,560 m^3 from any particular well is about 1 in 60,000 to 1 in 1.6 million (0.000000625 to 0.000017).

The probability of a well blowout in the Baffin Bay/Melville Bay region depends on the number of wells drilled. There are no data available to calculate this with any precision. Cairn Energy[57] stated that it had planned to drill up to four exploration wells in West Greenland during 2011 in Eqqua, Napariaq, Lady

[57] Cairn 2011.

Franklin, and Atammik blocks (Figure 20). If one assumes that there are a total of about 15 wells in the blocks in total, the probability would increase to 1 in 4,000 to 1 in 107,000 (0.0000094 to 0.00025).

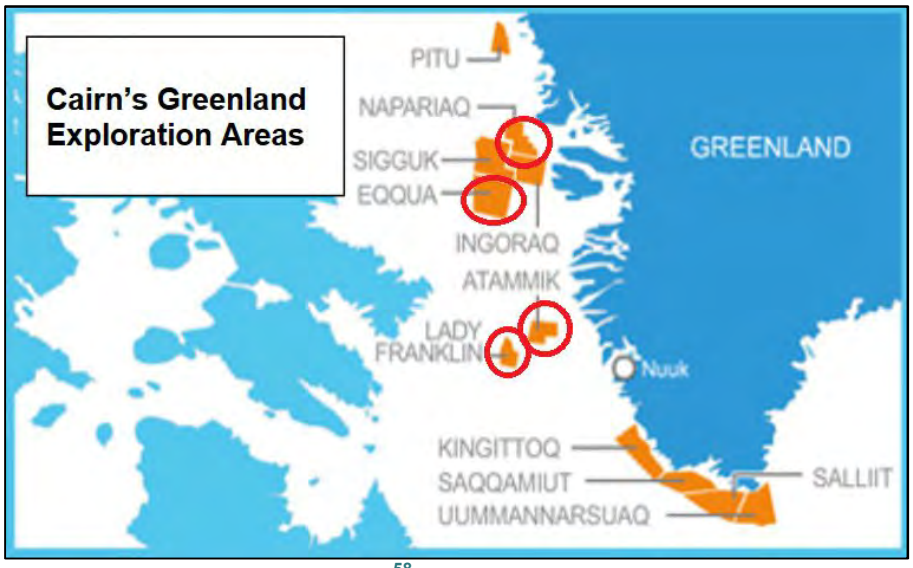

Figure 20: Cairn Blocks for 2011 Exploration[58]

[58] http://www.cairnenergy.com/files/pdf/factsheets/factsheet_cairn_greenland.pdf

Part III: Spill Probability Analysis: Vessel Spills

Vessel spills due to accidents are dependent on the specific vessel operations (numbers of transits, types of vessels, operational decisions) and the navigational and weather hazards in the region. An extensive vessel traffic modeling analysis was outside the scope of this study, but a brief analysis of probabilities of vessel spills follows.

Specific credible vessel spill scenarios were selected for modeling, as summarized in Table 13. These particular vessel spill scenarios were selected because they represented credible scenarios with known vessels and traffic patterns. There may be significant changes in vessel traffic patterns in this region with increased use of Polar Class vessels that can transit under ice conditions, as well as with changing patterns of ice coverage due to climate change. The probabilities of vessel spills described below do not take into account changes in future vessel traffic patterns. In addition, the types of scenarios described for the specific patterns of vessel traffic considered – cruise ships, and vessels transiting to the Baffinland Mines – do not take into account other vessel traffic that may transit the area.

Table 13: Summary of Hypothetical Vessel Oil Spill Scenarios for Modeling

Case #	Location	Spill Source	Oil Type	Volume (m^3)	Season(s)
3	Greenland coast Off Disko Island	Cruise Ship 68,000 GT2,800 m^3	IFO 180	280	Cruise Season: July to September
4	Lancaster Sound	Product Tanker ≈13,000 DWT 15,000 m^3 (cargo)	Arctic Diesel	2,400	Open water: June to September
5A	Eclipse Sound Milne Inlet	Bulk Carrier 85,000 DWT Polar Class 4 Panamax 6,250 m^3 (fuel)	IFO 380	1,000	Open water: August to October
5B					Ice: June 25 to July 31; Nov. 1 to March 7

Determining the probability of vessel oil spills due to accidents such as groundings and collisions involves determining the probability that there will be an accident and the probability that the accident will actually result in oil spillage. (Not all accidents result in the spillage of oil.) The probability that the oil spill will involve the release volumes designated for the study scenarios would be another factor to consider.

Cruise Ship Scenario

The cruise ship spill scenario involves the spillage of 280 m^3 of oil from the largest cruise ship in the region. There are about 15 to 20 trips per week with five ships during the cruise season of July to September[59] for Disko Lines and one trip annually for the *Crystal Serenity* – or about 240 trips per year.

Studies specifically on cruise ship accidents are limited, but available data indicate:

- 0.0156 accidents per year [study in Prince Rupert, BC, Canada][60]

[59] http://diskoline.dk/en/

- 0.0034 accidents per vessel per transit-day [Cook Inlet, Alaska, USA][61]
- 0.149 to 0.0252 collisions per vessel per year of operation [62]
- 0.0015 groundings per vessel per year of operation[63]

Collisions are unlikely to occur since the transit routes are not particularly busy, but groundings are a distinct possibility. If one assumes that there are 0.0015 groundings per year per vessel, this comes to a probability of 0.000004 groundings per day per vessel. For the 240 transits, there would be a probability of grounding of about 0.001 – or 1 in 1,013 years.

The accident rate from the Cook Inlet study might be applied to the 240 transits (about 120 transits, if each transit is about ½ day) to derive an estimate of accidents of 0.408 or 1 in 2.4 years. Not all accidents result in oil spillage. Assuming that the vessel has a double-hull on its bunker tanks, the probability that a grounding accident would result in a spill is 0.02.[64] This would mean that the likelihood of a grounding-related *spill* is about 0.0082 – or once in 122 years. Note that this spill may not necessarily be the volume selected for modeling.

Product Tanker Scenario

The probability that an oil tanker will have a serious grounding is 0.0026 per ship-year (a vessel operating for a year) – or about 0.000007 groundings per day per vessel.[65] Tanker traffic varies from year to year, and the specific routes taken also vary. This study did not include a specific vessel traffic study to determine the probabilities of tanker groundings or other accidents at specific locations, including the location selected for the modeling of the hypothetical product tanker spill scenario in Lancaster Sound.

However, for the purposes of analyzing the potential effects and impacts of tanker spills, the tanker traffic that could transit the general area for the study was considered in developing a probability estimate for tanker spills.

Based on data for the year 2013,[66] there are about 24 tanker trips through the region annually. Projections for the year 2030 go to as high as 43 trips annually. These tanker trips include those associated with supplying Arctic communities with fuel, [67] as well as mining activity.[68]

If one assumes that each voyage takes about 10 days, this would mean that there may be, at most, 0.0018 groundings per year – or a 1 in 556 chance that a serious grounding accident would occur in any year. This probability may increase to as much as 0.0032 per year – or a 1 in 310 chance in any year by the year 2030.

---

[60] Det Norske Veritas 2012.
[61] Etkin 2012.
[62] Papanikolaou et al. 2013. Nilsen et al. 2005.
[63] Det Norske Veritas 2011.
[64] Based on: Etkin and Michel 2003; Michel and Winslow 1999, 2000; Barone et al. 2007; Herbert Engineering et al. 2003.
[65] Det Norske Veritas 2011.
[66] Mariport Group Ltd. 2012.
[67] Mariport Group Ltd. 2012.
[68] Curran 2015.

The probability that the product tanker grounding will result in a spill is 0.18.[69] This means that the probability that there would presently be a spill associated with a product tanker grounding accident is about 0.0003, or 1 in 3,086. The probability increases to 0.00058 per year, or 1 in 1,736, by the year 2030, assuming the traffic projections are correct. Note that this spill may not necessarily be the volume selected for modeling.

With more tanker traffic, there would be a higher probability of spills, with less traffic, a lower probability. It is important to note that this is not the probability that a tanker spill would occur in this specific location or even only in Lancaster Sound, but rather the probability that there would be a tanker spill in the general region.

Bulk Carrier Scenarios

The iron ore bulk carrier selected for the hypothetical spill scenario is expected to make 12 transits during January and February of each year.[70] The probability of a serious grounding with a bulk carrier is about 0.0043 per ship-year, or about 0.000012 per day per ship.[71] Assuming the transits take about 10 days (an over-estimate), one might expect 0.00144 serious groundings – or a 1 in 694 chance of a grounding in a particular year from a bulk carrier transiting to or from the Baffinland Mines. The probability that the grounding would result in spillage of bunker fuel is 0.02.[72] The probability of a grounding-related spill from a bulk carrier is 0.00003, or 1 in 35,000. Note that this spill may not necessarily be the volume selected for modeling.

This probability is specific to the traffic expected for Baffinland Mines. With additional non-tank vessel traffic through this area, the probability of spills would increase.

Overall Conclusions on Vessel Spill Probabilities

In general, one may conclude that vessel spills are unlikely to occur, though the probability increases with the numbers of vessel transits. There may also be somewhat higher probabilities of vessel accidents in extreme weather conditions or specific navigational hazards.

When vessel accidents occur, there is not necessarily a spillage of oil involved. In fact, only between 2% and 18% of vessel accidents may actually result in spillage. If a spill does occur, the volume may be smaller than the volumes selected for consequence modeling. There is a slight probability that the spill may be larger.

The probability of a cruise ship spill is about 1 in 122 to 1 in 1,013 per year. This probability is based only on current cruise vessel traffic.

---

[69] Based on Yip et al. 2011; Rawson et al. 1998; NRC 1998; NRC 2001; IMO 1995; Etkin et al. 2002.
[70] Baffinland 2015.
[71] Det Norske Veritas 2011
[72] Based on Etkin and Michel 2003; Michel and Winslow 1999, 2000; Barone et al. 2007; Herbert Engineering et al. 2003.

The probability of a product tanker spill is about 1 in 3,086 based on current tanker traffic in the region. This probability may increase to as much as 1 in 1,736 by the year 2030, based on current traffic projections.[73]

The probability of a bunker spill from a bulk carrier spill is about 1 in 35,000. Any increases in vessel traffic may increase these overall spill probabilities.[74]

[73] Mariport Group Ltd. 2012.
[74] Étienne et al. 2013.

Part IV: Spill Response Development

Three of the hypothetical spill scenarios were selected by WWF-Canada for further analysis with respect to spill response effectiveness:

- **Case 1A:** Melville Bay One-Day Blowout 3,340 m^3/day (21,008 bbl/day) crude for 1 day = 3,340 m3 (21,008 bbl)
- **Case 1B:** Melville Bay 34-Day Blowout 3,340 m^3/day (21,008 bbl/day) crude for 34 days = 113,560 m^3 (714,271 bbl)
- **Case 2B:** Baffin Bay 34-Day Blowout 3,340 m^3/day (21,008 bbl/day) crude for 34 days = 113,560 m^3 (714,271 bbl)

The spill response simulations for the Melville Bay scenarios (Case 1A and Case 1B) involved a multi-faceted approach with mechanical containment/recovery operations, *in situ* burning, and surface dispersants. The Baffin Bay scenario (Case 2B) only involved sub-surface dispersant application.

SIMAP Response Modeling Basics

Modeling of spill response operations in SIMAP involves setting various parameters for oil removal rates through mechanical recovery, burning, or chemical dispersion, based on user inputs. The user defines reasonable assumptions regarding operations and logistics, maximized removal rates, thresholds for effectiveness, response timing, and areas of response operations.

The model (SIMAP) then simulates the behavior of the oil based on its chemical and physical properties in the particular environment into which the oil is released. Oil removal is then assumed to occur in the areas designated by the user as long as certain criteria are met and designated thresholds are not exceeded. SIMAP essentially determines whether oil removal is possible given the specific environmental conditions (wave height, winds, etc.) and the behavior of the oil (spreading on the water surface, evaporation, etc.).

Overall Daily Surface Operational Assumptions (Cases 1A and 1B)

All surface spill response operations (mechanical containment and recovery, *in situ* burning, and surface dispersants) are assumed to occur for 12 hours a day with a 12-hour rest period. In the per-day removal rates below, the operational period or "day" is assumed to be 12 hours.

While daylight hours will exceed 12 hours for significant portions of the response operations in these northern latitudes, the operational period is still considered to be 12 hours. The reason for this is that there will always be issues related to required down-time for equipment maintenance, mobilization times (on site), disposal of recovered liquids, and rest periods for workers (even with shift changes). This assumption is based on the consensus of response experts and research studies into this issue.

In addition to the daily 12-hour operational periods, another restriction was added with respect to logistical and safety concerns related to weather. Research studies[75] have indicated that spill response operations in Arctic conditions, even during open water and summer seasons, are compromised by weather, cold temperatures, and other factors that affect effectiveness about 52% of the time. When operations are halted, curtailed, or postponed due to weather issues, it generally takes another 20% of that

[75] For example, DeCola et al. 2006; Nuka 2014.

time to re-mobilize and get back up to speed. For all of the surface response operations, an assumption of 62.5% of non-operation time was assumed on top of the existing 12-hour operational time frames.

In the response modeling simulations, the initial starting times for all spill response operations are assumed to be 48 hours after the onset of the oil release from the well.[76] For the Baffin Bay spill site, the subsurface injection of dispersants was assumed to begin 72 hours after the onset of the spill. Based on expert opinion and research studies conducted for the US Bureau of Safety and Environmental Enforcement, it takes about 72 hours to begin subsurface dispersants operations.[77] Response operations were assumed to continue until hindered by ice coverage or the various thresholds for response effectiveness were exceeded, including the lack of recoverable oil on the water surface.

Parameters and Thresholds for Mechanical Response (Cases 1A and 1B)

In order for mechanical containment and recovery operations to be reasonably effective, certain environmental parameters need to be met:

- Maximum wind speed: 55.6 km/hour (30 knots)
- Maximum current speed: 0.36 meters/second (0.7 knots)
- Sea state (maximum wave height): 1.07 meters
- Ice coverage: less than 20%
- Minimum oil thickness: 8 µm (microns)

If these thresholds are exceeded (or not met, in the case of minimum oil thickness), oil removal operations are assumed to cease until the conditions next meet the criteria. In other words, the oil needs to be thick enough on the water surface for skimming equipment to be effective. In addition, the winds, currents, and sea state need to be such that containment booms are effective and there is no splashing over or entrainment (oil moving under the boom).

There were two types of mechanical recovery response operations included in the simulation. The first involved the offshore area near the well site and in deeper waters (the offshore zone). The second involved the nearshore areas along the coast (the nearshore zone). The *approximate* extents of these two response operation zones can be seen in Figure 21.

The operational zones were based on criteria of the approximate spread of the thickest oil, water depth, and distance from shore. Generally, response vessels and aircraft would be expected to work relatively near to the well site to remove the freshest oil. This oil would tend to be thicker on the water surface, less spread out, and less viscous to allow for greater removal efficiency. Responders may choose to follow larger oil patches up to a certain point offshore (about 180 km). Further offshore operations would cause safety concerns, as well as operational/logistical issues with regard to fueling.

[76] Based on information in the Cairn Oil Spill Contingency Plan (OSCP) (Cairn Energy 2011) and Steiner 2011.
[77] This report has not yet been released by BSEE.

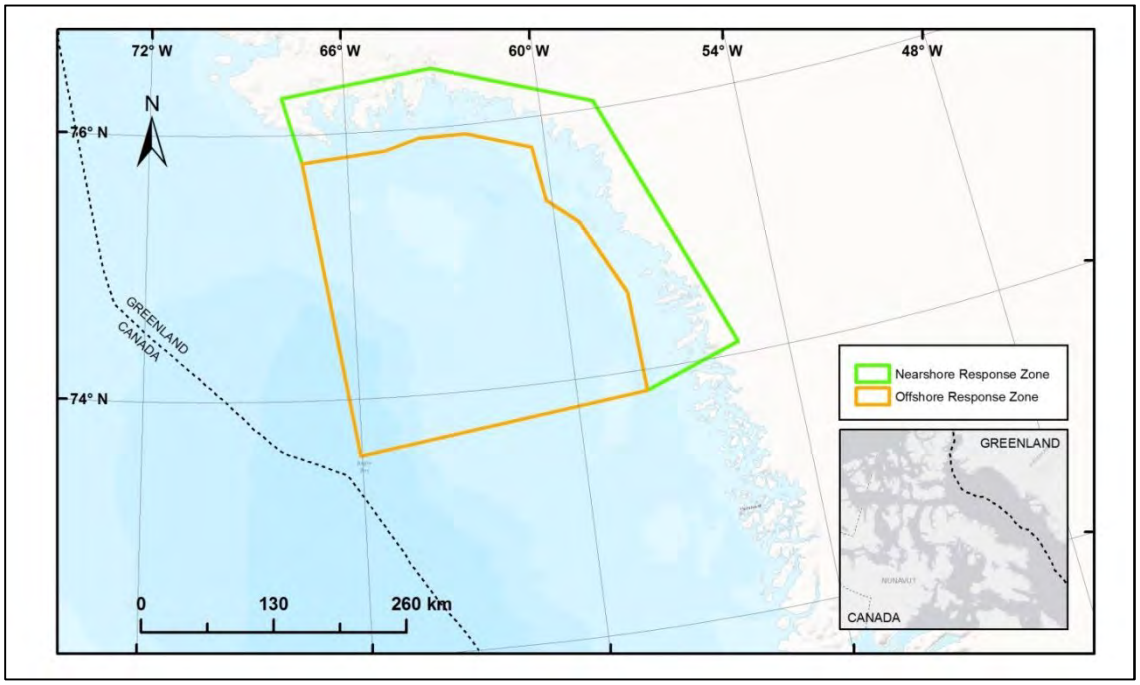

Figure 21: Nearshore and Offshore Response Operation Zones

Nearshore operational zones are for equipment that operates in shallower waters. The configuration of nearshore zones will also be dependent on the degree of land-fast ice. [Note that SIMAP takes the presence of land-fast ice into account with regard to defining the movement of oil and subsequent response operations.]

Offshore and nearshore mechanical recovery operations are compromised when ice coverage exceeds about 20%, and becomes relatively ineffective above 40% (Figure 22).[78]

		Ice coverage									
Response method	Open water	10 %	20 %	30 %	40 %	50 %	60 %	70 %	80 %	90 %	100 %
Mechanical recovery:											
- Traditional configuration (boom and skimmer)											
- Use of skimmer from icebreaker											
- Newly developed concepts (Vibrating unit; MORICE)											
In-situ burning:											
- Use of fireproof booms											
- In-situ burning in dense ice											
Dispersants:											
- Fixed-wing aircraft											
- Helicopter											
- Boat spraying arms											
- Boat "spraying gun"											

Figure 22: Expected Operational Limits of Spill Response by Ice Coverage[79]

[78] Evers et al. 2006.
[79] Evers et al. 2006.

In the offshore operations zone, the window for mechanical recovery operations was assumed to be about July through October, based on monthly average ice coverage data from TOPAZ. For the nearshore area, an additional month was assumed, through November, based on ice coverage data as well.

Another factor that significantly affects mechanical removal effectiveness in the field is the viscosity of the oil. Mechanical recovery (skimming) systems are usually most effective on relatively fresh oil. Once emulsification occurs, the oil becomes more viscous (by as much as 1,000 times) and increases its water content to about 70%.[80] These changes in oil properties present challenges for spill response operations. Many oil skimmers work considerably less efficiently (if at all) on emulsified, viscous oil, though some types of systems work better with increasing viscosity. The high water content of emulsified oil means considerably more volume of oil-water emulsion to recover, which increases the requirements for temporary storage capacity and transport for disposal or processing.

Different types of equipment have different limitations with respect to viscosity and other conditions (Figure 23).

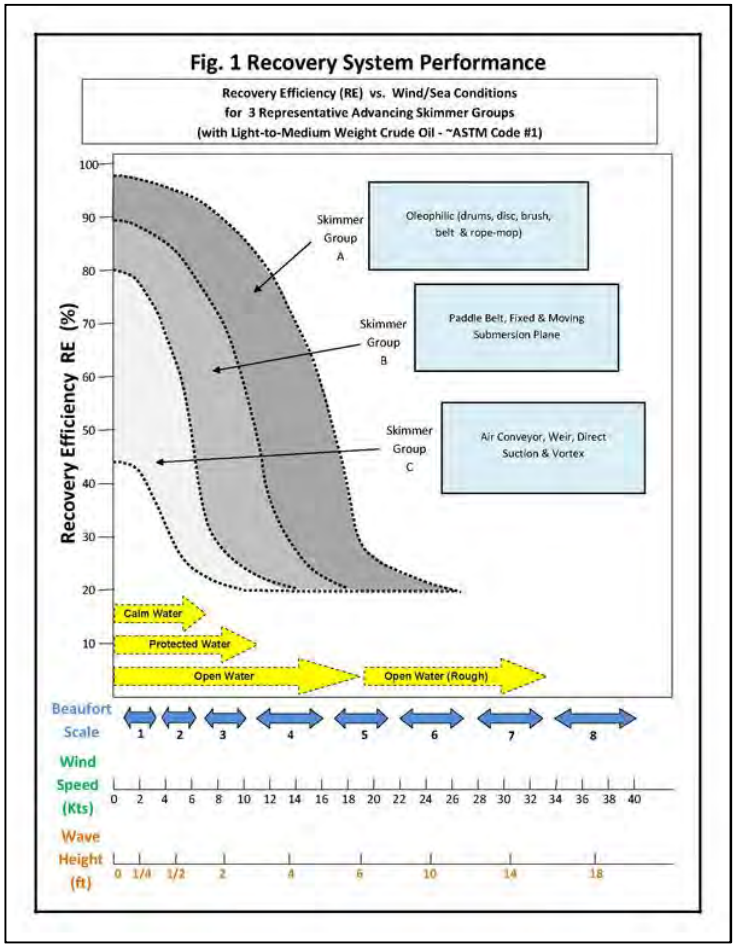

Figure 23: Factors that Affect Skimmer Efficiency[81]

[80] Fingas 2001, 2011.
[81] Dale 2011a, 2011b.

Based on research into skimmer effectiveness the thresholds for viscosity (i.e., the viscosities above which skimmers are ineffective) were assumed to be 80 cP in the nearshore zone, where the equipment would be mainly weir skimmers, and 15,000 cP in the offshore zone, where the equipment would mainly be oleophilic skimmers.[82]

Total mechanical recovery rate for the offshore equipment listed in the Cairn OSCP[83] is reported to be 5,000 bbl/day, or 795 m^3/day. Assuming this is the "effective daily recovery capacity" (EDRC) and not the manufacturers' reported nameplate capacities, this volume was then de-rated based on the Estimated Recovery System Potential (ERSP) calculator,[84] which comes to roughly 15% of the EDRC – or 120 m^3/day, or 10 m^3/hour. The ERSP calculator takes into account the way in which the conditions of encountering oil on the water surface, swath widths, and other factors will effectively reduce the amount of oil that would realistically be removed.

This amount is then apportioned to the offshore and nearshore sectors, with more being allocated to offshore operations. SIMAP (with the inputs of operational thresholds) then further reduces the total removal capabilities based on the temporally- and spatially-varying environmental conditions and weathering properties of the oil.

The mechanical recovery rates for the offshore zone would remove oil at the rate of about 7.5 m^3 per hour in a 12-hour operational day, provided the oil was of a viscosity of less than 15,000 cP and was thick enough on the water surface (8 µm) within the offshore recovery zone (as in Figure 21), and all of the environmental parameters (sea state, wind speed, current velocity) were met. Likewise, for the nearshore zone (as in Figure 21), the recovery rate would be 2.5 m^3 per hour in a 12-hour operational day. Over the course of each operational day, this would provide a removal capability of 90 m^3 per day for the offshore area, and 30 m^3 per day in the nearshore area.

In the modeling algorithms, the overall removal rate was also de-rated by an additional 62.5% to take into account that there will inevitably be compromised Arctic weather conditions, as previously described. This would result in a further overall reduction of removal capability.

Parameters and Thresholds for Surface Dispersant Response (Cases 1A and 1B)

In the response modeling, it was assumed that surface dispersants would be used in conjunction with mechanical recovery operations. Dispersants also have limitations in effectiveness depending on environmental conditions and oil properties throughout the weathering process. For effective dispersion, all of the following criteria needed to be met:

- Maximum oil viscosity: 20,000 cP
- Minimum oil thickness: 8 µm (microns)
- Minimum wind speed: 5.6 km/hour (3.0 knots)
- Maximum wind speed: 50.0 km/hour (27 knots)
- Minimum water depth: 10.0 meters
- Ice coverage: less than 30%

[82] Cairn Energy 2011.
[83] Cairn Energy 2011.
[84] BSEE and Genwest 2015; NRC 2013.

In the SIMAP modeling, surface dispersants were effective only if these criteria were met and there were sufficient chemical dispersants available (until the supply ran out.) Dispersant operations would only be successful if the oil were of sufficient thickness on the water surface and of a viscosity below 20,000 cP. In order to be effective, there needs to be sufficient mixing energy in the water, which requires a minimum wind speed of 5.6 km/h. The maximum wind speed would be 50 km/h. The maximum wind speed is not related to mixing energy, but rather to the safety of flying aircraft.

In order not to cause damages to nearshore organisms through higher concentrations of chemically-dispersed oil, a minimum water depth of 10 meters was assumed. Surface dispersant operations were assumed to occur in both the offshore and nearshore zones (Figure 21), provided the minimum water depth requirement was met.

Based on the ice coverage restriction (see Figure 22),[85] and monthly average ice cover data from TOPAZ, it was expected that dispersants would only be applied during July through October. As with the mechanical recovery operations there was assumed to be a 62.5% reduction in operations based on Arctic weather conditions.[86]

Dispersant applications were assumed to begin 48 hours after spill, because of delays associated with getting equipment and dispersant supplies on site. The operations were assumed to continue for 34 days (i.e., through Day 36 post-spill for both scenarios 1A and 1B), if there still is any treatable oil on the water surface. This duration is based on the amount of dispersant chemical available.

The Cairn OSCP[87] states that responders have access to 400,000 gallons of dispersant available for surface applications. The volume of dispersant can treat 8 million gallons of oil (190,476 bbl or 30,284m^3 total) at a 1:20 dispersant to oil ratio. Based on the operating assumptions described above, this volume of dispersant would be exhausted after 34 days of operations.

For a 12-hour operational day 74 m^3 of oil would be treated per hour, or 888 m^3 per day until the chemical dispersant supplies ran out.

Parameters and Thresholds for *In Situ* Burning Response (Cases 1A and 1B)

Another option for removing oil is to burn it through *in situ* burning operations. In the modeling it was assumed that this strategy was applied in addition to mechanical containment and recovery operations and surface dispersant applications.

In order for *in situ* burning to be effective the following criteria needed to be met:

- Maximum water content: 60%
- Minimum oil thickness: 8 µm (microns)
- Maximum wind speed: 55.6 km/hour (30 knots)
- Sea state (maximum wave height): 0.3 meters
- Maximum Current Speed: 0.36 meters/second (0.7 knots)

[85] See also Steiner 2011.
[86] DeCola et al. 2014; Evers et al. 2006.
[87] Cairn Energy 2011.

Burning was assumed to occur during the 12-hour daily operational window, provided the criteria were met and no thresholds were exceeded. The oil needed to be thick enough on the water surface, and be relatively free of emulsification, because the higher water content would hinder ignition and burning.

Wind speed needed to be low enough to allow burning to occur and to hinder the smoke plume from moving too far.

Sea state and current speed needed to be below thresholds that would significantly reduce the effectiveness of containment boom. Oil needs to be contained within fire boom to allow for burning to be effective.

In situ burning would only be conducted in the offshore response zone (see Figure 21) or a minimum distance of 10 kilometers from shore.[88]

For *in situ* burning, ice coverage needs to be less than 30% or more than 70% (see Figure 22). The oil needs to be either held by ice, be on top of ice, or be in relatively open water for the burning operations to be effective. Based on analysis of average monthly ice cover data from TOPAZ, it was assumed that there would be no particular seasonal restrictions on burning activities in the simulations.

The operations were assumed to begin 48 hours after the spill occurs and continued for the duration of the spill until there was no more burnable oil, i.e., it became too thin, too spread out on the water surface, or became too emulsified.

The burning rate was assumed to be 73 m^3 per hour, or about 878 m^3 per 12-hour operational day.[89] Again, the 62.5% Arctic weather factor was applied.

Sub-Surface Dispersant Operations (Case 2B)

Subsurface dispersants were applied for the first and only time during the 2010 Macondo MC252 (Deepwater Horizon) well blowout in the Gulf of Mexico. Approximately 770,000 gallons (2.9 million liters or 2,915 m^3) were applied over the course of about 80 days. As the result of the measured success of those operations, US regulatory agencies and industry operators are currently incorporating subsurface dispersant application into the strategy in offshore well spill response plans, including for Arctic operations.

There is no mention of subsurface dispersant application in any oil spill response plans associated with operations in Baffin Bay. The modeling of subsurface dispersant operations was conducted for the Baffin Bay 34-day blowout scenario (Case 2B) to evaluate the potential effectiveness of this response strategy, as it is likely that this strategy may be part of future response plans.

In the modeling of subsurface dispersants for Case 2B, it was assumed that there would be no surface operations, as modeled for the Melville Bay scenarios (Cases 1A and 1B). The only response modeled was subsurface dispersants.

[88] Steiner 2011.
[89] Based on Cairn Energy 2011.

Subsurface injection of dispersants at the wellhead was assumed to begin 72 hours after the onset of the spill and continue through the remaining duration of the 34-days blowout. Based on expert opinion and research studies conducted for the US Bureau of Safety and Environmental Enforcement, it takes about 72 hours to begin subsurface dispersants operations.[90] The model simulations assumed that the blowout plume was 100% treated at a dispersant to oil ratio of 1:100. To carry out this response, a supply of about 274,000 gallons (1,037,203 liters or 1,037 m^3) of dispersants would be required. Unlike the surface operations, there would be no limitations on operational time periods or weather-related down-times.

The subsurface injection simulations are described in more detail in the main report.

Summary of Spill Response Scenarios

The user inputs and modeling assumptions for the three selected hypothetical spill response scenarios are summarized in Table 14.

Table 14: Summary of Inputs and Assumptions for Spill Response Modeling

Response Strategy	Input or Assumption[91]	Scenario		
		Case 1A	**Case 1B**	**Case 2B**
		Melville Bay 1-day blowout of 3,340 m^3/day	**Melville Bay 34-day blowout of 3,340 m^3/day**	**Baffin Bay 34-day blowout of 3,340 m^3/day**
Mechanical Containment & Recovery	**Maximum Wind Speed**	55.6 km/h (30 kts)	55.6 km/h (30 kts)	--
	Maximum Current Speed	0.36 m/s (0.7 kts)	0.36 m/s (0.7 kts)	--
	Sea State (Max. Wave Height)	1.07 meters	1.07 meters	--
	Ice Coverage	<20%	<20%	--
	Minimum Oil Thickness	8 µm	8 µm	--
	Max. Oil Viscosity- Offshore	15,000 cP	15,000 cP	--
	Max. Oil Viscosity- Nearshore	80 cP	80 cP	--
	Daily Removal - Offshore	90 m^3	90 m^3	--
	Daily Removal - Nearshore	30 m^3	30 m^3	--
	Arctic Conditions Adjustment	62.5%	62.5%	--
Surface Dispersants	**Dispersant:Oil Ratio**	1:20	1:20	--
	Daily Oil Treated	888 m^3	888 m^3	--
	Maximum Oil Viscosity	20,000 cP	20,000 cP	--
	Minimum Oil Thickness	8 µm	8 µm	--
	Minimum Wind Speed	5.6 km/h (3.0 kts)	5.6 km/h (3.0 kts)	--
	Maximum Wind Speed	50 km/h (27 kts)	50 km/h (27 kts)	--
	Ice Coverage	<30%	<30%	--
	Arctic Conditions Adjustment	62.5%	62.5%	--
	Minimum Water Depth	10 meters	10 meters	--
	On-Scene Response Time	48 hours after spill	48 hours	--
In Situ Burning	**Maximum Water Content**	60%	60%	--
	Minimum Oil Thickness	8 µm	8 µm	--

[90] This report has not yet been released by BSEE.
[91] Daily removals are maximum removal rates before application of the Arctic condition adjustment factor.

Table 14: Summary of Inputs and Assumptions for Spill Response Modeling				
Response Strategy	**Input or Assumption[91]**	**Scenario**		
		Case 1A	**Case 1B**	**Case 2B**
		Melville Bay 1-day blowout of 3,340 m^3/day	**Melville Bay 34-day blowout of 3,340 m^3/day**	**Baffin Bay 34-day blowout of 3,340 m^3/day**
	Maximum Wind Speed	55.6 km/h (30 kts)	55.6 km/h (30 kts)	--
	Sea State (Max. Wave Height)	0.3 meters	0.3 meters	--
	Maximum Current Speed	0.36 m/s (0.7 kts)	0.36 m/s (0.7 kts)	--
	Ice Coverage	<30%, >70%	<30%, >70%	--
	Distance from Shore	10 km	10 km	--
	Daily Oil Burned	878 m^3	878 m^3	--
	Arctic Conditions Adjustment	62.5%	62.5%	--
Subsurface Dispersants	**Dispersant:Oil Ratio**	--	--	1:100
	Daily Application	--	--	33.4 m^3
	On-Scene Response Time	--	--	72 hours

References

Alpine Geophysical Associates. 1971. *Oil Pollution Incident: Platform Charlie, Main Pass Block 41 Field, Louisiana.* Prepared for the Water Quality Office, Environmental Protection Agency. Water Pollution Control Research Series Project #15080 FTU 05/71. 138 p.

Baffinland Iron Mines Corporation. 2015. *Terms of Reference for the Social Impact Assessment: Baffinland Iron Mines Corporation Trans-Shipping of Iron Ore in Greenland Waters*. March 2015. 73 p.

Barone, M., A. Campanile, F. Caprio, and E. Fasano. 2007 The impact of new MARPOL regulations on Bulker design: A case study. *Proceedings of the 2nd International Conference on Marine Research and Transportation*: 10 p.

Bercha, F.G. 2010. Arctic offshore oil spill probabilities. *Proceedings of Canada United States Northern Oil and Gas Research Forum*, Calgary, Canada. November 2010. 34 p.

Boehm, P.D. and D.L. Fiest. 1982. Subsurface distributions of petroleum from an offshore well blowout. The Ixtoc I Blowout, Bay of Campeche. *Environmental Science and Technology* Vol. 16(2):67-74.

Bureau of Safety and Environmental Enforcement (BSEE) and Genwest Systems. 2015. *ERSP Calculator User Manual.* US Department of the Interior, Bureau of Safety and Environmental Enforcement (BSEE). February 2015. 45 p.

Cairn Energy. 2011. *Oil Spill Prevention and Contingency Plan: Exploration Drilling Programme 2011 – Greenland.* Report No. ED/GRL/RSK/29/10/2071. 214 p.

Christensen, T., K. Falk, T. Boye, F. Ugarte, D. Boertmann, and A. Mosbech. 2012. *Identifikation af sårbare marine områder i den grønlandske/danske del af Arktis.* Aarhus Universitet, DCE – Nationalt Center for Miljø og Energi. 72 pp.

Commonwealth of Australia. 2011. *Final Government Response to the Report of the Montara Commission of Inquiry.* Australia Department of Resources, Energy, and Tourism. 132 p.

Curran, O. 2015. *Shipping and Marine Wildlife Management Plan*. BAF-PH1-830-P16-0024 Rev 5. Baffinland Iron Mines Corporation, Sustainable Development, Health, Safety & Environment. Appendix J10. 9 March 2015. 198 p.

Dale, D. 2011a. *Response Options Calculator (ROC) Users Guide.* Genwest Systems, Inc. May 2011. 72 p.

Dale, D. 2011b. *Response Options Calculator (ROC) Technical Documentation.* Genwest Systems, Inc. May 2011. 45 p.

DeCola, E., T. Robertson, and S. Fletcher. 2006. *Offshore Oil Spill Response in Dynamic Ice Conditions: A Report to WWF on Considerations for the Sakhalin II Project.* Prepared for WWF UK and WWF Germany by Nuka Research and Planning Group LLC, Alaska, USA. 74 p.

Det Norske Veritas. 2011. *Ship Oil Spill Risk Models*. Det Norske Veritas Project No. PP002916. Prepared for Australian Maritime Safety Authority. December 2011. 50 p.

Det Norske Veritas. 2012. *Prince Rupert Marine Risk Assessment: Navigational Risk Assessment Report.* Prepared for Prince Rupert Port Authority. Report No./DNV Reg. No. 13JIMVK-8. Rev 3, 2012-02-29. 160 p.

Dokken, Q. 2011. Ixtoc I versus Macondo well blowout: Anatomy of an oil spill event then and now. *Proceedings of the 2011 International Oil Spill Conference*. 8 p.

Dyb, K., L. Thorsen, and L. Nielsen. 2012. *Technical Report: Blowout Risk Evaluation in the Labrador Sea.* Report No. AFT-2011-0444-02.3. March 2012.Prepared by Acona Flow Technology AS for Denmark Bureau of Minerals and Petroleum. 72 p.

Egevang, C., D. Boertmann, and O. Stenderup Kristensen. 2005. *Monitering af havternebestanden på Kitsissunnguit (Grøne Ejland) og den sydlige del af Disko Bugt, 2002–2004.* Teknisk rapport nr. 62. Pinngortitaleriffik, Grønlands Naturinstitut. 41 p.

Étienne, L., R. Pelot, and C. Engler. 2013. *Analysis of Marine Traffic: Phase 2-Part 2: A Spatio-Temporal Simulation Model for Forecasting Marine Traffic in the Canadian Arctic in 2020.* Prepared for Defence R&D Canada Centre for Operational Research and Analysis, by Maritime Activity and Risk Investigation Network (MARIN) Research Group, Dalhousie University, Halifax, Nova Scotia, Canada. 198 p.

Etkin, D.S. 2009. *Analysis of U.S. Oil Spillage*. American Petroleum Institute Publication 356. August 2009. Environmental Research Consulting, Cortlandt Manor, New York. 71 p.

Etkin, D.S. 2012. *Cook Inlet Maritime Risk Assessment: Spill Baseline and Accident Casualty Study – Spill Scenarios and Impacts.* Prepared by Environmental Research Consulting and The Glosten Associates for Cook Inlet Risk Assessment, Anchorage, AK. March 2012. 142 p.

Etkin, D.S. 2015. Offshore well blowout probability model. *Proceedings of the 38th Arctic and Marine Oilspill Program Technical Seminar on Environmental Contamination and Response.*

Etkin, D.S., and K. Michel. 2003. Bio-Economic Modeling of Oil Spills from Tanker/Freighter Groundings on Rock Pinnacles in San Francisco Bay. Vol. II: Spill Volume Report. Prepared for US Army Corps of Engineers, Sacramento District. Contract DACW07-01-C-0018). 42 p.

Etkin, D.S., D. French-McCay, N. Whittier, S. Subbayya, and J. Jennings. 2002. Modeling of response, socioeconomic, and natural resource damage costs for hypothetical oil spill scenarios in San Francisco Bay. *Proc. of 25th Arctic & Marine Oilspill Prog. Tech. Sem.*: 1,075–1,102.

Evers, K-U., K.R. Sørheim, and I. Singsaas. 2006. *Oil Spill Contingency Planning in the Arctic: Recommendations*. ARCOP Growth Project GRD2-2000-30112. Prepared by Hamburgische Schiffbay-Versuchsanstalt GmBH (HVSA), Hamburg, Germany, and SINTEF, Trondheim, Norway. 47 p.

Fingas, M. 2001. *The Basics of Oil Spill Cleanu*p. Second Edition. Lewis Publishers, CRC Press LLC, Boca Raton, Florida. 233 p.

Fingas, M. 2011. Physical Spill Countermeasures. In *Oil Spill Science and Technology: Prevention, Response, and Cleanup*, edited by M. Fingas. Elsevier, Inc. pp. 303 – 338.

Fitch, W.A., K.E. Kirby, J.J. Dragna, D.D. Kuchler, D.K. Haycraft, R.C. Godfrey, J.A. Langan, B.E. Fields, H. Karis, M.T. Regan, and R.C. Brock. 2013. *BP and Anadarko's Phase 2 Pre-Trial Memorandum Quantification Segment.* Document Submitted in the U.S. District Court for the Eastern District of Louisiana MDL No. 2179 Section J. In Re: Oil Spill by the Oil Rig "Deepwater Horizon" in the Gulf of Mexico, on April 20, 2010. Document 11266 Filed 5 September 2013. 14 p.

Hauck, B., P. Frost, S.G. Flynn, S. Shutler, L. Mayberry, M. Lawrence, R.G. Dreher, S.Himmelhoch, N. Flickinger, S. Cernich, R. Gladstein, A.N. Chakeres, A. Cross, B. Engel, J. Harvey, R. King, E. Pencak, R.M. Underhill, D.J. Boente, S.D. Smith, and S. O'Rourke. 2013. *United States of America's Pre-Trial Statement for Phase Two: Number of Barrels of Oil Discharged and BP's Statements and Actions Related to Quantification and Source Control. Document Submitted in the U.S. District Court for the Eastern District of Louisiana MDL No. 2179 Section J. In Re: Oil Spill by the Oil Rig "Deepwater Horizon" in the G*ulf of Mexico, on April 20, 2010. Document 11265 Filed 5 September 2013. 14 p.

Herbert Engineering Corp., and Designers & Planners, Inc. 2003. *Evaluation of Accidental Oil Spills from Bunker Tanks (Phase 1).* Prepared for US Coast Guard Ship Structure Committee and Research, Washington, DC, and US Coast Guard Development Center, Groton, Connecticut. Report No. SSC-424. 54 p.

Holand, P. 2006. *Blowout and Well Release Characteristics and Frequencies.* SINTEF Report STF50 F06112. SINTEF Technology and Society, Trondheim, Norway. 77 p.

Holand, P. 2013. *Blowout and Well Release Characteristics and Frequencies, 2013*. SINTEF Report F25705. SINTEF Technology and Society, Trondheim, Norway. 114 p.

International Maritime Organization (IMO). 1995. *Interim Guidelines for Approval of Alternative Methods of Design and Construction of Oil Tankers under Regulation 13F(5) of Annex I of MARPOL 73/78. Resolution MEPC.66(37)*. Adopted September 14, 1995.

Ji, Z-G., W.R. Johnson, and G.L. Wikel. 2014. Statistics of extremes in oil spill risk analysis. *Environmental Science & Technology* 48:10505-10510.

Joint Division for Investigation of Maritime Accidents & Bahamas Maritime Authority Report. 2008. *Marine Accident Report: Quest Grounding on 27 June 2007*. Danish Maritime Authority Case No. 200708695. Bahamas Maritime Authority Case No. 80011365/2007/5545/ 15 p.

Mariport Group Ltd. 2012. *Arctic Shipping Developments for World Wildlife Canada.* Prepared for World Wildlife Fund Canada, by The Mariport Group, Ltd., Digby, Nova Scotia, Canada. 72 p.

McNutt, M.K., R. Camilli, T. J. Crone, G.D. Guthrie, P.A. Hsieh, T.B. Ryerson, O. Savas, and F. Shaffer. 2012. Review of flow rate estimates of the Deepwater Horizon spill. *PNAS, Proceedings of National Academies of Science* 109(50):20260-20267.

McNutt, M.K., S. Chu, J. Lubchenco, T. Hunter, G. Dreyfus, S.A. Murawski, and D.M. Kennedy. 2012. Applications of science and engineering to quantify and control the Deepwater Horizon oil spill. *PNAS, Proceedings of National Academies of Science* 109(50):20222-20228.

Michel, K., and T.S. Winslow. 1999. Cargo ship bunker tanks: Designing to mitigate oil spillage. *Society for Naval Architects and Marine Engineers (SNAME) Joint California Sections Meeting.* 14 May 1999. 13 p.

Michel, K., and T.S. Winslow. 2000. Cargo ship bunker tanks: Designing to mitigate oil spillage. *Marine Technology* Vol. 37 (4): 191 – 199.

Mosbech, A., D. Boertmann, and M. Jespersen. 2007. S*trategic Environmental Impact Assessment of Hydrocarbon Activities in the Disko West Area*. National Environmental Research Institute, University of Aarhus, Denmark. NERI Technical Report No. 618. 192 p.

National Research Council (NRC). 1998. *Double-Hull Tanker Legislation: An Assessment of the Oil Pollution Act of 1990*. National Academy Press, Washington, DC. 266 p.

National Research Council (NRC). 2001.*Environmental Performance of Tanker Designs in Collision and Grounding: Method for Comparison*. National Academies Marine Board/Transportation Research Board Special Report No. 259. National Academy Press, Washington, DC. 136 pp., plus appendices.

National Research Council. 2013. *A Review of Genwest's Final Report on Effective Daily Recovery Capacity (EDRC)*. National Academy of Sciences Ocean Studies Board, Washington, DC. 42 p.

Nilsen, O.V., C.B. Johansen, and M. Knight. 2005. *Formal Safety Assessment for Cruise Ships.* Prepared for SAFEDOR. Document Id. SAFEDOR-4.1.1. 2005-12-31 DNV rev. 1. 60 p.

Nuka Research and Planning Group. 2014. *Estimating an Oil Spill Response Gap for the US Arctic Ocean.* Prepared for US Bureau of Safety and Environmental Enforcement (BSEE), US Department of the Interior (Contract E13PC00024), by Nuka Research and Planning Group LLC, Alaska, USA.86 p.

Oldenburg, C.M., B.M. Freifeld, K. Pruess, L. Pan, S. Finsterle, and G.J. Moridis. 2012. Numerical simulations of the Macondo well blowout reveal strong control of oil flow by reservoir permeability and exsolution of gas. *PNAS, Proceedings of National Academies of Science* 109(50):20254-20259.

Papanikolaou, A., R. Hamman, B.S. Lee, C. Mains, O. Olufsen, E. Tvedt, D. Vassolos, and G. Zaraphonitis. 2013. GOALS – Goal Based Damage Stability of Passenger Ships. *Proceeedings of the 2013 Society of Naval Architects and Marine Engineers (SNAME) Annual Meeting.* 33 p.

Perry, J. and R. Bright. 2010. *Capricorn Greenland Exploration 1: Capricorn Sigguk Exploration Drilling Environmental Impact Assessment Exploration Drilling Programme, Sigguk Block, Disko West, Greenland.* Prepared by Environmental Resources Management Ltd. for Cairn Energy. Reference No. 0108885. March 2010. 501 p.

Rawson, C., K. Crake, and A. Brown. 1998. Assessing the environmental performance of tankers in accidental grounding and collision. *SNAME Transactions* Vol. 106: 41 – 58.

Speer, L., and T.L. Laughlin. 2011. *IUCN/NRDC Workshop to Identify Areas of Ecological and Biological Significance or Vulnerability in the Arctic Marine Environment: Workshop Report.* 40 p.

Steiner, R. 2011. *Review of Cairn Oil Spill Prevention and Contingency Plan (OSCP), Exploration Drilling Programme – 2011 Greenland.* 7 p.

van Oudenhoven, J.A.C.M. 1983. The Hasbah 6 (Saudi Arabia) blowout: The effects of an international oil spil as experienced in Qatar. *Proceedings of the 1983 International Oil Spill Conference*: pp. 381 – 388.

Yip, T.L., W.K. Talley, and D. Jin. 2011. The effectiveness of double hulls in reducing vessel-accident oil spillage. *Marine Pollution Bulletin*. Vol. 62 (11): 2,427 – 2,432.